Development of UHF RFID tags for traceability and quality control of food products, Application : Cheese production

Abanob Abdelnour

Communauté
UNIVERSITÉ Grenoble Alpes

THÈSE

Pour obtenir le grade de

DOCTEUR DE LA COMMUNAUTE UNIVERSITE GRENOBLE ALPES

Spécialité : **Optique et Radio-fréquence**

Arrêté ministériel : 25 mai 2016

Présentée par

Abanob Abdelnour

Thèse dirigée par **Pr. Smail Tedjini, Grenoble INP**
codirigée par **Dr. Darine Kaddour, Grenoble INP**

préparée au sein du : **Laboratoire de Conception et d'Intégration des systèmes (LCIS)**

dans **l'École Doctorale : Electronique, Electrotechnique, Automatique et Traitement du Signal**

Développement d'étiquettes RFID UHF pour la traçabilité et le contrôle de qualité des produits alimentaires, Application: production de fromage

Thèse soutenue publiquement le **25 Octobre 2018**,
devant le jury composé de :

Mme. Leena UKKONEN
Professeur à Tampere University of Technology (Rapporteur)
M. Robert STARAJ
Professeur à l'Université Nice-Sophia Antipolis (Rapporteur)
M. Raphaël GILLARD
Professeur à l'Université de Rennes (Président du jury)
M. Antonio LAZARO
Professeur associé à Universitat Rovira i Virgili (Rapporteur)
Mme Darine KADDOUR
Maître de conférences à Grenoble-INP/LCIS (Co-encadrant de thèse)
M. Smail TEDJINI
Professeur à Grenoble-INP/LCIS (Directeur de thèse)

Thesis background and Author's contributions

In the food sector, the use of RFID makes it possible to improve the safety of food while ensuring better traceability and better monitoring of products. The work of the thesis was mainly carried out within the framework of a project in cooperation with several academic and industrial partners in the cheese sector where the main objective of the project is to master all the manufacturing steps by providing efficient traceability and control of cheese ripening. The work carried out in this thesis fits into this context and aims at developing UHF RFID tags adapted to the constraints of food products by ensuring a dual function: a traceability function with unitary identification, and then a sensing function of cheese maturation by indirect measurement of its electromagnetic and physicochemical properties.

The first step of the project was the characterization of the electromagnetic parameters of food products during ripening in order to achieve an appropriate design of the tag antenna. In radiofrequencies, it is mainly the substrate that dictates the electromagnetic properties of the components, in particular the size of the antennas and their radiation pattern. Knowledge of these properties is essential to meet industrial requirements and to integrate systems in good conditions. In addition, a correlation study is carried out between the variation of the dielectric properties and that of the chemical properties during the period of cheese ripening. This study helps to understand the difference between cheese types and allows determining the main parameters to follow during cheese maturation for the design of the sensor tag.

The second step was the design of identification tags for the traceability of food products during the manufacturing process. The main objective is to create a UHF RFID tag with a performance that meets the needs of manufacturers in the cheese sector regarding the size, memory and reading distance while respecting the health standards at the packaging level as well as the substrate used. Several UHF RFID tag configurations were realized and tested in an industrial environment where the results obtained show the effectiveness of using an RFID system to automate the traceability of products in the cheese sector.

The third step is the design of sensor tags to track the degree of maturation of products during the ripening period. A first solution, based on the exploitation of

the effect of variation of the dielectric properties on the tag reading distance, shows a lack of performance due to the small variations as well as the difficulties of measurement in a real environment. A second solution based on the measurement of gas evolution rate shows the possibility of estimating the degree of cheese maturation. However, the sensor activation power and the high cost represent great challenges and thus make it difficult to adopt this solution. Finally, two alternative solutions to measure the effect of gas evolution were presented. The idea is based on monitoring other parameters varying due to the increase of gas release during cheese maturation. The first sensor tag configuration is based on product dimension tracking using a resistive sensor. On the other hand, the second sensor tag configuration is based on the pressure change tracking in the product packaging due to gas production. The results obtained show that these two sensor RFID tag configurations can offer simple and effective solutions for controlling the cheese ripening process.

The work presented in this thesis is organized into six chapters:

- **Chapter 1** presents an introduction to RFID technology as well as a state of the art about the application of RFID technology in the food industry and especially the cheese sector.
- **Chapter 2** presents a study of the electromagnetic properties of materials and the main methods of dielectric characterization.
- **Chapter 3** presents the results of dielectric characterization of several food products during their ripening period as well as their correlations with the variation of their chemical properties.
- **Chapter 4** introduces the main steps of UHF RFID tag design for cheese product traceability. Several configurations are realized and tested.
- **Chapter 5** introduces the difficulties of measurement in an industrial environment and proposes several solutions to improve the performance of the system at the tag and reader level.
- **Chapter 6** presents several sensor tag configurations based on tracking different parameters to detect the degree of cheese maturation.

Acknowledgments

This thesis was carried out at the Laboratory of Design and Integration of Systems (LCIS) located in Valence and attached to the polytechnic institute of Grenoble (Grenoble INP).

I would like to express my thanks to my thesis supervisor M. Smail TEDJINI, Professor at the polytechnic institute of Grenoble, for his help and generous support during my Ph.D. work. Thank you very much for your valuable advice, your availability and especially all the confidence you have given me during the thesis.

I would also like to thank my co-supervisor Mrs. Darine KADDOUR, Associate Professor at the polytechnic institute of Grenoble, for her constant support and for always providing encouraging and constructive feedback.

Many thanks to all partners in the project “AFFINID” especially M. Jean-Paul le Maître, M. Thomas Batier and M. Fabrice Buchin with all Enilbio team for their positive cooperation and their great help during the project.

As a member of ORSYS team, I have been surrounded by glorious colleagues who have provided a rich and fertile environment to study and explore new ideas. I acknowledge valuable discussions with all team members, in particular: Etienne Perret, Nicolas Barbot, Romain Siragusa, Pierre le MaÎtre and Yvan Duroc.

Thank you to all previous and current LCIS members, in particular: Jennyfer Duberville, Carole Seyvet, David Hely, Vincent Beroulle, Karim Oumahma, Sélim Azzouni, Cedric Carlotti and Laurent Lefevre.

Thanks for Dr. Antonio Lazaro, Pr. David Girbau and Dr. Ramon Villarino for welcoming me during my mobility program at University of Rovira I Virgili.

Special thanks to all my dear friends for their advice and support since my first day at LCIS, in particular: Duy-Thong, Gianfranco, Marco, Angel, Mossab, Tsitoa, Arash, David, Dahmane, Ahmed, Mushir, Zeshan, Rina, Fateh, Newton, Kostas, and Hatem.

Finally, but most importantly, I would like to give my deepest gratitude to my family members, for their enormous help and support. All of my achievements have an invisible part of your contribution.

Contents Page

List of figures

Page

Chapter 1

Chapter 2

Chapter 4

List of tables **Page**

Chapter 1

RFID technology in the food industry

1. Introduction

Nowadays there is a great need to ensure availability of food to overcome the continued growth in the world's population and to maintain the stability of markets and economy. Despite the great advances in science and technology that have helped to increase the food production, there is still a significant amount of wastage that occurs during the production process of food as well as on its way to the consumers. In addition to direct food wastage, health risks associated with food safety play a major role in food consumption. In this context, an efficient and reliable traceability system of food items can provide appropriate matching between food supplies and demands, as well as proper handling during storage and transit, which in turn reduces food wastage and ensures better food quality through tracing from farm to fork [1].

Recently, there are several intelligent packaging technologies that can effectively be used to trace food and to improve food safety and quality [2]. Among these technologies, RFID technology allows updating the item data as it moves along a supply chain and is able to sense and report ambient conditions (e.g., temperature, humidity, and pressure) through on-board or connected sensors. The

ability to update stored information is very useful for tracing purposes because information about the characteristics of every node passed by the item can be recorded in enough details to enable robust traceability. Also, continual measurement and reporting of ambient conditions can help detecting contamination if occurred. The main drawback of RFID technology is its relatively high cost compared to other traceability systems, which makes it limited to some parts of the production chain.

Nowadays, bar-codes and other visual traceability techniques are widely applied in the food sector despite their limited features. Compared to RFID, bar-codes do not possess the capability to store and update information locally. Moreover, none of the bar-code variants has the capability to sense and report ambient conditions or to hold two-way communication with a reader. Therefore, when entire set of costs and benefits are together taken into account, the cost-based distinction between bar code and RFID tag disappears or becomes less significant. Indeed, RFID technology is gradually surpassing bar-code technology in the field of food traceability, and more industrial food sectors are adopting RFID solutions..

This chapter presents a state of art about the RFID technology in the food industry. A basic high-level introduction to RFID to help understand its general characteristics along with the main features and differences between RFID systems is first provided. Then, the chapter discusses actual works developed to test the ability of RFID technologies to perform food traceability in a variety of sectors (wine, fish, and meat) with a specific focus on RFID applications in cheese industry. Finally, the main theme of the presented research, the author's contribution and the thesis organization are described in detail.

2. RFID Classification and Principles of Operation

An RFID system is composed of a tag and a reader which generates and transmits an interrogation signal to the tag and then decodes the backscatter signal produced by the tag. There are different types of RFID systems that have emerged due to continuous development of RFID technology over years[3]. Each system has its own features where the main differences between one system and another are based on operation frequency, communication protocol, power regulations and

reading distance. RFID systems can be categorized in terms of the tag as 'near-field' RFID (Low Frequency & High Frequency) based mainly on inductive coupling and 'far-field' RFID (Ultra High Frequency) based on signal propagation and backscattering [4].

Other classification, based on the way of activating the tags, divides the RFID systems into 'active' and 'passive', where an active tag powers its chip from a battery and transmits signal to the reader whereas a passive tag is activated by harvesting power from the reader interrogating signals. Between active and passive systems, there is a 'semi-passive' configuration where a passive tag can be enhanced with a battery allowing to power additional sensors or to increase the tag read range [4].

2.1 Near-field Coupling

This family of RFID systems includes both LF and HF systems where the transponders use magnetic coupling. A near field tag is constituted of an inductive inductance coil L acting as an "antenna", an electronic chip containing the identifier of the tag and carrying out the communication operations, and finally a capacitance C adjusting the circuit LC resonant frequency at the working frequency. In this configuration, a reader passes a large alternating current through a reading coil, resulting in an alternating magnetic field in its locality. Once the near field tag is placed in this magnetic field as shown in figure 1, an alternating voltage will appear across the inductive loop. This voltage is first rectified in order to power the tag chip, which allows the demodulation of the interrogation signal. RFID Tags based on near-field coupling send data back to the reader using load modulation [4]. A current variation proportional to the load applied to the tag's coil give rise to its own small magnetic field which will oppose the reader's field and therefore the reader coil can detect data as a small variation in current flowing through it.

Thus, if the tag's electronics applies a load to its own antenna coil and varies it over time, a signal can be encoded as tiny variations in the magnetic field strength representing the tag's ID. The reader can then recover this signal by monitoring the change in current through the reader coil. A variety of modulation encodings are possible depending on the number of ID bits required, the data transfer rate, and additional redundancy bits placed in the code to remove errors resulting from noise in the communication channel. Near-field coupling is the most straightforward approach for implementing a passive RFID system. This is why it

was the first adopted approach and has resulted in many subsequent standards, such as ISO 15693 and 14443, and a variety of proprietary solutions [5].

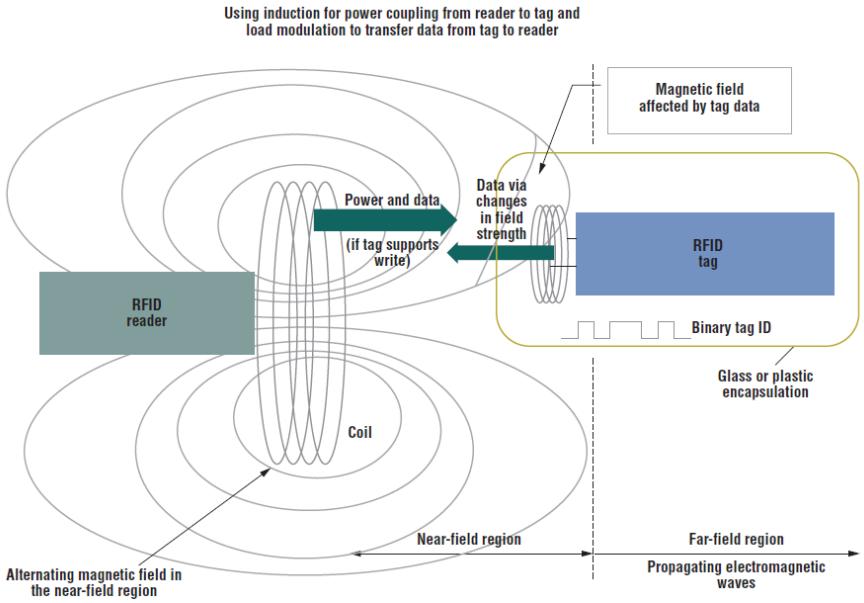

Fig. 1. Near-field power/communication mechanism for RFID tags operating at less than 100 MHz [5].

However, near-field communication has some physical limitations. The magnetic field drops off at a factor of $1/r^3$, where r is the separation of the tag and reader, along a center line perpendicular to the coil's plane and thus the energy available for induction decreases significantly with distance. Also, as applications require more ID bits as well as discrimination between multiple tags in the same locality for a fixed read time, each tag requires a higher data rate and thus a higher operating frequency. These design constraints have led to new passive RFID designs based on far-field communication.

2.2 Far-field Coupling

In far-field RFID systems, the antenna is comparable in size to the wavelength and uses radiative coupling to communicate between the reader and tag. The EM waves radiating from the reader antenna are captured by the tag antenna developing thus an alternating voltage difference across the tag antenna and therefore the microchip ports. A diode circuit can rectify this voltage and link it to a

capacitor, which results in an accumulation of energy in order to power up the electronic circuitry of the microchip [6].

As the tags are located beyond the near-field zone of the reader in far-field RFID systems, the communication between the reader and the tag is based on backscattering principle. The reader antenna emits an interrogating signal as illustrated in figure 2, which is received by the tag antenna. A part of the incident energy is then reflected from the tag and detected by the reader. The variation of the tag's load (microchip) impedance causes the envisioned impedance mismatch between the tag antenna and the load. As a consequence, the varying impedance mismatch produces a variation in the amplitude of the reflected signals. Therefore, by changing the tag antenna's load over time, the tag can reflect incoming signal (with amplitude modulation) back to the reader in a pattern that encodes the tag's ID. This category of communication is called 'backscattering modulation' [7].

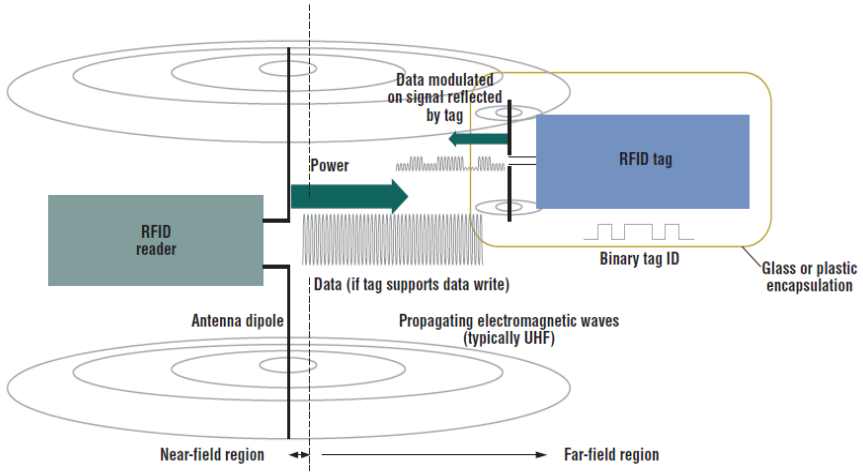

Fig. 2. Principle of backscattering in Far-field RFID system [5].

A far-field system's range is limited by the amount of energy that reaches the tag from the reader and by how sensitive the reader's radio receiver is to the reflected signal. The actual return signal is very small, because it's the result of two attenuations, each based on an inverse square law—the first attenuation occurs as EM waves radiate from the reader to the tag, and the second when reflected waves travel back from the tag to the reader. Thus the returning energy is $1/r^4$ (r is the separation of the tag and reader). In addition, only a part of the incident signal will be reflected, while another part is absorbed by the microchip.

However, the energy required to power a tag at a given frequency continues to decrease (currently lower than -20dBm; i.e. few microwatts). So, with modern semiconductors, tags can be read at increasingly large distances possible a few years ago. Furthermore, inexpensive radio receivers have been developed with improved sensitivity so they can now detect signals, for a reasonable cost, with power levels on the order of –100 dBm.

2.3 Passive RFID Systems

In passive RFID systems, as the RFID tag has no on-board power source, it uses instead the power emitted from the reader to activate itself. Passive RFID tags are based on the principle of backscattering modulation to transmit their stored data back to the reader. Compared to active or semi-active tags, passive tags are simpler in structure, lighter in weight, and less expensive while offering a virtually unlimited operational lifetime.

The trade-off is that passive tags have shorter reading distances than active tags and require higher-power readers. They are also constrained in their capacity to store information and their ability to perform well in electromagnetically noisy environments [8]. The reading range of passive RFID systems can be varying between 3 up to 20 meters depending on the transmission power of the RFID reader and the chip sensitivity. The presence of a reader is necessary for such a tag to transmit its data where the reader always communicates first, then followed by the tag response.

2.4 Semi-Passive RFID Systems

Semi-passive tags are a compromise between active and passive tags. They have as active tags their own power sources. However, they do not have a radiofrequency transmitter; instead they are based on the principle of backscattering modulation to transmit their information to readers. The cost of this type of tags is therefore lower compared to active tags. Therefore, this type of transponder can be considered as a good compromise for some applications because the cost is less than active tags and the reading distance is greater than passive tags.

2.5 Active RFID Systems

In active RFID systems, tags have an on-board power source and electronics for performing specialized tasks [9]. An active tag uses its on-board power supply to support microchip operation and transmit data to the reader. It does not require the power emitted from the reader for data transmission. The on-board electronics incorporate microprocessors, sensors, and input/output ports, and so on. In an active RFID system, the tag always communicates first, followed by the reader. As the presence of a reader is unnecessary for the data transmission, an active tag can broadcast its information to surroundings even in the absence of a reader. This type of active tag, which continuously transmits data with or without the presence of a reader, is also called a transmitter. Another type of active tag enters into a sleep or low-power state in the absence of interrogation by the reader. The reader wakes up the tag from its sleep state by issuing an appropriate command. The ability to enter into a sleep state conserves battery power, and consequently this type of tag generally has a longer battery life than an active transmitter tag. This type of active tag is called a transmitter/receiver [10].

Active RFID tags are mainly used in telemetry applications, to communicate a large amount of information over large distances. It makes it possible to reach operating distances of the order of a few hundred meters. The main drawback of active tags is that their cost is very high compared to passive tags and can reach one hundred dollars per unit.

2.6 Comparison between different RFID systems

Table 1 provides a qualitative comparison between LF, HF and UHF RFID systems based on their reading distances, data rates, and costs. This table shows that HF and UHF technologies stand out in terms of cost whereas UHF technology has more interests in reading distance and data rate.

Table 1. Comparison between different RFID systems

	LF	HF	UHF
Frequency	125 KHz, 134.2 KHz	13.56 MHz	865-928 MHz (Regionally dependent)
Read range	Few centimeters	Less than 1 meter	Up to 20 meters
Data rate	Slow	Fair	Very Fast

Scan capability	Single read	Single read	Multiple reads
Tag cost	High	Intermediate	Low
Reader cost	Low	Low	High
Tag memory	Very limited	256 bits to 8 Kbytes	96 bits to 8 Kbytes

Each of these RFID technologies has advantages and features that guarantee them a place in the market. Generally, the LF/HF RFID systems are more used compared to the UHF RFID systems because historically they came first on the market. However, due to high demands in terms of speed and reading distance in the field of traceability, UHF RFID technology is recently becoming more suitable for many applications and its implementation is increasing considerably in many fields.

3. Benefits of RFID technology in the food industry

In recent years, traceability aspects have become recognized as an essential tool for guaranteeing food safety and food quality. The quality of a food product depends mainly on its specific characteristics and its production process. Food characteristics can vary as function of weather conditions, biological variations, seasonality, storage, transportation, and cooling facilities. Based on these characteristics, specific risks may be introduced such as cross contamination of batches when different batches are mixed or when the same resource is used for the production of different intermediate products. Moreover, there are challenges associated with quality assurance when raw materials are sourced from different suppliers.

On the other hand, according to FAO (Food and Agriculture Administration) standards of Food Hygiene [11], “food safety is the assurance that food will not cause harm to the consumer when it is prepared and/or eaten according to its intended use.” Numerous opportunities exist for food safety violations during the processes, procedures, or stages that any given food product passes through on its way from farm to fork.

Therefore, as the scope of both food quality and food safety increases with the globalization of food supply chains, efficient traceability systems should be installed in order to ensure:

- ✓ Effective and efficient management of raw-material production.
- ✓ Identification of imminent potential deviations or errors in processes and procedures.
- ✓ Better food quality and safety through immediate identification of deficits or compromises in production equipment before or as soon as they take place.
- ✓ Appropriate quality and safety measures throughout the food supply chain to prevent contaminants.
- ✓ Continuous tracking of perishables in order to ensure that they reach the consumer in good condition.
- ✓ Extended shelf life of food products through proper management of their ambient conditions (e.g., gas, temperature, humidity) throughout the food supply chain.
- ✓ Effective inventory management and reduction of overall shrinkage.
- ✓ Reduction of overall wastage of food products so that more people can be fed with fewer raw materials.

Based on currently available technologies, RFID technology is clearly superior in terms of functionality as well as the management of information flow within the supply chain. Moreover, the development of RFID sensors tags has improved monitoring of the cold chain of perishable food products, environmental monitoring, as well as the presence of microbial organisms. The next section presents the main benefits of applying RFID systems in the food industry and its effects on overall food quality and safety.

3.1. Supply chain management

In supply chain management, RFID tags are used to track food products during distribution and storage. RFID technology serves as a replacement for barcode scanners for this particular application due to its advantages over barcodes: RFID systems do not require line of sight to read the tag, their range of operation is larger as compared to that of a barcode, readers can simultaneously communicate with multiple RFID tags, and tags can store more data as compared to a barcode. With its ability to scan multiple tags throughout 3-D space, known as the interrogation zone, RFID technology also facilitates automated product shipments from a warehouse to a retail store. Table 2 [12] shows the main differences between RFID technology and barcodes.

Table.2. Comparison RFID vs Barcode

Characteristics	RFID	Barcode
Traceability: communication to readers over the whole distribution chain	✔✔✔	✘
Multiple reading	✔✔✔	✘
Reading rate	✔✔✔	✔
Tag scanning	✔✔	✔
Multiple write and read	✔✔✔	✘
Reading through multiple materials (paper, plastic)	✔✔	✘
Life span	✔✔	✔
Cost	✔	✔✔
Robustness	✔✔	✔
Security	✔✔	✔
Environmental impact	✔	✔✔
Market	✘	✔✔✔

An RFID system implemented in a store can be used to maintain an accurate database of its inventory that automatically alerts a warehouse management system once the inventories are low. Thus, RFID technology will provide benefits such as greater speed and efficiency in stock operations, better inventory tracking throughout the supply chain, and enhanced forecasting [13] [14].

Wal-Mart stores Inc. was the 1st major company to push for RFID implementation in supply chain management. In June 2003, Wal-Mart announced that it would require its top 100 suppliers to put RFID tags on shipping cases and

pallets by 1 January 2005. Each tag would store an Electronic Product Code (EPC) that would be used to track products as they enter Wal-Mart's distribution centers and then in turn are shipped to individual stores. Wal-Mart now requires its top 300 suppliers to place RFID tags on all its pallets and cases of products [15] as shown in figure 3.

a *b*

Fig.3. Example of RFID system for supply chain management a) RFID tag on pallet b) Vehicle-mounted readers are placed on forklifts to automatically read and record the data registered in the pallet's RFID tag [16], [17]

British Telecommunications has launched a new online real-time food traceability system based on RFID technology. This system, known as BT foodnet, tracks products in real-time to speed up and reduce the cost of recalling products. The online network provides retailers and their suppliers access to real-time synchronized data on the current and historical status of all stock items as they pass throughout the supply chain (from manufacturer to the point of sale). This system combines barcodes and RFID read/write tags with a secure data exchange platform on the Internet [18].

Spanish in-molding plastic company (Araven), specialized in manufacturing of food containers used in industrial kitchens at restaurants and hotels, has developed smart food containers which are enhanced with UHF RFID tags. Due to the addition of the RFID tags in these containers, more accurate and historic information about product and usage can be gathered. Hence, this new information RFID-based system helped to achieve better inventory control, improve events management such as cold-storage room replenishment, or reduce products close to expiration date [19].

eProvenance (Bordeaux France) has developed an RFID based tracking system to preserve the quality of fine wines and trace their origin. This RFID system consists of 3 components. The 1st component is a 13.56 MHz semi-passive RFID tag placed inside each case of wine. This semi-passive tag enables wine producers and distributors to monitor and log ambient temperatures in each case of wine 3 times a day. The 2nd component is a 13.56 MHz passive RFID tag with a unique code attached to the base of each bottle for tracking and inventory management. The 3rd component is a proprietary and tamper-proof neck seal at the base of the capsule of each bottle. The seal has a unique identifying code printed with invisible ink, which contains identification numbers of both the semi-passive and passive tags. All 3 components are linked together with their unique identification numbers on an online database [20].

United biscuits (Hayes, U.K.) uses RFID technology to control the movement of raw materials and in weighing, mixing, and baking processes involved in the preparation of biscuits and cakes [21].

RFID technology has been used by cheese manufacturers to trace cheese along the supply chain with great precision. This tracking system could result in rapid product recall in case of a problem. Customers can find the entire history of the cheese after purchase by entering an alphanumeric code on a website [22].

3.2. Monitoring of preservation conditions

Recently, RFID chips are enhanced with sensing capabilities which allow monitoring the environmental conditions, storing the data concerning the product, and then transmit the collected information upon request. Infratab Inc. (Oxnard, Calif., U.S.A.) developed RFID tags in both HF and UHF bands which can monitor the shelf life of foods to which they are attached. The tags are enhanced with temperature sensors and a visual display that provides green, yellow, and red indicators depending upon the status of the item. The range of operation for these tags is from −30 to 70 °C with an accuracy of 0.5°C [23].

Other works [24] proposed a low power system for food monitoring which is compliant with the standard ISO15693 for identification purposes and used proprietary commands for temperature logging. The temperature operation range is from -40°C to 85°C being accurate of ±0.5°Cover the whole temperature range with an average power consumption around 8.4 µW when active.

D. Cartasegna et al. presented an integrated smart label for tracing food information and monitoring its preservation conditions. The system includes humidity, temperature, and light intensity sensors with the respective interface circuits, an A/D converter, and a 13.56-MHz RFID transponder for transmitting and receiving data, as well as for gathering from an external reader the energy for recharging the on-board microbattery and powering the transmitter [25].

A system based on a combination of RFID technology and variable sensor types was proposed by [26] where the integration of different sensors is possible depending on the requirements. In this work, the main attention was turned on the temperature monitoring in truck environment during the food transport. Furthermore, the system was capable to communicate with the driver's cabin and with a central base in case of temperature range violation, allowing the driver or the fleet manager to proactively intervene before damage occurs.

3.3 Food safety

Nowadays, the Food market demands new smart solutions that can send the information of the food spoilage for a long distance without any physical intervention. RFID systems can be used to ensure that food products such as meat, fruits, and dairy products remain within a safe range of surrounding conditions such as temperature, humidity and pressure during transportation and storage [27]. Beside improving food safety, RFID technology can help to reduce operating costs, meet compliance requirements, and improve efficiency in the food industry [28].

Peng Liu et at [29] proposed a traceable safety information coding for beef cattle based on RFID and improved EPC. The proposed system solves the coding problems of key information in the procedures of tracing the quality and safety of beef cattle, which is featured with low cost and strong scalability. Operation in the field showed the efficiency of the proposed coding system which can allow the establishment of an efficient traceability system for quality and safety of beef cattle.

A wireless RFID compatible sensor tag using gold nanoparticles was developed for pathogen detection in the liquid food supply chain [30]. The goal of this project was to coat microscopic structures with bacteriophages or viruses that bind with

pathogens. Detection is based on resonance frequency shift of RFID tag response which is correlated with the concentration of bacteria in the milk.

4. RFID Applications in food industry

RFID applications have been progressively developed in the past decade in different fields of food production in relation to good traceability through all stages of the production/distribution chain [31]. In some cases, RFID applications allowed increased production efficiency; a group of examples are presented below in relation to development attempts, trials and obtained results.

4.1 Wine sector

For added-value products like wine, the importance of obtaining precise information on the overall process, from the grape to the bottled wine, lies in the fact that consumers would rather pay more for a product with proven attributes [32]. It also lies in avoiding counterfeit products. The wine supply chain is a complex chain, where a large amount of data has to be handled. A solution to systematically store and recover information about products and processes generated throughout the wine supply chain can thus help to overcome the inherent difficulties associated with data management in the wine sector. Therefore, a complete traceability system can be developed in the wine production sector by joining RFID technology with the use of wireless sensor networks for monitoring at the vineyards.

Expósito et al [33] developed a proposal of such a merged solution for a winery in Spain. It was shown that the system could provide a competitive advantage to the company by improving visibility of the processes performed and the associated control over product quality. The RFID implementation began at the harvesting of the grapes. Origin authentication was enabled by means of tags glued to the boxes/containers transporting the grapes from the vineyards to the winery as shown in figure 4.

Fig.4. RFID tags attached to containers of grapes [33]

RFID tagging of the boxes/containers helped to select or classify the received grapes by categories as the RFID tags were linked with the data previously collected from the region of origin (variety of grape, degree of ripening, etc.). Moreover, RFID tags also allowed to identify all the different tanks where the wine was processed, which is an important issue in those stages of processing where mixtures of different wines/musts are performed (e.g., blending operations).

Once the wine is bottled, a specific identifier is created for each single bottle, in order to link each bottle with its complete history of production, starting from some months before the harvesting time. Data can be obtained by querying the identifier on a website or an application, which obtains the data from the general database of the production company. However, the radio propagation in presence of liquids presents important differences compared to tags installed on boxes or containers. Wine bottles suffer from this disadvantage. Once the wine is bottled, the location of the tags on the bottle surface is problematic: the liquid content is a good conductor, and so the transmission capabilities of the tag are reduced. A good selection of the type of tags, as well as its location in the body of the bottle, is a key factor to achieve good performances. In this context, Gonçalves et al [34] studied the performance of different RFID tag configurations designed on the cork of wine barrel as well as wine bottle as illustrated in figure 5. The UHF RFID tags proposed in this paper achieved good performance in terms of reading range (varying between 3 to 6 meters depending on cork type).

a *b* *c*

Fig. 5. Different configurations of RFID tags designed on cork a) Meander tag on wine barrel cork b) Meander monopole on wine bottle cork c) compact size tag on regular bottle stoppers [34]

The transportation of wine from the cellars to storage areas and to points of sale is also crucial for the final consumer. Therefore, the information on the production environment as well as temperature and humidity along the transport and storage processes must be recorded. Bernardi et al [35] reported a case study evaluating the RFID implementation on an anti-counterfeit mechanism in selected wine production environments. The suggested system used a personal digital assistant (PDA) with a public/private key mechanism involving both, passive RFID internal memory and unique RFID identifier to allow the reseller and the final user to verify whether the bottle is original. Also, Anastasi et al [36] implemented a system for monitoring the productive cycle of Sicilian winery, where sensor nodes were deployed both in the field and in the cellars where the wine aging occurs.

According to previously stated works, the application of RFID technology had a great impact on improving the traceability in the wine sector especially in the case where farm-to-fork (F2F) Web service has been designed to link each item identifier to the data incorporated at the vineyards and winery. RFID technology allowed thus the consumers to obtain the full tracking of the bottle they are going to taste.

4.2 Fish sector

Seafood represents a highly perishable food category; the stay-time of its products within different production stages and market installations directly affect their purchase probability. Recently, average distances that the products need to

cover to reach the destination markets have increased due to the developing global trade. Therefore, the time needed to ship fish products abroad also increased which generates additional problems in terms of appearance and freshness maintenance [37]. As a result, the traceability of seafood is becoming an important aspect to be considered during the industrial processing where both producers and consumers are looking at food traceability as a mean to restore confidence in the food supply and limit damages incurred by distribution of unsafe products [38]. In this context, the integration of RFID technology in the fish production sector can have a great impact on improving the traceability system by providing accurate production information about items as well as monitoring the preservation conditions using sensor tags. The RFID system can be based on identification and monitoring by batch or in some cases it can be by item when the unit is of high value to allow integrating an RFID tag per item as shown in figure 6.

a *b*

Fig.6. Different RFID system configurations for traceability in the fish sector a) RFID HF tag placed inside a polystyrene box with the fish for identification and temperature monitoring [39] *b) RFID HF tag implanted into Tuna caudal fin root* [40].

The efficient management of preservation conditions is crucial during the cold chain distribution of seafood goods where temperature is the most important factor in prolonging the quality of items. Temperature fluctuations affect negatively the cold chain and are considered as the main reason for quality losses occurring during the production stages of seafood items [41]. In this context, E. Abad et al [39] developed a real-time traceability and cold chain monitoring system based on HF RFID for food applications. The smart tag attached on the product to be tracked integrates light, temperature and humidity sensors, a microcontroller, a memory chip, low power electronics and an antenna for RFID communications. The sensor

logged data were stored in the memory together with traceability data and a commercial reader was used for reading and writing data on the smart tag, with a wireless reading distance of 10 cm, in real-time at any time of the food chain. The results obtained showed the potential of applying RFID technology in this field where the main advantage was the possibility of reading data at any time of the logistic chain without opening the polystyrene boxes containing the fish and the tags. Therefore, the RFID system proposed in this work can help to improve the competitiveness of the fish/food companies, their logistic management, and also to reinforce the confidence of the consumers in the fish/food logistic chain.

Besides monitoring temperature through the cold chain, the fishing industry requires an effective information management system which covers the entire life-circle of seafood from fishing vessel to the market. Miyamoto et al [40] presented a solution based on an HF RFID tag, implanted into tuna fish body, which records fishing time and position (latitude & longitude) along with biological data of caught fish such as species name, sex, and body length and weight. Then, the recorded data and the RFID tag ID number are simultaneously transmitted to an information control base through a communication satellite system ORBCOMM. This system allowed managers of tuna fisheries and fish markets to read the data from the RFID tag in the fish body, and request for data verification from the data storage center over the Internet.

Similar work [42] proposed an RFID system where fishermen can scan the fish's tag at or near the moment of capture with a compatible RFID reader and then transmit the fish's data file to a personal smartphone pre-installed with a reporting application. The developed application allows the fisherman to input any missing data, or add richer data (i.e. a photo of the fish, GPS coordinates) before saving the form and storing the data on internal phone memory. Then, once connected to a cellular or wireless network, the data will be immediately uploaded to the fisheries group database. In addition, this system allows improving "catch and release" fishing activities which enables scientific researchers to access data collected from the same tag over the entire lifetime of a fish.

Recent works also discussed the possibility of integrating RFID technology in fish sales as well as combining RFID systems with other technologies such as drones and artificial intelligence techniques in order to provide a totally automating process for the fish sector. In Taiwan, a group of researchers studied the feasibility

of combining RFID systems with drones in order to improve the management of oyster farms [43]. The realized tests showed that the proposed system can provide a useful tool in analyzing and identification of oyster rafts farming with less man power and time. In Indonesia, another work proposed an integrated fish auction system [44] where the usage of RFID technology and digital weighing scale helped to decrease the chance of data manipulation and improved auction total sales by automatically generating fish data into database.

From temperature monitoring to identification by drones and automated auction systems, theworks, mentioned in this section, showed the feasibility of combining RFID systems with other technologies and clearly demonstrated the great impact of applying RFID technology in the fishing industry. RFID application greatly improved the process of fish tagging and reporting while allowing automating the process of collecting, parsing, and transmitting data without requiring supervision from the user which opens the doors towards the integration of IoT in the fish sector.

4.3 Meat sector

With the development of society and the improvement of living standards, meat quality became an important primary public concern. Thus, legislation is progressively imposing the development of a suitable monitoring technology for meat products evaluation during production, processing, storage and distribution. For meat traceability, EU food policies are progressively imposing the implementation and use of different RFID applications. However, the implementation of RFID tracking systems in the meat supply chain apparently involves a greater level of technological difficulties in comparison with other sectors, since monitoring is extended to live animals.

In this context, a series of works were published in the past few years proposing different and interesting solutions. Tomes et al. [45] focused on the use of RFID systems to identify cattle specimens in association with a large Biotrack database. In this work, each ID was associated to a whole set of biometric identifiers in order to allow the correct identification of meat sold units with the animal of origin. This integrated RFID-Biotrack database system could eventually replace barcodes with the purpose of full traceability between the participants.

Kong et al. [46] developed an RFID architecture for a meat supply chain safety control. RFID was used to identify each animal in pig farms, and to organize the information into a farm database. Similar works also proposed a solution based on combining RFID technology and SQL Server 2000 databases to realize information traceability for the entire pork production [47].

Luo et al. [48] went further, by designing RFID system based on an online reading and writing system for meat production lines within poor environment conditions (i.e., Chinese pig slaughterhouses). Authors were able not only to collect, transmit and deal with the crucial information essential for the good traceability and regarding the key processes but also printed a set of commercial meat RFID tags to be used directly on carcass and cuttings in the sales stores.

Later, Shougang et al. [49] developed an RFID system that worked from customers back to manufacturers, by connecting each product to the related points of interest. At sale, data from the meat products with RFID tags are entered into a database allowing the connection of the meat unit with the data flow of all other products in circulation. If necessary, this procedure facilitates the monitoring and management of product flow and thus the time needed by the authorities for an eventual withdraw was significantly reduced.

Chen et al. [50] studied the development of a management system for pig matching and breeding based on combining RFID and Quick Response (QR) code technologies with an electronic database management system to keep track of the farm situation at all times. Results obtained in pig farms showed that aside from effectively improving the efficiency of breeding and matching, this system can also significantly improve and upgrade administration of vaccines and efficiency of breeding.

Recently, studies are more oriented towards the integration of sensing capabilities in RFID systems which allow remote sensing of food quality. In this context, Nguyen et al. [51] presented a solution for the detection of meat quality based on the correlation between the physical read-range of passive UHF RFID tags and the permittivity of the object on which the tags are placed as shown in figure 7. By studying the variation of meat permittivity as function of time, it was possible to detect the contamination time from which the meat becomes improper for consumption based on the measurement of the tags read-range.

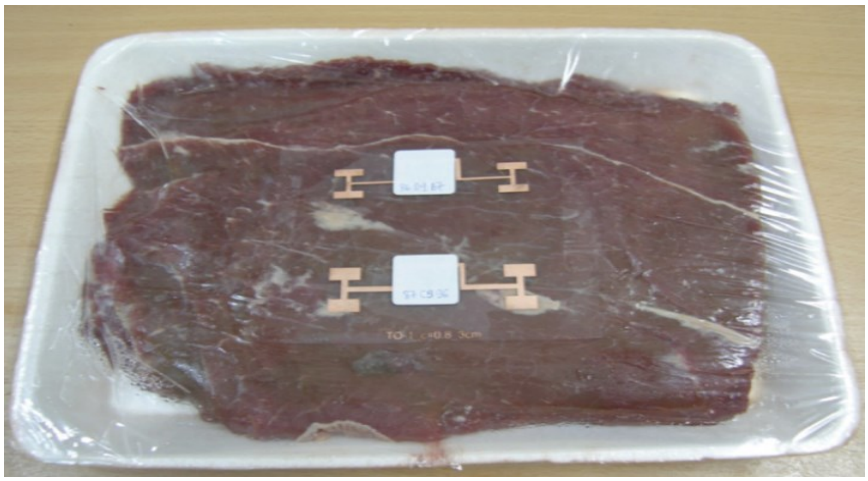

Fig. 7. An RFID tag-based sensor is tested on a sample of beef wrapped in plastic over ten consecutive days to detect when it becomes unfit for human consumption [52]

Based on previously stated works, the integration of RFID technology in the meat production sector showed great benefits. However, the majority of these works was mainly focused on traceability and management of production chain in farms. Therefore, there is still need for more development by integrating sensing capabilities in the RFID systems which allow consumers to verify meat quality at sales in order to reduce manipulations and increase the confidence in the market.

4.4 Cheese sector

Nowadays, the sector of cheese production does not have an automated procedure that guarantees a proper traceability throughout all the fabrication stages. The traceability in the sector of cheese production is based on casein plaques or special types of stamps. As a result, the production and quality control are performed by batches and the data are stored manually by written records. The main problem in this scenario is the cheese ripening which is done in special chambers where the surrounding conditions such as humidity, temperature, product handling and mold growing affect the readability of the products labels. Therefore, there is a great need for developing innovative systems and technologies that could improve the performance of traceability systems in the cheese sector. By automating information collection, ripening chambers and warehouse management can be optimized which reduces costs and thus improves the competitiveness.

Nowadays, published studies relative to the use of these technologies in Europe within the cheese industry are still few. Pérez-Aloe et al. [53] tested different RFID systems based on fixed and portable reader configurations using two different types of RFID HF tags. The tags have been tested under different conditions of temperature, humidity, saline solutions immersions or in the presence of preservative substances and oils. Besides, physical tests including friction and flexibility have been also achieved. No significant negative effects on tags readability were reported, with the exception of those cases where metallic materials occurred in the range of the reader. Later, similar work realized by Regattieri et al. [54] proposed a traceability system for the supply chain of Parmigiano Reggiano cheese, which was developed based on an integration of alphanumerical codes and HF RFID technology. Results obtained showed the benefits of applying RFID technology compared to barcode and alphanumerical codes despite the relatively higher cost of RFID systems.

In a subsequent study, Varese et al. [55] tested the applicability of RFID technology to the dairy cheese production not only for item identification but also for authentication in order to avoid cases of imitations of Protected Designation of Origin (PDO). Two different types of small-sized tags were used and their efficiency was compared: an embedded tag directly inserted on the side of the cheese at the end of the forming process; an external tag inserted in a casein plate after the first or second turning over of the cheese. The results indicated that the positioning of the tags did not affect readability. The embedding tag proved to be more resistant during the various stages of processing, while the casein plate was more subjected to losses at handling, but only in those cases in which the cheese has a rough/uneven rind.

Papetti et al. [56] proposed the integration of an RFID system with quality analysis for single product of a typical Italian cheese. The tracing and quality information (chemical and spectrophotometric) are combined on a web platform where any details about the product shelf-life from producer to consumer can be easily obtained. The categories involved in this system are divided into manufacturers, wholesalers, resellers, retailers and consumers who contribute separately, according to their level of membership, to provide a set of data related to each product. All collected data are then registered into a centralized database.

In the same context of applying RFID systems in the cheese production sector, Barge et al. [57] realized an interesting study by investigating the effectiveness of RFID technology in tracing single cheese wheels, from curd making to final packaging and delivery. RFID systems, operating at low, high and ultra-high frequencies (LF, HF and UHF respectively), were tested and compared with the aim of evaluating the performances and limits of each solution at different stages of the production process. According to the authors, the HF RFID system is considered to be more suitable for cheese traceability than UHF tags due to its lack of performance when used in direct contact with high water content material such as cheese. However, this conclusion is not accurate as the authors used commercial UHF tags for testing and they did not design appropriate UHF tags for this specific application and thus the UHF tags performance degraded significantly.

In all previously mentioned works, the RFID systems applied in the cheese sector were limited to identification and in some few cases the quality analysis was realized separately then combined with the product RFID identifier on a database, which improved the traceability and control management of the supply chain considerably. However, both cheese producers and consumers are looking for monitoring of the quality of cheese in real time to obtain a procedure for info-tracking systems, together with the combination with a web platform to access production history and quality of product using the RFID sensors. In this context, a French company realized smart shelves enhanced with RFID sensor tags for monitoring temperature and humidity in cheese maturation chambers [58]. The system is based on active RFID tags which can communicate with the reader antenna inside the ripening chamber in a range of 100 meters. Then, the reader will transmit the acquired data to the web interface which can be accessible at any time from a computer, tablet or smartphone.

Moreover, Google research department in France launched recently an innovative project called “Google cheese master” with the aim of developing smart sensing nodes combined with artificial intelligence techniques to detect cheese quality as shown in figure 8. However, the main challenge for these works is the capability of detecting the major varying parameters during the ripening of different types of cheese and the ability to integrate the sensors on a smart label such as RFID tags.

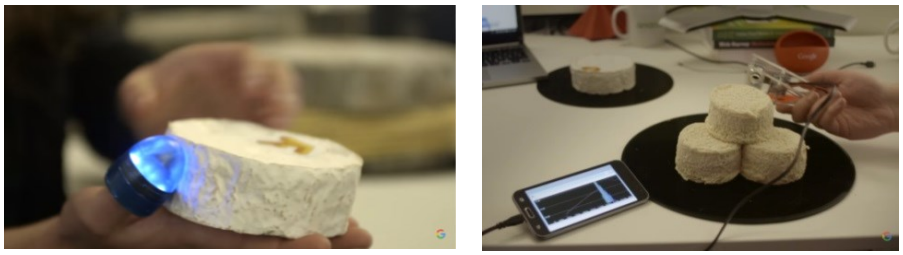

a b

Fig. 8. Google cheese master research project for monitoring cheese quality based on several types of sensors a) Optical sensor b) Ultrasound sensor [59]

4.5 Other Food Products

Besides cattle and pigs traceability, RFID technology has also played an important role in poultry farming [60]. Moreover, RFID readers and semi active tags integrated with gas sensors were used to assess the quality of apples by monitoring produced gases such as ethylene [61]. RFID tags integrated with gas sensors (O_2 and CO_2) were used for checking freshness of Broccoli [62]. In addition, Semi-passive RFID loggers were used for prediction of shelf life of lettuce transported in refrigerated container [63]. It has also been reported that keeping quality of tomatoes and shelf-life of Soybean sprouts as well as control management of Kiwi supply chain were also realized using RFID systems [64]–[66].

5. Conclusion

In the food sector, safety of the product is a major concern in several countries, in particular, the traceability of food products which is mandatory by law. Radio Frequency Identification is a promising technology with the potential to improve the management of information flow within the supply chain and security in the food sector. RFID is already being used for years in animal identification and tracking and in the food chain for traceability control. Moreover, integration of RFID tags with sensors has improved monitoring of the cold chain of perishable food products, environmental monitoring, irrigation, specialty crops and farm machinery. This chapter describes how the widening use of RFID technology for the traceability of food products takes place within the different stages of the supply chain from production, through distribution, up to the final merchandizing of different food products.

As referenced, RFID implementation in the food sector is increasing at a great rate due to the possibility of coupling different types of radio frequency smart tags to environmental sensors through new tools provided by the fast developing WSN technology. Nevertheless, real applications of RFID technologies are still limited because of various technical and economical obstacles. From a management point of view, the main challenge preventing the wide application of RFID systems is its higher cost compared to other technologies commonly used in the food sector. The cost of traceability is a very delicate question, especially in the food sector because the value of the product is normally very low and so the solutions adopted for the tracking and tracing system must be very cheap. For this reason, alphanumerical codes and bar codes are today the most promising. However, Radio frequency identification systems proved to have more potential and more advantages; which is encouraging food processing companies not to consider traceability as an economic burden but can view it as an opportunity for system growth especially for ‘‘high value” products such as famous cheeses and wines where integration of RFID systems can be feasible and affordable.

Another important issue concerning the application of RFID in the food sector is the choice of system configuration. The majority of works discussed in this chapter were based on HF RFID near field configuration which is limited in terms of speed and reading distance compared to UHF RFID tags. This choice is basically because near field RFID systems (LF & HF) were applied in the industry before the UHF RFID systems and also because the lack of performance of UHF tags when they are placed in proximity of food products compared to LF and HF tags which are less sensitive to water content. However, developing appropriate UHF tag designs for food products can improve the system performance and add more advantages and benefits which can lead to adoption greater potential of RFID technology in the food sector.

According to previously stated works, the application of RFID technology in the cheese sector is very limited compared to other food sectors such as wine and fish industries. The traceability in the cheese sector is still based on visual marks or alphanumerical codes. In this context, the objective of the thesis is to study the feasibility of applying UHF RFID systems with the aim of improving traceability and quality monitoring in the cheese supply chain. The following chapters will discuss in detail the main works realized starting by characterization of different properties of cheese till design and validation of several tags configurations for traceability and sensing of cheese during its production chain.

References

[1] R. Nukala, K. Panduru, A. Shields, D. Riordan, P. Doody, and J. Walsh, "Internet of Things: A review from 'Farm to Fork,'" 2016, pp. 1–6.

[2] M. Ghaani, C. A. Cozzolino, G. Castelli, and S. Farris, "An overview of the intelligent packaging technologies in the food sector," *Trends Food Sci. Technol.*, vol. 51, pp. 1–11, May 2016.

[3] J. Landt, "The history of RFID," *IEEE Potentials*, vol. 24, no. 4, pp. 8–11, Oct. 2005.

[4] D. M. Dobkin, *The RF in RFID: Passive UHF RFID in Practice*. Elsevier, 2007.

[5] R. Want, "An introduction to RFID technology," *IEEE Pervasive Comput.*, vol. 5, no. 1, pp. 25–33, Jan. 2006.

[6] C. C. Yen, A. E. Gutierrez, D. Veeramani, and D. van der Weide, "Radar Cross-Section Analysis of Backscattering RFID Tags," *IEEE Antennas Wirel. Propag. Lett.*, vol. 6, pp. 279–281, 2007.

[7] C. Boyer and S. Roy, "Coded QAM Backscatter Modulation for RFID," *IEEE Trans. Commun.*, vol. 60, no. 7, pp. 1925–1934, Jul. 2012.

[8] M. R. Souryal, D. R. Novotny, D. G. Kuester, J. R. Guerrieri, and K. A. Remley, "Impact of RF interference between a passive RFID system and a frequency hopping communications system in the 900 MHz ISM band," *IEEE Electromagn. Compat. Mag.*, vol. 1, no. 3, pp. 97–102, Third 2012.

[9] W. J. Yoon, S. H. Chung, S. J. Lee, and Y. S. Moon, "Design and Implementation of an Active RFID System for Fast Tag Collection," in *7th IEEE International Conference on Computer and Information Technology (CIT 2007)*, 2007, pp. 961–966.

[10] O. Aluf, "Active RFID TAGs system analysis of energy consumption as excitable linear bifurcation system," in *2009 IEEE International Conference on Microwaves, Communications, Antennas and Electronics Systems*, 2009, pp. 1–9.

[11] "Codex Alimentarius: Food Hygiene (Bsasic texts) - Fourth edition." [Online]. Available: http://www.fao.org/docrep/012/a1552e/a1552e00.htm. [Accessed: 15-May-2018].

[12] Y. Xiao, S. Yu, K. Wu, Q. Ni, C. Janecek, and J. Nordstad, "Radio frequency identification: technologies, applications, and research issues," *Wirel. Commun. Mob. Comput.*, vol. 7, no. 4, pp. 457–472, May 2007.

[13] I. Cuiñas, R. Newman, M. Trebar, L. Catarinucci, and A. A. Melcon, "Rfid-based traceability along the food-production chain [Wireless Corner]," *IEEE Antennas Propag. Mag.*, vol. 56, no. 2, pp. 196–207, Apr. 2014.

[14] D. Wang and D. Huang, "Food Supply Chain Management under Conditions of Food Safety," in *2010 International Conference on Management and Service Science*, 2010, pp. 1–4.

[15] R. Weinstein, "RFID: a technical overview and its application to the enterprise," *IT Prof.*, vol. 7, no. 3, pp. 27–33, May 2005.
[16] "Flex Hard Tag - Durable RFID Tag For Returnable Containers." [Online]. Available: http://www.universalrfid.com/product/flex-hard-tag/rfid-tags-rfid-labels-and-asset-tags. [Accessed: 29-Jun-2018].
[17] "RFID Readers Information | Engineering360." [Online]. Available: https://www.globalspec.com/learnmore/data_acquisition_signal_conditioning/data_input_devices/rfid_readers. [Accessed: 29-Jun-2018].
[18] C. Connolly, "Sensor trends in processing and packaging of foods and pharmaceuticals," *Sens. Rev.*, vol. 27, no. 2, pp. 103–108, Apr. 2007.
[19] B. B. Bravo, J. C. Fernandez, M. M. Barrera, and J. R. Sanchez, "Implementation of RFID tags in food containers in catering business," in *European Workshop on Smart Objects: Systems, Technologies and Applications*, 2010, pp. 1–6.
[20] "eProvenance applies RFID technology to monitor temperature and assure the quality of fine wine." [Online]. Available: https://www.eprovenance.com/news/pressReleases-030801.htm. [Accessed: 16-May-2018].
[21] R. Angeles, "Rfid Technologies: Supply-Chain Applications and Implementation Issues," *Inf. Syst. Manag.*, vol. 22, no. 1, pp. 51–65, Dec. 2005.
[22] A. Regattieri, M. Gamberi, and R. Manzini, "Traceability of food products: General framework and experimental evidence," *J. Food Eng.*, vol. 81, no. 2, pp. 347–356, Jul. 2007.
[23] Infratab, "Infratab Unwraps Freshtime™ Sensor Platform at Internet of Things." [Online]. Available: https://www.prnewswire.com/news-releases/infratab-unwraps-freshtime-sensor-platform-at-internet-of-things-300186286.html. [Accessed: 16-May-2018].
[24] F. O. O. Gomes *et al.*, "A low-power RFID enabled temperature sensor for cold chain management," in *2015 IEEE International Symposium on Circuits and Systems (ISCAS)*, 2015, pp. 2113–2116.
[25] D. Cartasegna *et al.*, "Smart RFID label for monitoring the preservation conditions of food," in *2009 IEEE International Symposium on Circuits and Systems*, 2009, pp. 1161–1164.
[26] I. Schumacher, J. Wollenstein, and J. Kalbitzer, "Low-power UHF-RFID sensor tags for a complete monitoring and traceability of the cold chain," in *Smart SysTech 2012; European Conference on Smart Objects, Systems and Technologies*, 2012, pp. 1–6.
[27] K. Y. Chetanraj, K. S. Shushrutha, A. R. Phani, and C. S. Naveen, "The design of active RFID for food quality and safety sensors," in *2017 International Conference On Smart Technologies For Smart Nation (SmartTechCon)*, 2017, pp. 1124–1127.

[28] J. Ren, "RFID enable food supply chain traceability and safety," in *2015 International Conference on Logistics, Informatics and Service Sciences (LISS)*, 2015, pp. 1–5.
[29] P. Liu, W. Liu, Q. Li, M. Duan, Y. Wang, and Y. Dai, "A research on tracing code of culture of food safety traceability based on RFID and improved EPC," in *2016 International Conference on Logistics, Informatics and Service Sciences (LISS)*, 2016, pp. 1–6.
[30] S. Karuppuswami, L. L. Matta, E. C. Alocilja, and P. Chahal, "A Wireless RFID Compatible Sensor Tag Using Gold Nanoparticle Markers for Pathogen Detection in the Liquid Food Supply Chain," *IEEE Sens. Lett.*, vol. 2, no. 2, pp. 1–4, Jun. 2018.
[31] L. Ruiz-Garcia and L. Lunadei, "The Role of RFID in Agriculture: Applications, Limitations and Challenges," *Comput Electron Agric*, vol. 79, no. 1, pp. 42–50, Oct. 2011.
[32] M. G. C. A. Cimino and F. Marcelloni, "Enabling Traceability in the Wine Supply Chain," in *Methodologies and Technologies for Networked Enterprises*, Springer, Berlin, Heidelberg, 2012, pp. 397–412.
[33] I. Expósito, J. A. Gay-Fernández, and I. Cuiñas, "A Complete Traceability System for a Wine Supply Chain Using Radio-Frequency Identification and Wireless Sensor Networks [Wireless Corner]," *IEEE Antennas Propag. Mag.*, vol. 55, no. 2, pp. 255–267, Apr. 2013.
[34] R. Gonçalves *et al.*, "RFID-Based Wireless Passive Sensors Utilizing Cork Materials," *IEEE Sens. J.*, vol. 15, no. 12, pp. 7242–7251, Dec. 2015.
[35] P. Bernardi, F. Gandino, F. Lamberti, B. Montrucchio, M. Rebaudengo, and E. R. Sanchez, "An anti-counterfeit mechanism for the application layer in low-cost RFID devices," in *2008 4th European Conference on Circuits and Systems for Communications*, 2008, pp. 227–231.
[36] G. Anastasi, O. Farruggia, G. L. Re, and M. Ortolani, "Monitoring High-Quality Wine Production using Wireless Sensor Networks," in *2009 42nd Hawaii International Conference on System Sciences*, 2009, pp. 1–7.
[37] U. Schröder, "Challenges in the Traceability of Seafood," *J. Für Verbraucherschutz Leb.*, vol. 3, no. 1, pp. 45–48, Feb. 2008.
[38] Thompson M., Sylvia G., and Morrissey M. T., "Seafood Traceability in the United States: Current Trends, System Design, and Potential Applications," *Compr. Rev. Food Sci. Food Saf.*, vol. 4, no. 1, pp. 1–7, Nov. 2006.
[39] E. Abad *et al.*, "RFID smart tag for traceability and cold chain monitoring of foods: Demonstration in an intercontinental fresh fish logistic chain," *J. Food Eng.*, vol. 93, no. 4, pp. 394–399, Aug. 2009.
[40] Y. Miyamoto, Y. Katoh, K. Uchida, D. Shiode, T. Tokai, and T. Kakihara, "Development of The Tuna Fish Catch Information Management System using RFID and a Communications Satellite," in *OCEANS 2006 - Asia Pacific*, 2006, pp. 1–5.

[41] C. Costa, F. Antonucci, P. Menesatti, F. Pallottino, C. Boglione, and S. Cataudella, "An Advanced Colour Calibration Method for Fish Freshness Assessment: a Comparison Between Standard and Passive Refrigeration Modalities," *FOOD BIOPROCESS Technol.*, vol. 6, no. 8, pp. 2190–2195, Aug. 2013.

[42] A. Bennett *et al.*, "Fish tagging via RFID and bluetooth: Crowdsourced fish tracking through better reporting tools," in *OCEANS 2016 MTS/IEEE Monterey*, 2016, pp. 1–5.

[43] J. H. Yang and Y. Chang, "Feasibility study of RFID-Mounted drone application in management of oyster farms," in *2017 IEEE International Geoscience and Remote Sensing Symposium (IGARSS)*, 2017, pp. 3610–3613.

[44] S. Liawatimena, "Design of an Integrated Fish Auction System in Indonesia Using RFID," in *2015 3rd International Conference on Artificial Intelligence, Modelling and Simulation (AIMS)*, 2015, pp. 179–181.

[45] T. J, D. Lukešová, and M. J, "Meat Traceability from farm to slaughter using global standards and RFID," *Agric. Trop. Subtrop.*, vol. 42, pp. 98–100, Apr. 2009.

[46] Q. Kong, L. Zhao, S. Sun, X. Wang, and M. Zhang, "Safety Control Meat Supply Chain: A Case Study of SUTAI Pigs," in *2009 Fourth International Conference on Innovative Computing, Information and Control (ICICIC)*, 2009, pp. 709–712.

[47] Z. De-an, T. Cui-feng, and W. Xian-wang, "Design of Traceability System for Pork Safety Production Based on RFID," in *2009 Second International Conference on Intelligent Computation Technology and Automation*, 2009, vol. 3, pp. 562–565.

[48] Q. Luo, B. Xiong, Z. Geng, L. Yang, and J. Pan, "A Study on Pig Slaughter Traceability Solution Based on RFID," in *Computer and Computing Technologies in Agriculture IV*, 2010, pp. 710–720.

[49] R. Shougang, Lian, X. Huanliang, and Z. Guanghong, "Research on RFID-based meat product track and traceability system," in *2010 International Conference on Computer Application and System Modeling (ICCASM 2010)*, 2010, vol. 8, pp. V8-458-V8-462.

[50] P.-J. Chen, Y.-C. Du, K.-A. Cheng, and C. Y. Po, "Development of a management system with RFID and QR code for matching and breeding in Taiwan pig farm," in *2016 13th International Conference on Electrical Engineering/Electronics, Computer, Telecommunications and Information Technology (ECTI-CON)*, 2016, pp. 1–5.

[51] S. D. Nguyen, N. N. Le, P. T. Lam, E. Fribourg-Blanc, C. M. Dang, and S. Tedjini, "A wireless sensor for food quality detection by UHF RFID passive tags," in *2015 International Conference on Advanced Technologies for Communications (ATC)*, 2015, pp. 258–263.

[52] D. Nguyen, T. Tien Pham, E. Fribourg-Blanc, N. Le, C. Mau Dang, and S. Tedjini, “RFID beefs up,” Jan. 2013.
[53] R. Perez-Aloe, J. M. Valverde, A. Lara, J. M. Carrillo, I. Roa, and J. Gonzalez, “Application of RFID tags for the overall traceability of products in cheese industries,” in *2007 1st Annual RFID Eurasia*, 2007, pp. 1–5.
[54] A. Regattieri, M. Gamberi, and R. Manzini, “Traceability of food products: General framework and experimental evidence,” *J. Food Eng.*, vol. 81, no. 2, pp. 347–356, Jul. 2007.
[55] E. Varese, S. Buffagni, and F. Percivale, “Application of RFID technology to the agro-industrial sector: analysis of some case studies,” *J. Commod. Sci. Technol. Qual. - 1971-4483*, vol. 47, pp. 171–190, Jan. 2008.
[56] P. Papetti, C. Costa, F. Antonucci, S. Figorilli, S. Solaini, and P. Menesatti, “A RFID web-based infotracing system for the artisanal Italian cheese quality traceability,” *Food Control*, vol. 27, no. 1, pp. 234–241, Sep. 2012.
[57] P. Barge, P. Gay, V. Merlino, and C. Tortia, “Item-level Radio-Frequency IDentification for the traceability of food products: Application on a dairy product,” *J. Food Eng.*, vol. 125, pp. 119–130, Mar. 2014.
[58] “Accueil,” *Skware*. [Online]. Available: https://www.skware.com/. [Accessed: 23-May-2018].
[59] Google France, *Google Cheese Master - Vers l’Affiné et Au Delà - Google France*. .
[60] J. Wisanmongkol and P. Pongpaibool, “A Passive UHF RFID Tag for Poultry Traceability,” May 2018.
[61] A. Vergara *et al.*, “An RFID reader with onboard sensing capability for monitoring fruit quality,” *Sens. Actuators B Chem.*, vol. 127, no. 1, pp. 143–149, Oct. 2007.
[62] K. H. Eom, M. C. Kim, S. Lee, and C. won Lee, “The Vegetable Freshness Monitoring System Using RFID with Oxygen and Carbon Dioxide Sensor,” *Int. J. Distrib. Sens. Netw.*, vol. 8, no. 6, p. 472986, Jun. 2012.
[63] R. Jedermann, R. Schouten, A. Sklorz, W. Lang, and O. Kooten, “Linking keeping quality models and sensor systems to an autonomous transport supervision system,” *Proc. 2nd Int. Workshop Cold Chain Manag.*, Jan. 2006.
[64] R. Gautam, A. Singh, K. Karthik, S. Pandey, F. Scrimgeour, and M. K. Tiwari, “Traceability using RFID and its formulation for a kiwifruit supply chain,” *Comput. Ind. Eng.*, vol. 103, pp. 46–58, Jan. 2017.
[65] R. Jedermann, L. Ruiz-Garcia, and W. Lang, “Spatial Temperature Profiling by Semi-passive RFID Loggers for Perishable Food Transportation,” *Comput Electron Agric*, vol. 65, no. 2, pp. 145–154, Mar. 2009.
[66] D. S. Lee, K. J. Hwang, D. S. An, J. P. Park, and H. J. Lee, “Model on the microbial quality change of seasoned soybean sprouts for on-line shelf life prediction.,” *Int. J. Food Microbiol.*, vol. 118, no. 3, pp. 285–293, Sep. 2007.

Chapter 2

Dielectric properties & Measurement techniques

1. Introduction

Recently, there are many applications where the electromagnetic properties of different materials are studied as key parameters for quality monitoring and sensing. In this context,the electromagnetic properties of food products and biological materials have become valuable parameters in food engineering and technology. As the majority of food products have very little magnetic properties due to small concentration of magnetic materials such as iron, cobalt and nickel, the main focus is usualy on their dielectric properties as they do not have a significant magnetic behavior. Therefore, the dielectric characterization of food products has become of great importance as it allows better understanding and modeling of the material response to the electromagnetic field over a wide range of frequencies under different conditions of temperature, pressure, moisture, etc... The primary interest in the dielectric characterization of food products had focused on predicting and describing the behavior of food materials when they are exposed to potential electromagnetic fields in microwave heating applications. For instance, some electro-heating processes have been applied in the industry, while microwave heating is commercially employed and is also widely used in households.

The exploitation of electromagnetic properties of biological materials plays a significant role in the development of improved sensing devices for the control and automation of several agricultural, environmental, and industrial food processes. It is worth noting that, several studies have demonstrated relationships between materials physicochemical properties and their dielectric properties. Indeed, food dielectric properties can be related to some quality parameters, such as humidity and pH levels. Moreover, dielectric parameters of some types of food can also be related to the maturation level, storage, or processing such as pasteurization or sterilization. Thus, there is an absolute need for better understanding of the dielectric properties of materials and techniques for measuring these properties. Among several characterization methods, the choice of characterization technique depends on several criteria such as the frequency band of interest, measurements accuracy, speed and time of characterization, but also the nature, shape, and ease of handling of the material.

This chapter discusses the dielectric properties, modeled by the complex permittivity, their role, and importance in the agri-food sector as well as the main measurement methodologies used for the characterization of food products and their development.

2. Dielectric properties

Analysis of the dielectric properties of foods over a vast range of frequencies is essential in research, modeling and development of thermal treatments based on radio frequency and microwave energy. For RF circuit design, the dielectric properties of the circuit substrate and the medium play a major role in optimizing the system performance. In the frame of RFID traceability, the knowledge of dielectric properties of the tag substrate is an essential step for tag antenna design to achieve the optimum performance. Moreover, these properties can provide interesting information about the interaction between the foodstuff and electric fields which can be very useful in the development of many food sensing applications.

2.1 Definition

From the electromagnetic point of view, any material can be modeled by its permittivity, which is a complex quantity mostly used to describe the ability of a material to polarize in response to an applied electromagnetic field as well as estimating the attenuation and transit time of the wave energy propagating within the material. The relative complex permittivity, ε_r , describes permittivity normalized to free space permittivity ε_0 and it is represented as:

$$\varepsilon_r = \varepsilon'_r - j\varepsilon''_r \tag{2.1}$$

where ε'_r and ε''_r are the dielectric constant and loss factor, respectively and $j = \sqrt{-1}$

The real part, the dielectric constant (ε'_r), describes the ability of a material to store energy when it is subjected to an electric field. It influences the electric field distribution and the velocity of waves travelling through the material. Physically it means, the greater the polarization developed by a material in an applied electric field of given strength, the greater the dielectric constant will be.

The imaginary part, the loss factor (ε''_r), influences both signal attenuation and field power absorption. One more important parameter used in EM theory is the tangent of loss angle: $\tan(\partial) = \frac{\varepsilon''_r}{\varepsilon'_r}$. This parameter describes the ability of the dielectric material to dissipate energy in response to an applied electric field which transfoms into heat [1], [2]. The amount of thermal energy converted in the food is proportional to the value of the loss factor [3].Therefore, a material with a high loss factor is easily heated by microwave. On the other hand, a material with a very low ε''_r, is quasi-transparent to microwave signal. Power dissipation (Q_g) is given by the common form of the average power loss density (power dissipation per unit volume, W/m3) drawn from the Poynting's theorem [4]:

$$Q_g = \frac{1}{2}\omega\varepsilon_0\varepsilon''|E|^2 \tag{2.2}$$

Where ε_0 is the permittivity of free space (≈ 8.854 x 10^{-12} F/m) and *E* is the electric field strength [V/m].

In the presence of an external electric field, the material molecules and charges try to align with the applied field. A dielectric loss results mainly from the inability of molecules polarization to follow the rate of change of the oscillating electric field

applied to the material. This inability arises from the relaxation time (τ) in a material which is the time the dipoles need to return to their original random orientation. It does not occur instantaneously, but the polarization diminished exponentially. If the relaxation time is shorter or close to the rate of the oscillating electric field, then there would be no or minimum loss. However, when the oscillation rate increases, the polarization becomes unable to follow the oscillating frequency and thus resulting in the energy absorption which is dissipated as heat.

The increase in temperature of a material due to dielectric heating can be calculated as [5]:

$$\rho C_p \frac{dT}{dt} = 55.63\ x\ 10^{-12}\ f E^2 \varepsilon'' \tag{2.3}$$

where C_p is the specific heat of the material in J kg^{-1} °C^{-1}, ρ is the density of the material in kg/m3, E is the rms electric field intensity in V m^{-1}, f is the frequency in Hz, $\frac{dT}{dt}$ is the time rate of temperature increase in °C s^{-1}. It is clear from equation (2.3) that the rise in temperature is proportional to the loss factor of the material, in addition to electric field intensity, frequency and treatment time[6], [7].

2.2. Polarization mechanisms

Physically, polarisability is induced when there is electric field applied onto the materials. In the absence of electric field, the molecules and charges are randomly oriented inside the dielectric material. When the electric field is applied the molecules, antoms and electon cloud are aligned according to the applied field which causes separation of positive and negative charges and the molecules behave like an electric dipole. Different kinds of polarization mechanisms occur within a dielectric material:

2.2.1 The orientation polarization (dipole polarization)

This type of polarization mechanism is due to the reorientation of the permanent dipoles under the influence of the electric field. Inside a dielectric material, there are some molecules which possess a permanent dipole where there is always a separation of charges within the molecule. The dipoles in a dielectric material are randomly oriented as a result of thermal motion. Therefore, in the

absence of an external field, the dipole moments from different molecules cancel out, and the net polarization is zero. As the material is exposed to an electric field, the dipoles rotate to align with the applied field and to align also with each other.

Dipole polarizability is frequency dependent and can be shown as in Equation (2.4)

$$\alpha_d = \frac{\alpha_0}{1 + j\omega t} \tag{2.4}$$

where α_d is the dipole polarisability and α_0 is the low frequency (static) polarisability.

Thus, dipole moments no longer cancel out, and the material develops a net polarization as shown in figure 1.

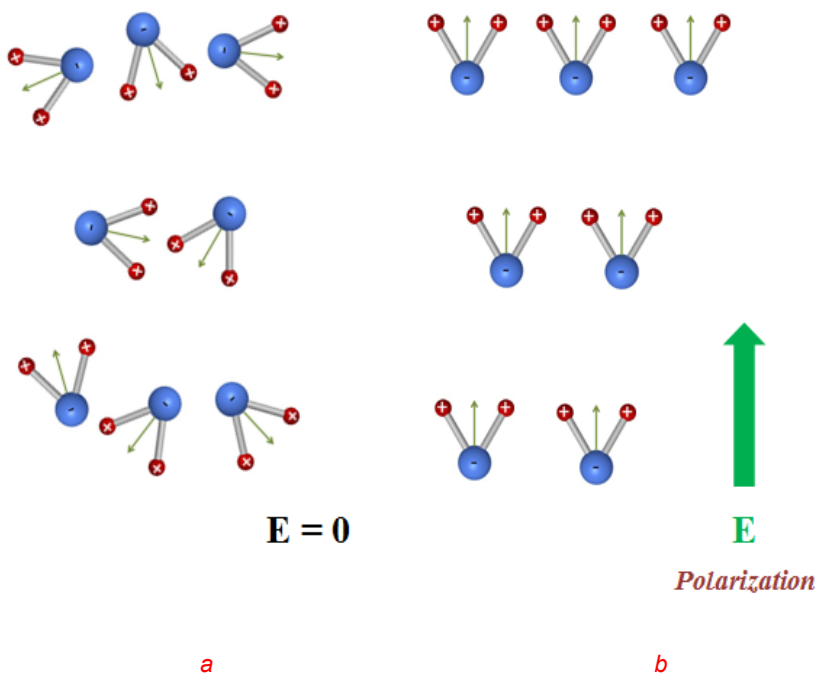

a b

Fig. 1. Dipole polarization mechanism a) randomly oriented dipoles in the absence of electric filed b) dipoles aligned with the applied filed resulting in a net polarization.

2.2.2. The atomic polarization

This type of polarization occurs in dielectric materials having an ionic structure composed of cations and anions. A cation and anion of equal and opposite charges are held together by an ionic bond. This ion pair has a dipole moment before the application of an electric field. However, the sum of these moments is usually zero over the entire structure. These ionic bonds stretch due to the applied field and thus the net polarization increases as the magnitude of individual dipole moments increases as illustrated in figure 2.

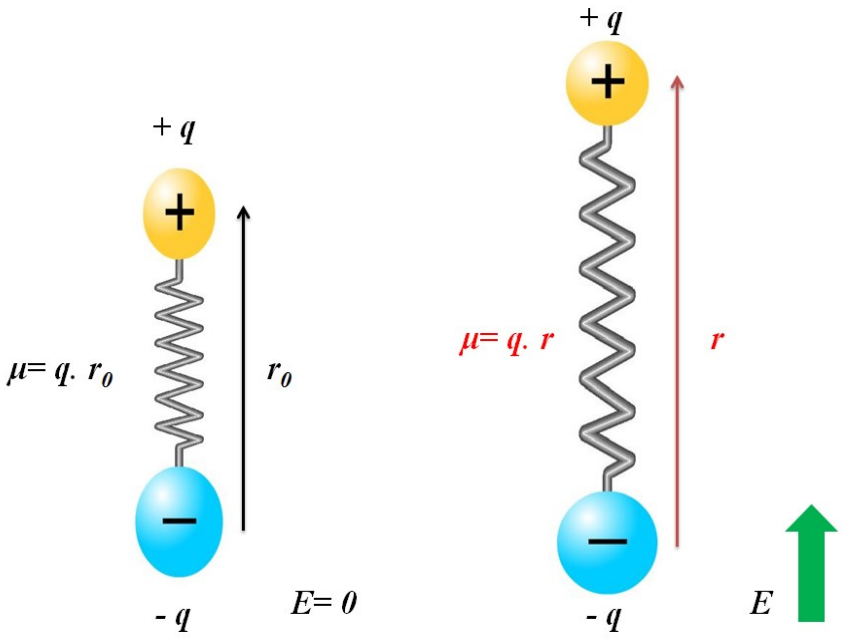

Fig. 2. Atomic polarization mechanism where the ionic bonds stretch due to the applied field.

2.2.3. The electronic polarization

This kind of polarization is caused by modification of electrons position around the nucleus.The applied field causes the electron cloud around the nucleus to distort in one direction while the nucleus moves in the opposite direction. A dipole

moment is developed as the center of electron cloud is no longer coinciding with the nucleus as shown in figure 3.

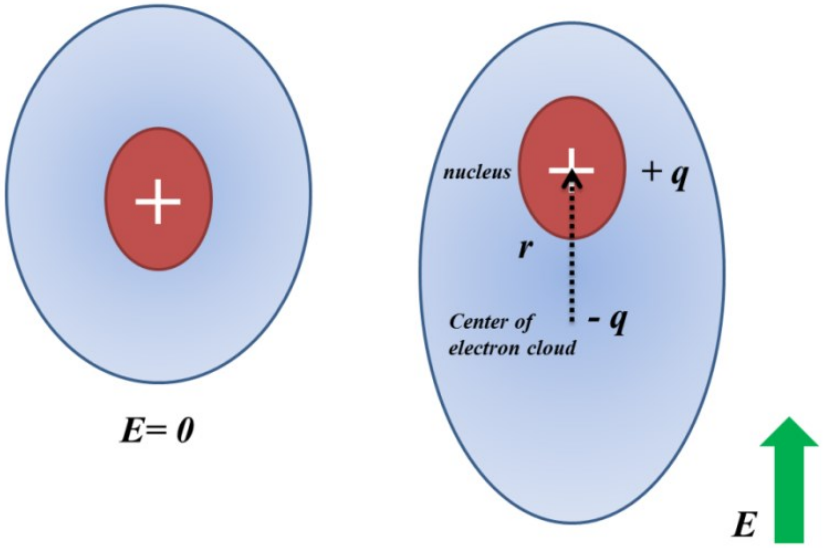

Fig. 3. Electronic polarization mechanism caused by modification of electrons position around the nucleus due to the applied field.

Depending on the frequency of the applied field, one or two mechanisms dominate over the others. Electronic polarization can occur in all dielectric materials whereas the atomic and orientation mechanisms are only available to materials possessing ions and permanent dipoles respectively. In general, the dipoles rotation is the dominant polarization mechanism in irradiating materials rich in water (such as biological tissues, foods, mixtures based on water or polar solvents) in the microwave electromagnetic spectrum region (industrial high-frequency heating $\left(10^7 < f_{(Hz)} < 10^9\right)$. The atomic and the electronic polarization mechanisms are relatively weak, and usually constant over the microwave region (Figure. 4).

There is another mechanism called the " Interface polarization " and is observed in materials containing free electrons build-up at the interface between

components in heterogeneous systems (Maxwell-Wagner effect) [4]. However, its contribution, in general, is small compared to the other polarization mechanisms.

As it is difficult to separate conduction losses from dielectric losses due to polarization, the following equation expresses the overall dissipative feature (loss factor) of a material:

$$\varepsilon''_{total}(\omega) = \underbrace{\varepsilon''_{ep}(\omega) + \varepsilon''_{ap}(\omega) + \varepsilon''_{dp}(\omega) + \varepsilon''_{interfp}(\omega)}_{\text{Losses due to plarization mechanisms}} + \underbrace{\frac{\sigma}{\varepsilon_0 \omega}}_{\text{conductivity loss}}$$

$$= \varepsilon''_{p}(\omega) + \varepsilon''_{\sigma}(\omega)$$

where ε''_{ep}, ε''_{ap} , ε''_{dp} and $\varepsilon''_{interfp}$ correspond to electronic, atomic dipolar and interfacial polarization mechanisms, respectively; and σ is the medium conductivity.

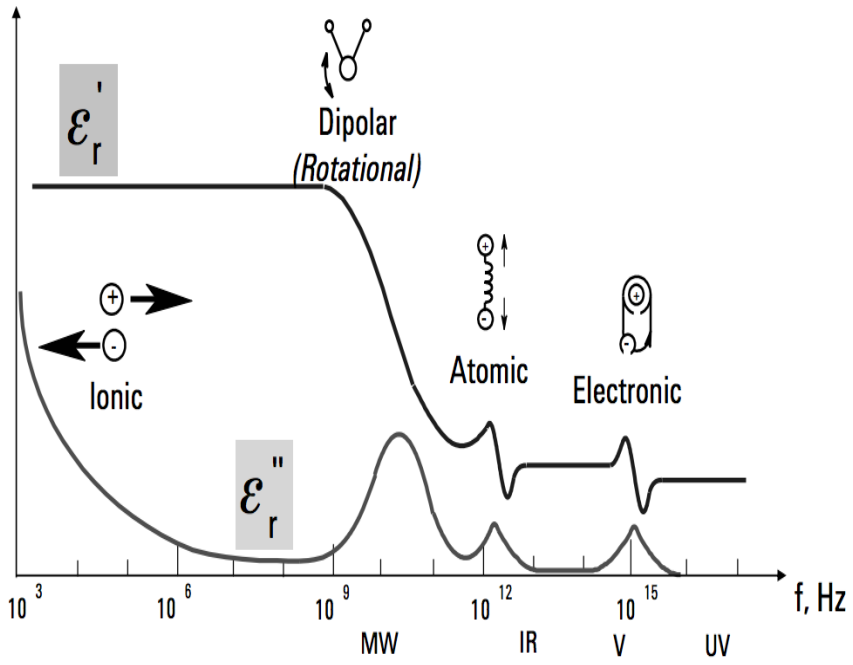

Fig. 4.Typical frequency-regions of the loss mechanisms

2.3. Other properties related to dielectric parameters

2.3.1. Penetration depth

Food materials are, in general, poor electrical conductors as they can store and dissipate electric energy when exposed to an electromagnetic field [8]. The following equation describes the decay of electric field strength as a function of material thickness (z):

$$E = E_0 e^{-\alpha z} \tag{2.5}$$

where the attenuation factor α depends on the dielectric properties of the material [9] and operating frequency f (or free space wavelength $\lambda_0 = c/f$) and is given by :

$$\alpha = \frac{2\pi}{\lambda_0}\left[\frac{1}{2}\varepsilon'_r\left(\sqrt{1+\left(\frac{\varepsilon''_r}{\varepsilon'_r}\right)^2}-1\right)\right]^{\frac{1}{2}} \tag{2.6}$$

The penetration depth (d_p) is usually defined as the depth into a sample where the microwave and RF power has dropped to $1/e$ or 36.8% of its transmitted value as shown in figure 5. The penetration depth in a lossy material can be calculated as a function of ε'_r and ε''_r:

$$d_p = \frac{c}{2\pi f\sqrt{2\varepsilon'_r\left[\sqrt{1+(\varepsilon''_r/\varepsilon'_r)}-1\right]}} \tag{2.7}$$

where c is the speed of light in free space (3 x 10^8 m/s) and f is the frequency (Hz).

Under some conditions ($(\varepsilon''_r/\varepsilon'_r)$ << 1, i.e. small tan δ) the penetration depth can be calculated by:

$$d_p = \frac{\lambda_0\sqrt{\varepsilon'_r}}{2\pi\,\varepsilon''_r} \tag{2.8}$$

Common food products have ε''_r< 25, which implies a d_p of 0.6 to 1 cm at 2.45 GHz [10]. According to [11] and [12], the penetration of microwaves at 915 and

2450 MHz in foods with high moisture content at room temperature is typically between 0.3 and 7 cm, depending on the salt content and frequency.

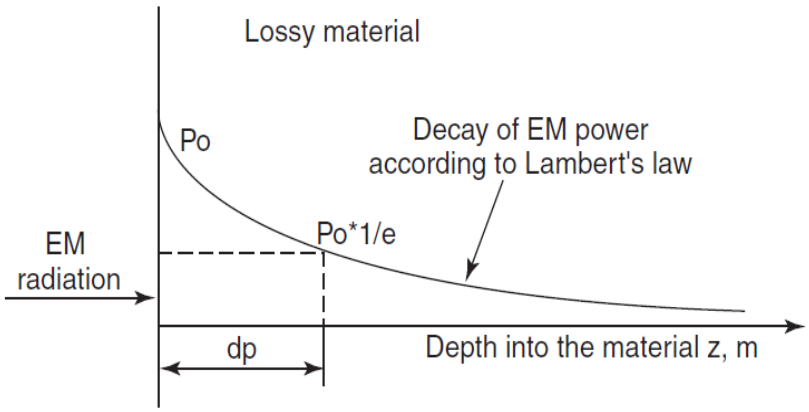

Fig. 5. Penetration depth inside a lossy dielectric material. [6]

Knowing or measuring the dielectric properties, the penetration depths of electromagnetic energy in selected materials can be then easily calculated. For given fixed dielectric properties, the penetration depth of a material is inversely proportional to frequency *f*, as equation (2.7) states. So, deeper penetration corresponds to lower frequencies, and higher frequencies result in a more significant surface heating. Thus, the penetration depth of RF energy in foods can be as large as one order of magnitude compared with MW; for example, at 27.12 MHz a six times greater penetration depth in mangoes was calculated compared to microwave energy at 1800 MHz at 20 ºC [13].

2.3.2. Temperature Effect

Temperature has a significant effect on the dielectric properties. The way these properties vary due to temperature is highly depended on the material's characteristics. For example, as temperature rises, relaxation time for water decreases. Therefore, the dispersion peak moves to higher frequencies and the peak of loss factor of pure water decreases with increasing temperature.

The dielectric constant ε'_r of free water also decreases with increasing temperature as the result of increased Brownian movement as shown in figure 6.

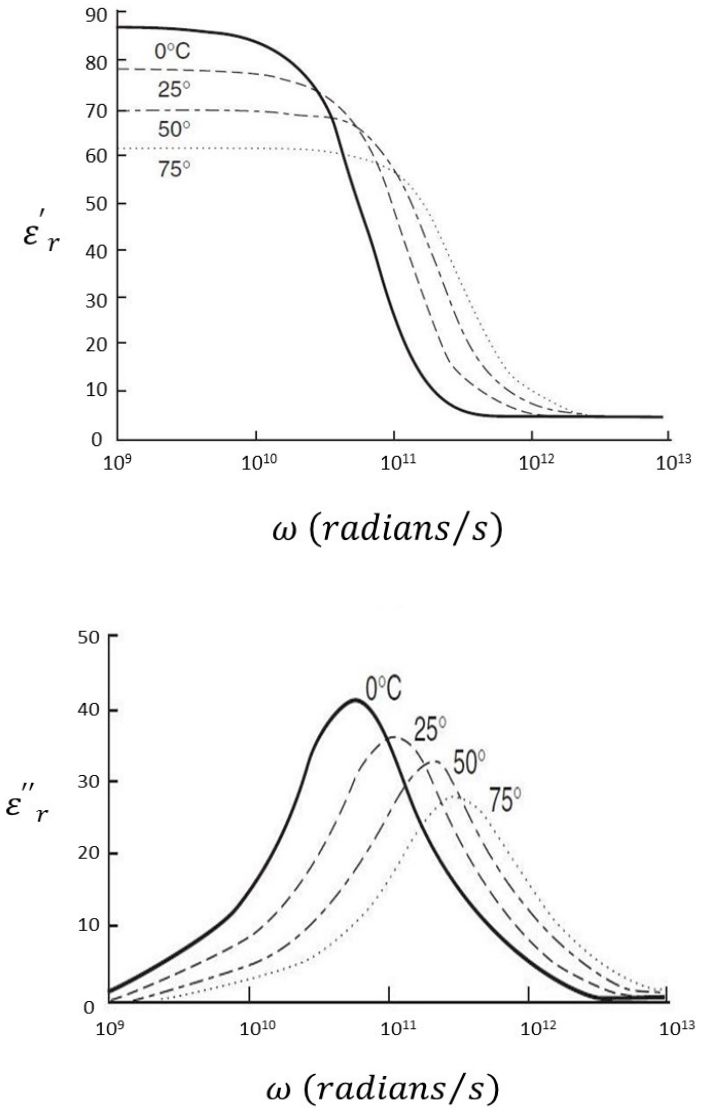

Fig. 6. Temperature effect on dielectric properties of free water ($\omega = 2\pi f$, where f is the frequency in Hz)[14].

In multi-dispersion materials, for example, the transition is gradual because of the combined effects of relaxation and the ionic conduction. This combination results in a U-shape frequency response of ε''_r as shown in figure 7. At a specified frequency, the electric conductivity in ionic solutions increases with temperature due to decreased viscosity and hence increased ion mobility [9]. Therefore, at 915 MHz the dielectric constant of ionic solutions generally increases with temperature.

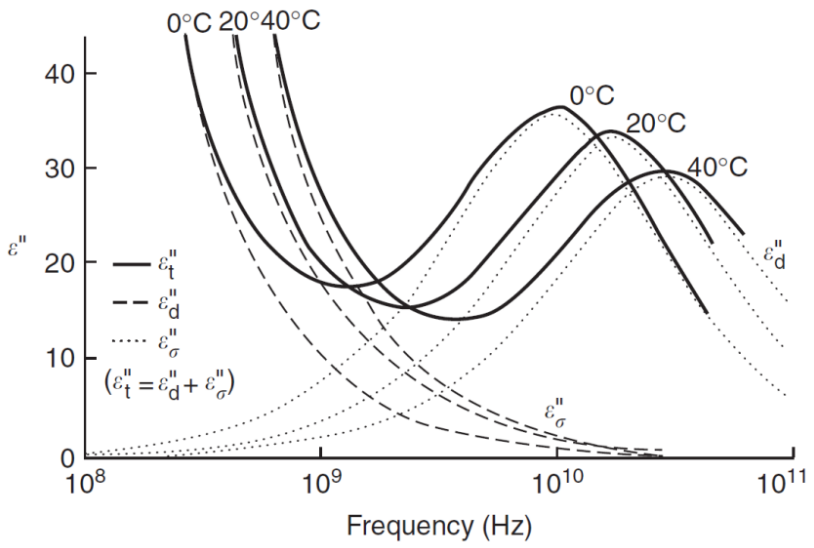

Fig. 7. Effect of temperature on dielectric loss factor ε''_r of 0.5N aqueous sodium chloride at three temperatures[15].

Figure 8 shows the loss factor of a typical dry nut (walnut kernels) over the frequency range from 1 to 1800MHz at five temperatures. The ε''_r values are less than 1 at frequencies below 50 MHz. The ε''_r values peak in the range between 500 and 1000 MHz. The peak value of ε''_r for walnut kernels decreases with increasing temperature, while the frequency corresponding to the peak ε''_r shifts to a higher value.

This temperature-dependent trend is typical of polar molecules [16]. At any selected frequency in the tested range, the loss factor of the walnut kernel generally decreases with increasing temperature; that is, for a given EM field intensity, higher temperature walnuts will absorb less energy than cooler ones, resulting in improved heating uniformity.

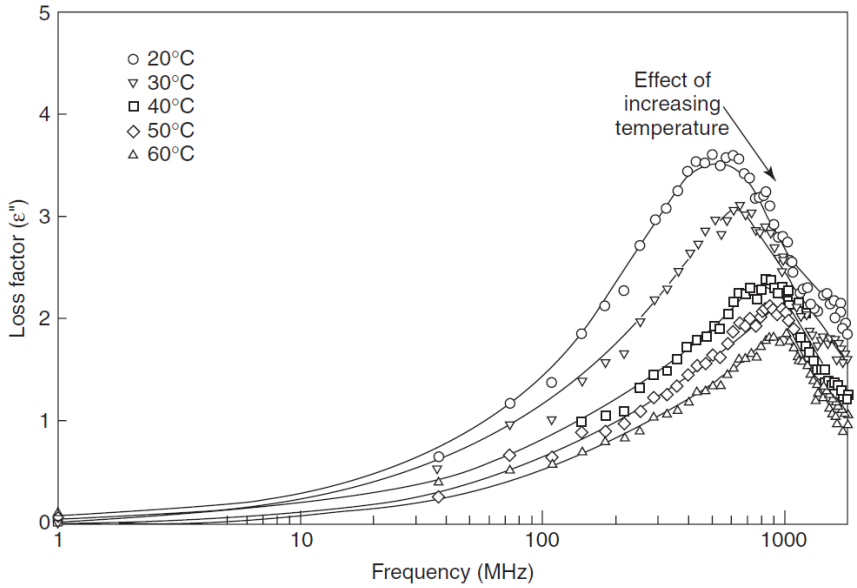

Fig. 8. Dielectric loss factor of walnut kernels as a function of frequency at five temperatures [17].

2.3.3. Moisture Effect

Moisture content is one of the major components of most biological materials. As the moisture content increases, the dielectric constant and loss factor of the materials become more significant [14] [16] [18]. Generally, at low moisture content water primarily exists in bounded form, thus possessing a limited mobility in the presence of electromagnetic waves. As moisture content in material increases, a critical level (or critical moisture content, Mc) is attained as shown in figure 9. When water exceeds this critical level, all the available binding sites for water molecules become saturated and an increase in the population of free water molecules occurs which consequently result in an increase of dielectric losses. The free-water molecules have dielectric properties similar to those of liquid water, while the bound water exhibits lower dielectric properties. Dielectric properties of biomaterials, in general, decrease rapidly with decreasing moisture content to the critical moisture level. During microwave drying, the wetter parts of biomaterials absorb more microwave energy and tend to level off the uneven moisture distribution.

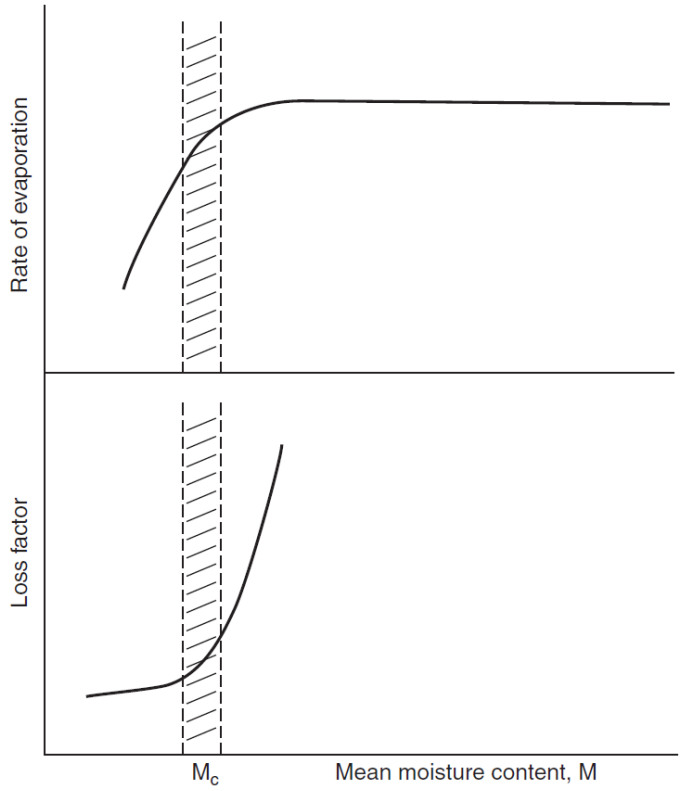

Fig. 9. The rate of evaporation and dielectric loss factor as affected by food moisture content.

2.4. Dielectric properties of foods

As discussed in the previous sections, dielectric characterization is considered as a key for understanding the response of a material when subjected to EM fields for the purposes of heating, drying or processing. Other applications based on dielectric properties of food are explored such as disinfestation treatment for several commodities using dielectric heating. Therefore, to develop a treatment protocol based on RF or MW heating, the first step is to gain knowledge of the dielectric properties of the fruit. Previous works presented and classified the values of dielectric properties of different food products as function of frequency, temperature and food nature. Table.1 shows dielectric constants and loss factors of fresh fruits and vegetables at common frequencies.

Table. 1. Dielectric properties of fruits and vegetables.

Fruit or vegetable	Temp (°C)	Moisture Content %	Dielectric constant Frequency		Dielectric Loss factor Frequency		Ref
			27,12 MHz	915 MHz	27,12 MHz	915 MHz	
Apple (Golden)	20	-	72.5	74.3	120.4	8.5	[15]
	50	-	68.1	67.8	202.2	8.3	
Apple (Red)	20	-	74.6	77.0	92.0	10.0	[15]
	50	-	68.7	68.9	153.8	9.8	
Avocado	20	-	115.7	59.9	699.6	27.4	[19]
	50	-	137.9	57.9	1136.2	39.8	
Banana	23	78	-	64.0	-	19.0	[20]
Cantaloupe	23	92	-	68.0	-	14.0	[20]
Carrot	23	87	-	59.0	-	18.0	[20]
Cherimoya	20	-	71.5	59.0	238.5	25.4	[19]
	50	-	72.0	57.5	406.4	29.1	
Cherry	20	-	91.2	73.7	293.0	16.4	[15]
	50	-	89.6	66.7	501.0	19.3	
Cucumber	23	97	-	71	-	11	[20]
Grape	23	82	-	69	-	15	[20]
Grapefruit	20	-	89	72.7	202.4	12.1	[15]
	50	-	93.8	66.1	345.3	14.2	
Kiwifruit	-	87	-	70	-	18	[20]
Lemon	-	91	-	73	-	15	[20]
Lime	-	90	-	72	-	18	[20]
Longan	20	-	75.2	68.2	230.1	13.3	[19]

	50	-	69.7	60.8	377.7	15	[20]
Mango	20	86	83.1	74	250.1	13.8	[21]
	50	79.8	67.3	404.6	16.0		
Onion	-	92	-	61	-	12	[20]
Orange	20	-	84	72.9	223.3	16.5	[15]
	50	-	78	66.1	367.7	17.5	
Papaya	-	88	-	69	-	10	
Passion fruit	20	-	82.7	59.7	264.1	15	[19]
	50	-	91.6	55.5	441.2	17.6	
Peach	-	90	-	70	-	12	[20]
Pear	-	84	-	67	-	11	[20]
Persimmon	20	-	79.8	68.4	207.5	21.1	[19]
	50	-	76.6	68.5	346.4	16.1	
Potato	-	79	-	62	-	22	[20]
Radish	-	96	-	68	-	20	[20]
Squash fruit	-	95	-	63	-	15	[20]
Strawberry	-	92	-	73	-	14	[20]
Sweet potato	-	80	-	55	-	16	[20]
Turnip	-	92	-	63	-	13	[20]
White sapote	20	-	76	62.6	258.6	24	[19]
	50	-	74.5	60.3	433.1	24.9	

In the same context, a vast amount of information has been published on the dielectric properties of meat and fish products using different methods, frequencies and temperatures as shown in table.2 which presents the dielectric properties of meats (chicken, lamb, beef, pork and turkey) and fish products such as Salmon and Caviar.

Table. 2. Dielectric properties of meats, salmon and caviars.

Species (anatomical location)	Type	Temp (°C)	Dielectric constant Frequency		Dielectric Loss factor Frequency		Ref
			27.12 MHz	2450 MHz	27.12 MHz	2450 MHz	
Beef	**Lean**		70.5	43.7	418.7	13.7	[22]
Lamb (leg)	**Lean**		77.9	49.4	387.2	15.0	[22]
Pork (shoulder)	**Lean**		69.6	51.3	392.0	15.1	[22]
Pork (back)	**Fat**		12.5	7.9	13.1	0.76	[22]
Chicken (breast)	**Lean**		75.0	49.0	480.8	16.1	[22]
Turkey (breast)	**Lean**		73.5	56.3	458.4	18.0	[22]
			40 MHz	915 MHz	40 MHz	915 MHz	
Pink salmon	**Anterior**	20	87.6	55.1	296.3	22.6	[23]
		60	100.8	51.4	525.5	33.0	[23]
		120	116.8	47.1	890.8	47.1	[23]
	Middle	20	85.3	57.0	313.9	22.8	[23]
		60	99.1	53.7	581.4	34.8	[23]
		120	119.7	50.7	1085.2	60.4	[23]
			27.12 MHz	915 MHz	27.12 MHz	915 MHz	
Sturgeon caviar	**Salted**	20	129.8	29.8	1349.4	40.5	[24]
		50	121.5	22.7	1501.1	43.3	[24]
		80	182.0	25.0	2614.5	73.6	[24]
	Unsalted	20	70.7	30.7	470.8	18.7	[24]
		50	46.4	18.3	375.9	14.1	[24]
		80	59.6	18.9	642.7	22.2	[24]

Recently, there is more interest about analyzing and studying the dielectric properties of different food products not just for heating but also for sensing applications and quality monitoring during food production chains. Therefore, there is a great need for accurate and effective dielectric measurement techniques which suit different types of food as well as being able to realize dielectric characterization over large bands of frequencies and at different levels of temperature. The next section will discuss in detail the main dielectric measurement methods used for characterization of food products.

3. Dielectric characterization methods

In order to ensure food security and monitoring products, the dielectric permittivity of materials should be characterized accurately. It is essential to know the electromagnetic characteristics of each product in order to have a good RFID response and meet the industrial requirements as well as to integrate, under good conditions, the products in their appropriate systems.

Although several electromagnetic characterization techniques exist, not all of them are suitable to characterize food products. Hereinafter we discuss the main dielectric measurement techniques used for dielectric characterization of different food products.

3.1. Open ended coaxial line method

Open-ended coaxial probe (OCP) method is currently one of the most popular techniques for measuring of complex dielectric permittivity of many materials. Non-destructive, broadband (RF and microwave ranges), and high-temperature measurements can be performed with this method using commercially available instrumentation. Its well-developed theory makes it possible to obtain sufficiently accurate results for both medium-loss and high-loss media [19]–[21].

The open-ended coaxial probe is a cut off section of transmission line that has been sealed so moisture cannot seep into it. The material is measured by immersing the tip of the probe into a liquid sample under test, or can be pressed against a solid or a semi-solid sample. The fields at the probe end “fringe” into the material and change as they come into contact with the material under test (MUT) as illustrated in figure 10. The dielectric properties of the MUT can be then

extracted as function of the measured reflection coefficient S_{11} with the network analyzer.

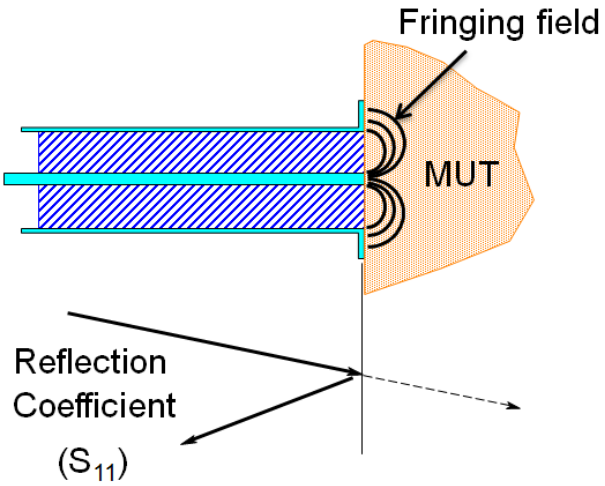

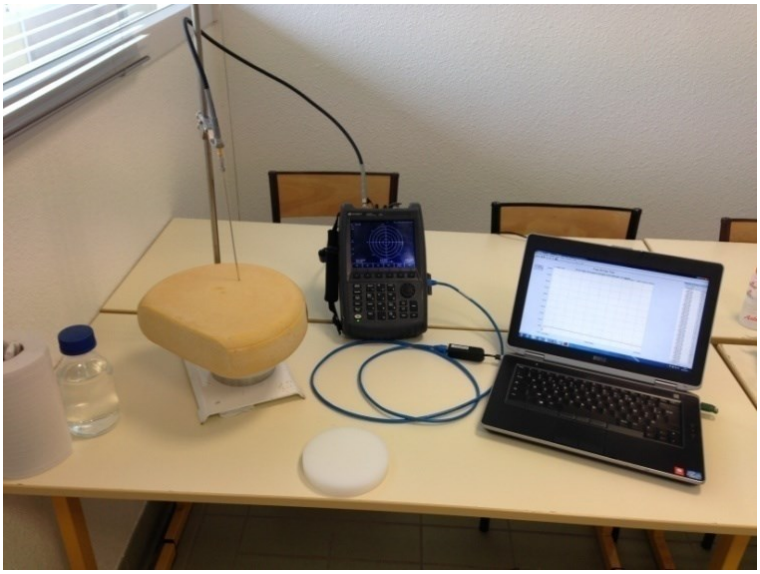

Fig. 10.Coaxial probe method and measurement setup for cheese dielectric characterization using portable VNA (Field fox) and a software for extracting dielectric properties from S parameters

The sensing element of an OCP system is an open-ended cylindrical coaxial line that is excited by transverse electromagnetic (TEM) wave. Parameters (amplitude and phase) of incident and reflected signals are detected by the Network analyzer. The complex dielectric permittivity is determined according to the reflected coefficient ($\Gamma = \Gamma' - j\Gamma''$) [26] as follows:

$$\varepsilon'_r = (A_e\, f)^{-1} \left\{ \frac{-2\Gamma''}{(1+\Gamma')^2 + \Gamma''^2} \right\} \tag{2.9}$$

$$\varepsilon''_r = (A_e\, f)^{-1} \left\{ \frac{1-\Gamma'^2 - \Gamma''^2}{(1+\Gamma')^2 + \Gamma''^2} \right\} \tag{2.10}$$

where A_e is the empirical coefficient dependent on characteristic impedance of the probe and sample size. In order to eliminate the influence of reflections caused by transmission-line discontinuities, a calibration procedure is utilized. The EM characteristics of the measurement system are analyzed using three standard terminations (open, short, and a well-known dielectric properties such as de-ionized water, for example). The actual reflection coefficient is given as a function of calibration parameters and the reflection coefficient measured using Network analyzer Γ_m

$$\Gamma = \frac{\Gamma_m - \mathrm{a}_{11}}{\mathrm{a}_{22}(\Gamma_m - \mathrm{a}_{11}) + \mathrm{a}_{12}} \tag{2.11}$$

where a_{11} is the directivity error, $\mathrm{a}_{12}$is the frequency response error, and a_{22} is the source match error. Taking into account propagation constant (□) and distance from the connector to the probe head (z) we can calculate a_{ij} in terms of S parameters obtained for the three calibration terminations [28].

The OCP method is very well suited for liquids or soft solid samples. It is accurate, fast, and broadband (from 0.2 to up to 20 GHz). The measurement requires little sample preparation. A major disadvantage of this method is that it is not suitable for measuring food materials with low dielectric property like oils (dielectric constant ≈ 2.5 at 1 GHz) [29], [30].

3.2. Resonant cavity method

The method of measuring the permittivity with the resonant cavity is based on a theory called "Perturbation Method" [31]. This method is based on a comparative analysis of certain EM characteristics between empty and a partially loaded rectangular or cylindrical resonance cavity [32] as shown in figure 11.

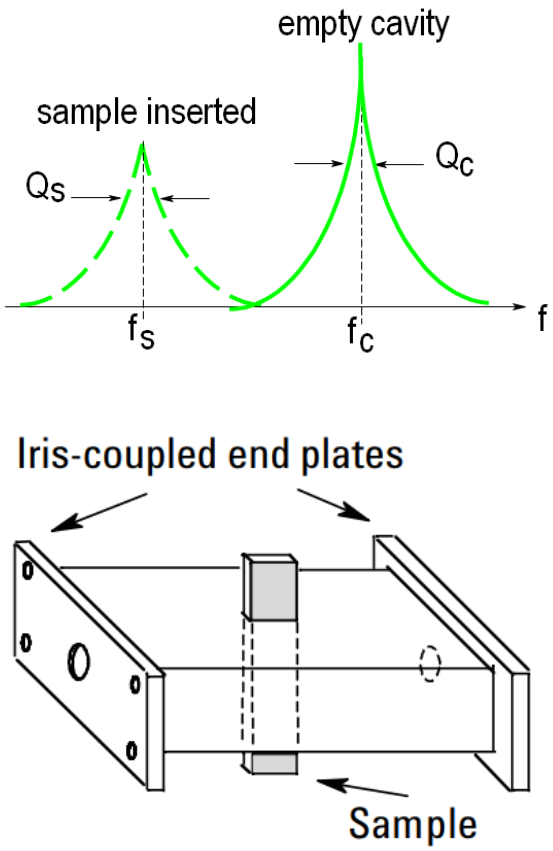

Fig. 11.Resonant cavity measurement technique

Indeed, the presence of the material causes the modification of the resonant frequency and the quality factor of the cavity. The dielectric constant (the real part) is calculated from the resonance frequency offset whereas the dielectric losses are estimated from the variation of the quality factor by:

$$\varepsilon'_r = 1 + \frac{V_c(f_c - f_s)}{AV_s f_s} \tag{2.12}$$

$$\varepsilon''_r = \frac{V_c}{BV_s}\left(\frac{1}{Q_s} - \frac{1}{Q_c}\right) \tag{2.13}$$

where : V_c is the volume of empty cavity, V_s is the volume of the loaded sample, f_c is the resonant frequency of empty cavity, f_s is the resonant frequency of filled cavity, Q_c is the quality factor of Empty Cavity,and Q_s is the quality factor of Filled Cavity

A & B are the coefficients that depend on several parameters: shape, sizes, location of the sample in the cavity, and excited operating mode of the cavity. In some cases, A and B may be found analytically [32] or they may be determined empirically with calibration of the experimental setup. Appropriate location of the sample is also a very important factor that affects the accuracy of the measurement. Sometimes, measurement errors are possible when there are air gaps between the specimen and the conducting parts of the metallic resonator.

The perturbation method is more accurate than the waveguide methods and it is particularly suited for medium-loss and low-loss materials. Precisely shaped small-sized samples are usually used with this technique. Biodegradable substrates such as Poly-lactic acid (PLA) and casein thin films are characterized using the resonant cavity in the GHz frequency band. However, this method has some drawbacks as it provides dielectric properties measurements only at fixed frequency points and it is considered to be more expensive than the open-end coaxial probe system.

3.3. Transmission line method

The transmission-line method (TLM) belongs to a large group of non-resonant methods of measuring complex dielectric permittivity of different materials in a microwave range [33], [34]. There are two main types of transmission lines used for dielectric measurements:

- Rectangular waveguide

- Coaxial line

where the choice of measurement technique depends on rapidity of the method, simplicity and precision of the parameters to be characterized. Rectangular waveguide and coaxial line methods involve placing the material inside a portion of an enclosed transmission line as shown in figure 12 where the complex permittivity is computed from the measurement of the reflected signal (S_{11}) and transmitted signal (S_{21}).

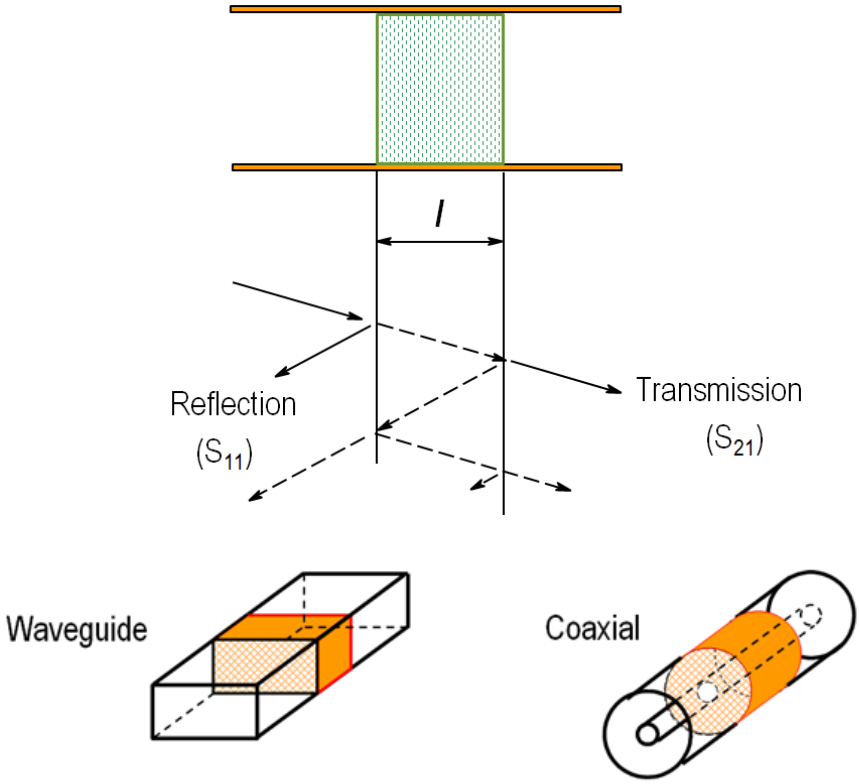

Fig. 12.Dielectric characterization based on enclosed transmission lines

The material sample is assumed to completely fill the cross section of the fixture with no air gaps, have smooth flat faces and to be uniform throughout. The material thickness should also be known as measurements are based on both reflection and transmission through the material. The sample must be sufficiently long to contain enough of the wavelength to be measurable. However, with today

sensitive network analyzers, reasonable measurements can be obtained with shorter samples. This method is more suitable for liquid and powder food materials. Elsewise, the material should be transformed to liquid state as in [35] where melt cheedar cheese was poured inside the waveguide and special calibration was applied to de-embed the effect of Teflon window at the waveguide boundaries as shown in figure 13.

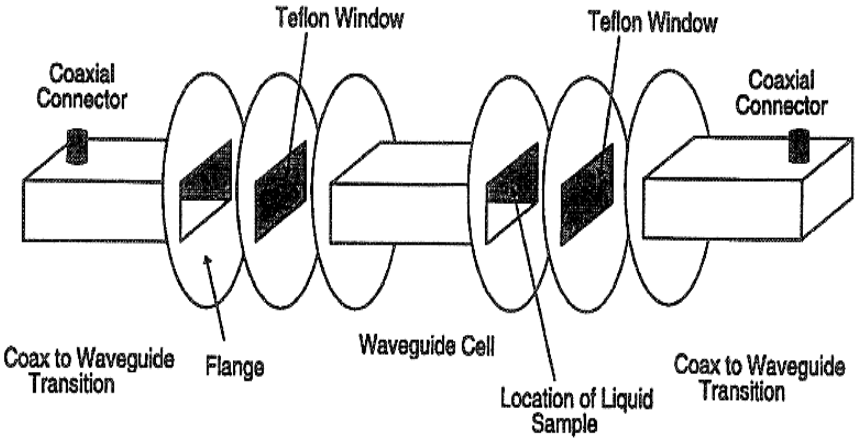

Fig.13. Experimental configuration for cheese dielectric characterization using waveguide cell [35]

In this experiment, the waveguide was assumed to be single mode (propagating only the TE10 mode), completely filled with the material under test, which has a complex relative permittivity $\varepsilon_r = \varepsilon'_r - j\varepsilon''_r$ where ε'_r is the dielectric constant and ε''_r is the loss factor. The material was assumed to be non-magnetic (having complex relative permeability μ_r= 1) and the effect of ohmic losses in the waveguide walls were neglected. The cutoff wavelength in the waveguide is λ_c= 2a, the propagation constant in the waveguide is given by the following expression [36]:

$$\gamma = j\sqrt{\frac{\varepsilon_r \omega^2}{c^2} - \left(\frac{2\pi}{\lambda_c}\right)^2} \tag{2.14}$$

where $\omega = 2\pi f$ is the angular frequency in rad/s.

The wave impedance of the waveguide is defined as:

$$Z = \frac{j\omega\mu_0}{\gamma} \tag{2.15}$$

where μ_0 is the magnetic permeability in free space ($= 4\pi\ x\ 10^{-7}\ H/M$).

The voltage reflection coefficient ρ is :

$$\rho = \frac{Z(\varepsilon_r) - Z(1)}{Z(\varepsilon_r) + Z(1)} \tag{2.16}$$

where $Z(\varepsilon_r)$ is the waveguide impedance filled with the dielectric material and $Z(1)$ is the impedance of the waveguide filled with air.

The transmission coefficient T is given by:

$$T = e^{-\gamma d} \tag{2.17}$$

From [36] the S parameters can be driven as function of the voltage reflection coefficient ρ and the transmission coefficient:

$$S_{11} = \frac{(1 - T^2)\rho}{1 - T^2\rho^2} \tag{2.18}$$

$$S_{21} = \frac{(1 - \rho^2)T}{1 - T^2\rho^2} \tag{2.19}$$

Thus, the dielectric properties of the material can be then extracted from the measured S parameters [37], [38].

Basic principles of coaxial transmission line technique are given in [6], [39]. In general, a TLM measurement system is more expensive for the same range of

frequency than the open ended coaxial probe system, and the measurements are more difficult and time-consuming. Moreover, this method can be hardly applicable on some types of food materials which cannot be easily transformed to suit the waveguide shape.

3.4. Parallel plate capacitor system

Among the methods for measuring the permittivity of materials is the use of the parallel plate capacitance method. This dielectric measurement technique covers a frequency band from [10KHz to 100MHz]. The sample is placed as the dielectric inside a parallel plate capacitor. Permittivity is calculated from knowing the area of the plate and the thickness of sample, and measuring the capacitance using an LCR or Impedance analyzer as shown in figure 14.

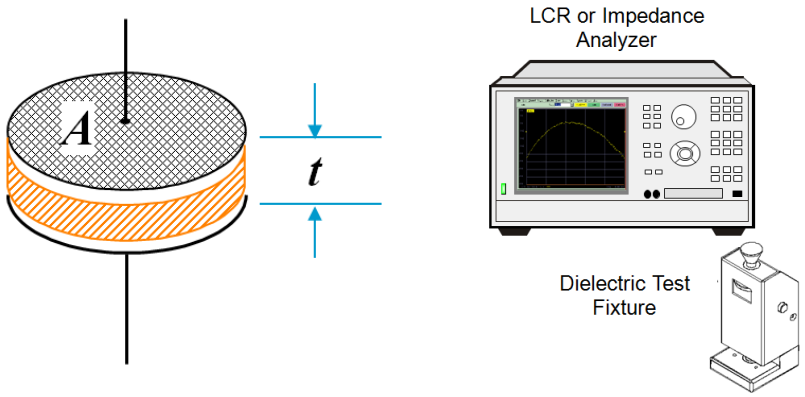

Fig. 14. Typical analyzer and parallel plate capacitor fixture set up

The complex permittivity of the material inserted between the capacitor plates is calculated as:

$$\varepsilon'_r = \frac{C}{\varepsilon_0 \frac{A}{t}} \tag{2.20}$$

$$\varepsilon''_r = D.\varepsilon'_r \tag{2.21}$$

where C is the capacitance, ε_0 is the vacuum permittivity (8.85 e^{-12} F/m), A is the plate area, t is the material thickness and D is the dissipation factor.

In most analyzers the calculation is automated, making this a convenient technique for accurately measuring permittivity of sheet materials at low frequencies.

3.5. Free space method

Free-space methods is considered as the oldest dielectric measurement technique [40][41]. It is based on focusing microwave energy at or through a sample of a material by using antennas. This method has several advantages as it covers wide range of frequencies, non-destructive and it does not require a contact between the sample and the measuring tool. Moreover, it can be applied to materials to be tested under high temperatures and hostile environments.

Figure 15 shows the two main free space measurement setups:

a) S-parameter configuration based on field transmission through the material.

b) NRL (Navy Research Laboratory) arch method based on the signal reflection from the material under test.

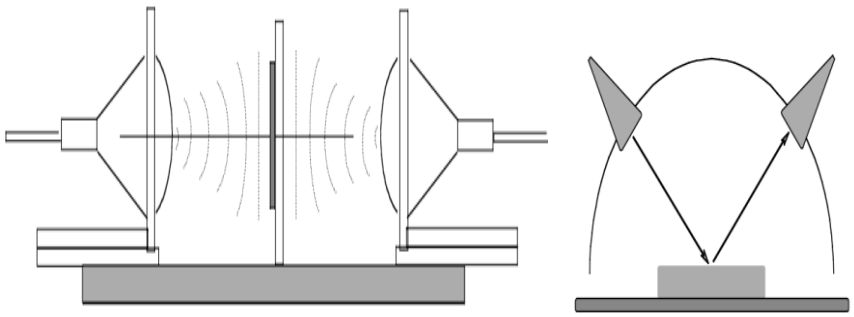

a *b*

Fig. 15. Free space method a) measurement by transmission b) NRL arch reflectivity test

The test bench contains two antennas and the location of the material between the two antennas must be selected carefully (plane wave theory). A full two-port calibration is required in order to obtain accurate results. A TRL (Thru-Reflect-Line) or TRM (Thru-Reflect-Match) calibration may actually be easier than other

calibration techniques in free space. The dielectric properties of the material under test are then extracted as function of transmitted and reflected signals.

Figure 16 shows a free space quasi-optical system covering the frequency band of 75-110 GHz.

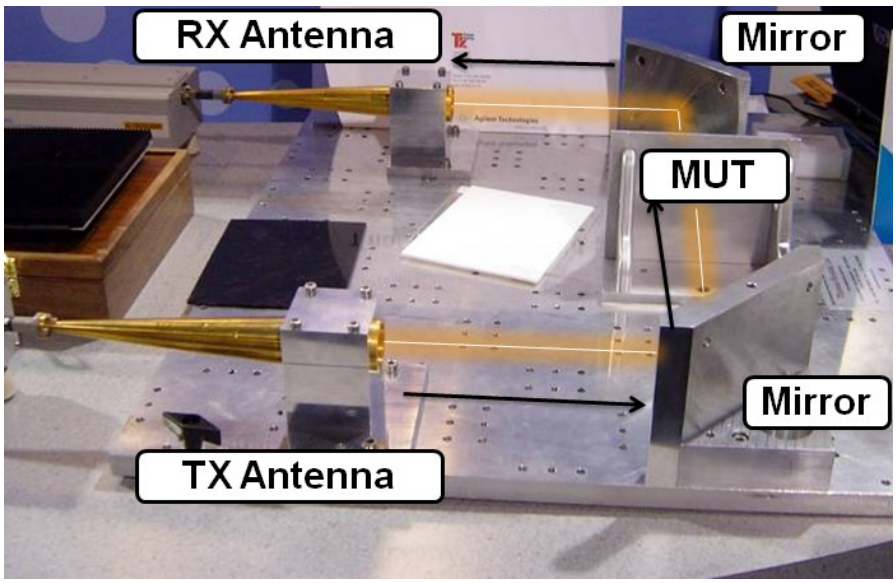

Fig. 16. Measurement setup of free space quasi-optical system [42]

The transmitted signal from the antenna is reflected off the mirror and passes through the sample to the mirror on the other side and then redirected to the receiving antenna. The total loss in the S_{21} path through this fixture is less than 1dB which is quite remarkable at such high frequency band.

3.6. Dipole antenna method

As discussed in the previous sections, the most popular method for food dielectric characterization is the open-ended coaxial line probe. Its popularity is largely due to its relatively simple calibration procedures, measurement frequency range, and commercial availability. However, the coaxial probe is very expensive to implement and is suitable only for homogeneous samples.

Therefore, for heterogeneous dielectric samples such as food products, an alternative method that is capable of measuring the average permittivity and easy

to handle would be useful. This section presents a simple non-destructive dielectric characterization method based on reflection coefficient measurement of a dipole antenna placed on the material under test (MUT).

3.6.1 Principle of the proposed method

A simple half-wavelength dipole antenna placed on a dielectric substrate having relative dielectric constant ε_r and surrounded by free space is analyzed as if the antenna was placed in a homogenous medium having an effective dielectric constant ε_e.The effective permittivity ε_e depends mainly on the substrate's relative dielectric constant ε_r and the antenna geometry.

For this structure, the resonance frequency f_r of the antenna is directly related to the medium according to the following relation:

$$f_r = \frac{c}{2L\sqrt{\varepsilon_e}} \tag{2.22}$$

where c is free space velocity of light, L is dipole length and ε_e is the effective permittivity. The technique to estimate ε_e is based on a capacitance method using coplanar strips structure equivalent to a center fed dipole [43]. Hence, the effective capacitance between the two arms of the dipole due to the electric field is the main parameter that defines the effective relative permittivity as seen by the antenna. The total effective capacitance of center fed half-wavelength dipole between air and a dielectric substrate with finite thickness is given by:

$$C_e = \varepsilon_0 W[2K_1 + (\varepsilon_r - 1)K_2] \tag{2.23}$$

where ε_r the relative permittivity of the substrate, W is the dipole arm width, K_1 and K_2 represent the filling factors of the electric field lines between the two dielectric mediums depending mainly on the dipole dimensions and the substrate thickness. The effective relative permittivity, as seen by the dipole, is the ratio of the capacitor C_e to its value in air, and is given by:

$$\varepsilon_e = 1 + \left(\frac{\varepsilon_r - 1}{2}\right)\frac{K_2}{K_1} \tag{2.24}$$

From equations 22 & 24, the dielectric permittivity of the substrate can be described as a function of the dipole's resonance frequency:

$$\varepsilon_r = 2\left[\left(\frac{K_1}{K_2}\right)\left(\frac{c}{2\,Lf_{fr}}\right)^2\right] - 1 \qquad (2.25)$$

From [43], the filling factors (K_1&K_2) will vary as the sample's thickness changes and thus, the antenna resonance frequency.

Figure 17 shows relative permittivity variation as function of the resonance frequency of a dipole designed to resonate in air at 867 MHz for three different substrate's thicknesses using equation (25).

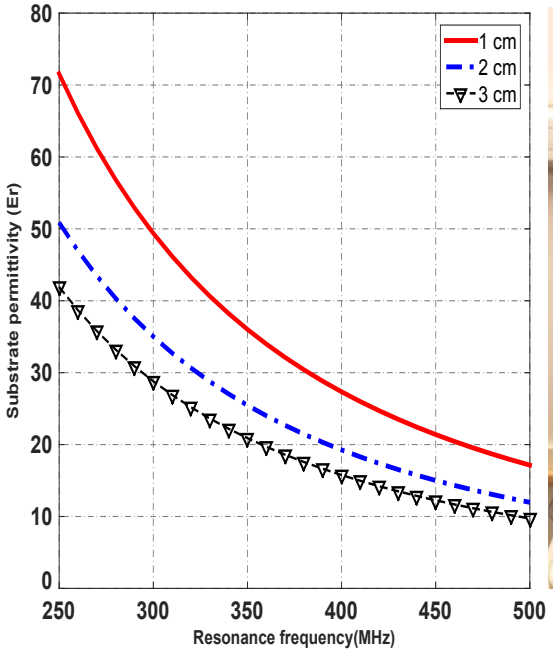

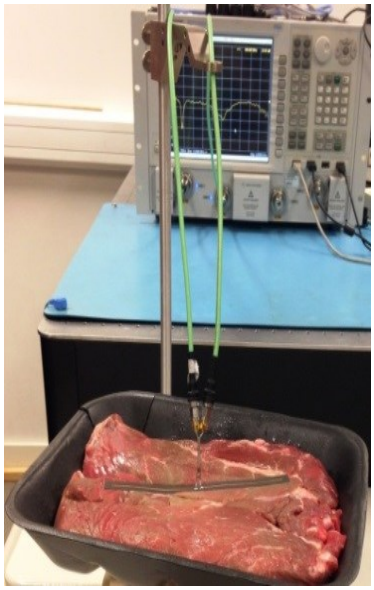

a b

Fig.17.a) Dielectric constant variation versus the resonance frequency of a dipole for three different substrate's thicknesses = 1, 2 and 3 cm. b) Measurement setup [44]

For a given dielectric permittivity, as the sample thickness increases, the resonance frequency decreases. Thus, the dielectric permittivity of a sample can be directly extracted from the measured reflection coefficient of a simple dipole in a good contact with the material's surface.

3.6.2 Measurement results

Figure 18 shows the reflection coefficient measurements of the half wavelength printed in contact with a cheese sample of 3 cm thickness and a lean meat sample of 1 cm thickness. The cheese measurement curve fits with the HFSS model of ε_r =15 while the meat measurement curve fits with the HFSS model of ε_r = 55.

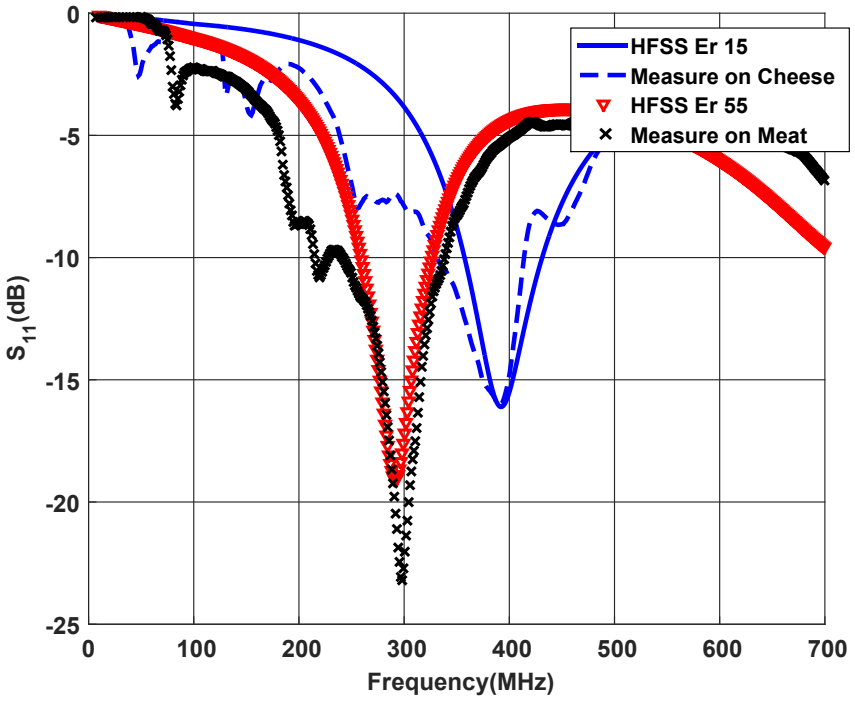

Fig.18. Dipole reflection coefficient measurements (in contact with a sample of cheese and a sample of lean meat) versus HFSS models [44]

From equation (25), for sample thickness of 3 cm, the measured resonance frequency of the dipole on the cheese sample = 390 MHz, which corresponds to a value of $\varepsilon_r \approx 15$ with a precision of ±1.For a lean meat sample of 1 cm thickness, the measured resonance frequency is around 295 MHz, which corresponds to a value of $\varepsilon_r \approx 50$ with a precision of ±2.

Table.3 shows a comparison between the values of ε_r obtained by this method and the values obtained by simulation on HFSS, as well as the average permittivity

of the cheese and meat samples measured by a commercially available coaxial-line probe at the same frequency of antenna's resonance (867 MHz).

Table. 3. Comparison between values of ε_r obtained by three different methods

Sample	Dipole Method	HFSS Model	Dielectric probe
$\boldsymbol{\varepsilon_r}$ **(cheese)**	15 ± 1	15	14
$\boldsymbol{\varepsilon_r}$ **(Meat)**	50 ± 2	55	56

The main drawback of this method is its limitation to the characterization of the real part of the material permittivity. However, it can be very useful in many food applications where the dielectric constant is the main parameter of interest.

4. Conclusion

Nowadays, in a large number of modern applications, the knowledge of the electromagnetic properties of used material is highly required for purpose of proper and effective design of the considered applications. Beside the exploitation of dielectric properties of food products for RF heating applications, permittivity of some types of food can also be related to the maturation level, storage, or processing such as pasteurization and sterilization which could be developed to improve the food safety as well as providing better quality monitoring based on determination of moisture content, density, maturity and other parameters. Moreover, in the field of RFID traceability systems for food items, a good knowledge of the dielectric constant is required for an appropriate tag antenna design to achieve the best performance. This chapter discussed in detail the main parameters which affect the dielectric properties of food products and provided a summary about previously published works which studied the dielectric properties of different types of food products as function of frequency and temperature.

In this context, the dielectric measurement techniques became of great importance in order to understand the behavior of the material when it is submitted to electromagnetic field. Although several electromagnetic characterization techniques exist, not all of them are suitable to characterize food products. An overview on the main dielectric characterization techniques is

presented. Finally, a new measurement technique showed the possibility of measuring the dielectric constant of food products using a simple dipole antenna which represents a simple and cost effective method compared to costly measurement techniques.

References

[1] J. N. Ikediala, J. Tang, S. R. Drake, and L. Neven, “Dielectric properties of apple cultivars and codling moths,” Trans. ASAE, vol. 43, pp. 1175–1184, Sep. 2000.

[2] R. E. Mudgett, “Microwave properties and heating characteristics of foods,” Food Technol. USA, 1986.

[3] H. Schubert and M. Regier, “The microwave processing of foods.,” Microw. Process. Foods, 2005.

[4] A. C. Metaxas, R. J. Meredith, and I. of E. Engineers, Industrial microwave heating. London : Peter Peregrinus Ltd. on behalf of the Institution of Electrical Engineers, 1983.

[5] M. E. Sosa-Morales, L. Valerio-Junco, A. López-Malo, and H. S. García, “Dielectric properties of foods: Reported data in the 21st Century and their potential applications,” LWT - Food Sci. Technol., vol. 43, no. 8, pp. 1169–1179, Oct. 2010.

[6] V. Komarov, S. Wang, and J. Tang, “Permittivity and Measurements,” in Encyclopedia of RF and Microwave Engineering, John Wiley & Sons, Inc., 2005.

[7] S. O. Nelson, “Review and assessment of radio-frequency and microwave energy for stored-grain insect control,” Trans. ASAE, vol. 39, no. 4, pp. 1475–1484, 1996.

[8] C. R. Buffler, Microwave Cooking and Processing: Engineering Fundamentals for the Food Scientist. Springer US, 1993.

[9] A. R. V. Hippel, Dielectrics and waves. Wiley, 1954.

[10] M. S. Venkatesh and G. S. V. Raghavan, “An Overview of Microwave Processing and Dielectric Properties of Agri-food Materials,” Biosyst. Eng., vol. 88, no. 1, pp. 1–18, May 2004.

[11] M. E. Sosa-Morales, L. Valerio-Junco, A. López-Malo, and H. S. García, “Dielectric properties of foods: Reported data in the 21st Century and their potential applications,” LWT - Food Sci. Technol., vol. 43, no. 8, pp. 1169–1179, Oct. 2010.

[12] Y. Wang, T. D. Wig, J. Tang, and L. M. Hallberg, “Dielectric properties of foods relevant to RF and microwave pasteurization and sterilization,” J. Food Eng., vol. 57, no. 3, pp. 257–268, May 2003.
[13] M. E. Sosa-Morales, G. Tiwari, S. Wang, J. Tang, H. S. Garcia, and A. Lopez-Malo, “Dielectric heating as a potential post-harvest treatment of disinfesting mangoes, Part I: Relation between dielectric properties and ripening,” Biosyst. Eng., vol. 103, no. 3, pp. 297–303, Jul. 2009.
[14] B. S. Schweigert, Microwaves in the Food Processing Industry, 1 edition. Orlando, Fla: Academic Press, 1985.
[15] S. Wang et al., “Dielectric Properties of Fruits and Insect Pests as related to Radio Frequency and Microwave Treatments,” Biosyst. Eng., vol. 85, no. 2, pp. 201–212, Jun. 2003.
[16] H. Feng, J. Tang, and R. P. Cavalieri, “Dielectric Properties of Dehydrated Apples as Affected by Moisture and Temperature,” Trans. ASAE ONLINE, 2002.
[17] S. Wang, J. Tang, R. P. Cavalieri, and D. C. Davis, “Differential Heating of Insects in Dried Nuts and Fruits Associated with Radio Frequency and Microwave Treatments,” Trans. ASAE, 2003.
[18] S. O. Nelson, W. R. Jr Forbus, and K. C. Lawrence, “Permittivities of Fresh Fruits and Vegetables at 0.2 to 20 GHz,” J. Microw. Power Electromagn. Energy Publ. Int. Microw. Power Inst., vol. 29, pp. 81–93, Feb. 1994.
[19] S. Wang, M. Monzon, Y. Gazit, J. Tang, E. J. Mitcham, and J. W. Armstrong, “Temperature-dependent dielectric properties of selected subtropical and tropical fruits and associated insect pests,” Trans. ASAE, 2005.
[20] M. S. Venkatesh and G. S. V. Raghavan, “An Overview of Microwave Processing and Dielectric Properties of Agri-food Materials,” Biosyst. Eng., vol. 88, no. 1, pp. 1–18, May 2004.
[21] M. E. Sosa-Morales, G. Tiwari, S. Wang, J. Tang, H. S. Garcia, and A. Lopez-Malo, “Dielectric heating as a potential post-harvest treatment of disinfesting mangoes, Part I: Relation between dielectric properties and ripening,” Biosyst. Eng., vol. 103, no. 3, pp. 297–303, Jul. 2009.
[22] J. G. Lyng, L. Zhang, and N. P. Brunton, “A survey of the dielectric properties of meats and ingredients used in meat product manufacture,” Meat Sci., vol. 69, no. 4, pp. 589–602, Apr. 2005.

[23] Y. Wang, J. Tang, B. Rasco, F. Kong, and S. Wang, “Dielectric properties of salmon fillets as a function of temperature and composition,” J. Food Eng., vol. 87, no. 2, pp. 236–246, Jul. 2008.
[24] M. Al-Holy, Y. Wang, J. Tang, and B. Rasco, “Dielectric properties of salmon (Oncorhynchus keta) and sturgeon (Acipenser transmontanus) caviar at radio frequency (RF) and microwave (MW) pasteurization frequencies,” J. Food Eng., vol. 70, no. 4, pp. 564–570, Oct. 2005.
[25] J. Wang, J. Tang, Y. Wang, and B. Swanson, “Dielectric properties of egg whites and whole eggs as influenced by thermal treatments,” LWT - Food Sci. Technol., vol. 42, no. 7, pp. 1204–1212, Sep. 2009.
[26] M. A. Stuchly and S. S. Stuchly, “Coaxial Line Reflection Methods for Measuring Dielectric Properties of Biological Substances at Radio and Microwave Frequencies-A Review,” IEEE Trans. Instrum. Meas., vol. 29, no. 3, pp. 176–183, Sep. 1980.
[27] D. V. Blackham and R. D. Pollard, “An improved technique for permittivity measurements using a coaxial probe,” IEEE Trans. Instrum. Meas., vol. 46, no. 5, pp. 1093–1099, Oct. 1997.
[28] G. P. Otto and W. C. Chew, “Improved calibration of a large open-ended coaxial probe for dielectric measurements,” IEEE Trans. Instrum. Meas., vol. 40, no. 4, pp. 742–746, Aug. 1991.
[29] J. Vrba and D. Vrba, “Temperature and Frequency Dependent Empirical Models of Dielectric Properties of Sunflower and Olive Oil,” Radioengineering, vol. 22, pp. 1281–1287, Dec. 2013.
[30] T. Mathew, A. D. Vyas, and D. Tripathi, “Dielectric properties of some edible and medicinal oils at microwave frequency.,” Can. J. Pure Amp Appl. Sci., vol. 3, no. 3, pp. 953–957, 2009.
[31] P. Banerjee, G. Ghosh, and S. K. Biswas, “A simple technique for the measurement of the permittivity of medium loss samples using cavity perturbation method,” in 2007 IEEE Applied Electromagnetics Conference (AEMC), 2007, pp. 1–3.
[32] V. V. Komarov and V. V. Yakovlev, “Modeling control over determination of dielectric properties by the perturbation technique,” Microw. Opt. Technol. Lett., vol. 39, no. 6, pp. 443–446, Dec. 2003.
[33] A. C. Metaxas, R. J. Meredith, and I. of E. Engineers, Industrial microwave heating. London : Peter Peregrinus Ltd. on behalf of the Institution of Electrical Engineers, 1983.
[34] G. Torgovnikov, Dielectric Properties of Wood and Wood-Based Materials. Berlin Heidelberg: Springer-Verlag, 1993.

[35] A. D. Green, “Measurements of the Dielectric Properties of Cheddar Cheese,” J. Microw. Power Electromagn. Energy, vol. 32, no. 1, pp. 16–27, Jan. 1997.
[36] J. Baker-Jarvis, E. J. Vanzura, and W. A. Kissick, “Improved technique for determining complex permittivity with the transmission/reflection method,” IEEE Trans. Microw. Theory Tech., vol. 38, no. 8, pp. 1096–1103, Aug. 1990.
[37] A. M. Nicolson and G. F. Ross, “Measurement of the Intrinsic Properties of Materials by Time-Domain Techniques,” IEEE Trans. Instrum. Meas., vol. 19, no. 4, pp. 377–382, Nov. 1970.
[38] W. B. Weir, “Automatic measurement of complex dielectric constant and permeability at microwave frequencies,” Proc. IEEE, vol. 62, no. 1, pp. 33–36, Jan. 1974.
[39] C. C. Courtney, “Time-domain measurement of the electromagnetic properties of materials,” IEEE Trans. Microw. Theory Tech., vol. 46, no. 5, pp. 517–522, May 1998.
[40] S. B. Kumar, U. Raveendranath, P. Mohanan, K. T. Mathew, M. Hajian, and L. P. Ligthart, “A simple free-space method for measuring the complex permittivity of single and compound dielectric materials,” Microw. Opt. Technol. Lett., vol. 26, no. 2, pp. 117–119, Jul. 2000.
[41] D. K. Ghodgaonkar, V. V. Varadan, and V. K. Varadan, “A free-space method for measurement of dielectric constants and loss tangents at microwave frequencies,” IEEE Trans. Instrum. Meas., vol. 38, no. 3, pp. 789–793, Jun. 1989.
[42] “Agilent VNA Quasi-Optical Systems.” [Online]. Available: http://www.terahertz.co.uk/tk-instruments/products/agilentvna. [Accessed: 26-Feb-2018].
[43] A. Abbosh, “Accurate Effective Permittivity Calculation of Printed Center-Fed Dipoles and Its Application to Quasi Yagi-Uda Antennas,” IEEE Trans. Antennas Propag., vol. 61, no. 4, pp. 2297–2300, Apr. 2013.
[44] A. Abdelnour, A. Rennane, D. Kaddour, and S. Tedjini, “Non-destructive dielectric characterization method for food products,” in 2017 IEEE MTT-S International Microwave Symposium (IMS), 2017, pp. 2022–2024.

Chapter 3

Analysis of dielectric & chemical properties of cheese during ripening

1. Introduction

The ripening of rennet-coagulated cheeses, and hence their flavor, texture and quality, are largely predetermined by the manufacturing process. Many important factors which affect cheese ripening such as moisture content, levels of NaCl, pH, and physical size of the cheese are influenced by manufacture. Indeed, it is difficult, and often impossible, to remedy during the maturation stage any mistake made during curd manufacture.

This chapter studies the variation of dielectric properties of several kinds of cheese during the maturation process. The main objective is to determine is the dielectric propreties can be considered as sensing parameters for cheese quality monitoring. The second objective is to use these dielectric properties for antenna design of UHF RFID tags in order to provide a robust traceability solution for cheese production sector which will be discussed in detail in the next chapter.

The first section of this chapter discusses the main parameters affecting cheese maturation as well as detailed explanation of the different stages of ripening process. The second section presents the dielectric characterization including

measurement setup and results of dielectric properties of three types of cheese during maturation. The third section provides a study of correlation between dielectric and chemical properties. Finally, the chapter concludes with a discussion about the feasibility of a ripening sensor based on the dielectric properties.

2. Cheese manufacture and ripening

Most cheese varieties are subjected to a ripening period after manufacture. The ripening time may vary in duration from weeks to years depending on cheese variety. The primary aim of the ripening process is the development of the desired flavor, texture and functionality (eg. grated cheese, sliced or processed) of the cheese. This ripening process may be carried out in moisture-impermeable packages (foil-ripening) or under natural conditions where the coated cheese is subject to moisture loss during ripening.

Ripening duration and temperature and, in the case of natural ripening, ripening temperature are specific for each cheese variety allowing the optimal balance between flavor, texture and functionality. Careful treatment of the cheese during ripening is also required to prevent growth of undesirable microorganisms and physical defects.

Swiss-type cheese, known as *Emmental* in France, belongs to the family of cooked pressed cheese. The term cooked is a cheese whose curd has been heated at the time of slicing whereas the term pressed means that the cheese curd is pressed at the time of molding to obtain the volume by eliminating the maximum whey, and then left to ripening. Compared to other types of fresh cheese like Feta and Mozzarella, pressed cheese has a significantly lower moisture content which affects its dielectric properties.

An Emmental passes by several stages of ripening after being pressed as shown in figure 1. The first step is salting or brining where the primary objective is to slow down or stop the bacteria process of converting lactose to lactic acid. The secondary purpose is to pull moisture from the surface and begin forming the rind of the cheese. The period of this stage depends on the cheese density and volume. A very dense low moisture cheese such as Emmental will need more time than a moist open texture cheese.

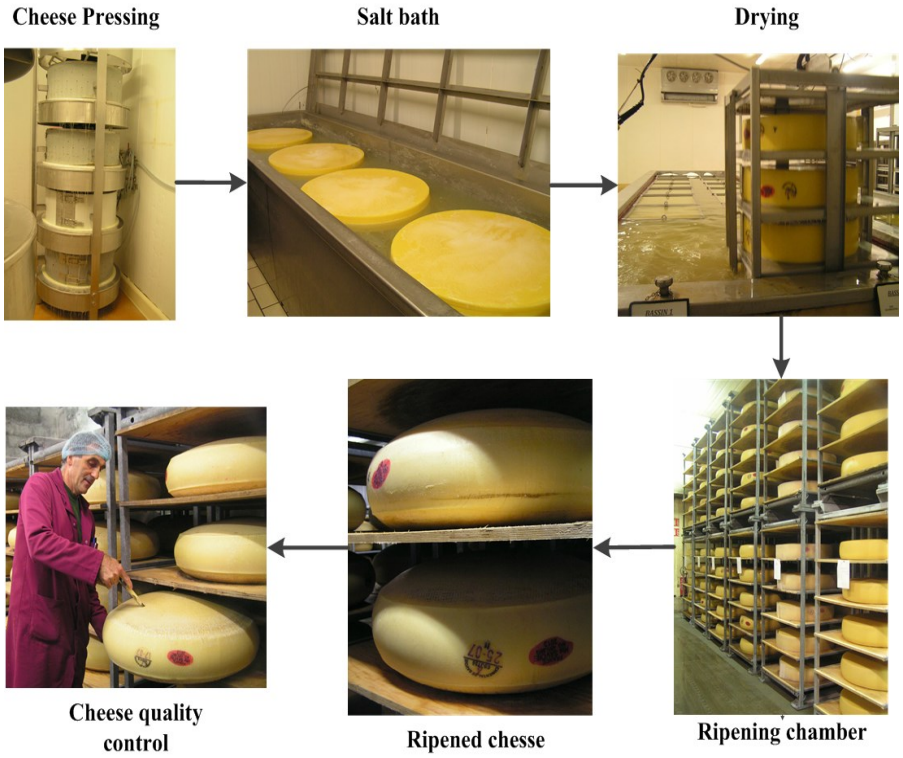

Fig.1. Emmental cheese production process [1], [2]

The cheese wheels are then transferred to temperature controlled ripening chambers or caves where the maturation process proceeds. It begins by cool or cold cave where the temperature is in the range of 10ºC in order to allow cheese to stabilize after brining. This stage lasts between two to three weeks depending on the size and volume of cheese wheels.

The temperature of ripening chamber is then raised to reach around 20ºC to 25ºC. By increasing the temperature, a very specific fermentation then begins where the activity of propionic acid bacteria (PAB) increases and releases carbon dioxide inside the loaf (up to 150 liters).

Unable to escape through the impermeable rind of cheese, these gas bubbles create holes (also called "openings" or "eyes") in the loaf. This also explains why

the flat cheese wheels at the beginning of ripening gradually become bulging during maturation under the effect of pressure.

After a period of 4 weeks to 6 weeks in the warm caves, the cheese wheels are placed in a cold ripening chamber at 6 °C for ~ 15 days.

The following sections mainly focused on the analysis of dielectric and chemical properties of Swiss-type cheese during ripening process. A complementary study is realized on similar types of pressed cheese (Morbier & Grimont) which are ripened under different conditions (see figure 2). In the following sections, the dielectric properties of three types of cheese as well as the correlation with their chemical properties are analyzed under different ripening conditions.

a *b* *c*

Fig.2 . Three types of cheese studied a) Emmental b) Morbier c) Grimont

3. Dielectric characterization of cheese

3.1. Dielectric measurement method

As discussed previously in chapter 2, there are several measurement techniques for dielectric characterization. In this study, an open-ended coaxial probe is used as it is considered the most adequate and accurate measurement technique for semi-solid materials such as cheese.

Dielectric measurements were achieved using a Keysight Technologies open-ended co-axial slim form probe (Outer diameter 2 mm) (Model No. N1501A) [3] connected to an ENA Vector Network Analyzer (Model No. E5080A) [4], with the

aid of the N1500A Materials Measurement Suite software package as illustrated in figure 3.

The system was calibrated using three known standards namely air, a short circuit and distilled water at 25 °C. The automated electronic calibration refresh feature was activated using an ECal module. This feature allows recalibrating the system automatically, in seconds, just before each measurement is made. This virtually eliminates cable instability and system drift errors.

Cheese samples were left to equilibrate to room temperature in an air conditioned laboratory at 23 C, and the temperature of each sample was recorded immediately prior to the dielectric measurement using a thermocouple.

Figure 3 shows the measurement setup where several measurements were realized on two sides of each cheese wheel. The dielectric properties were mainly analyzed on the cheese rind as it is the most accessible spot for later installation of RFID tags.

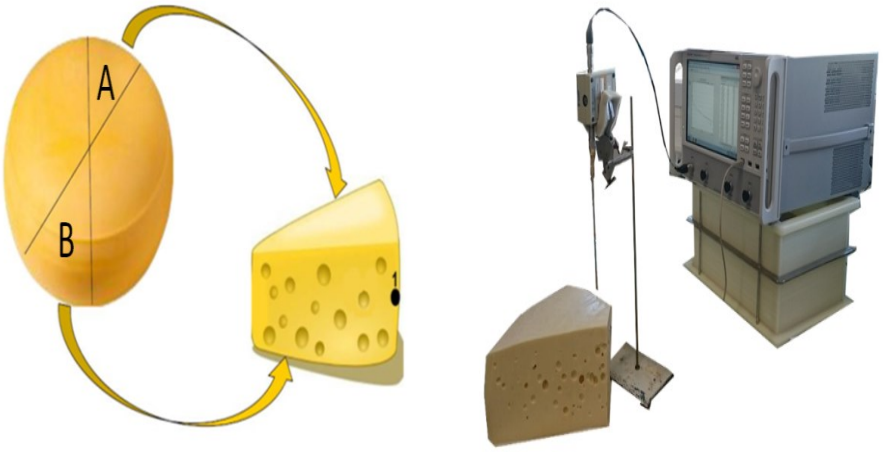

Fig. 3. Dielectric characterization measurement setup using an open ended coaxial probe

The cheese samples were raised using a plastic fixture until in constant contact with the dielectric probe in order not to affect the calibration. The probe is inserted at 5 mm depth inside cheese and dielectric properties of each sample were

measured over a range of frequencies varying from 100 MHz to 2 GHz. A substantial number (more than 6) of dielectric measurements were performed on samples for each side at different ripening stages. As the frequency increases, both permittivity and loss tangent decreases due to dielectric relaxation of the material as shown in figure 4.

The standard deviations of the replicates for each sample, across the dielectric spectra, were calculated. In general the standard deviation among replicates at any frequency was less than 4% and this was used as a guide to identifying and rejecting outliers.

Outliers were most likely the result of poor or uneven contact between the probe and the sample or the presence of air bubbles close to the probe.

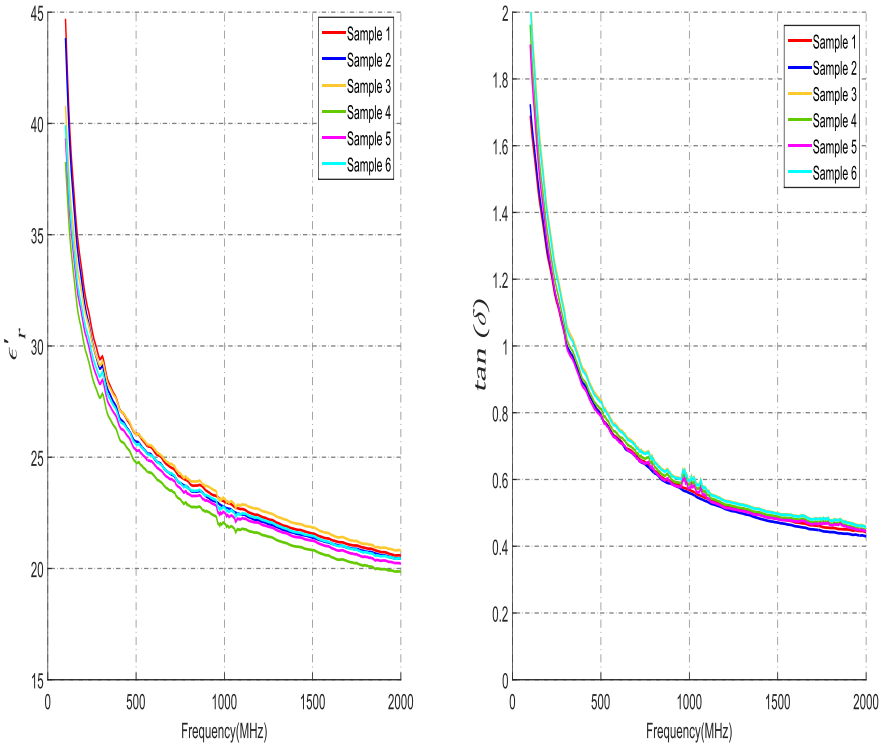

Fig. 4. Several measurements of Emmental dielectric properties over a range of frequencies varying from 100 MHz to 2000 MHz.

3.2 Dielectric properties of Emmental

For this study, experimental Emmental cheeses were manufactured according to the usual process in the same week by the same cheese producer and from the same standardized milk. The samples were wrapped in plastic foil during the entire maturation process and measurements were realized at two sides of each sample (A & B).

Figure 5 shows a comparison between the average value of dielectric constant ε'_r of four different Emmental cheese samples (C1, C2, C3& C4) at 867 MHz for four steps of ripening: 1) End of brining; 2) Cold cave; 3) Warm cave and 4) End of ripening.

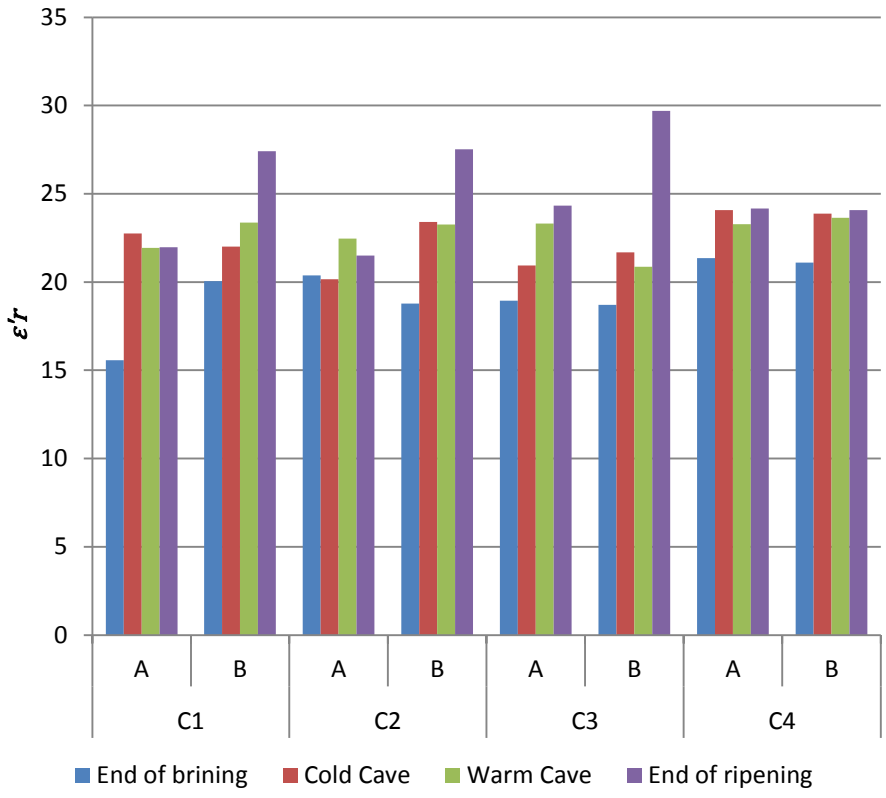

Fig. 5. Dielectric constant variation of four different Emmental cheese samples (C1, C2, C3& C4) at 867 MHz

The first measurements were realized at the end of the brining process just before transferring the samples to the cold caves. The dielectric constant of most samples is relatively lower in this stage of ripening compared to the other stages. This can be explained by the high concentration of NaCl on the surface of cheese at this stage which reduces the dielectric constant. However, this behavior can be different from one sample to another or even on the same sample between its two sides as the rate of diffusion of NaCl from the surface towards the center of cheese is not uniform like in C1 where the value of side A is around 15 whereas the other side B presents a higher permittivity of 20.

Then measurements were repeated at the end of cold and warm caves. The dielectric constant of most samples almost did not change during these two stages of ripening. At the end of ripening, relatively higher values of ε'_r compared to previous stages are noticed as in C1(B), C2(B) and C3. However, this variation was very weak and undistinguishable for the rest of samples

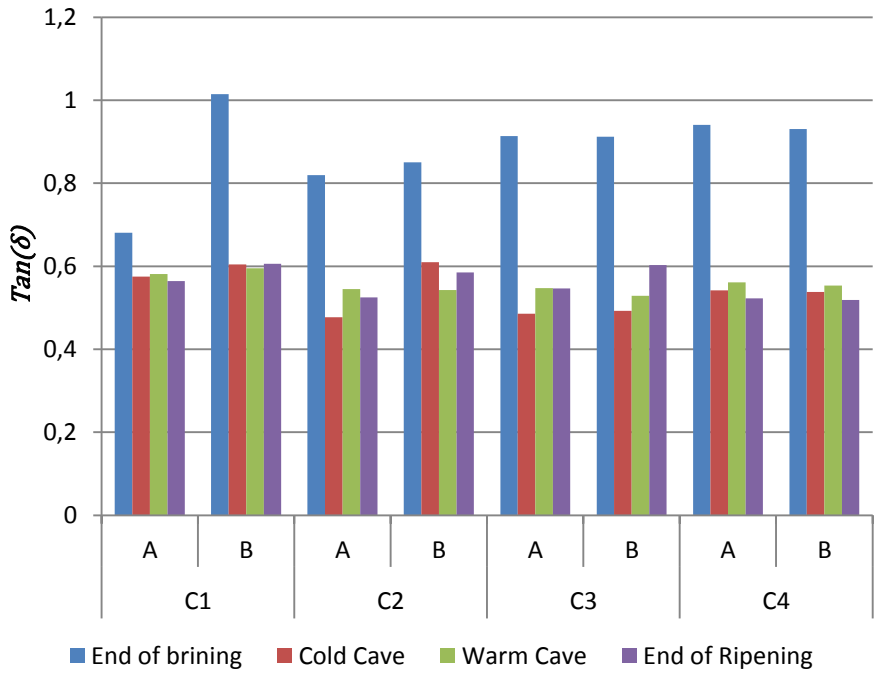

Fig. 6. Dielectric loss tangent variation of four different Emmental cheese samples (C1, C2, C3& C4) at 867 MHz

Figure 6 presents the variation of the loss tangent of the same cheese samples during maturation. It is clearly noticeable the effect of salting on the loss factor as the conductivity on the cheese surface is higher compared to the rest of ripening stages. This effect decreases as the cheese samples are left to stabilize and ripe as the NaCl is absorbed and diffused towards the center of cheese samples. The dielectric losses do not change considerably during the rest of the maturation process. The average of loss tangent before the cold cave stage is around 0,87 and it decreases during ripening to reach around 0,55 at the end of cheese maturation.

As a conclusion, the analysis of dielectric properties of four samples of Emmental cheese shows a slight and irregular variation of ε'_r during ripening process. On the other hand, there is a significant and clear variation of loss tangent between the brining stage and the rest of maturation stages. However, dielectric losses did not present a noticable change during the rest of cheese ripening.

3.3 Dielectric properties of Grimont

Grimont is another type of french cheese which belongs to the family of pressed cheese. The main difference between this type and Emmental is the maturation period as it is shorter in the case of Grimont (around 6 weeks). Also, this kind of cheese is not ripened under plastic foil which impacts a lot the variation of its dielectric properties. After pressing and salting, the cheese wheels are left to dry in cool cave under a temperature of around 6ºC to 10ºC.

For this type of cheese, experimental samples were manufactured according to the usual process in the same week by the same cheese producer and from the same standardized milk. Measurements were realized on three different wheels (C1, C2 &C3) at the beginning and at the end of their maturation period. Figure 7 shows a comparison between the mean value of measured dielectric properties at start and end of ripening at UHF RFID European frequency 867 MHz.

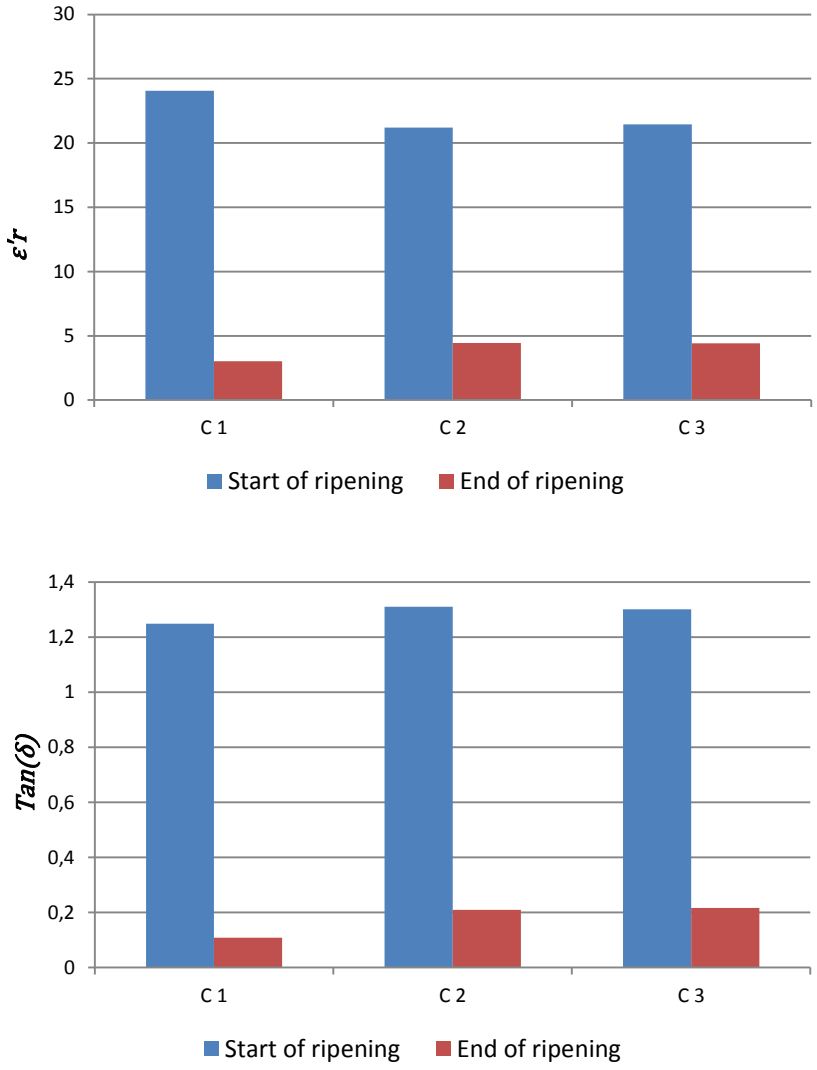

Fig. 7. Dielectric properties variation of three different samples of Grimont cheese (C1, C2 & C3) at 867 MHz

An important variation of both dielectric parameters ε'_r and *Tan (δ)* occurs during the maturation process. Measuring as high as 22 at the beginning of maturation, the dielectric constant decreases until it reaches around 4 at the end of ripening. Similar behavior is observed for the dielectric losses as they decrease

significantly during maturation to reach around 16% of its initial value. Compared to Emmental, there are no holes in the texture of this type of cheese which increases the stability and the accuracy of dielectric measurements.

3.4 Dielectric properties of Morbier

The third type of cheese in this study is “Morbier” which also belongs to the same family of pressed cheese as the previous cases. The maturation period is quite similar to “Grimont” where cheese wheels are placed after pressing in cool caves for around six weeks. The main difference between Morbier and the previous cases is the salting process. During their ripening, the Morbier is rubbed on both sides with salty water once or twice a week which makes its texture more firm compared to Emmental and Grimont.

For this type of cheese, experimental samples were manufactured according to the usual processin the same week by the same cheese producer and from the same standardized milk. Measurements were realized on three different wheels (C1, C2 &C3) at the beginning and at the end of their maturation period. Figure 8 shows a comparison between the average of measured dielectric properties at start and end of ripening at UHF RFID European frequency 867 MHz.

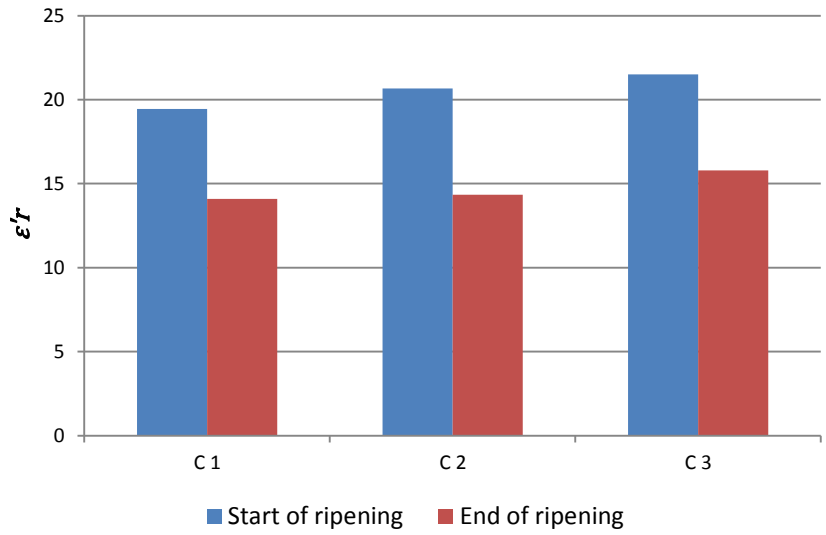

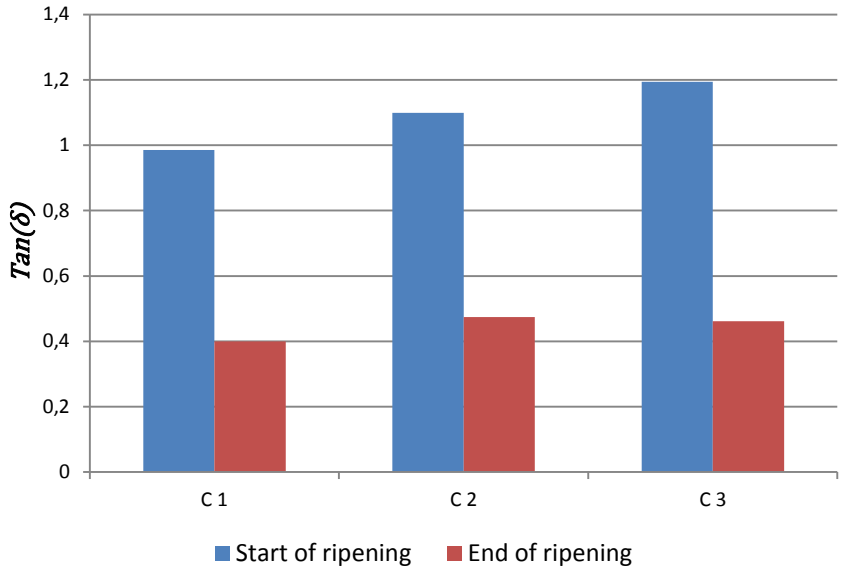

Fig. 8. Dielectric properties variation of three different samples of Morbier cheese (C1, C2 & C3) at 867 MHz

The Morbier cheese does not have holes in its texture like Emmental. However, compared to Grimont, a less significant variation of both dielectric parameters ε'_r and *Tan (δ)* took place during the ripening process. The dielectric constant decreases until it reaches at the end of ripening around 70%o f its initial value. Similar behavior is observed for the dielectric losses as they decrease significantly during maturation to reach around 40 % of its initial value.

4. Correlation between dielectric and chemical properties

This section study the correlation between the main chemical properties of cheese and the dielectric properties presented in the previous section. The aim of this study is to have a deeper knowledge about the main parameters which affect the dielectric properties during maturation as well as the difference between the variations of chemical properties of several types of cheese under different maturation conditions.

4.1. Main parameters and methods of extraction

The chemical composition (dry matter, fat, pH, calcium, sodium chloride and total nitrogen) of all samples of three types of cheeses (Emmental ,Grimont&Morbier) was studied in the laboratory of National School of Dairy Industry and Biotechnologies in Poligny (ENILBIO).

Analytical methods and uncertainty values for each parameter are reported in table 1. Samples were extracted at 5 mm from the cheese top rindwith a thickness of around 1 cm. Possible variations in the sample conditions during the experiments where monitored by measuring the weight and pH of the samples both before and after the experiment.

Table.1. Analytical methods and uncertainty values for each chemical parameter

Parameters		**Measurement method**	**Uncertainty**
DM	Dry Matter	NF EN ISO 5534 [5]	0,57 g/kg
Fat	Fat	NF V 04-287 [6]	1,27 g/kg
pH	pH	pH meter	0,05 upH
Ca	Calcium	Method of Pearce [7]	0,28 g/kg
NaCl	Sodium chloride	NF EN ISO 5943 [8]	0,19 g/kg
TN	Total nitrogen	NF EN ISO 8968-1 [9]	0,28 g/kg

4.2 Correlation between dielectric and chemical properties of Emmental

A total of eight measurements were obtained for Emmental samples (2 sides of four cheese wheels). Figures 9 to 14 show the variation of dielectric properties as function of each chemical parameter over different ripening stages.

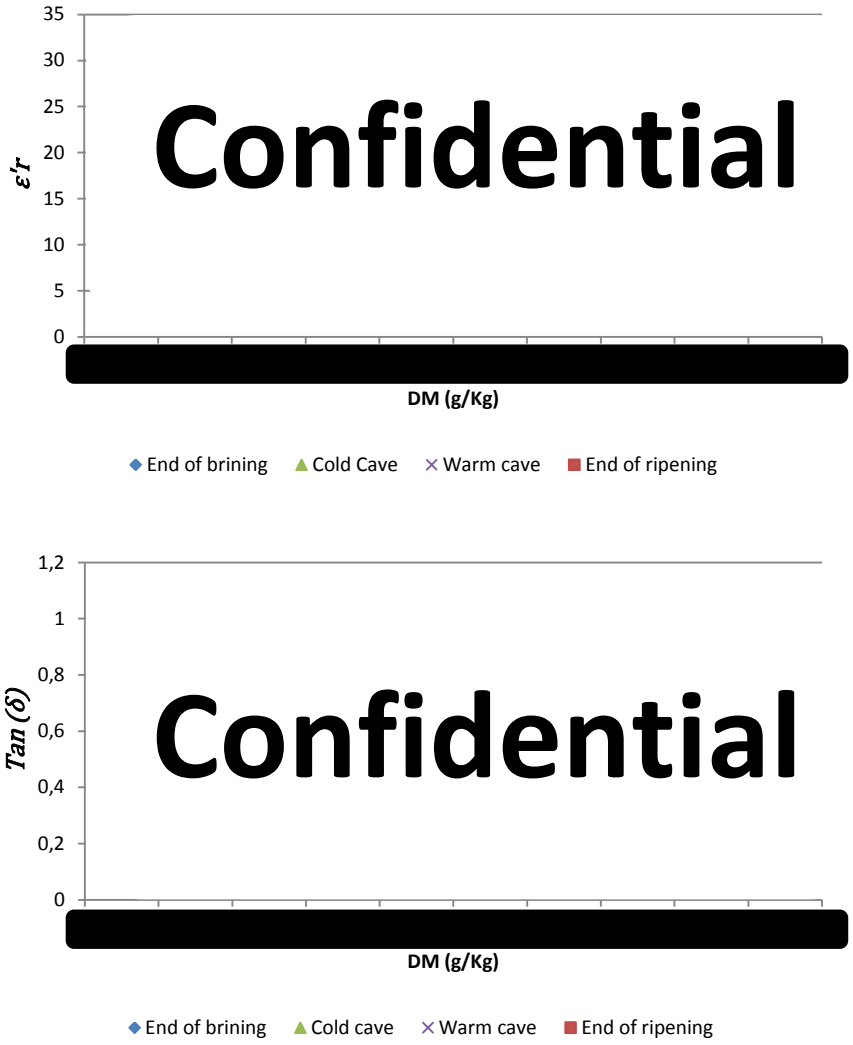

Fig.9 Variation of Emmental dielectric properties during maturation as function of dry matter

As the analyzed samples correspond to Emmental wheels wrapped under foil, the variation of dry matter over the entire period of ripening is around 20 g/Kg which is almost negligible. Therefore, the variation of dielectric constant was very weak. Similar behavior is observed in figure 10 where the fat concentration also did not

change significantly during maturation explaining thus the low variation of the dielectric properties.

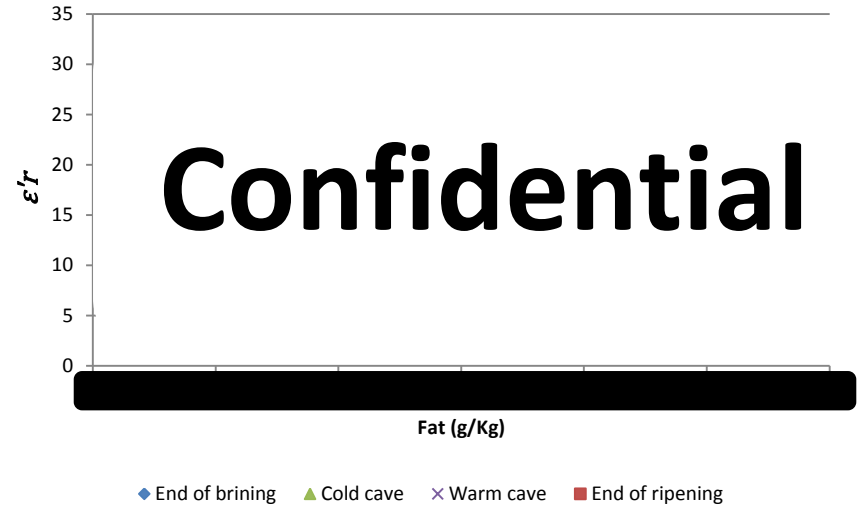

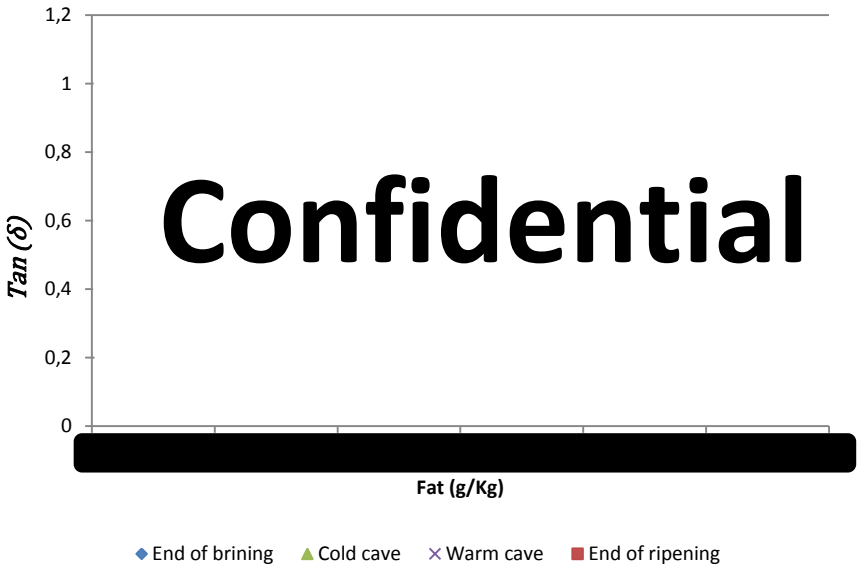

Fig.10 Variation of Emmental dielectric properties during maturation as function of fat concentration

Figure 11 shows clearly the effect of pH on dielectric properties of Emmental. Despite the small variation of pH during ripening (around 0,4), the difference between each ripening stage is quite distinguishable as function of dielectric parameters.

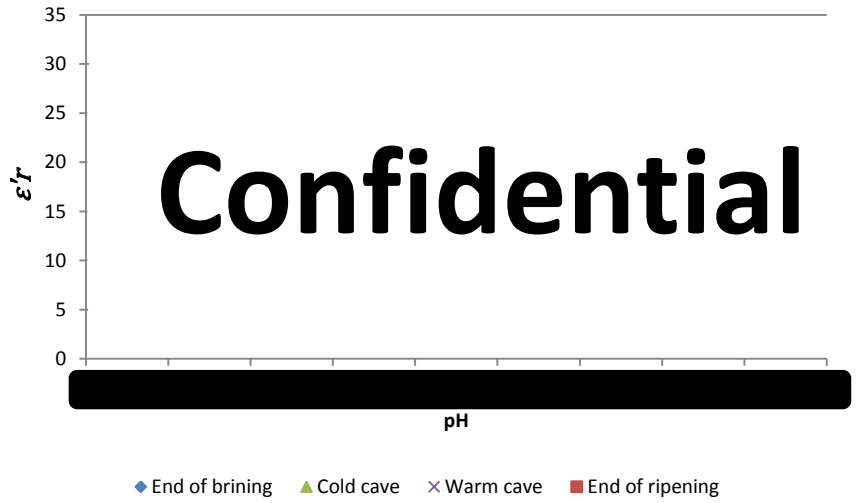

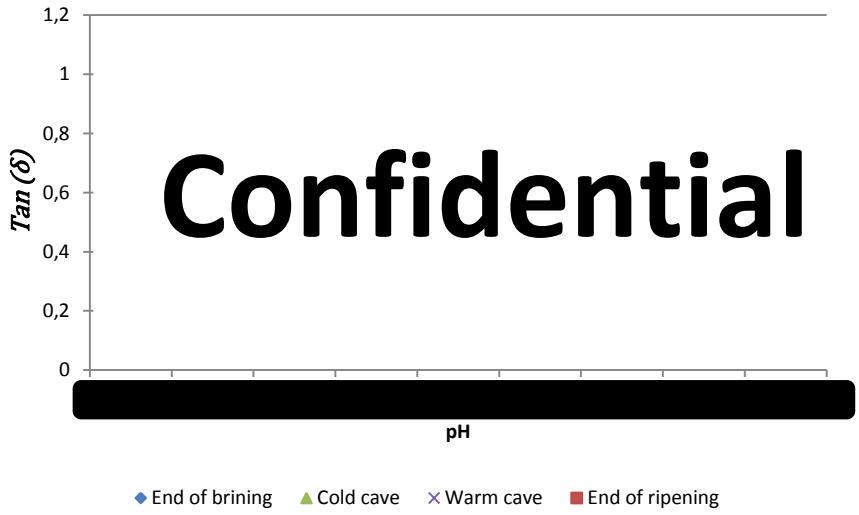

Fig.11 Variation of Emmental dielectric properties during maturation as function of pH level

On the other hand, figure 12 shows no effect of calcium concentration on dielectric properties.

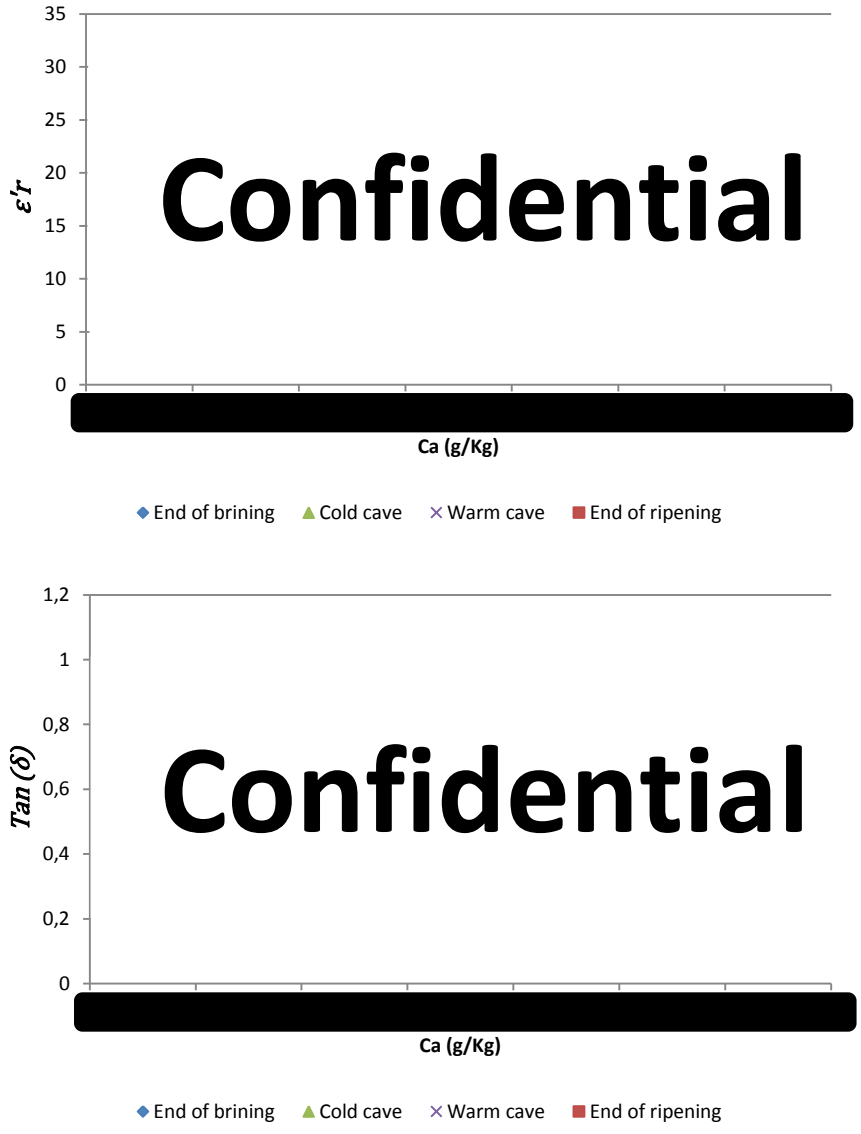

Fig.12 Variation of Emmental dielectric properties during maturation as function of calcium concentration

The concentration of NaCl basically affects the conductivity and thus the losses. Figure 13 shows the strong correlation between the NaCl and Tan (δ) where the losses decreased around 40% of its initial value as the salinity concentration decreased on the surface.

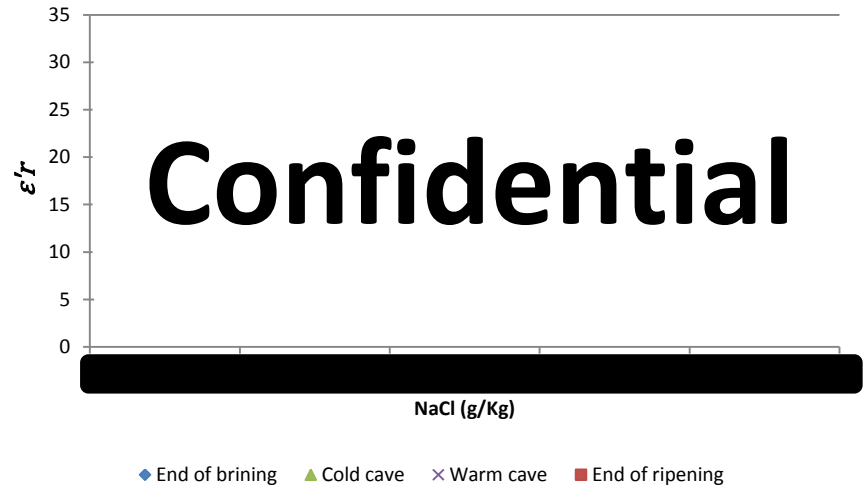

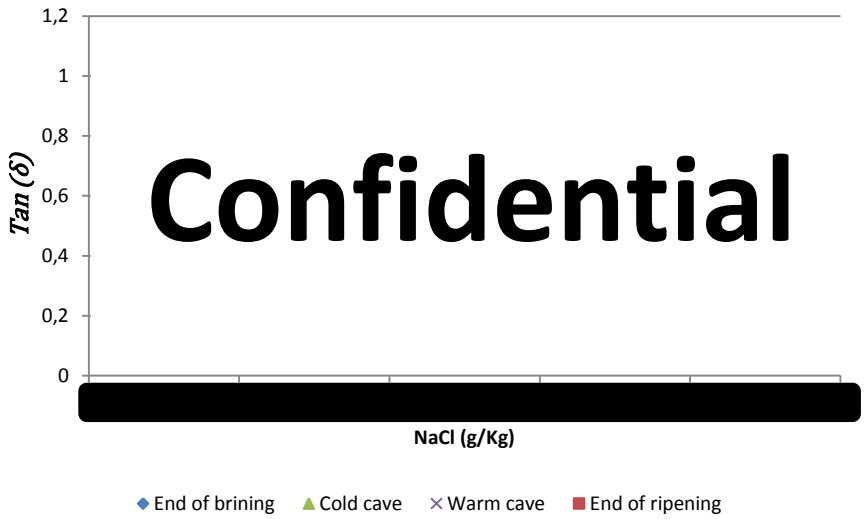

Fig.13 Variation of Emmental dielectric properties during maturation as function of NaCl concentration

Insignificant correlation is observed between the dielectric properties and the total nitrogen inside the cheese texture as illustrated by figure 14.

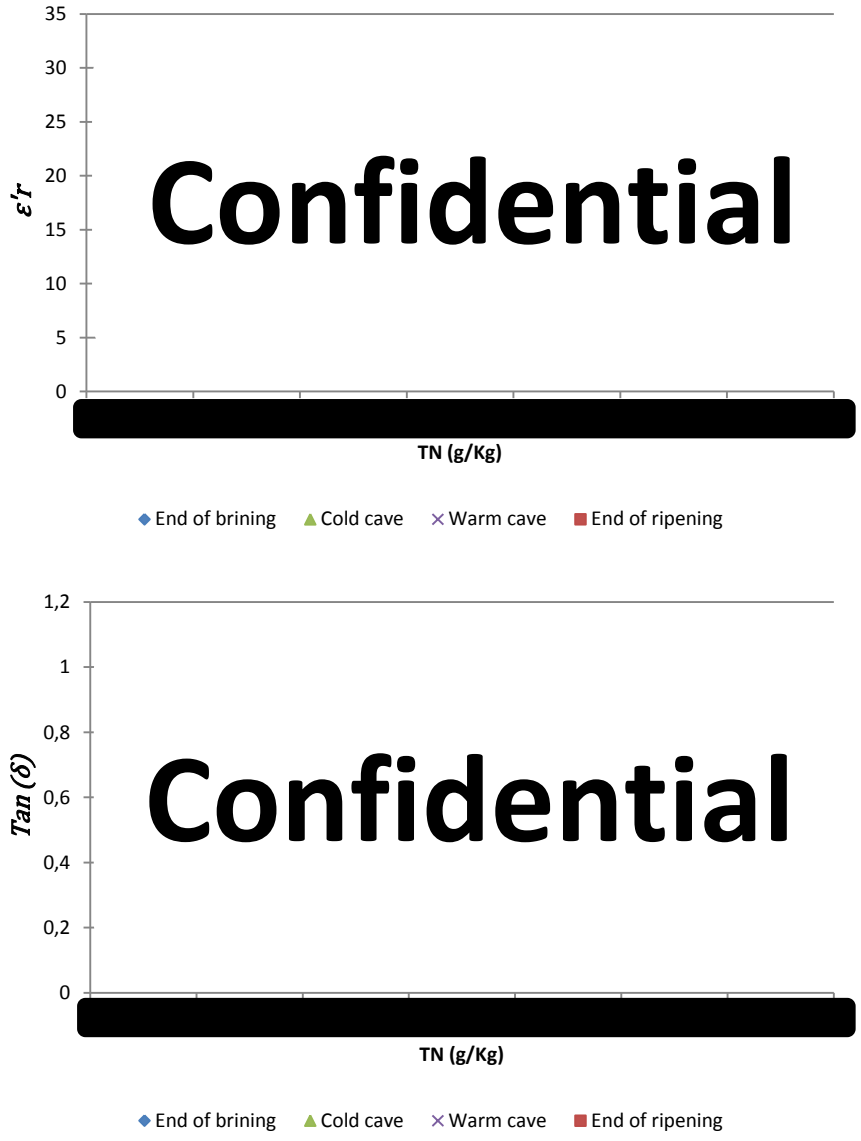

Fig.14 Variation of Emmental dielectric properties during maturation as function of nitrogen concentration

In general, the variation of dielectric properties of Emmental cheese is more correlated to some chemical parameters than other ones. Dry matter, pH and salt concentration are the three main parameters which mostly affect the behavior of dielectric properties of Emmental, whereas the effect of Fat, Calcium and nitrogen are less significant and often negligible.

4.3 Correlation between dielectric and chemical properties of Grimont

A total of three measurements were obtained for Grimont samples as its wheel size is much smaller compared to Emmental. Figures 15 to 20 show the variation of dielectric properties as function of each chemical parameter at start and end of ripening period.

Figure 15 & 16 show a strong correlation between the dielectric properties of Grimont versus the variation of dry matter and fat concentration. It is obvious that the concentration of fat increases with the evaporation of moisture content and thus has similarly strong correlation with the dielectric properties. Compared with Emmental ripened under foil, the dry matter effect is much more significant in the case of Grimont ripened in air which highlights the great effect of packaging on the maturation process.

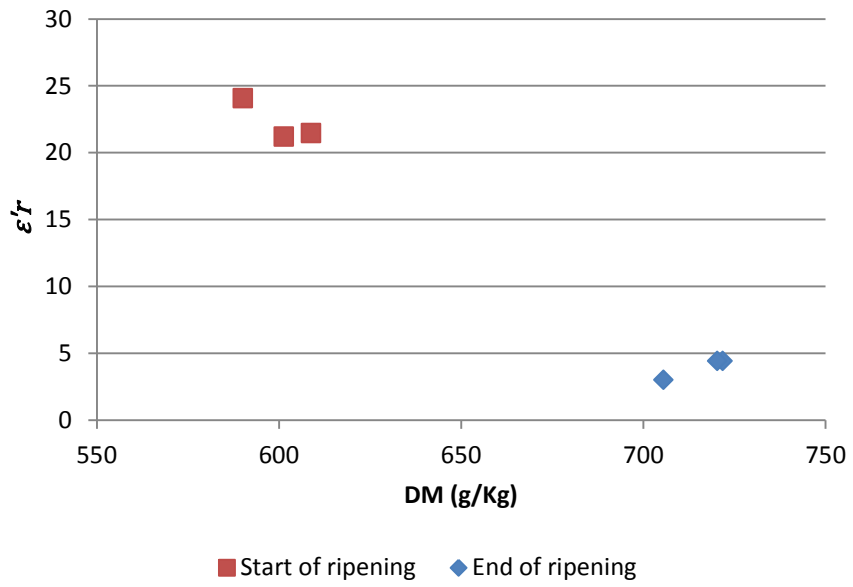

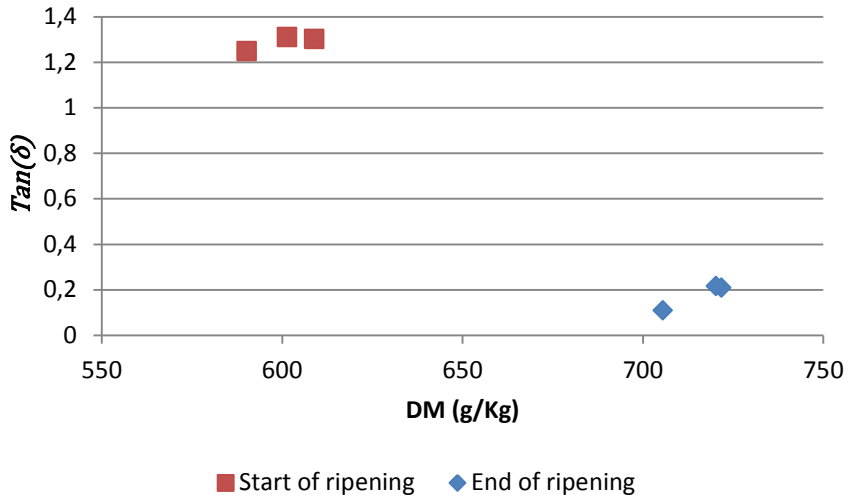

Fig.15 Variation of Grimont dielectric properties during maturation as function of dry matter

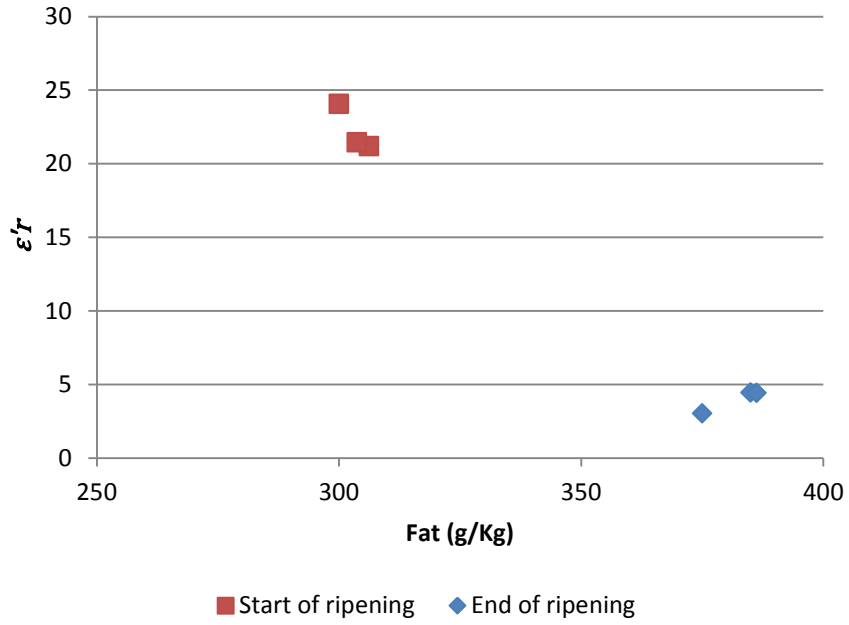

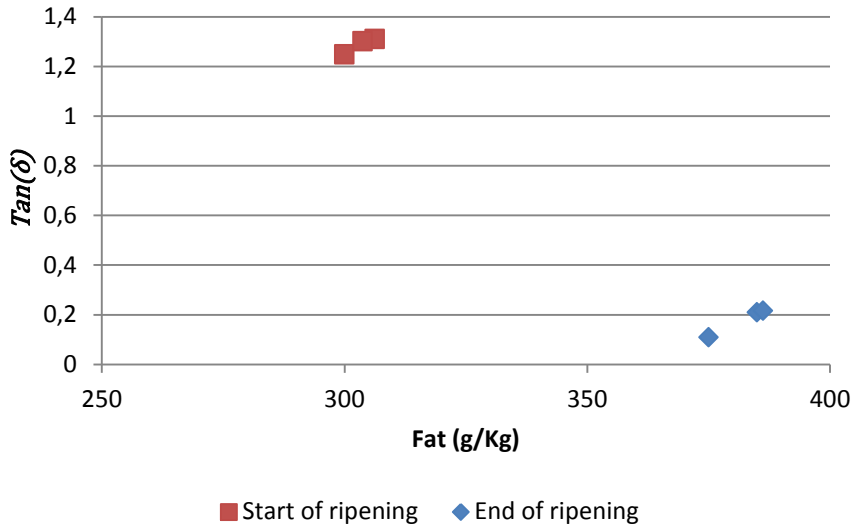

Fig.16 Variation of Grimont dielectric properties during maturation as function of fat concentration

pH and NaCl concentration are two major parameters which affect the dielectric properties of Grimont. Figure 17 & 18 show a stronger correlation with the dielectric properties of this type of cheese compared to Emmental.

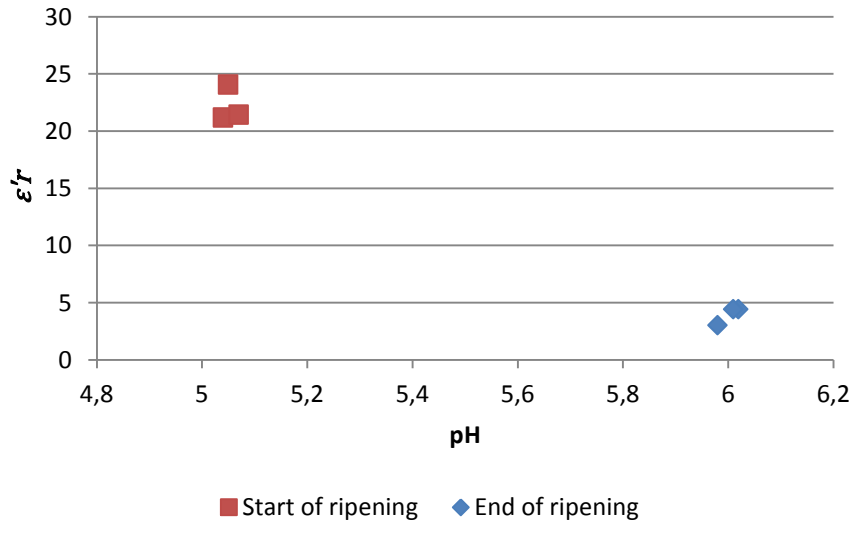

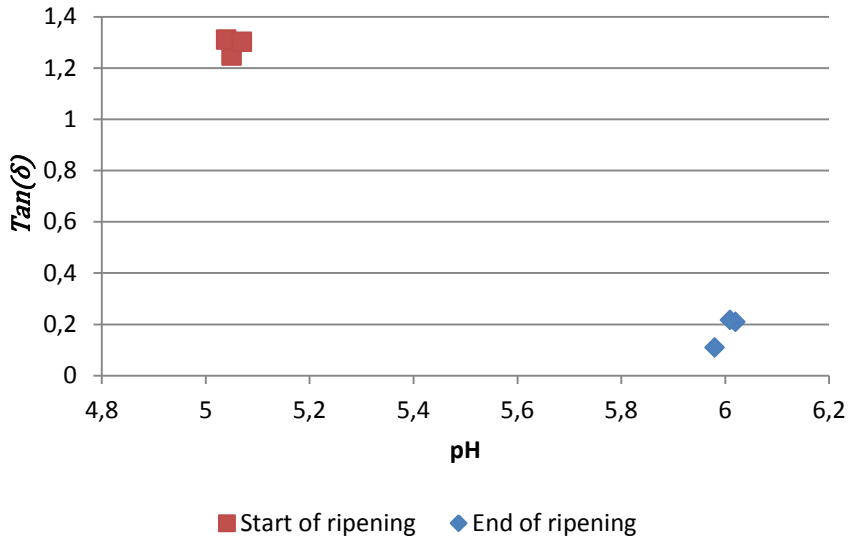

Fig.17 Variation of Grimont dielectric properties during maturation as function of pH

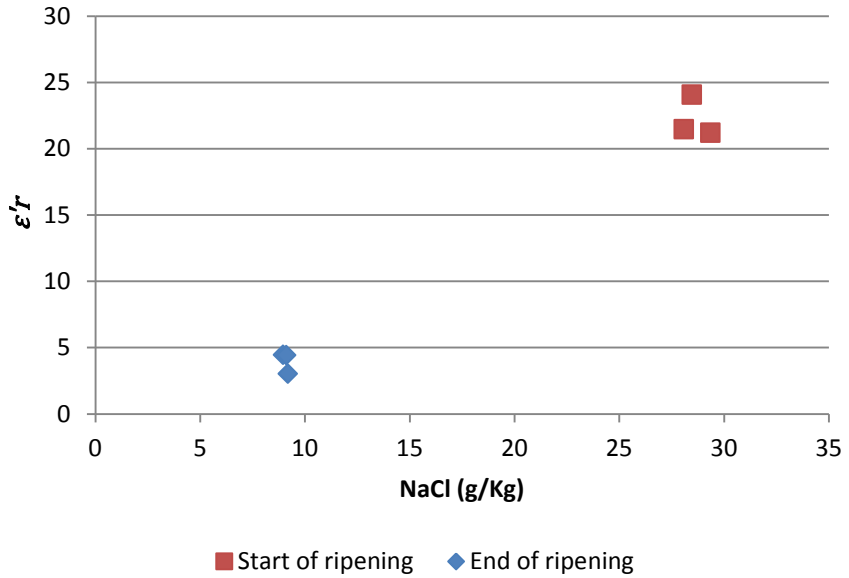

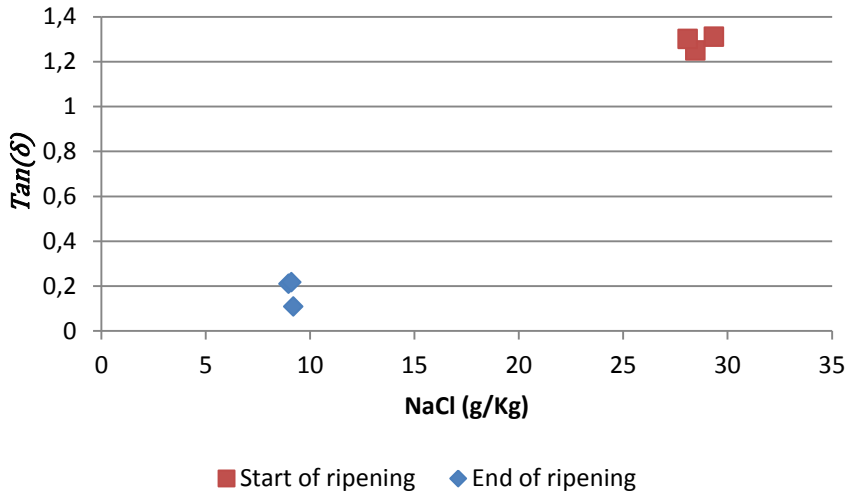

Fig.18 Variation of Grimont dielectric properties during maturation as function of NaCl

Despite the significant correlation of Calcium and nitrogen concentrations with dielectric properties as shown in figure 19 & 20, these parameters have lower effect due to their relatively small variation in grams during maturation compared with the other chemical parameters.

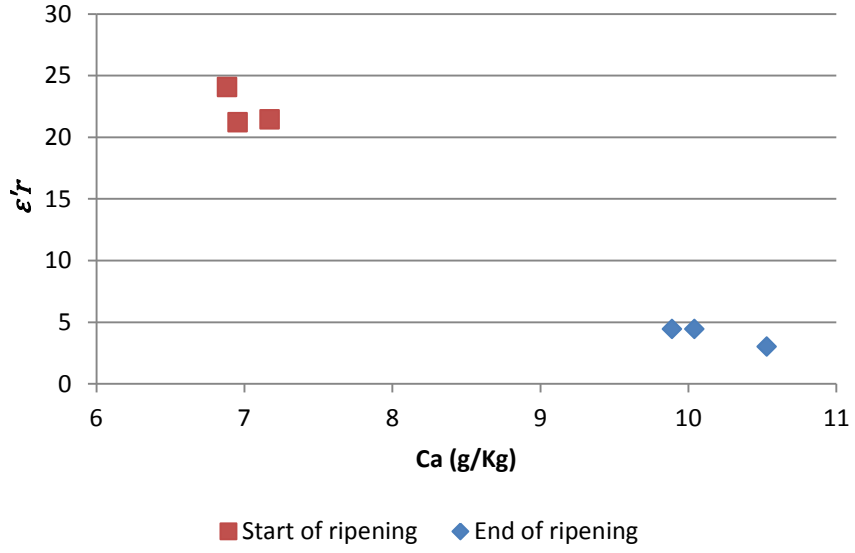

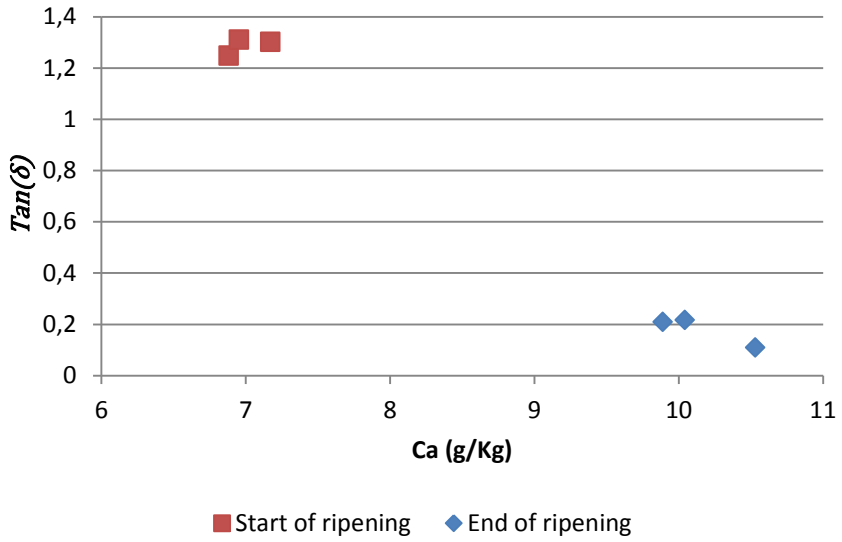

Fig.19 Variation of Grimont dielectric properties during maturation as function of calcium concentration

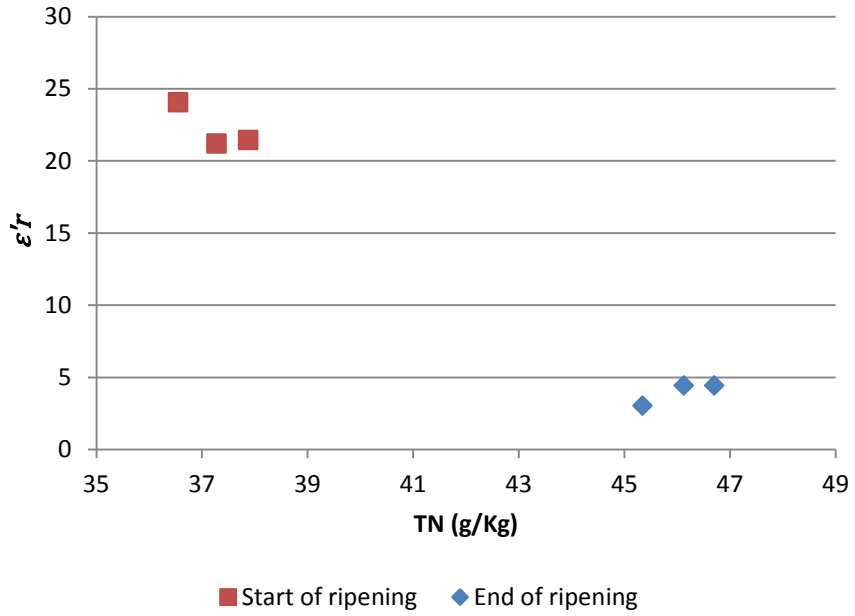

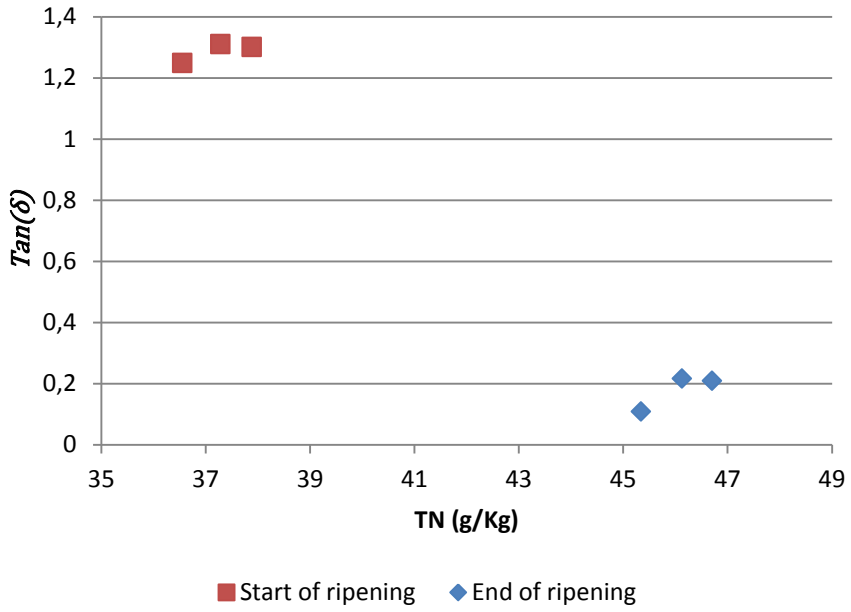

Fig.20 Variation of Grimont dielectric properties during maturation as function of nitrogen concentration

As a conclusion, all three samples of Grimont showed a significantly strong correlation between their dielectric and chemical properties. As in the previous case of Emmental, dry matter, pH and NaCl are the key parameters affecting the dielectric properties of cheese.

4.4 Correlation between dielectric and chemical properties of Morbier

Similar to Grimont, a total of three measurements were obtained for Morbier samples as its wheel size is much smaller compared to Emmental. Figures 21 to 26 show the variation of dielectric properties as function of each chemical parameter at start and end of ripening period. Ripened in similar conditions as Grimont, samples of Morbier showed a quite comparable behavior during maturation where dry matter and fat concentration have significant correlation with the dielectric properties as shown in figure 21 & 22

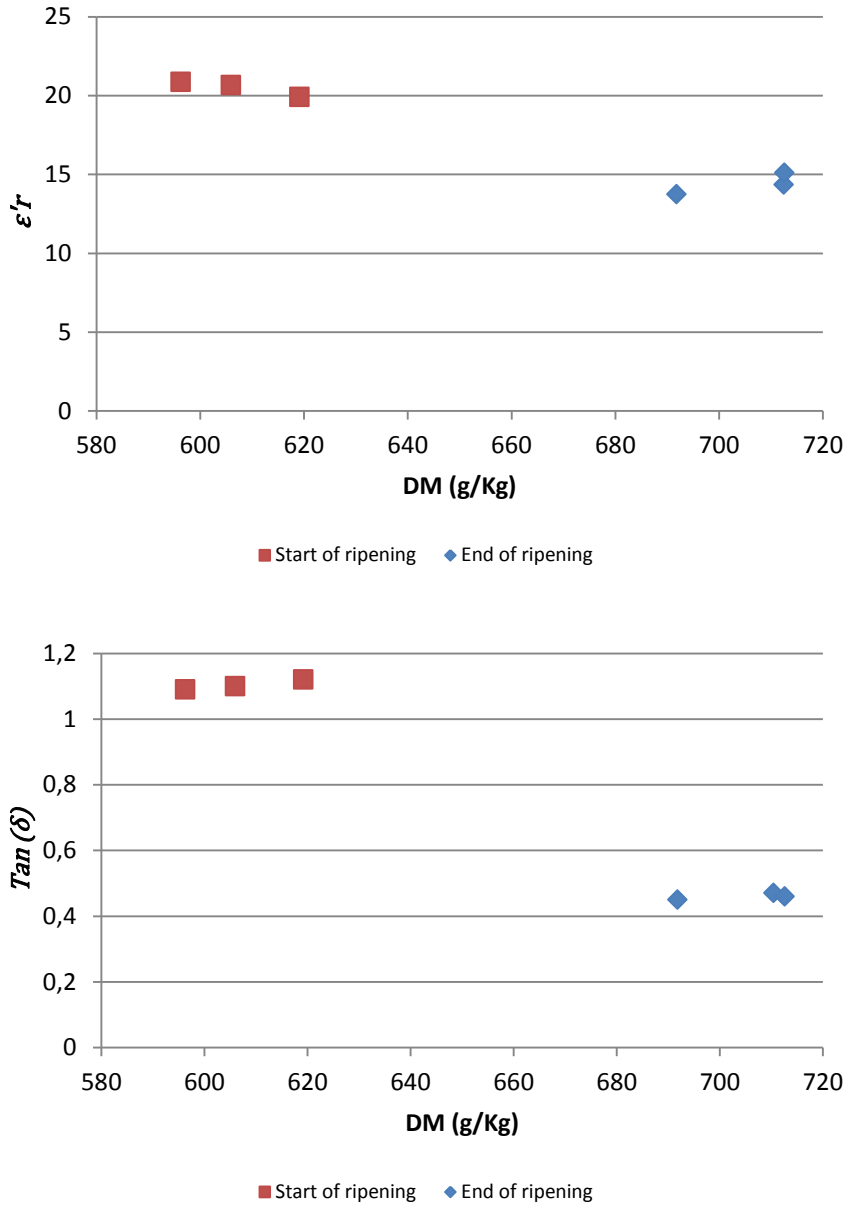

Fig.21 Variation of Morbier dielectric properties during maturation as function of dry matter

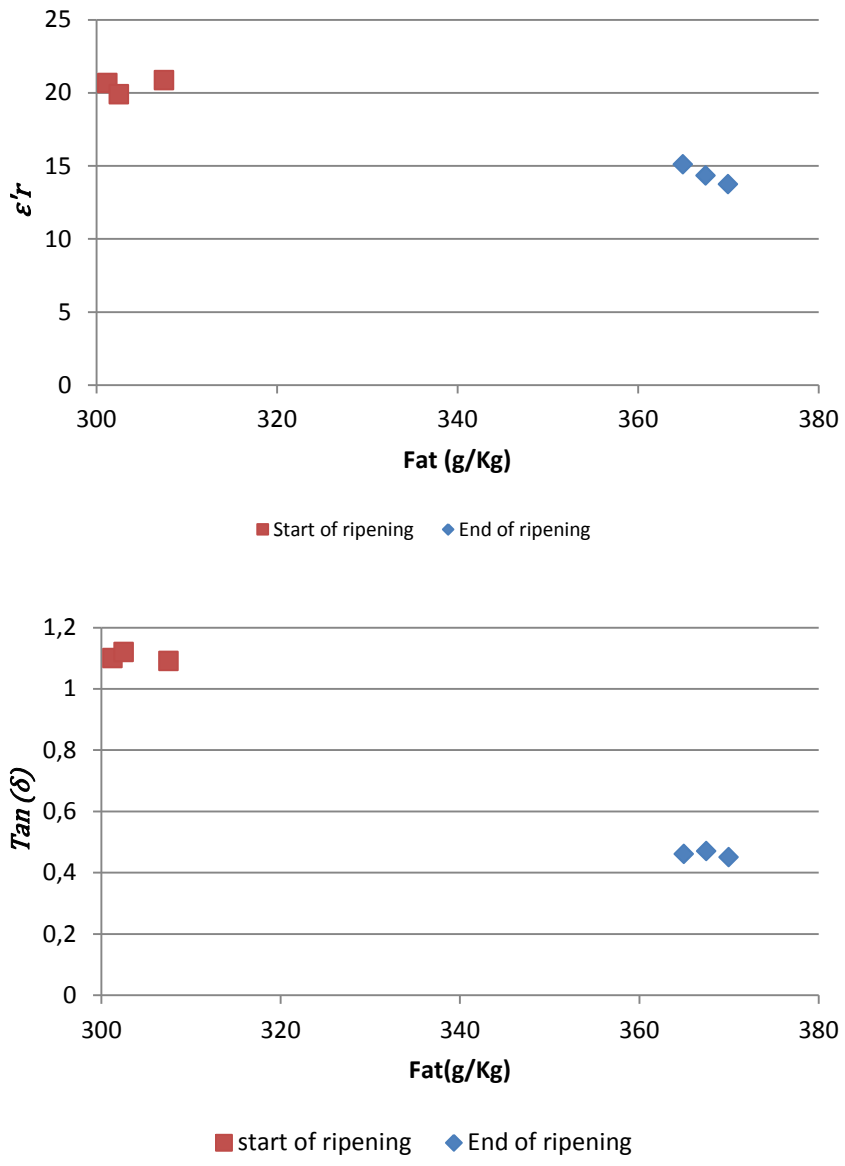

Fig.22 Variation of Morbier dielectric properties during maturation as function of fat concentration

The variation of pH in Morbier samples is quite higher compared to Grimont and Emmental, whereas NaCl showed identical behavior to Grimont as shown in figure 23 & 24 respectively.

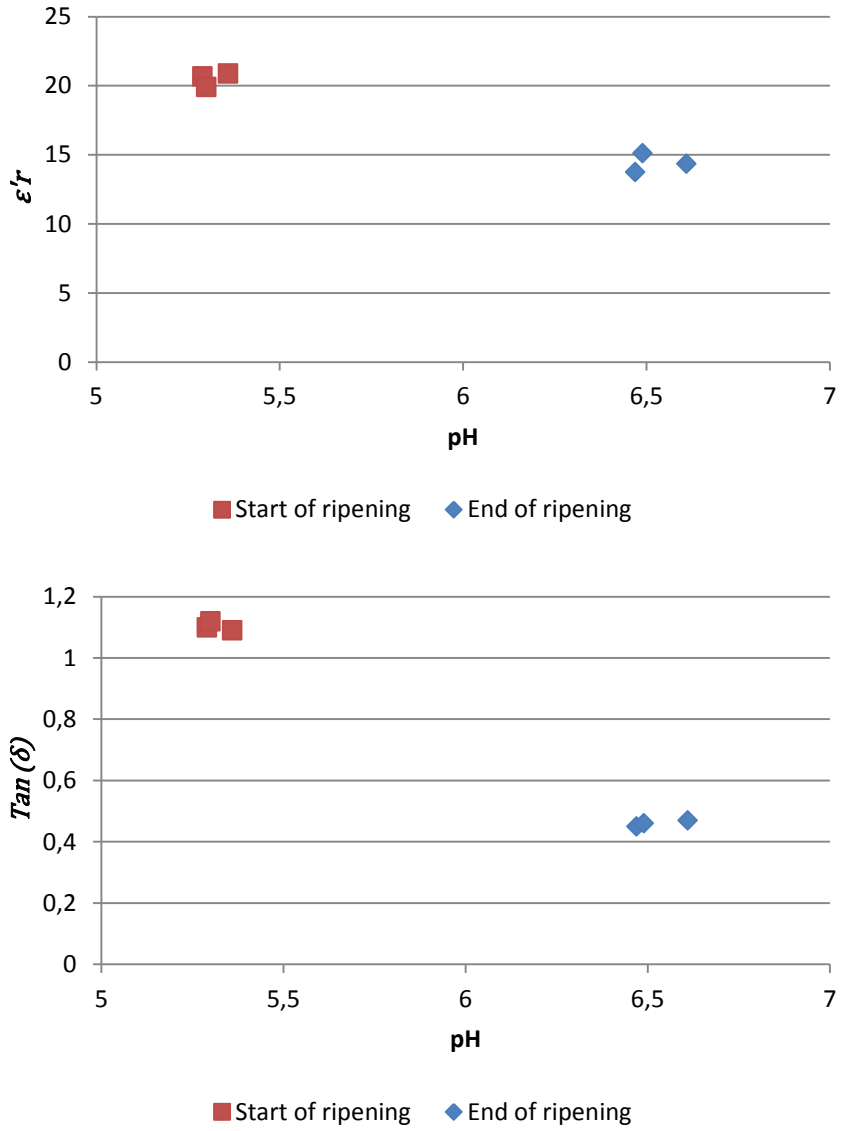

Fig.23 Variation of Morbier dielectric properties during maturation as function of pH

Both parameters have an important effect on dielectric properties. However, the dielectric constant showed lower dependence compared to loss tangent.

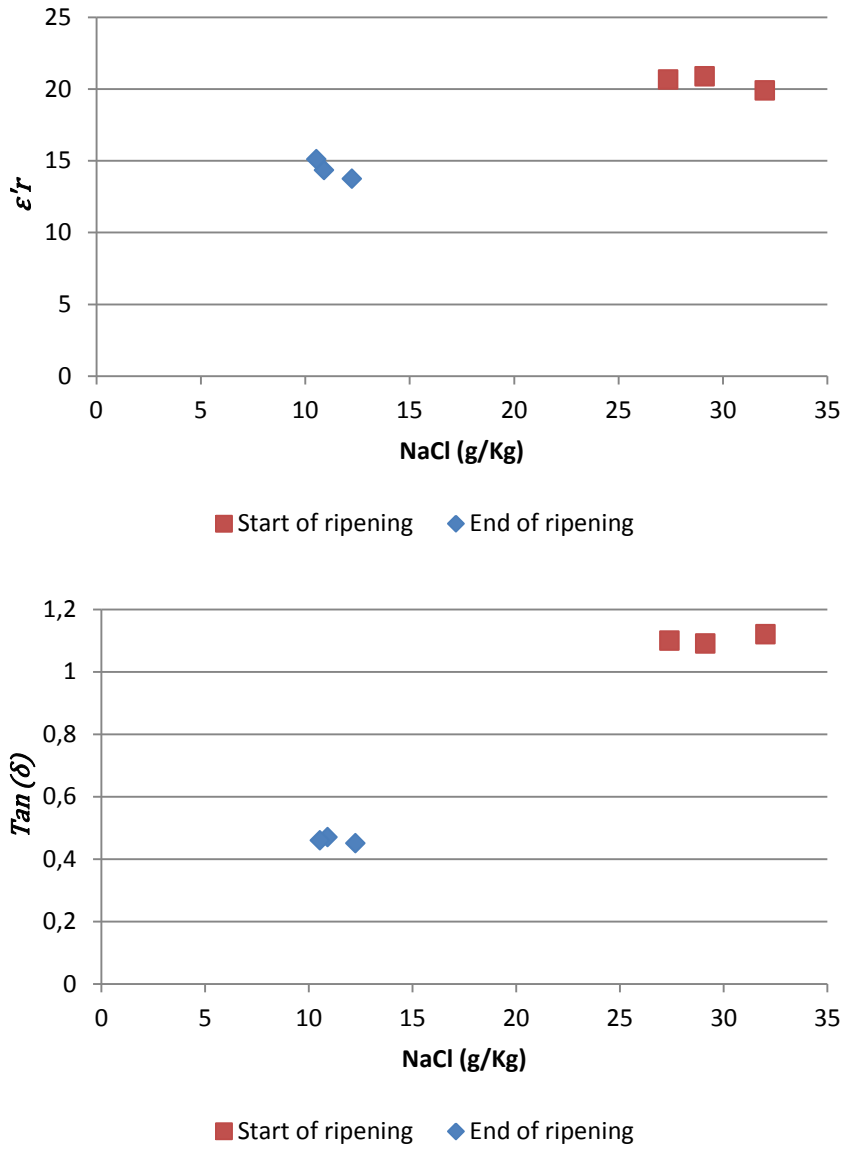

Fig.24 Variation of Morbier dielectric properties during maturation as function of NaCl

Similar to pH, the variation of calcium and nitrogen concentrations is more important in Morbier samples than the other types of cheese as shown in figures 25 & 26 respectively.

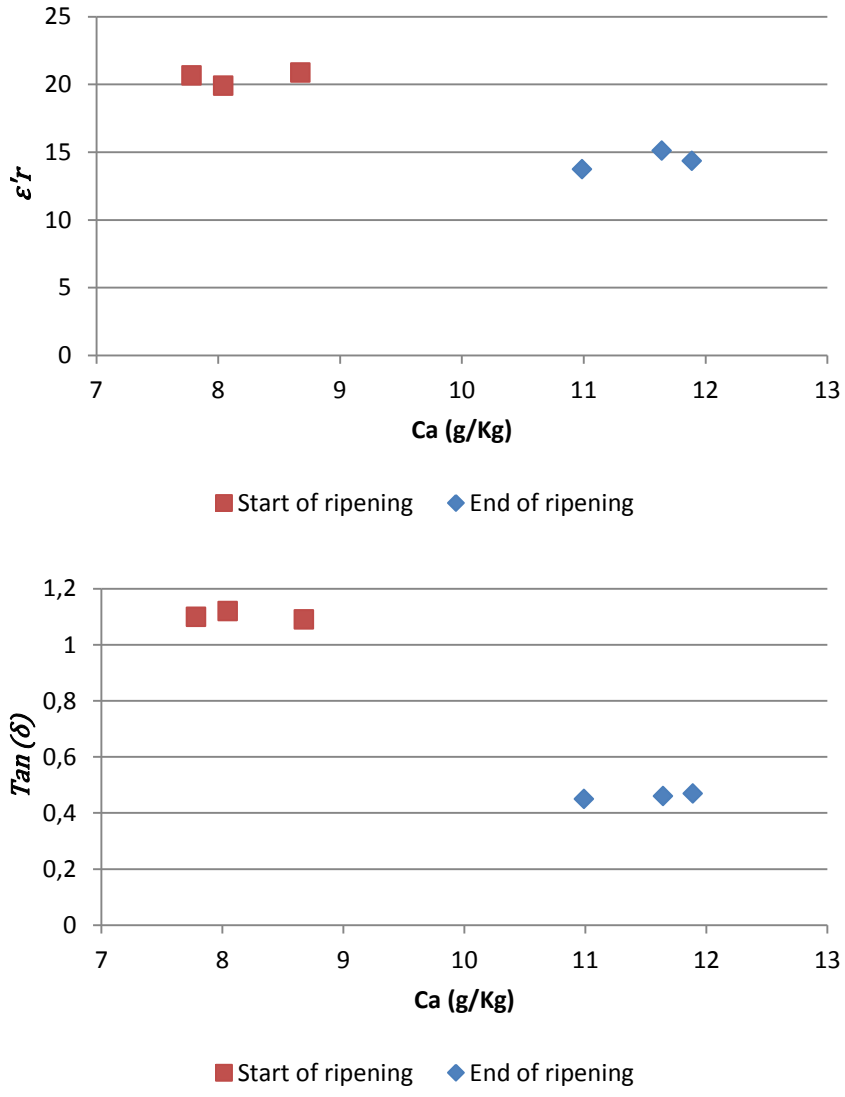

Fig.25 Variation of Morbier dielectric properties during maturation as function of calcium concentration

As their overall concentrations are much smaller than the other parameters, their effect on dielectric properties would be inconsiderable.

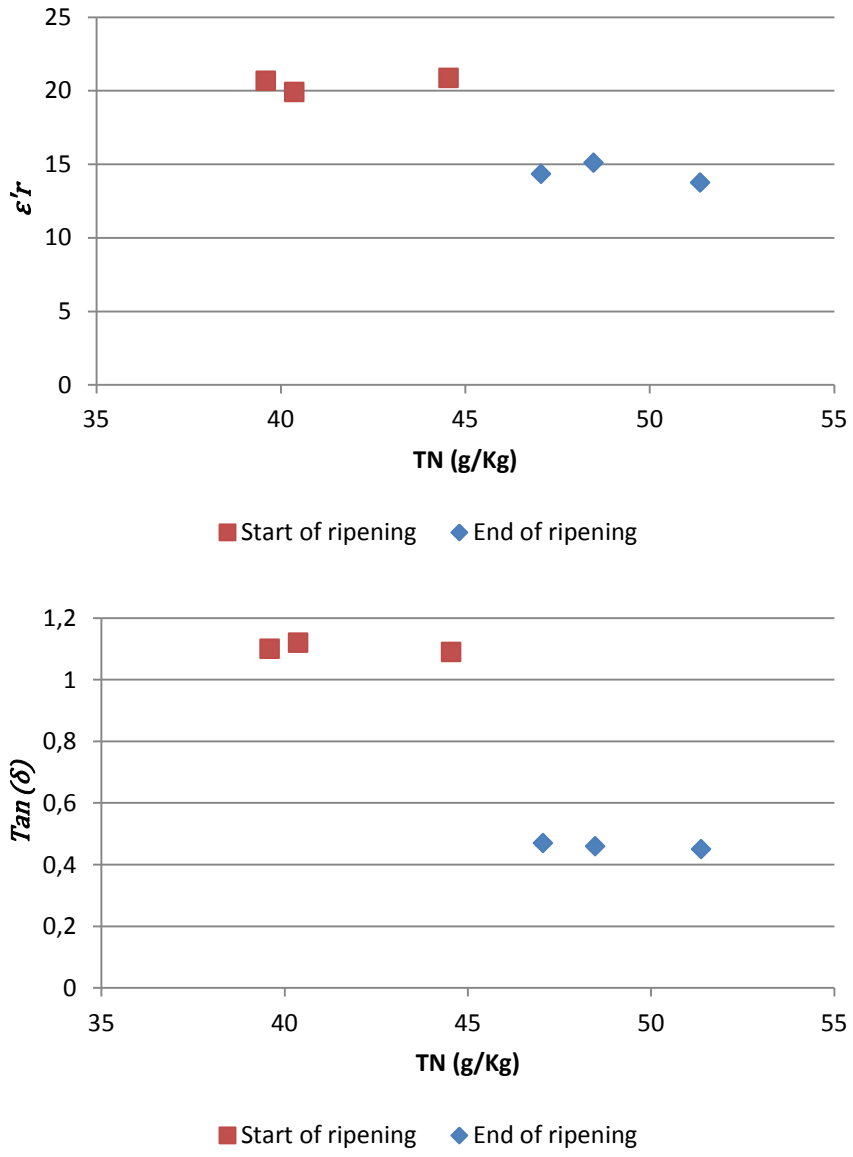

Fig.26 Variation of Morbier dielectric properties during maturation as function of nitrogen concentration

Table 2 summarizes the correlation factors between dielectric and chemical properties as well as the correlation between the chemical parameters of all three types of studied cheeses

Table 2 Correlation factors of dielectric and chemical properties

Emmental							
Parameter	ε	Tan(δ)	DM	Fat	pH	Ca	NaCl
Tan(δ)	-0,400						
DM	**-0,783**	0,453					
Fat	-0,269	-0,069	0,450				
pH	**0,631**	**-0,712**	**-0,603**	0,102			
Ca	-0,432	0,066	0,480	0,152	-0,216		
NaCl	**-0,664**	**0,904**	**0,674**	-0,030	**-0,856**	0,184	
TN	**-0,655**	0,263	**0,779**	0,432	-0,490	**0,587**	0,451
Grimont							
Parameter	ε	Tan(δ)	DM	Fat	pH	Ca	NaCl
Tan(δ)	**0,991**						
DM	**-0,989**	**-0,981**					
Fat	**-0,988**	**-0,985**	**0,997**				
pH	**-0,992**	**-0,995**	**0,994**	**0,996**			
Ca	**-0,994**	**-0,995**	**0,977**	**0,977**	**0,988**		
NaCl	**0,992**	**0,997**	**-0,992**	**-0,994**	**-1,000**	**-0,991**	
TN	**-0,989**	**-0,982**	**0,999**	**0,997**	**0,995**	**0,977**	**-0,993**

Morbier							
Parameter	ε	Tan(δ)	DM	Fat	pH	Ca	NaCl
Tan(δ)	**-0,957**						
DM	**0,923**	**-0,986**					
Fat	0,595	-0,752	0,827				
pH	0,913	**-0,949**	**0,981**	0,787			
Ca	0,855	-0,915	**0,965**	0,848	**0,987**		
NaCl	-0,865	**0,922**	**-0,964**	-0,783	**-0,986**	**-0,968**	
TN	0,752	-0,750	0,792	0,505	0,874	0,869	-0,856

Highlighted cells indicate the parameters with relatively stronger correlation factor compared to the others whereas the sign indicates the sense of variation dependence if it is direct or inverse proportional.

5. Conclusion

This chapter discussed the variation of dielectric and chemical properties performed on samples of three types of pressed cheese during maturation. The dielectric measurements of Emmental samples showed an average variation of dielectric constant around 28% between start and end of ripening process. However, this variation did not exceed 2% between Cold and Warm caves. On the other hand, the average variation of loss tangent was more important between start and end of ripening process (around 36%) due to the diffusion of NaCl from the surface towards the center of cheese during maturation. This variation was much lower between the other ripening stages, reaching around 5%. Despite the significance of the dielectric variations between early and late ripening, it is difficult to exploit because these variations are not repeatable from one sample to another.

A complementary study was realized on two more types belonging to the same family of pressed cheese as Emmental. This study showed that the correlation factors between dielectric and chemical parameters vary differently from one type of cheese to another. Packaging as well as ripening period and conditions play a major role in the variation of dielectric and chemical properties during maturation. Moreover, the development of holes in the texture of Emmental during ripening makes the estimation of dielectric properties more complicated compared to other types of cheese without holes such as Morbier and Grimont. A significantly stronger variation of dielectric and chemical properties is observed in the case of cheese samples ripened in air compared to much weaker variations in the case of cheese maturation wrapped in foil. This is merely due to the effect of evaporation of moisture content which leads to an important change in both dielectric and chemical parameters. For all the three studied types of cheese, dry matter along with the pH and NaCl concentration are the main chemical parameters which affect their dielectric properties.

References

[1] "A la découverte de l'Emmental de Savoie - le secret des fruitières (2) - Mag'cuisine," 25-Nov-2013. [Online]. Available: http://www.magcuisine.fr/archives/2013/11/25/28458996.html. [Accessed: 19-Jun-2018].

[2] "A la découverte de l'Emmental de Savoie - le temps de l'affinage et de la dégustation (3) - Mag'cuisine," 02-Dec-2013. [Online]. Available: http://www.magcuisine.fr/archives/2013/12/02/28459023.html. [Accessed: 19-Jun-2018].

[3] "N1501A Dielectric Probe Kit | Keysight (formerly Agilent's Electronic Measurement)," 03-Mar-2018. [Online]. Available: https://www.keysight.com/en/pd-2492144-pn-N1501A/dielectric-probe-kit?nid=-536902475.1128377&cc=FR&lc=fre. [Accessed: 03-Mar-2018].

[4] "E5080A ENA Vector Network Analyzer | Keysight (formerly Agilent's Electronic Measurement)," 03-Mar-2018. [Online]. Available: https://www.keysight.com/en/pdx-x202208-pn-E5080A/ena-vector-network-analyzer?cc=FR&lc=fre. [Accessed: 03-Mar-2018].

[5] "ISO 5534:2004(en), Cheese and processed cheese — Determination of the total solids content (Reference method)." [Online]. Available: https://www.iso.org/obp/ui/#iso:std:iso:5534:ed-2:v1:en. [Accessed: 23-Jun-2018].
[6] "ISO 3433:2008(en), Cheese — Determination of fat content — Van Gulik method." [Online]. Available: https://www.iso.org/obp/ui/#iso:std:iso:3433:ed-2:v2:en. [Accessed: 23-Jun-2018].
[7] K. N. Pearce, L. K. Creamer, and J. Gilles, "Calcium lactate deposits on rindless Cheddar cheese," *NZ J Dairy Sci Technol*, vol. 8, pp. 3–7, Jan. 1973.
[8] "ISO 5943:2006 - Cheese and processed cheese products -- Determination of chloride content -- Potentiometric titration method." [Online]. Available: https://www.iso.org/standard/43922.html. [Accessed: 23-Jun-2018].
[9] "ISO 8968-1:2014 - Milk and milk products -- Determination of nitrogen content -- Part 1: Kjeldahl principle and crude protein calculation." [Online]. Available: https://www.iso.org/standard/61020.html. [Accessed: 23-Jun-2018].

Chapter 4

Passive UHF RFID tag design steps for cheese traceability

1. Introduction

In the food industry, an efficient and effective system transmitting accurate, timely, complete, and consistent information about products through the supply chain can significantly reduce operating costs and can increase productivity. At the same time, such a system contains many product safety elements which make consumers safer by providing detailed information about where an item comes from, what its components and origin are, and about its processing history. In this context, RFID systems could be exploited for traceability as well as chain management and logistics improvements to guarantee the highest level of traceability efficiency in terms of quality and safety. However, RFID adoption is rarely deployed in the cheese industry, and cheese traceability is generally managed and documented by written records.

This chapter presents the main legal and regulatory aspects of cheese traceability and discusses the advantages of UHF RFID systems compared to

conventional methods applied in the cheese production sector. Then, the design steps of an UHF RFID tag are explained in detail including the selection of substrate material approved for food contact, selection of the RFID chip and measurement of its impedance, simulation of physical variations during ripening and the realization of final prototypes. Several UHF tag topologies are designed and a comprehensive comparison of their read ranges on different types of cheese is presented.

Finally, the installation of tags during cheese fabrication process is described and an improved detection technique of randomly oriented tags is discussed.

2. Regulations and conventional methods

2.1 Traceability regulations in the cheese industry

Regulation (EC) No. 178/2002 of the European Parliament and of the Council of 28th January 2002 sets the general principles and requirements of food law and it defines traceability as “the ability to trace and follow a food, feed, food-producing animal or substance intended to be, or expected to be incorporated into a food or feed, through all stages of production, processing and distribution” [1]. The focus on traceability today is based on automatic data acquisition technologies, in order to allow the maximum of information flow management.

A product traceability system requires the identification of all the physical entities, locations and dates from which the product originates, that is to say, where and when the product is processed, packaged, and stocked, and so this includes every agent in the supply chain. Nowadays, technical and operative resources available are fundamentally alphanumerical code, bar code, and radio-frequency identification (RFID).

2.2. Alphanumerical codes

In order to mark the production information on cheese wheels, the sector of cheese production uses particular types of stamps or/and casein plaques enhanced with alphanumerical codes. Throughout the cheese ripening, these marks can be affected by the environmental conditions such as temperature, moisture, product handling (mechanical movement like turning) and shape evolution which can reduce the readability of these labels, as shown in figure 1. It is for this reason that

the production and quality control are for the most part performed by bunches and the information stockpiling is done manually by the company personnel [2].

Alphanumerical codes are a sequence of numbers and letters of various sizes placed on labels. They provide information of great importance for the cheese making industry by indicating the product's country of origin, region, cheese type and date of fabrication as well as quality and certification markers. The design phase of this system is very simple and economic, but its management requires significant human resources (and so cost) because code writing and code reading are not automatic. Furthermore, performance is not particularly good: there are many problems associated with the large amount of managed manually data. Not to mention the high risk of data integrity corruption and security breaches.

Fig. 1. Casein labels used for the cheese identification where the production information is unclear due to moisture and polishing.

Another major drawback is that no standards are defined for alphanumerical codes. These codes are generally developed by the owners, which makes this technique limited and unpractical over large scale as there is a unique and not standard tie between the different actors (raw material suppliers, manufacturers and distributors).

2.3. Barcode system

Today, alphanumerical codes are not frequently used because barcodes offer several significant advantages. Indeed, optical barcodes are very popular and commercially successful to identify items and automate checkout systems. Barcodes which represent data by varying the width and the spacing of some parallel lines are used in many other applications as automatic identification and data capture (AIDC). The automation, the high speed, the great precision guaranteed by a barcode structure permits simpler, more economical, and exact traceability systems. More and more industries, especially in the retail sector, use barcodes as a principal means of identifying items.

In a barcode system, each time items are moved from one point to another, their barcode labels must be positioned in a way that they can be detected and identified properly by the optical reader as shown in figure 2. This characteristic, often called line of sight positioning, requires time and effort for the scanning process and so there is room for error and inefficiency.

Fig. 2. Cheese traceability system based on Barcodes [3]

Besides their limitations in terms of reading distance and identification by family, not per item, they can be easily damaged (optical damage) which makes barcodes less attractive to the food sector, and their application is consequently limited.

2.4. RFID system

In addition to barcode technology, RFID systems are recently applied in the food sector. RFID tags are very small (a few millimeters reading distance) and they have no compatibility problems with foods. The tag is an isolated system, its materials can be aseptic and food compatible. The radio wave used for communication between tags and traceability database needs very little power, so electromagnetic interaction is practically non-existent [4].

Previous works discussed the benefits of using RFID tags for the traceability of dairy products [2], [5], [6]. Compared to alphanumerical casein labels and barcodes, RFID systems present some potential benefits like efficiency improvement with the increased speed of operations, increased accuracy of information, minimized labor cost and better inventory outcome.

With a specific reference to the cheese sector, RFID is a very promising system because it has several features compared to other conventional methods:

- It allows continuous monitoring of any item throughout the entire maturation process which has a great effect in reducing wastes.
- Based on identification per item not per family as barcodes, RFID systems are more efficient to react to any quality problem as it is possible to track and find only defective products.
- It allows improving management of product recalls and help producers and distributors to minimize damage.
- Being a major player in Internet of Things (IoT), RFID permits to easily convey products information to Internet on a web platform in order to become available to different end users [7].

However, the majority of the existing traceability systems used HF tags which are very limited in reading range (few centimeters) [7]. In an industrial environment, cheese wheels are kept in huge caves for maturation as shown in

figure 3. In such an environment, tracking each item using HF tags is very time-consuming making HF RFID, just like optical barcode,not practical for cheese wheels tracking.

Fig. 3. Thousands of cheese wheels kept in a huge cave for maturation [8]

On the other hand, an UHF RFID system offers more advantages:

- A relatively longer read range compared to HF tags, that could be in meters
- Comply with the global, universally adopted UHF Gen2 Class1standard (EPC global Gen2 ISO 18000-63)
- Lower costs of labels in comparison to HF labels in a large production scale.
- Good performance in data transmission and in environments with high tag density.

Therefore, using an UHF RFID system is an interesting alternative that will mainly reduce the time for identification and information storing during the cheese production process.

The following sections describe the design steps of UHF tags and present different tag topologies compatible with food safety regulations and constrains of cheese traceability in an industrial environment.

3. Passive UHF RFID tag design steps

The objective is to design a tag for the traceability of the cheese wheels during the different stages of ripening and which is appropriate with the constraints of the food products.

The main design steps of an UHF RFID tag are:

3.1 Choice of substrate material

The labels used for traceability in the food sector should be compatible with norms and regulations of food safety. According to the European Food Safety Authority, *food contact substances* is defined as “any substance that is intended for use as a component of materials used in manufacturing, packing, packaging, transporting, or holding food.”. The framework regulation (EC) No. 1935/2004 [9] contains general safety requirements and determines all food contact materials. In cheese production sector, casein is the common material used for fabrication of labels for cheese traceability. Casein labels are used to mark batch number, date, separation between specific experimental batches, etc. They are produced from the milk protein casein so they become part of the rind. There is no adhesive as the whey in the cheese acts as one [10].

However, casein is not a common material for RFID tag realization and thus other materials should be used. Plastics such as Polyethylene Terephthalate (PET), Polypropylene (PP), and Polycarbonate (PC) are among the list of safe materials for food contact and can be used for tag fabrication as well as encapsulation. Recently, biodegradable materials such as PolyLactic Acid (PLA) are widely used for food packaging in order to reduce plastic wastes and can also be used as a flexible substrate for RFID tag fabrication [11].

3.2. Dielectric characterization

As discussed in previous chapters, dielectric characterization of materials is an essential step for efficient tag antenna design in RFID systems. The dielectric constant of the substrate mainly affects the antenna resonance frequency whereas

the loss factor affects the antenna radiation efficiency. The choice of measurement technique depends on the texture of material (Solid, Semi-solid or liquid) as well as its size (large samples or thin sheets). Figure 4 shows example of the methods used for characterization of different materials. For cheese characterization, an open-ended coaxial probe is used as it can penetrate inside cheese texture and easy to handle compared to the resonant cavity method which suits better thin and uniform substrates such as plastics.

a *b*

Fig. 4. Different characterization methods a) dielectric characterization of cheese using a coaxial probe b) characterization of thin sheets of casein in a resonant cavity

Table 1 summarizes the measured dielectric properties of casein and polypropylene that are compatible materials for tag fabrication. Three measurements were realized by a resonant cavity for each sample and average values of dielectric properties correspond to the UHF RFID frequency of 866 MHz.

Table.1 Dielectric properties of casein and polypropylene

Material	ε_r'	Tg (δ)
Casein	**5,85 ± 0.2**	**0,24 ± 0.03**
Polypropylene	**2,74 ± 0.05**	**0,005 ± 0.001**

3.3 Chip selection

Recently, there are a lot of commercially available UHF RFID chips provided by many manufacturers. However, for a specific application, there is always a trade-off between many factors such as chip sensitivity, available memory, chip packaging (wafer type or SMD), sensing capabilities (temperature sensing, analog entries), serial bus for communication with µc (I^2C or SPI) and cost.

In order to provide an efficient solution for cheese traceability, chip sensitivity and memory are the two most important parameters which affect the choice of a RFID chip. In order to reach the longest distance possible, the selected chip should have a very high level of sensitivity.. Moreover, the chip should have a reasonable memory size to store all required production data.

Table 2 presents a comparison between the most recent RFID chips used for identification based on chip Read and Write sensitivity as well as available memory and average price.

Table.2 Comparison between commercial RFID chips

Type	EPC (bits)	User Memory (bits)	Sensitivity Read/Write (dBm)	Average price in $ per 100 tags
Impinj Monza R6	96	NA	**-22,1/ -18,8**	65
Impinj Monza 5	128	32	-20 / -16	73
Impinj Monza 4D	128	32	-22/ -16,7	79
NXP UCODE 7xm+	448	**2 K**	-19 / -12	NA
NXP UCODE 7xm	448	1 K	-19 / -12	89
NXP UCODE 7m	128	32	-21 / -16	NA
NXP UCODE 7	128	NA	-21 / -16	64
Alien Higgs-4	128	128	-20,5 / x (Read only)	**57**
Alien Higgs-3	96-480	512	-20 / x (Read only)	60

Based on this comparison, the chip MonzaR6-P was considered for the design of tags for two main reasons. First, Monza R6-P has the highest sensitivity (-22 dBm) compared to the other chips and thus tags based on this chip can be detected at longer distances.

The second reason is due to a unique feature in this chip based on auto-tuning capabilities [12] which allow the chip to reach its maximum performance under variable conditions. These variations can be due to change in substrate characteristics with time or due to some defects in antenna realization. Therefore, this unique feature adds a lot of flexibility in the design of tags specially for food traceability applications. Figure 5 shows the variation of real and imaginary impedance as function of the input capacitance value.

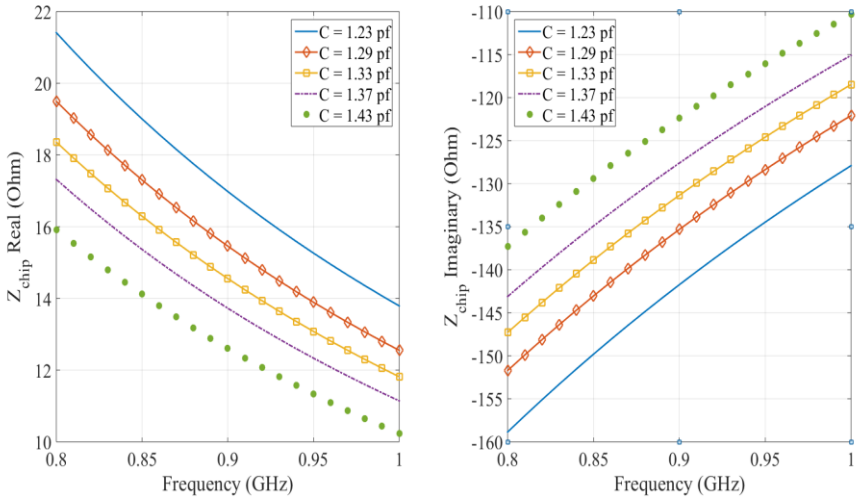

a b

Fig 5. Simulation results of Monza R6_P chip impedance variation due to auto-tuning according to the datasheet RC model a) Real b) Imaginary

The auto-tune feature can be enabled or disabled by setting a specific bit in the memory. When the auto-tune disable bit is zero, auto-tune works as normal. When the bit is one, auto-tune is disabled and the capacitance on the front end assumes the mid-range value (1.33 pf). According to simulation of input capacitance variation, the real part of chip impedance can vary between (13.58 Ω to 18.28 Ω) whereas the imaginary part vary between (-126.92 Ω to -146.97 Ω).

The main drawback of Monza R6 is its limited user memory (64 bits max) compared to other chips as MonzaX-2K or NXP Ucode 7m which have larger memories. However, the EPC bank can be used in combination with the User memory which allows using 96 more bits for storing data. Based on cheese traceability requirements, a total of 160 bits is quite reasonable.

Another tag configuration studied in this work is based on coupling of a near field RFID module (AK tag) to an external antenna like a dipole or meander antenna. The AK tag principle is inspired from the famous T-Match technique where a simple loop compensates the capacitance of the RFID chip while the two branches of the dipole or meander line increase the radiation resistance as shown in figure 6. The main advantage of this configuration is its quite easy realization as the AK tag is just coupled to the antenna without the need to solder the RFID chip where the strength of the coupling is controlled by the distance between the loop and the radiating body [13].

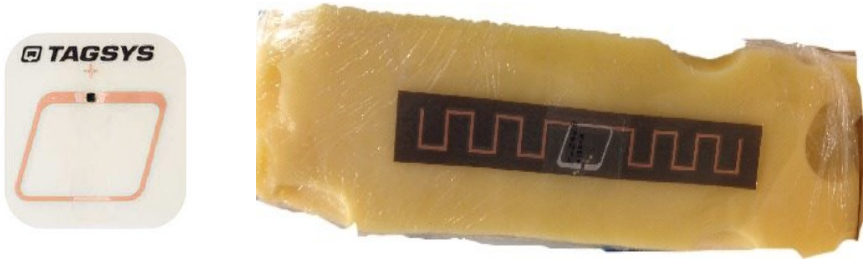

a *b*

Fig. 6. Tag configuration based on coupling a) AK tag module b) AK tag coupled to a meander antenna

3.4 Chip impedance measurement

All datasheets provide the RC model of the RFID chip or the value of its complex impedance at a specific frequency from which the chip impedance over a larger band of frequency can be calculated. However, there is always some uncertainty due to the mount parasitic or difference in chip packaging. In the case of Monza R6-P, it is already mentioned in the datasheet an approximate value of parasitic capacitance due to mounting in the range of 0.2 pf. This value is estimated based on wafer packaging of the chip which is different from the packaging used in this

study provided by murata [14] and thus the chip impedance should be measured in order to obtain more accurate results.

In order to design an efficient antenna, the chip impedance was measured using a vector network analyzer as shown in figure 7. However, most of the network analyzers and other measurement instruments are terminated by asymmetric ports (coax, SMA). Thus, reflection coefficient measurement of a balanced structure such as a RFID chip can-not be directly performed using a network analyzer. One of the most common ways of eliminating this problem for balanced structures is to use a balun. A balun is as a balance un-balance converter (basically a transformer), which can provide a differential signal at its output port.

With a differential measurement setup, a symmetric feed is realized. Two semi-rigid cables whose outer conductors are soldered together and the inner conductors are soldered to the chip pads form the differential probe (Fig.7.b).

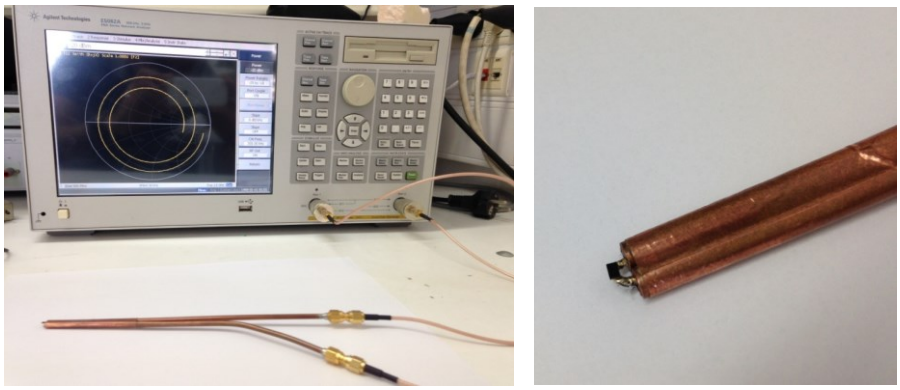

a *b*

Figure 7. a) Measurement setup b) Balun used for balanced impedance measurement

The testing fixture used in the measurement process also induces additional parasitic effects; accurate measurement cannot be achieved without taking the fixture impact into consideration. The fixture effects can be compensated by port extension to carry out the calibration plane to the end of the test probe. Another method is to de-embed these effects by post-processing. In this work, the delay introduced by the balun was de-embedded using post-processing. First, the balun is

measured in “open configuration” where each branch is connected to one port on the VNA and its S-parameters are saved under S2P format. The S2P file is then imported in Ansys designer in the model shown in figure 8 where the block TD presents the time delay (in seconds) that will be tuned to decompensate the fixture effects.

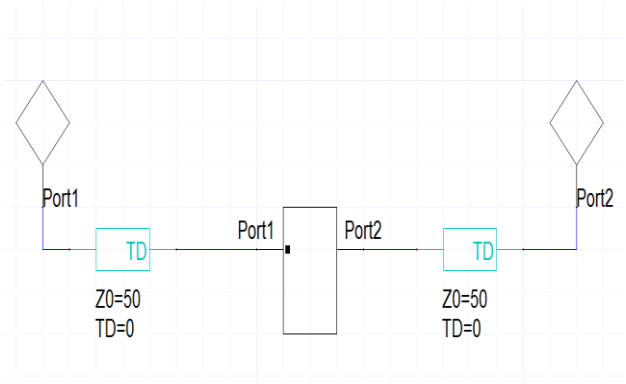

a

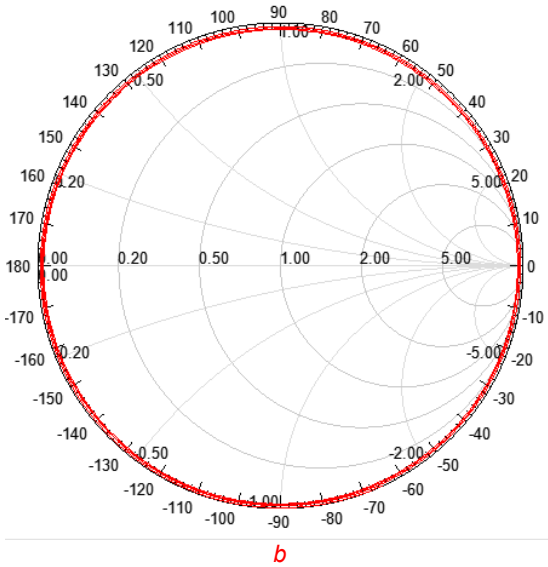

b

Fig. 8. a) S parameters analysis model in Ansys designer b) Measured S parameters at one port on Smith chart before de-embedding the delay introduced by the balun.

Then, the time delay block for each port is tuned until the delay introduced by each branch of the balun is removed as shown in figure 9. The delay introduced can be slightly different from one branch to another depending on their physical lengths.

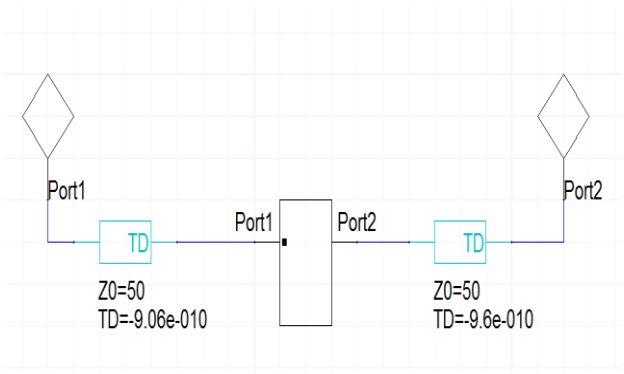

a

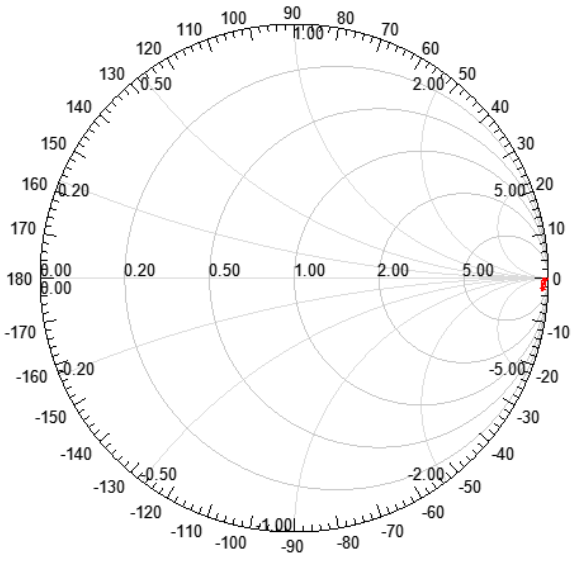

b

Fig. 9. a) S parameters analysis model in Ansys designer b) Measured S parameters at one port on Smith chart after de-embedding the delay introduced by the balun

The RFID chip is then soldered between the two inner conductors of the balun (Fig.7.b) and measurements are repeated. The new S2P file is imported to the Ansys *S*-parameters model and the chip complex impedance is extracted. In order to measure the chip impedance at the activation mode, the input power must be higher than the sensitivity level of the chip, however, the chip impedance will also vary as function of the input power. To study the effect of input power, the impedance of chip Monza-R6 was measured over a frequency band of 200 MHz (from 800 MHz to 1 GHz) at 4 power levels (-20 dBm, -10 dBm, 0 dBm, and 10 dBm).

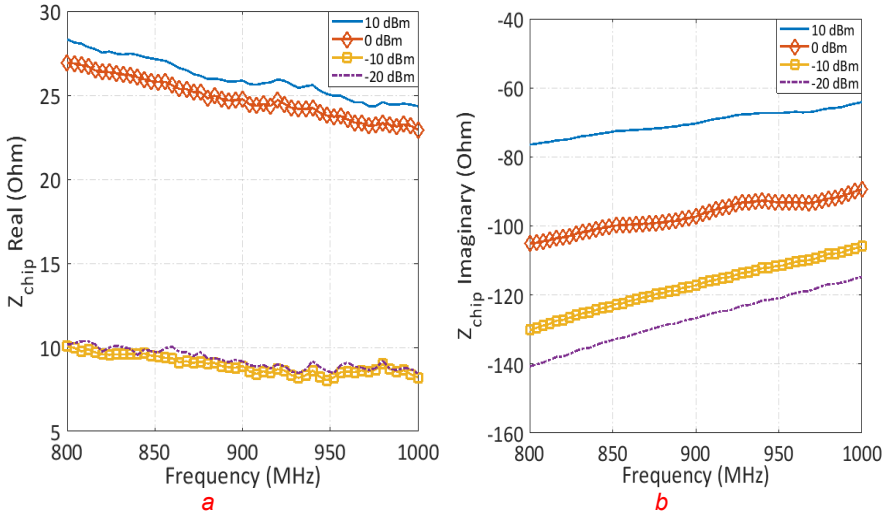

Fig.10. Measurement of Monza-R6 impedance at 4 power levels a) Real b) Imaginary

The real part of the chip impedance is around 10 Ohm at 866 MHz for a low power level (-20 dBm) and the imaginary part is around -132 Ohm. Big variation is noticed at higher power levels (0 & 10 dBm) as shown in figure 10. In general, the value of the RFID chip impedance provided by the datasheet (13 – j 127 ohm) is measured at an input power near the chip sensitivity or the lowest activation power which corresponds to the case of maximum read range of the tag. Therefore, the value of chip impedance measured at -20 dBm (10 –j 132 ohm) is used for design and simulation. This slight difference between the datasheet impedance and the measured one prove the feasibility of this method of measurement.

3.5 Tag antenna design and simulation

All previously discussed design steps are concluded in the design and simulation of the RFID tag antenna. Dielectric characterization of fabrication materials along with good selection of the RFID chip and accurate impedance measurement lead to a robust and effective tag design. The main objective of antenna simulation is to realize a good compromize between impedance matching and antenna gain leading thus to the optimal tag performance. Also, it allows better understanding of antenna radiation behavior when it is in contact with several substrate materials which helps selecting the appropriate design configuration for each application.

4. Different UHF RFID tag topologies for cheese traceability

This section introduces some design topologies dedicated to cheese traceability as they take into account the properties of cheese as substrate during different stages of the production chain. They are designed with the objective to allow tag reading at acceptable distance during the maturation process. Therefore, different UHF tag antenna designs are studied and the realized prototypes based on Monza R6-P were tested and measured showing the possibility of reaching a read range of several meters.

4.1. Tag on a polypropylene substrate

A French company specialized in the fabrication of labels for dairy products developed a traceability solution based on barcodes [15] which are realized on casein and polypropylene as shown in figure 11. A polypropylene label is easily recyclable and offers excellent resistance to water and chemicals which makes it compatible with food product constraints. This configuration can also be used to realize UHF RFID tag where the tag antenna is separated from the cheese surface by the casein and polypropylene layers, which turns in noticeable improvement of the tag performance as the read range is significantly increased.

A polypropylene substrate and a casein patch of 1 mm and 0.36 mm thicknesses respectively were considered for the simulation. The dielectric properties of polypropylene and casein were characterized at UHF RFID operational band using a

resonant cavity where dielectric constant and loss tangent of polypropylene are 2.74 and 0.005, respectively whereas casein has a higher dielectric constant of 5.85 and presents a loss tangent of 0.24 as previously mentioned in table 1.

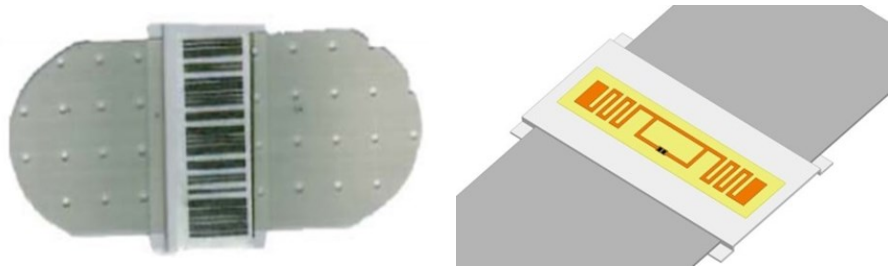

a *b*

Fig. 11. a) Barcode on casein and patch of polypropylene [10] b) 3D model of RFID tag on a substrate of polypropylene

The tag antenna was simulated on a substrate of cheese with ε_r'= 21 and $tan(\delta)$= 1. The design is based on a meander line antenna and the layout of the optimized RFID UHF tag on polypropylene is shown with detailed dimensions in figure 12 where the tag has a total area of 4.5 cm x 1.07 cm.

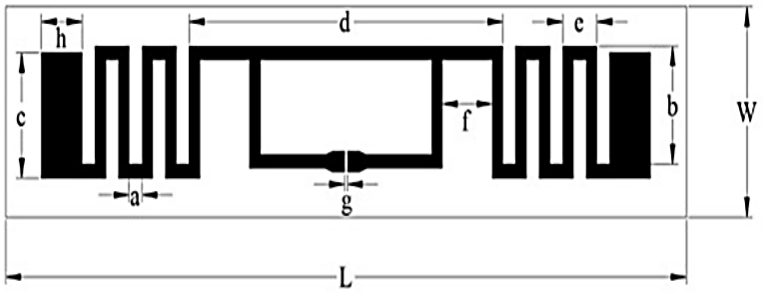

Dimensions (mm)	a	b	c	d	e	f	g	h	L	W
Tag Polypropylene	0.85	6	6.35	20.7	2.25	3.3	0.3	2.7	44.9	10.7

Fig. 12. The layout of the RFID tag on polypropylene.

Indeed, RFID tag read range is defined as the maximum distance at which the tag can be read. It depends on the chip sensitivity, the tag antenna gain, polarization, and the matching between the antenna and the chip.

Using Friis equation [16], it is possible to calculate the RFID tag's read range performance as:

$$ReadRange = \frac{\lambda}{4\pi}\sqrt{\frac{P_{eirp}G_{tag}\,p(1-|S|^2)}{P_{th}}} \tag{4.1}$$

where λ is the wavelength of the carrier emitted by the reader, P_{eirp} is the regulated equivalent isotropic radiated power, P_{th} is the activation power of the chip, G_{tag} is the tag antenna gain, p is the polarization loss factor between reader and tag antennas. $|S|^2$ is the power reflection coefficient given by:

$$|S|^2 = \left|\frac{Z_{chip} - Z_{ant}{}^*}{Z_{chip} + Z_{ant}}\right|^2 \tag{4.2}$$

where Z_{ant} and Z_{chip} are respectively tag antenna and IC impedances.

The polarization loss factor p describes the degradation in the system performance due to misalignment between the tag and reader antenna polarizations. In the case of a linearly polarized reader antenna, the best performance is achieved when the tag is perfectly aligned with the reader antenna. However, in a real case scenario, a deterioration of the tag orientation will induce degradation in the read range.

Figure 13. a shows the final prototype realized on polypropylene and casein label. The read range performance of the realized tags was measured using the Voyantic Tagformance measurement system [17]. This system can provide the backscattered signal strength from the tag under test and thus evaluates its read range. Figure 13. b presents a comparison between the simulated and measured read range of the realized prototype on a cheese sample in the frequency band 820-940 MHz. The maximum measured read range on cheese is around 1.3 meters at 866 MHz. These results of measurement and simulation correspond to a linearly

polarized reader antenna configuration where the tag was aligned with the polarization direction during measurements.

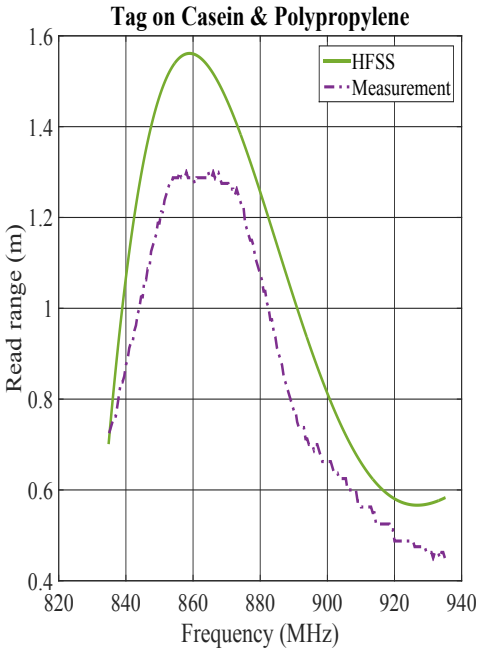

a *b*

Fig. 13. a) Realized prototype on casein and polypropylene b) Simulated vs Measured read range

This smaller read range compared to UHF tags in air is explained by the fact that this configuration has a lower directivity due to the absence of a reflective ground plane and the small distance separating between the tag antenna and the cheese surface which absorbs a significant part of the energy reaching the tag due to its high dielectric loss.

Better performance can be achieved by increasing the thickness of the polypropylene substrate which will provide better isolation between the tag antenna and the lossy surface of the cheese product. A parametric study on the effect of the substrate thickness on tag radiation efficiency is shown in figure 14 where three polypropylene thicknesses were considered for simulation (1-3 and 5 mm).

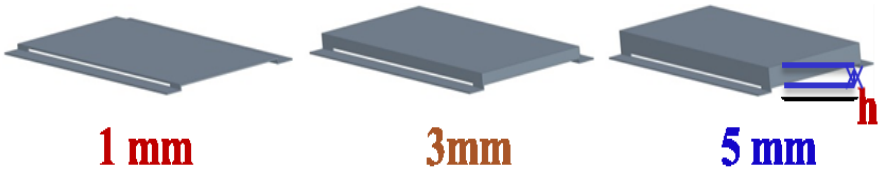

Fig. 14. Simulation models of polypropylene for three different values of thickness(h)

Simulation results show that the tag radiation efficiency improves considerably as the polypropylene thickness (h) increases and thus achieves better read range performance. Table 3 shows the tag gain and simulated read range at 866 MHz for 3 values of (h) as well as the case where the tag is simulated in direct contact with cheese without the polypropylene layer (h= 0).

Table.3 Simulated Gain and Read range at 866 MHz versus thickness(h)

PP thickness (*h*)	Gain (dB)	Read range (m)
Direct contact *h* = 0	-27	0.3
***h* = 1 mm**	-19	1.45
***h* = 3 mm**	- 16.6	1.80
***h* = 5 mm**	-15	2.10

A separation of just 1 mm between the tag antenna and cheese surface helped to increase the read range from 0.3 meter to 1.45 meters. At 5mm thickness, the tag can achieve a read range of around 2 meters which shows the potential of this design configuration for lossy materials such as food products.

4.2. Tag with reflective ground plane

Due to high dielectric cheese losses, a conventional RFID tag will have poor electrical performance as the cheese surface will act like a bad ground plane which shorts the tag antenna and reduces its directivity to the minimum. Designing a tag with a reflective ground plane, in this case, will be more efficient. Indeed, the reflective ground plane will separate the antenna from the cheese surface and on the same time will get the advantage of the conductivity of cheese surface to act as an infinite ground plane which will increase the directivity of the tag antenna and hence its read range. In the case of lossy ground plane, this advantage is counterbalanced by the unavoidable absorption effect.

As discussed in the previous configuration on Polypropylene, the primary parameter that affects the antenna's electrical performances is the thickness of the dielectric substrate (h) on which the tag is realized. The more the tag antenna is separated from the cheese surface, the more the read range increases. A conventional configuration [13] composed of a loop connected to a meander dipole antenna with a ground plane on FR4 substrate (ε'_r=4.3) is simulated with the electromagnetic simulation tool HFSS where three different thicknesses (h) are considered (1.6 mm, 3.2 mm and 5 mm). The detailed dimensions of the optimized RFID tags are shown in figure 15 where the maximum tag area does not exceed 1.4 cm x 7.5 cm.

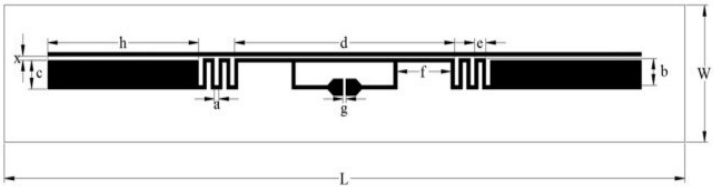

Dimensions (mm)	a	b	c	d	e	f	g	h	x	L	W
Tag FR4 1.6 mm	0.45	2.45	2.625	22.35	1.15	5.47	0.3	15.35	0.375	69.2	12.45
Tag FR4 3.2 mm	0.45	2.7	2.875	26.35	1.15	7.575	0.3	15.35	0.375	73.2	12.7
Tag FR4 5.0 mm	0.45	3.8	3.975	28.35	1.15	9.175	0.3	12.35	0.375	69.2	13.8

Fig. 15. The layout of UHF tag with a ground plane on FR4

Figure 16 presents a comparison between the three simulated antenna gains. The highest gain is achieved for h = 5mm, with an increase of ≈ 3dB compared to 3.2 mm and ≈ 6 dB compared to 1.6 mm.

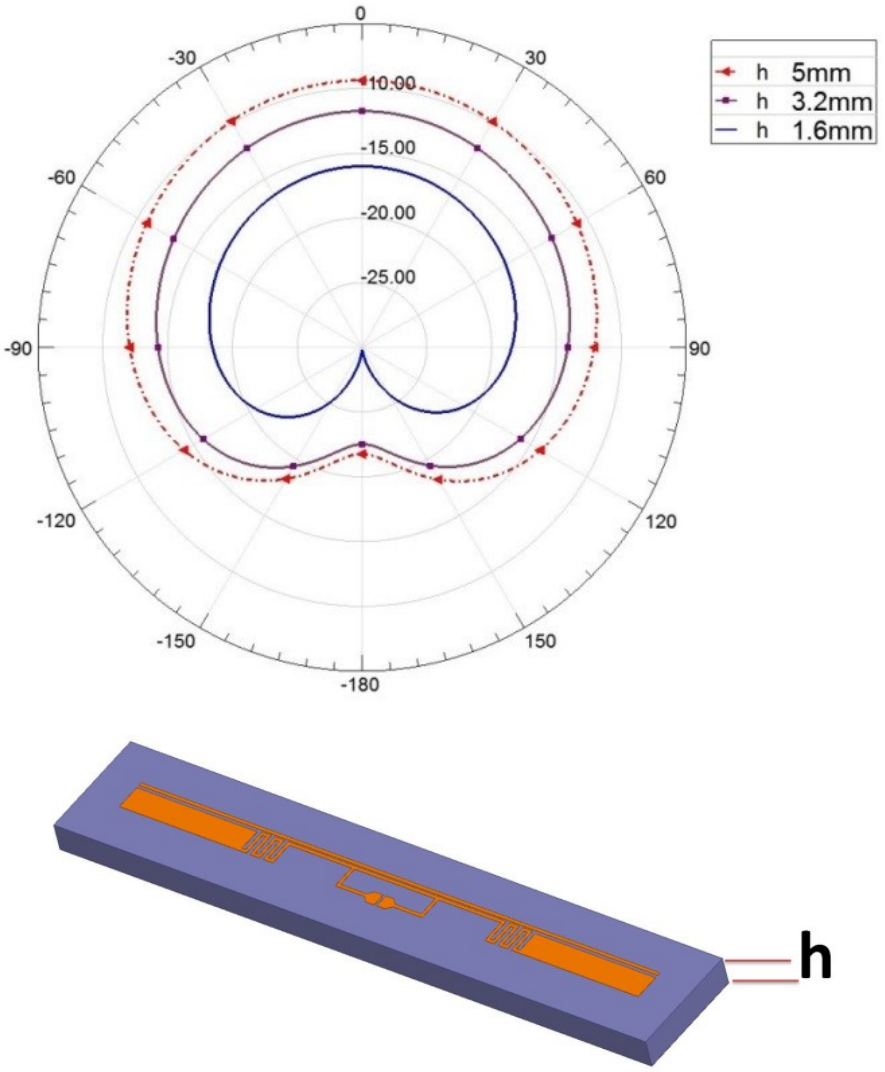

Fig. 16. 3D model of simulated tag on cheese and a comparison between the gains of the tag (at phi=90 deg) simulated on FR4 substrates for 3 different thicknesses

All simulated models are well matched to the chip impedance (reflection coefficient below -10 dB) and the estimated read ranges are around 2.4 meters, 4.2 meters and 5.3 meters as shown in figure 17 for *h* = 1.6 mm , 3.2 mm and 5 mm respectively.

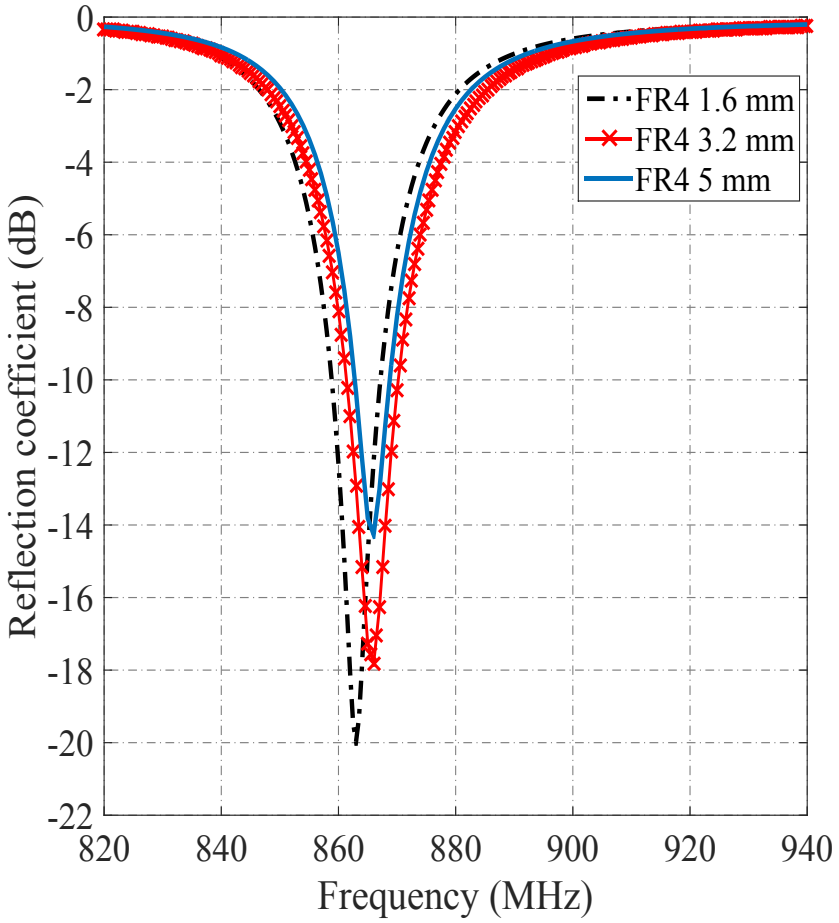

a

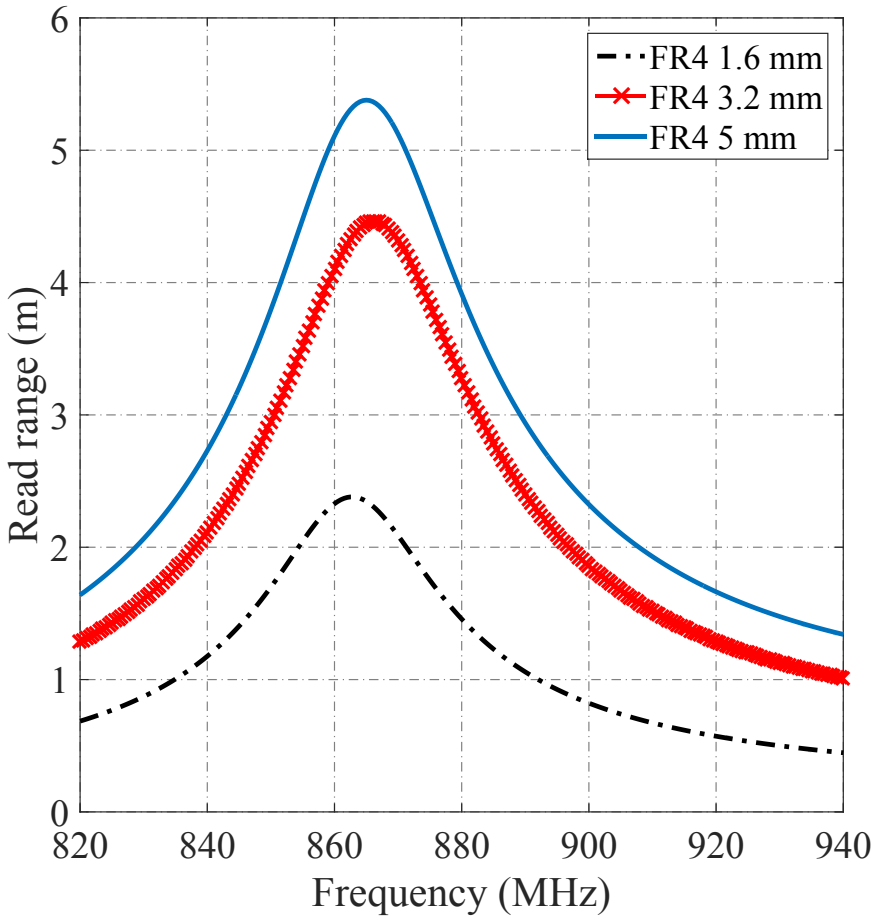

b

Fig. 17. Simulation results for 3 substrate thicknesses a) Reflection coefficient b) read range

Figure 18 shows a comparison between the measured read ranges of tags realized on FR4. The measurements were achieved on Emmental cheese samples in a frequency range between 835 MHz to 935 MHz with a frequency step of 1 MHz. The maximal read range of the tag fabricated on a standard 1.6 mm FR4 and having a size near to 10 cm² was around 2.2 meters. The read range increases to reach 3.5 meters and 4.6 meters for substrates of 3.2 mm and 5 mm thickness respectively.

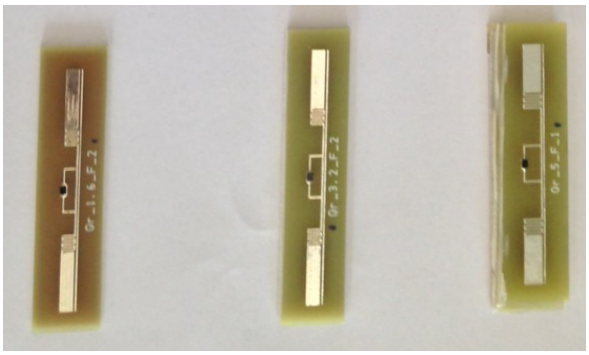

a

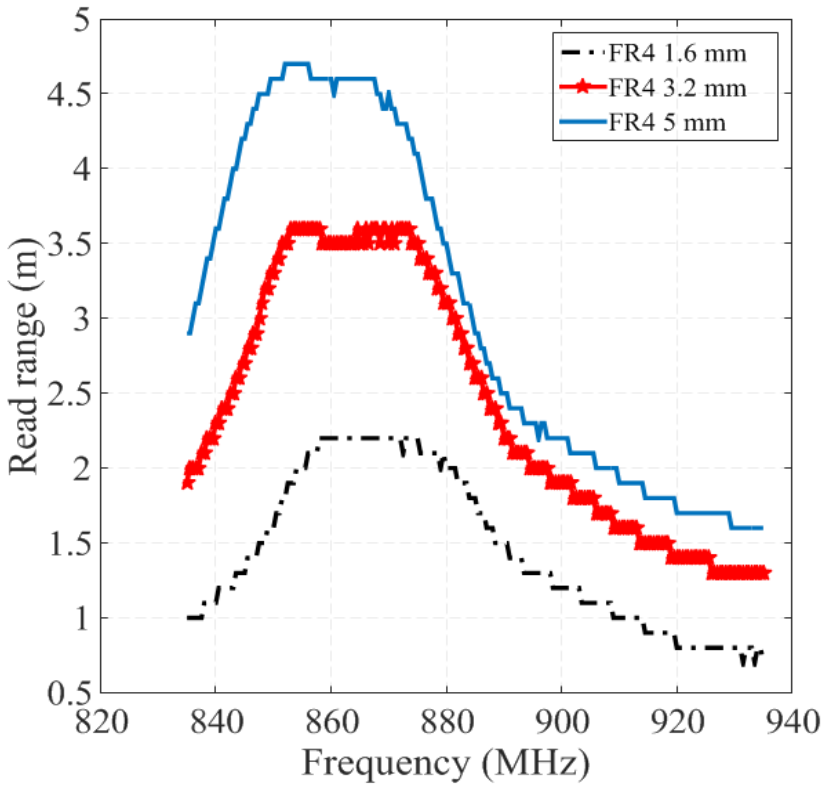

b

Fig. 18. a) prototypes realized on FR4 b) Comparison between the measured read ranges

The difference between the simulated and measured read range for each tag is in the range between 10% to 15%. This difference is mainly due to the nature of the cheese (heterogeneous product) and the quality of FR4 substrates.

A comparison between all the fabricated RFID tags was realized on three types of cheese: Emmental, Morbiet and Grimont. Figure 19 summarizes the average read range of several measurements for each tag where the deviation error does not exceed 15%. Results show that tags with ground plane have better performance compared to tags on polypropylene where the maximum read range can reach around four meters. These read ranges allow automating the process of identification and offer the possibility for more applications of data monitoring.

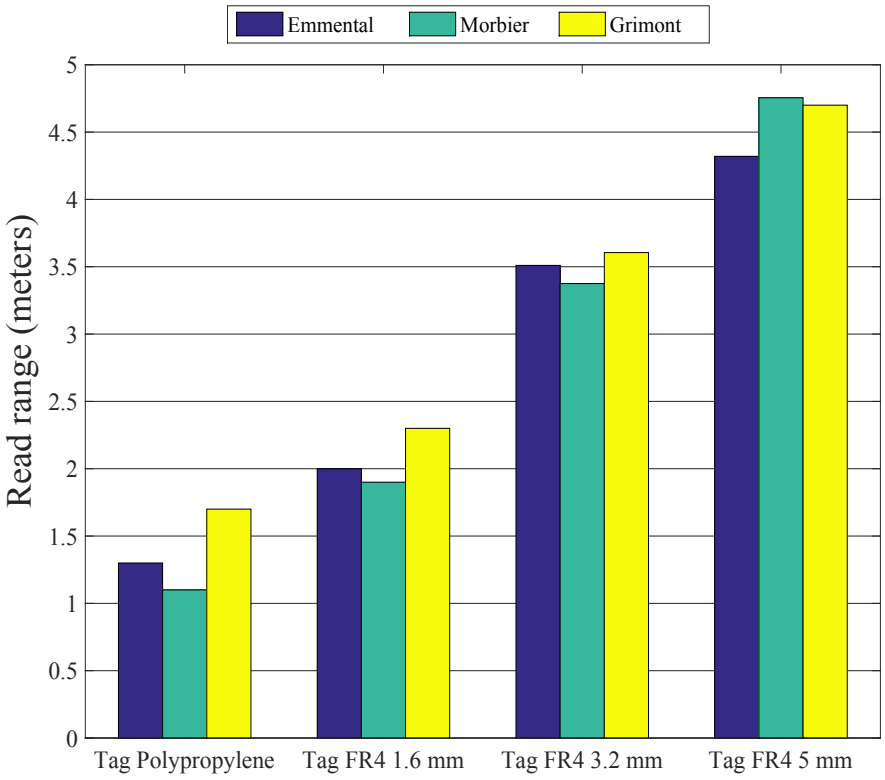

Fig. 19. Comparison between measured read ranges of different configuration on three types of cheese.

4.3. Green RFID Tag for smart packaging

The two previously discussed configurations based on polypropylene or tags with reflective plane are basically for cheese tracking during the fabrication process. At the end of the fabrication process, these tags will be removed and cheese wheels will be cut and sliced before being packaged for distribution. The production information is then printed on each item which makes this cycle of production chain very vulnerable to manipulation attempts latter by distributors. Therefore, smart packaging of food products is of a great importance in order to provide a continuous and robust traceability solution covering all the production cycle of the product from fabrication to consumers. This allows registering all the production information on the smart packaging and tracking each item till the end of chain which provides higher level of food security for consumers. Also, based on smart packaging of food products, there will be smart refrigerators that can detect when a particular food item is running low which will allow consumers to automatically order fresh groceries through the Internet.

Recently, the food sector is oriented towards green solutions using biodegradable materials for packaging to reduce non-recycled plastic wastes. In this context, RFID could indeed be a part of green IT which is cost effective as well as compatible with regulation and preservation of environmental health [18]. Previous works discussed the realization of RFID tags on different biodegradable substrates such as cellulose acetate (CA) [19], Plywood Substrates [20] and Polylactic Acid (PLA) using 3D printing [21]. Compared to previous works fabricated on rigid substrates, this work presents a UHF RFID tag realized on a very thin and flexible film of PLA which is more suitable for food packaging.

As the PLA is a biodegradable material, it was important to study the variation of its dielectric properties versus time and weather conditions. First, the thickness of PLA was measured accurately with a profilometer to obtain an accurate measurement of the permittivity. An average of 40 µm of thickness is obtained as shown in figure 20.

The permittivity and loss tangent of one factory sample of PLA have been measured using Damaskos cavity system [22]. Then the dielectric properties of the same sample have been measured again after being exposed to weather conditions during two weeks. The results are presented in table 4.

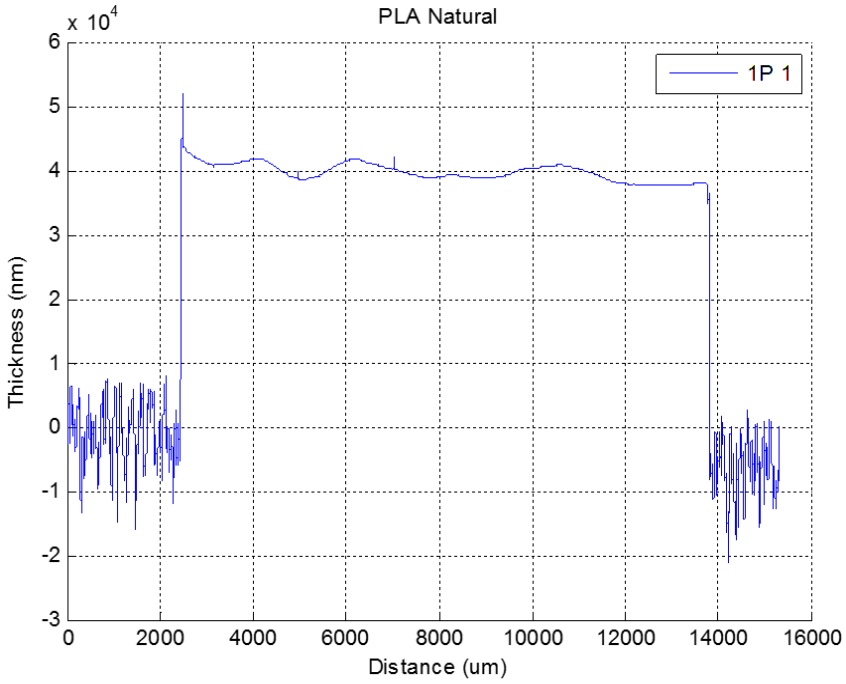

Fig. 20. Measurement of PLA thickness obtained by a profilometer.

We can notice that a small variation in the dielectric properties of PLA occurred due environmental conditions. In order to take into account this variation, the average of these two values was considered during the design and simulation.

Table 4. PLA Dielectric properties variation

Measurement Day	ε_r'	$\tan(\delta)$
Day 1	2.72	0.002
Day 15	2.94	0.004

The tag design is based on a meander line antenna where the final tag dimensions are 11 mm x 78 mm with line's width of 1.5 mm as shown in figure 21:

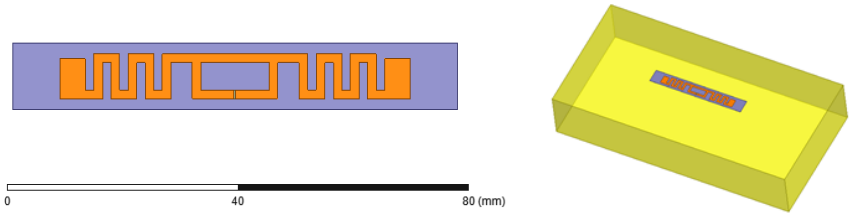

Fig. 21. HFSS simulation model of PLA tag on cheese

A parametric simulation of the read range versus frequency was realized for different permittivity and loss tangent values of the cheese substrate. The tag read range was simulated at ε_r' (15,17,19 & 21) and tan (δ) (0.6 & 0.8). As the cheese is a very lossy substrate, the maximum gain obtained is around -23 dB which affects the tag read range to be in the range between 0.65 m and 0.72 m at 866 MHz as shown in figure.22.

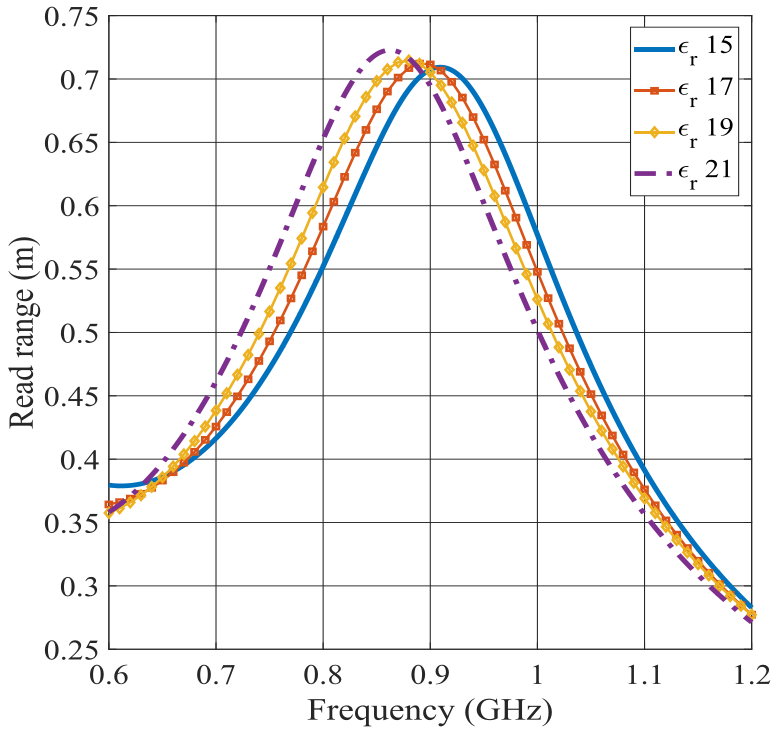

a

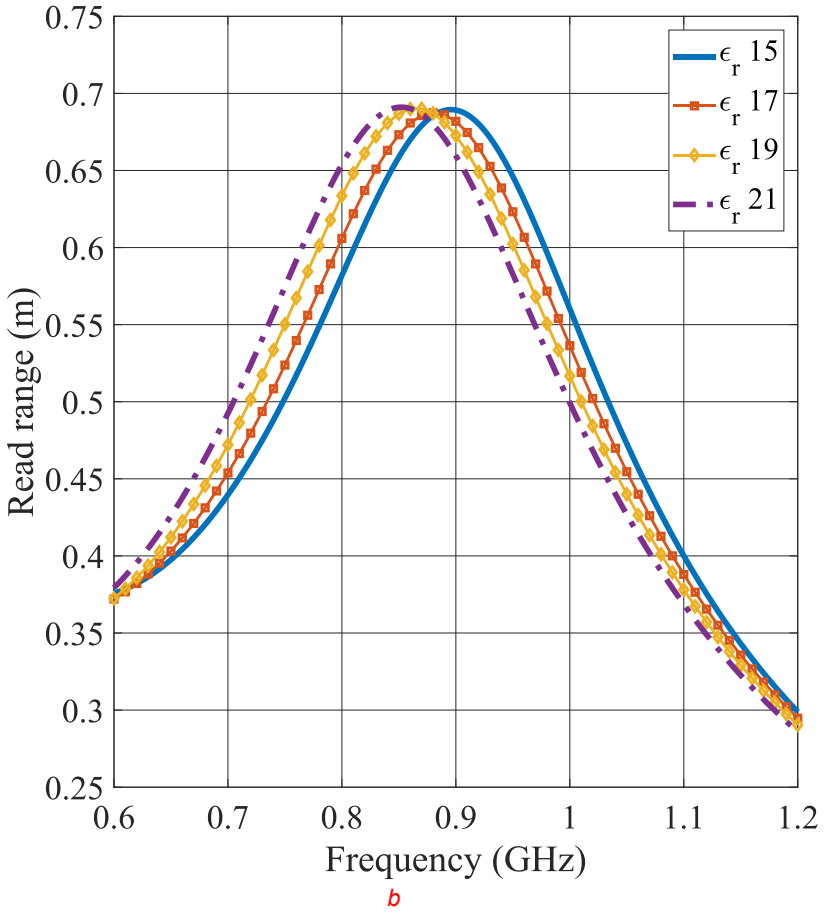

b

Fig.22. Read range versus frequency for ε_r (15, 17, 19 & 21) a) tan(δ)= 0.6 b) tan(δ)= 0.8

When the permiitivity ε_r' increases, the tag resonance frequency shifts towards lower frequencies. On the other hand, as the dielectric losses increase, the tag read range decreases.

The fabrication of RFID tag on PLA substrate was based on chemical etching of adhesive copper foil attached to the PLA as shown in figure 23. Read range measurements were realized using a commercial RFID reader (CAEN RFID) in a real environment. The read range obtained at maximum allowed power is around 55 cm which is too limited for identification of products on a large scale.

Fig. 23. a) Realized tag prototype on PLA b) Measurement setup

It is still too early to speak about standardizing smart packaging based on RFID tags for food products due to its relatively high cost. However, the rapid advance in fabrication technologies, in particular RFID IC and reader, will provide cheaper and more potential RFID IC for food tracking and thus smart packaging based on RFID will play a major role in the food production sector.

5. Conclusion

This chapter discussed some of the most relevant traceability solutions currently applied in the food sector. Despite their high efficiency compared to conventional methods, RFID systems are still rarely applied in the food sector. A study on advantages and limitations of both HF and UHF RFID showed the potential of applying UHF technique in large scale production such as cheese sector.

A comprehensive discussion about each design step of UHF RFID tag, for purpose of application to cheese sector, is presented. Two different tag topologies for cheese traceability during fabrication process are discussed. A first design approach based on Monza R6 RFID chip and fabricated on polypropylene substrate combined with a casein label realized a read range of around 1.2 meters. This configuration can be improved by increasing the substrate thickness to reach around 2 meters for a 5 mm thickness of polypropylene layer. Then, a second design approach based on a reflective ground plane is presented. Compared to the first design on PP, this configuration takes advantage of the cheese lossy surface to act as an quasi-infinite ground plane which helps to increase the tag directivity and thus the tag achieves larger read range. A prototype of an RFID tag based on Monza R6 RFID chip and realized on 5mm layer of FR4 showed the possibility of achieving a read range of around 4.5 meters. These read ranges of both configurations can provide an automated traceability solution and well comply with the requirements of cheese producers.

Finally, a tag design based on PLA is considered for smart packaging of food products. This tag configuration allows continuous food traceability from food producers to consumers and help to reduce plastic wastes by using biodegradable material for food packaging.

References

[1] Regulation (EC) No 178/2002 of the European Parliament and of the Council of 28 January 2002 laying down the general principles and requirements of food law, establishing the European Food Safety Authority and laying down procedures in matters of food safety, vol. 031. 2002.

[2] R. Perez-Aloe, J. M. Valverde, A. Lara, J. M. Carrillo, I. Roa, and J. Gonzalez, “Application of RFID tags for the overall traceability of products in cheese industries,” in 2007 1st Annual RFID Eurasia, 2007, pp. 1–5.

[3] “Cognex Readers Power LABELYS Solution for Comprehensive Cheese Production Management and Traceability | Cognex.” [Online]. Available: https://www.cognex.com/applications/customer-stories/food-and-beverage/cognex-readers-power-labelys-solution-

for-comprehensive-cheese-production-management-and-traceabilit. [Accessed: 08-Jun-2018].
[4] A. Regattieri, M. Gamberi, and R. Manzini, "Traceability of food products: General framework and experimental evidence," J. Food Eng., vol. 81, no. 2, pp. 347–356, Jul. 2007.
[5] L. Kumari, K. Narsaiah, M. K. Grewal, and R. K. Anurag, "Application of RFID in agri-food sector," Trends Food Sci. Technol., vol. 43, no. 2, pp. 144–161, Jun. 2015.
[6] F. Bibi, C. Guillaume, N. Gontard, and B. Sorli, "A review: RFID technology having sensing aptitudes for food industry and their contribution to tracking and monitoring of food products," Trends Food Sci. Technol., vol. 62, pp. 91–103, Apr. 2017.
[7] P. Papetti, C. Costa, F. Antonucci, S. Figorilli, S. Solaini, and P. Menesatti, "A RFID web-based infotracing system for the artisanal Italian cheese quality traceability," Food Control, vol. 27, no. 1, pp. 234–241, Sep. 2012.
[8] "Comté: How the Largest Small-Batch Cheese in France Is Made | Serious Eats." [Online]. Available: http://www.seriouseats.com/2011/07/comte-how-largest-small-batch-cheese-is-made-in-france.html. [Accessed: 08-Sep-2017].
[9] Regulation (EC) No 1935/2004 of the European Parliament and of the Council of 27 October 2004 on materials and articles intended to come into contact with food and repealing Directives 80/590/EEC and 89/109/EEC, vol. 338. 2004.
[10] "Green Casein Labels," cheesemaking. [Online]. Available: http://www.cheesemaking.com/casein-labels-green.html. [Accessed: 08-Jun-2018].
[11] A. Géczy, G. Horváth, L. Dudás, L. Gál, I. Hajdu, and G. Harsanyi, RFID cards on biodegradable substrates – Realization aspects and future trends. 2014.
[12] "Monza R6 RAIN RFID Tag Chip Optimized for Retail | Impinj." [Online]. Available: https://www.impinj.com/platform/endpoints/monza-r6/. [Accessed: 19-Mar-2018].
[13] G. Marrocco, "The art of UHF RFID antenna design: impedance-matching and size-reduction techniques," IEEE Antennas Propag. Mag., vol. 50, no. 1, pp. 66–79, Feb. 2008.
[14] "For electronic device management | UHF band RFID | RFID | Murata Manufacturing Co., Ltd." [Online]. Available:

https://www.murata.com/en-eu/products/rfid/rfid/uhf/smd. [Accessed: 19-Mar-2018].
[15] J. P. Maitre, “Food product e.g. cheese, information medium, has label having two slots that are positioned so that main part of slots constitutes central part of label, where side holding flanges are off-set on both sides of main part,” FR2884955 (A1), 27-Oct-2006.
[16] C. A. Balanis, Antenna theory: analysis and design, 3rd ed. Hoboken, NJ: John Wiley, 2005.
[17] “Tagformance Pro,” Voyantic. [Online]. Available: http://voyantic.com/products/tagformance-pro. [Accessed: 19-Oct-2017].
[18] I. Bose and S. Yan, “The Green Potential of RFID Projects: A Case-Based Analysis,” IT Prof., vol. 13, no. 1, pp. 41–47, Jan. 2011.
[19] A. Géczy et al., “Experimental 13.56 MHz RFID cards on biodegradable substrates,” in 2015 38th International Spring Seminar on Electronics Technology (ISSE), 2015, pp. 52–56.
[20] E. Sipilä, J. Virkki, L. Sydänheimo, and L. Ukkonen, “Heat-sintered and photonically sintered brush-painted silver UHF RFID tags on plywood substrates,” in 2015 1st URSI Atlantic Radio Science Conference (URSI AT-RASC), 2015, pp. 1–1.
[21] L. Catarinucci, R. Colella, P. Coppola, and L. Tarricone, “Microwave characterisation of polylactic acid for 3D-printed dielectrically controlled substrates,” Antennas Propag. IET Microw., vol. 11, no. 14, pp. 1970–1976, 2017.
[22] “Damaskos, Inc:::Cavities & Resonators.” [Online]. Available: http://www.damaskosinc.com/cavitiy.htm. [Accessed: 19-Mar-2018].

Chapter 5

Improved traceability solutions for cheese sector

1. Introduction

This chapter presents the installation procedure of the RFID tags during the production process of cheese. Different tag configurations discussed in the previous chapter are installed on several types of cheese and tested in a real industrial environment using a handheld reader. Compared to controlled measurements using a professional system like Tagformance, measurements in a real environment reveal new challenges which affect the performance of different tags such as the limited output power provided by the majority of commercial portable readers which affects considerably the reading range of RFID tags on cheese

In order to provide a totally automated solution for cheese traceability, using a fixed RFID reader configuration which can be installed on a robot is considered as it is the most practical and cost effective option. One of the major challenges of this configuration is the random tag orientation on cheese which is hard to control

during installation. For identification, using a circularly polarized reader antenna is not considered as a practical solution in this case as it means losing half of power reaching the tag in an already difficult environment and thus reducing the system read range. In this context, a novel reader antenna configuration based on rotating polarization is discussed as an effective solution which allows detecting randomly oriented tags based on backscattered RF signals from the tags without decreasing the system performance.

Another challenge is to provide visual identification on the cheese traceability labels as it is considered one of the requirements of cheese producers. A novel traceability technique combining both Barcode and RFID technologies on the same antenna design is presented. This configuration is of great interest as it offers more flexibility for cheese makers and combines the advantage of both technologies on the same label allowing thus a better traceability.

2. Tag installation and measurements in real environment

According to cheese production legislations and regulations [1] [2], all tags must be encapsulated before installation in order to maintain a high level of hygiene and to avoid any contact between the cheese and the tag electronics as shown in figure 1 where the tag is encapsulated between low layers of polypropylene and a casein plaque. The edges of the final prototype are sealed with resin which helps avoiding any water leakage to the tag during installation.

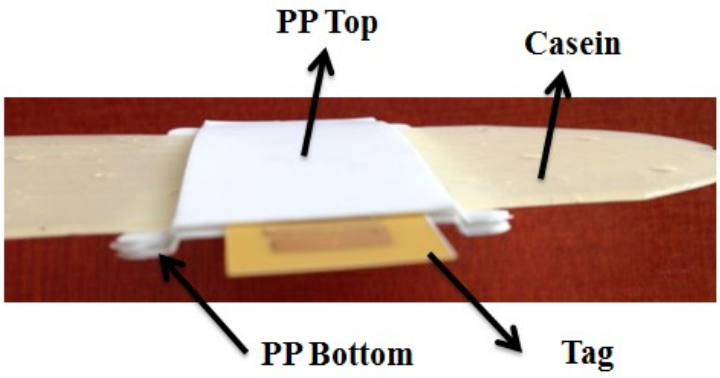

a

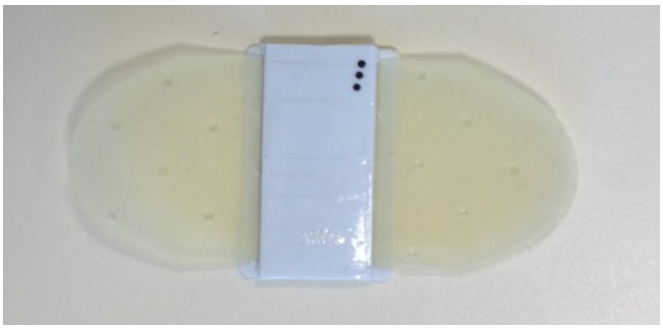

b

Fig. 1. a) Tag encapsulated between two layers of polypropylene b) tag sealed with resin before installation on cheese

Another technique is to envelop tags in PET foils under vacuum and insert them between the two layers of PP and thus avoid using resin for sealing.

The installation of RFID tags comes during the fabrication process of cheese after the curdling step where the tag is placed between the poured curd and the cheese mold. Then, the curd is pressed to allow evacuating the excessive proportion of water content, and the tag readability is checked before moving the cheese wheels to the ripening chamber as illustrated in figure 2.

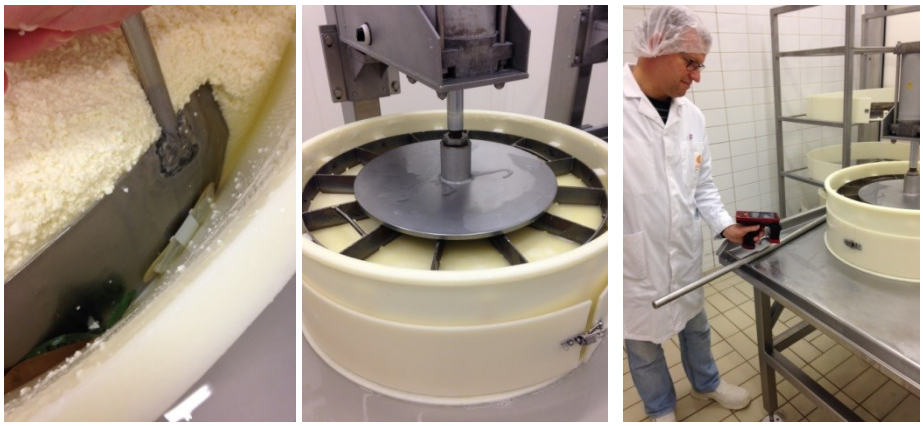

a b c

Fig. 2. Tag installation procedure : a) placing the tag between curd and cheese mold b) curd pressing c) Test of tag readability

The realized tags were installed on different types of cheese (Emmental, Grimont and Morbier) and measurements were achieved in a real industrial environment using a commercial RFID portable reader as shown in figure 3. The reader (Alien H450) used for measurements has a limited output power of 30 dBm and an antenna of 1dBi gain thus the portable reader effective radiated power (ERP) according to ETSI power standards is :

30 dBm (reader) + 1 dBi (antenna gain) – 2,15 dBi = 28,85 dBm.

Compared to Tagformance measurements based on transmitting the maximum allowed power (33 dBm ERP), this power difference of 4,15 dB will affect the system performance as the tags' read ranges are expected to be lower by a factor of ≈ 0,62. In such an environment, measurements were also affected by multipath due to signal reflections which makes the tags performances even lower.

Fig. 3. Measurement in an industrial environment using handheld RFID reader

All the realized prototype tags presented in chapter 4 (section 4) have been tested in the cheese ripening chambers. A comparison between the measured average read range for each tag configuration on Emmental, Morbier and Grimont cheeses is presented in figure 4.

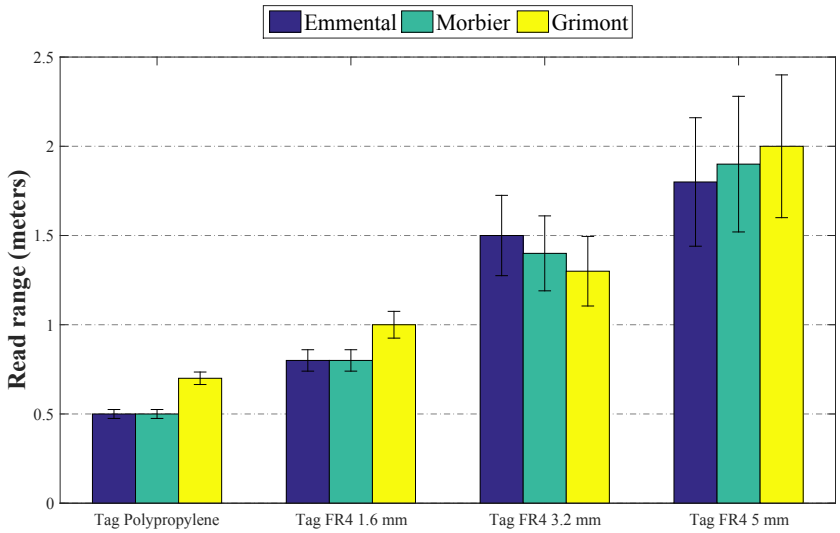

Fig. 4. Comparison between tags' read ranges (in meters) on three types of cheese in industrial environment using a portable reader

These measurements were realized at the first days of ripening after tags installation on cheese. As previously discussed in chapter 3, the dielectric properties of these three types of cheese are very similar at the beginning of maturation which explains the small differences of the first configuration (Tag Polypropylene) performance on the three cheeses. On the other hand, the other tag configurations with a ground plane are less sensitive to the variation of dielectric properties of cheese. However, as the read range increases, the uncertainty of measurements increases due to multi-path effect. Better performances can be achieved using a portable reader with higher output power.

3. Improved detection technique of randomly oriented UHF RFID Tags

International food trade brings many challenges to the table, not least for food manufacturers that constantly face high demands for food safety and traceability. In this frame, food manufacturers are looking more and more to automate the entire traceability process of food in order to guarantee high quality and to reduce wastes and human mistakes to the minimum. Based on our studies presented in previous chapters about the use of RFID systems in cheese sector, we found that

using a handheld RFIDreader for checking and tracing has some performance limitations. Moreover, cheese traceability realized by working personnel is a very time-consuming process and it does not suit large-scale production where thousands of products must be checked regularly. Therefore, cheese manufacturers are more interested about fixed reader configuration on a robot which can read and modify data on tags in a faster and more accurate way.

One of the major challenges of this configuration is the random tag orientation on cheese which is hard to control during installation. In general, circular polarized reader antennas are the most applied in RFID systems as the reading operation is not dependent on tag orientation. However, using a circularly polarized reader antenna is not considered as a practical solution in this case of cheese traceability as it means losing half of power reaching the tag in an already severe environment leading to a shorter read range especially in the writing mode where the sensitivity of RFID chips significantly decreases. On the other hand, using linear polarized antennas is also unpractical as it is difficult to control the tag orientation during the installation process as illustrated in figure 5.

Fig. 5. Randomly oriented tags on cheese wheels

In this section, a novel reader antenna configuration based on rotating polarization is discussed as an effective solution which allows detecting randomly oriented tags without decreasing the system performance. This is achieved by means of a polarization matching approach, using simple off-the-shelf components. A mono-static configuration composed of a dual polarized reader antenna along with some passive RF components, is used to sweep the interrogating signal polarization in any angle, where the maximum backscattered power received by the reader is dependent to the tag orientation.

3.1. Operation principle

For passive RFID, tag's antenna collects energy from the waves sent by the reader to turn on the chip, which transmits the identification information back to the reader by backscattering. In this context, the polarization matching between tag and reader antennas plays an important role in affecting tag's received power and thus the level of backscattered power received later by the reader. The backscattered power from the tag can be calculated using radar equation:

$$P_r = \frac{P_t {G_t}^2 \lambda^2 \sigma}{(4\pi)^3 r^4} (PLF)^2. \quad (5.1)$$

where, P_r is the backscattered power from the tag, P_t is the transmitted power from the reader, r is the distance between tag and reader antennas, λ is the wave-length of the signal transmitted, G_t is the gain of the transmitter antenna (reader) and σ is tag's radar cross-section. PLF is the Polarization Loss Factor and is given by :

$$PLF = cos^2 \alpha, \quad (5.2)$$

where α is the angle between the linear polarization of the tag and the reader antenna as shown in figure 6(a).

Based on (5.1) and (5.2), if the RFID tag antenna is randomly oriented while the polarization angle of the reader antenna is swept, the tag's orientation can be estimated from the power transfer between both antennas. In order to validate this concept, the antenna in figure 6(b) was used. It is able to transmit and receive a linear polarized signal in any direction between 0 (H) and 90 (V) degrees (figure 6(a)). It is composed of a dual polarization antenna with the two linear polarized horn antennas in cross-configuration, a power splitter, and two variable

attenuators as shown in figure 6(b). The transmitted signal polarization is swept with small a angle (Tx) by attenuating the power delivered to each linear polarized antenna as shown in Table 1. This configuration was tested in practical environment with a 50 ohm dipole centered at 867 MHz, and used as a probe. Figure 6(b) shows the bench and figure 6(c) shows the normalized insertion loss measured between the proposed transmitter's antenna configuration and the dipole for different values of α between 0 and 90 degrees. The orientation of the dipole was fixed at 90 (Vertical) degrees, while the transmitting signal direction was swept according to Table 1.

Table 1.Theoretical attenuators (dB) to configure the desired polarization direction

Tx angle	*Attenuator(H)*	*Attenuator (V)*
0	0	∞
9	1	9
17,5	1	6
32	2	4
45	3	3
58	4	2
72,5	6	1
81	9	1
90	∞	0

The minimum insertion loss corresponds to the attenuators for a polarization configuration of 90 degrees (α = 0 degree). The insertion loss increases till it reaches the maximum at 0 degree polarization where the dipole and transmitter antennas are cross-polarized (α = 90 degrees).

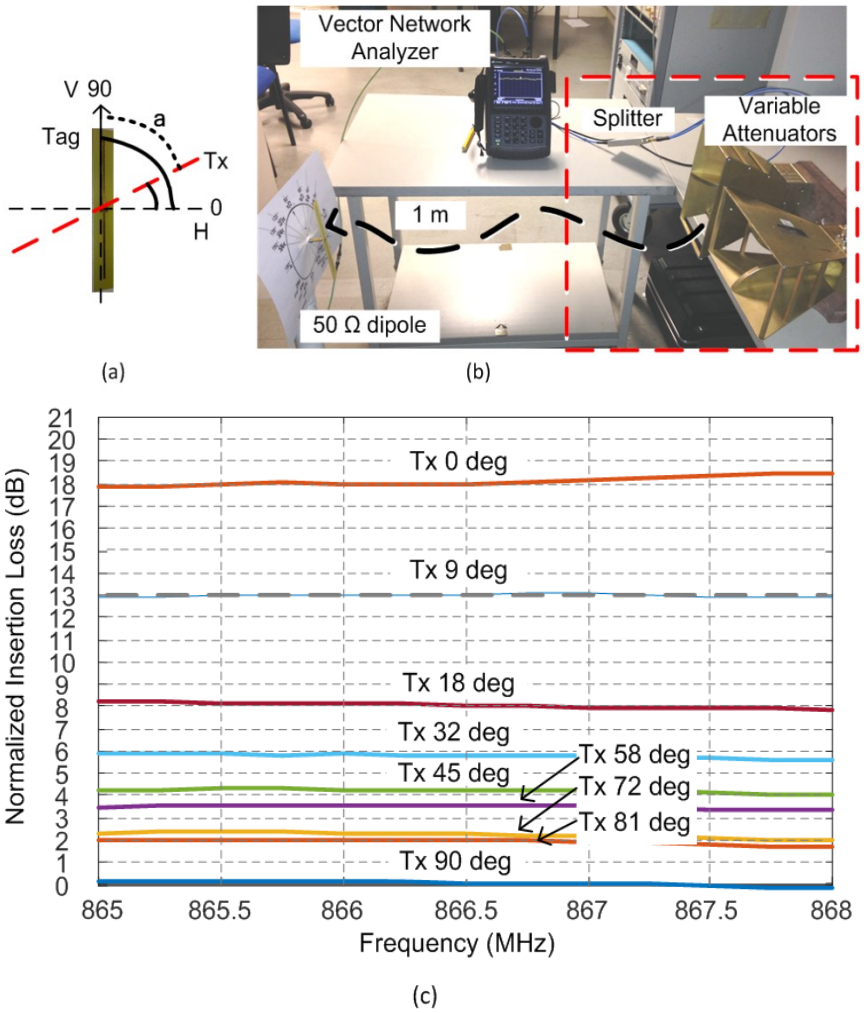

Fig. 6. Measurement of the insertion loss between the proposed reader antenna configuration and a 50 Ω dipole centered at 867 MHz and placed in vertical position (90 degrees). The minimum insertion loss was realized for a transmitted polarization which corresponds to dipole orientation (α = 0 degree)). (a) angles definition. (b) Bench. (c) Measurement result.

3.2. RFID reader architecture

The proposed approach is based on a mono-static antenna configuration as the same antenna is used as transmitter and receiver. Figure 7 shows the main blocks of an RFID reader where the antenna configuration described in the previous

section is connected to a passive RF circulator which isolates the transmitting and receiving channels.

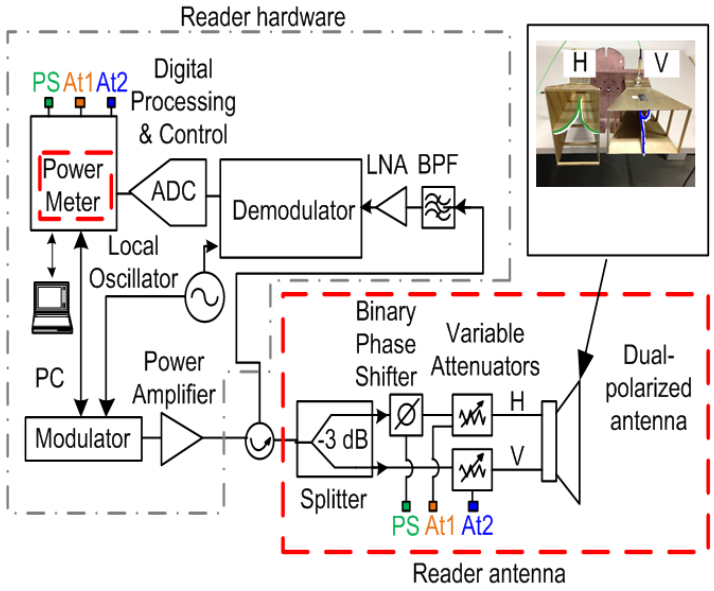

Fig. 7. Schematic block of the proposed reader architecture. The transmitting block is composed of passive RF components to sweep the linear polarized interrogating signal. The digital processing and control unit is equipped with a power meter to measure the backscattered signal.

The two attenuators of the antenna may be digitally controlled (*AT1 & AT2*). To sweep the polarization direction in a higher range between 0 and 180 degrees, a binary digitally controlled phase shifter (PS) with a value of 180 degrees may be used to change the phase of the horizontal antenna and thus allow covering all the possible tag orientations.

As the orientation detection is based on measuring the backscattered power from the tag exploiting the equation 5.1 and 5.2, the reader should be enhanced with a power meter module or Received signal strength Indicator (RSSI) which is already available in most of commercial RFID readers. By using a commercial RFID reader providing 30 dBm output power and two linearly polarized horn antennas with 8 dBi gain, the maximum equivalent radiated power (ERP) from each antenna is equal to :

30 dBm (reader output power) – 3dB (Power splitter) + 8 dBi (Horn antenna gain) – 2.15 dB = 32,85 dB which does not exceed the maximum allowed power.

The main advantage of this configuration is the possibility of transmitting the maximum allowed power in any angle without any loss at the level of receiving antenna as in the case of circular polarization. Therefore, the tag will receive the maximum power only when its orientation corresponds to the polarization of the transmitted signal in order to maximize the PLF. Knowing the angle of the reader interrogating signal, the tag orientation can be easily estimated as it is corresponding to the maximum backscattered power received by the reader. Once the tag orientation is estimated, the reader will automatically select the configuration of attenuators which realize the best performance and thus achieves better communication between reader and tag.

3.3. Experimental validation

Voyantic Tagformance measurement system was used to emulate the RFID reader hardware architecture in figure 7, as it can provide the backscattered signal strength from the tag under test over a large band of frequency [3]. Figure 8 shows the measurement setup where a commercial UHF RFID tag was placed in a real environment at 1 m from the reader antennas. The Tagformance was connected with a circulator to the reader antenna as illustrated in figure 8. We used ten attenuators values from 1 dB to 10 dB provided by mini-circuits with an accuracy varying between 0.4 and 0.6 dB [4].

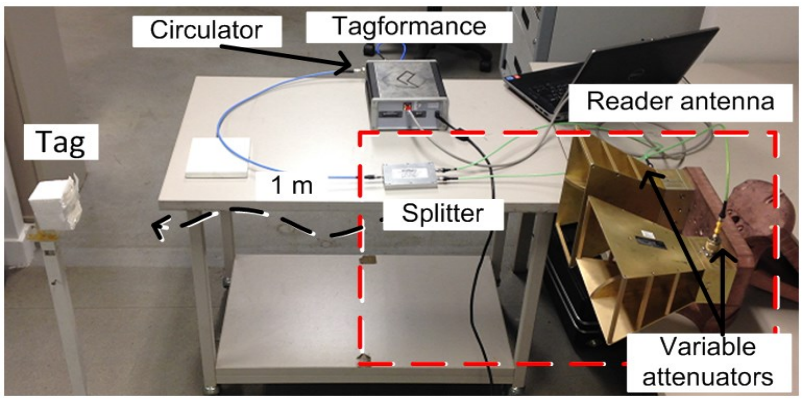

Fig. 8. Bench of the tag measurement using the Tagformance and the proposing reader antenna configuration to emulate the RFID system in Fig. 7.

The first measurement was realized with the tag placed horizontally. Figure 9 shows the measured of tag backscattered power at each transmitter polarization angle described in Table 1. The backscattered power is at maximum all over the European RFID frequency band for the 0 degree transmitter polarization which corresponds with the tag orientation (α = 0 degree).

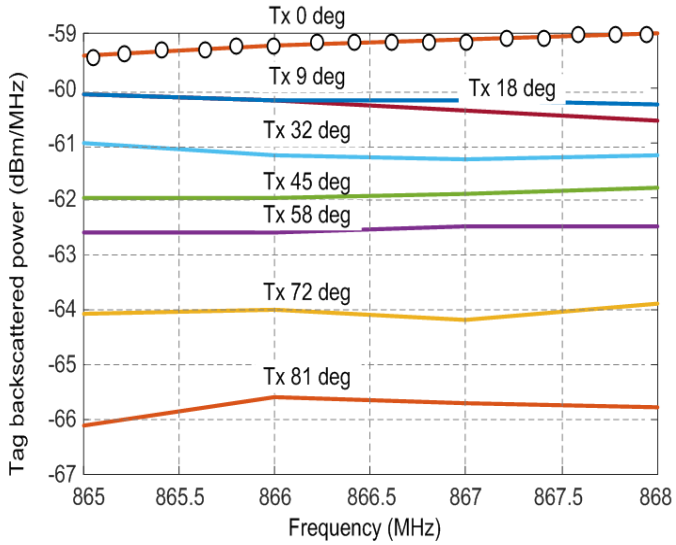

Fig. 9. Measurement results of the setup in Fig. 8 with the tag in horizontal position (0 degree).

A similar behavior was detected for attenuators configuration corresponding to Tx = 9 & 18 degrees. This is explained by the fact that for these two angles the dominant signal is the one provided by the horizontal antenna where the same value of attenuator is used for both configurations (Table 1).

Another measurement of the tag at 60 degrees angle orientation is presented in figure 10. The maximum backscattered power of two transmitter polarizations was at 58 degrees that correspond to an α angle of 2 degrees. However the measurement at 72 degrees shown a comparable receiving power (α = 10 degree), this ±10 degrees precision is basically due to the attenuators accuracy which varies between 0.4 and 0.6 dB. This performance can be improved by using smaller attenuator values, which can allow smaller polarization sweep, and a more sophisticated algorithm based on correlation with the PLF expression.

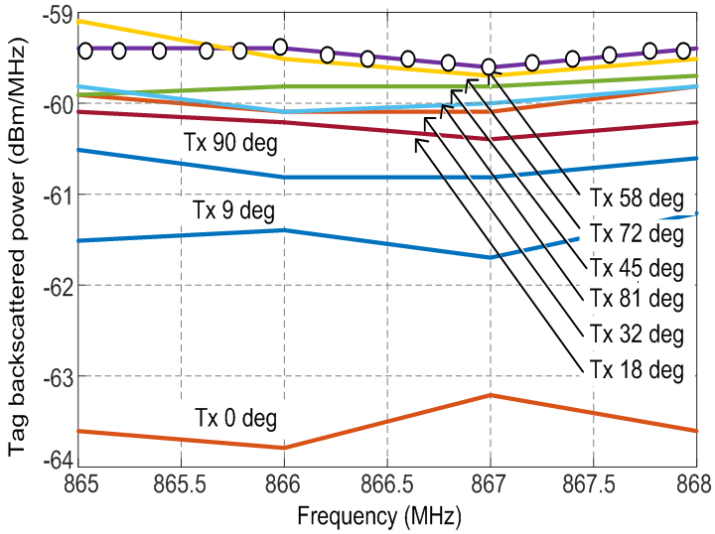

Fig. 10. Measurement result of the setup in Fig. 8 with the tag at 60 degrees.

In the frame of cheese traceability, the results obtained proved the feasibility of this new technique to detect randomly oriented tags without compromising the system performance which allow better and more reliable traceability solution based on a fixed reader configuration. Compared to circularly polarized reader antenna where only half of power reaches the tag, this configuration achieves better performance by optimizing the polarization of the interrogating signal according to the highest RSSI backscattered from the tag and thus achieving the best performance.

This method based on rotating the polarization of reader antenna can be also very useful for other applications such as determining the orientation of tags which can be very efficient in reducing wastes while extracting the tags automatically from cheese wheels at the end of the fabrication process.

4. Hybrid traceability solution based on RFID and barcode

As RFID systems are still not widely applied in the cheese sector, one of the most important requirements of the cheese manufacturers is to keep standard labels, mainly barcodes, along with RFID tags in order to avoid miscommunication while dealing with external partners in the field. In this context, it is worth noting that recently there are many other industrial sectors which install hybrid track and

trace systems based on both barcode and RFID technologies for identification. Hybrid traceability solutions are being deployed in a variety of healthcare applications, including producing hospital wristbands and labeling for pharmaceutical unit-dose medications [4]. Indeed, hybrid systems combining the advantages of both barcode and RFID technologies can be accurately adapted to meet the specific requirements of the food sector and provide better traceability.

The following section presents a single tag design combining both technologies on the same smart label with a simple and reduced cost fabrication.

4.1. Design technique

A traditional barcode is composed of several parallel bars with varied widths and gaps. A small modification of a barcode can transform it to an RFID tag antenna just by connecting its vertical bars with very thin horizontal stubs as shown in figure 11. By connecting the bars to each other's, the barcode readability would not be modified. However, in order to have a good RFID read range, impedance matching with the RFID chip and antenna directivity should be optimized.

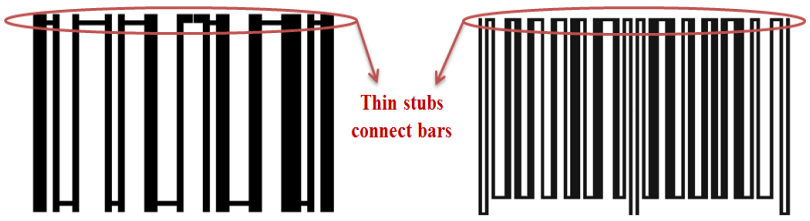

a *b*

Fig. 11. Transforming a barcode to Meander RFID tag by connecting its bars a) Code 128 b) EAN13 code

Impedance matching can be achieved by the optimization of both bars lengths and widths as illustrated in figure 12. While changing the barcode length does not affect its optical readability, the optimization of bars width should be realized carefully else wise the barcode cannot be scanned correctly. The optimization of bars width can be achieved merely by scaling the entire structure in the direction of the width axis and thus the width of all bars and gaps are scaled with the same factor, and the optical readability is maintained.

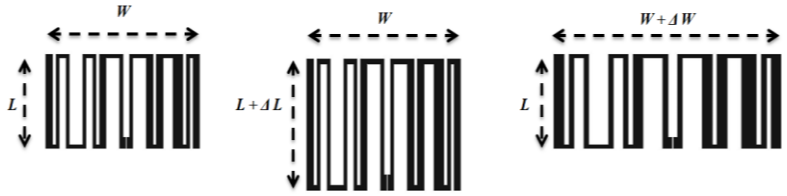

Fig. 12. Impedance matching based on optimization of barcode dimensions: Bar length (L) and Bar width (W)

Matching the IC impedance to the antenna is not the only parameter for designing RFID tags. Previous work [5] managed to match a QR code to RFID chip. However, the overall radiation efficiency and directivity of the structure were very low which decreased the read distance to the range of dozens of centimeters. Compared to conventional RFID tags, linear barcodes will have similar omnidirectional radiation pattern as well as a good directivity. Figure 13 shows a comparison between the simulated directivities of a meander tag and barcode tags of the same size using the 3-D full-wave electromagnetic simulation tool HFSS.

The meander antenna has a maximum directivity (at Phi 90 deg) of 1.98 dB whereas the barcode tag has a lightly lower directivity of 1.82 dB.

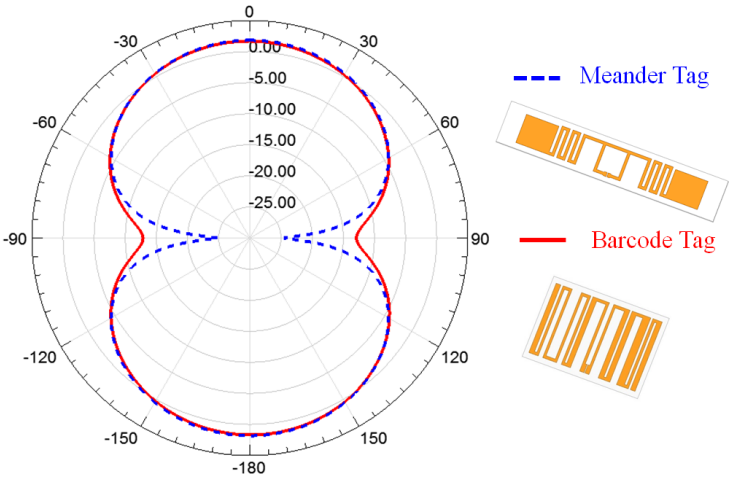

Fig. 13. Comparison between the simulated directivities of a conventional meander tag and proposed barcode tag design.

EAN-13, and Code 128 barcodes have been considered to design smart labels as they are the most used barcode standards to label consumer goods as well as in logistics and transportation industries for ordering and distribution worldwide [6]. Barcodes were generated using Microsoft® Office Barcode Add-In where all barcodes are pre-configured according to industry standards. Barcodes are then exported under .dxf format for simulation and optimization with ANSYS HFSS. Analysis frequency band goes from 820 MHz to 920 MHz where reflection coefficient, gain, and read-range are the main characteristics of interest.

Optical barcodes have standard sizes, and thus the tag design should not exceed these limits [7][8]. For EAN-13 barcodes, the recommended standard total width is 31.35 mm with narrow bar width = 0.33 mm. The EAN13 width can be reduced to 80% and can be increased up to 200% without affecting reliable scanning. For Code 128, the narrow bar width can vary from 0.13 mm to 1.02 mm. Code 128 total width is limited by the scanner resolution. Practically one should restrict the number of characters to whatever fits comfortably in a scanner's field of view [9]. The barcode height is recommended not to be less than 13 mm. All tag designs presented in the article respected these limits.

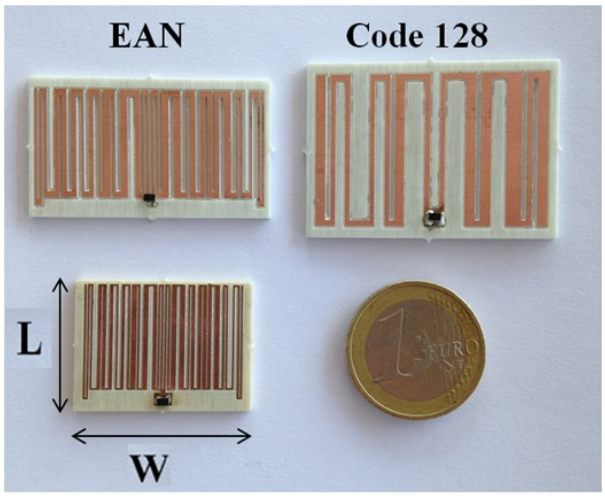

Dimension (mm)	Code128	EAN (Large)	EAN (Small)
W	41	40	29
L	29	23	22

Fig. 14. The realized prototypes on Rogers RO4003™ substrate, Code128 (right) two different sizes of EAN (left).

Two tags with different sizes based on EAN-13 barcode and a tag based on Code 128 are designed without exceeding the limits of barcodes standard sizes. They were fabricated on Rogers RO4003 substrate of 1.52 mm thickness as shown in figure 14. The dielectric constant and loss tangent of Rogers RO4003 are 3.55 and 0.0027, respectively, at the European UHF RFID operation frequency of 867 MHz.

Figure 15 shows a comparison between the gain of the proposed structure. As the tags are all realized on the same substrate, the main parameter which affects the tag directivity is the size of the antenna. Therefore, Code 128 tag and EAN (large) tag realized relatively higher gain (≈ 0 dB) compared to EAN (Small) tag (≈ -3 dB) as it has the smallest dimensions.

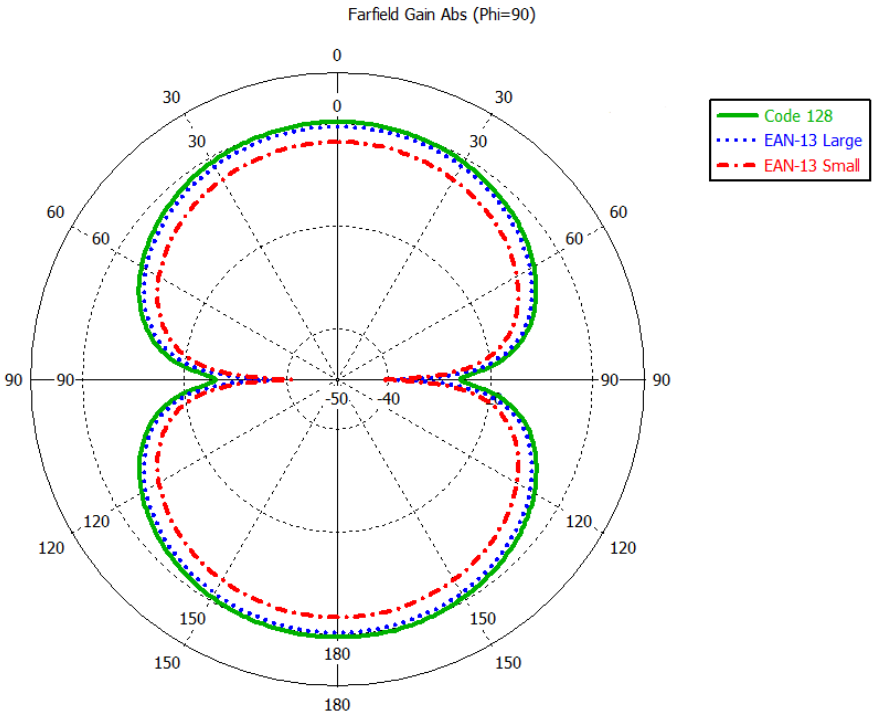

Fig. 15. Comparison between the gains of different barcode tag structures.

All realized prototypes were successfully read using a handheld optical barcode reader. The UHF read range performance of the realized tags was then measured using the Voyantic Tagformance measurement system. This system can provide the backscattered signal strength from the tag under test and thus estimates its read range. Figure 16 presents a comparison between the read ranges measured and simulated for each of the three realized smart labels. A good agreement between measurements and HFSS simulations is achieved.

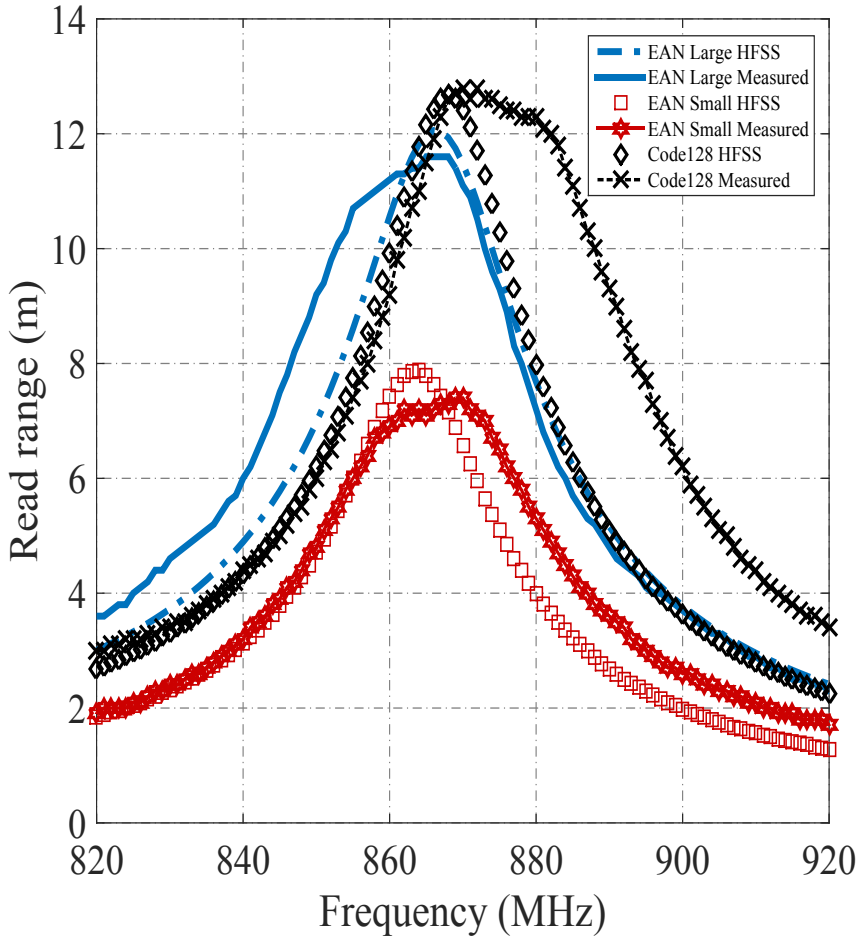

Fig. 16 Comparison between the read ranges of realized prototypes: HFSS simulations vs. Measurements

Code128 & EAN-13 (large) achieved a read range of 12.5 and 11 meters respectively. The small configuration design of EAN-13 achieved a lower performance of 8 m. This lack of performance is expected because a tag with smaller size presents a lower directivity reducing thus its read range. These results demonstrate the feasibility of smart labels combining both barcodes and RFID technologies.

4.2. AK Tag Smart labels

In the previous section, the Monza-R6 chip was soldered on the three presented prototypes. In order to avoid the soldering step, the Adaptive Kernel Tag or AK Tag can be considered. It consists of an RFID IC deployed in conjunction with a small loop antenna based on a parallelogram shape (Dimensions = 11.54 mm X 9.2 mm). The AK tag principle is inspired from the famous T-Match technique where a simple loop compensates the capacitance of the RFID chip while the two branches of the dipole or meander line increase the radiation resistance [10]. The main advantage of this configuration is its quite easy realization as the AK tag is just coupled to the barcode without the need to solder the RFID chip. To do so the strength of the coupling between the AKtag and the barcode antenna is controlled by the distance between the loop and the radiating body [10].

The Ak tag model provided by tagsys is based on a parallelogram shape (Dimensions = 11.54 mm x 9.2 mm) with curved edges. For our application, the actual AK tag shape is not optimal. Indeed, the AK tag is better to be designed based on a rectangular shape with right edges and thus avoids scanning error in some zones where the parallelogram sides interfere with barcode gaps as illustrated in figure 17. This alternative Ak Tag rectangular model was simulated and optimized where the sides' dimensions are 11.8 mm x 10 mm.

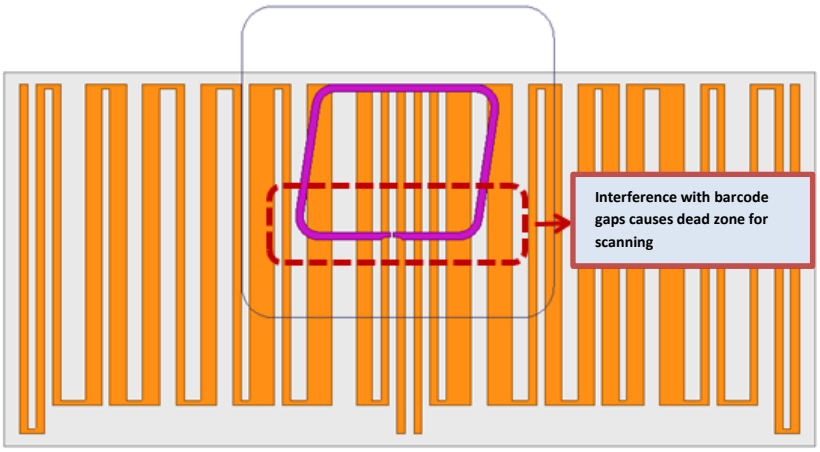

a

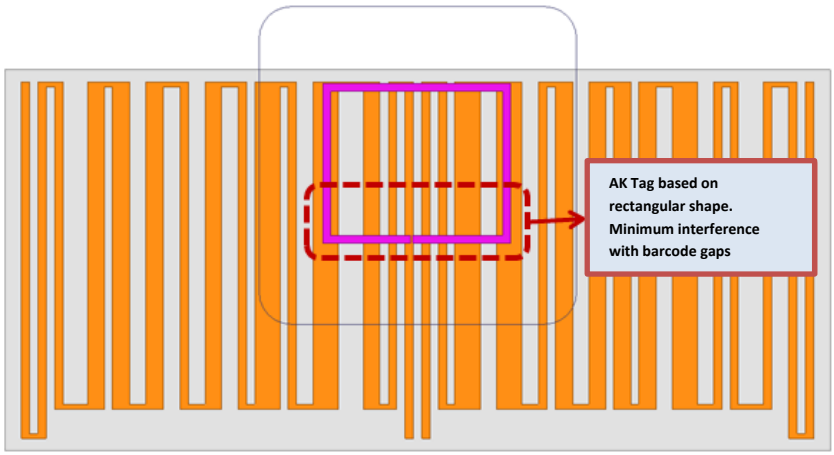

b

Fig. 17. Comparison between two shapes of Ak Tag model a) original parallelogram shape provided by tagsys b) modified rectangular form more suitable for this application as it reduces the scanning dead zone due to interference between Ak Tag and barcode gaps.

Figure 18 shows a comparison between the reflections coefficients of both configurations matched to the same chip Monza-5. The radiation patterns of both tags are quite similar with a maximum gain of -1.4 dB and a slight difference of only 0.3 dB between both configurations.

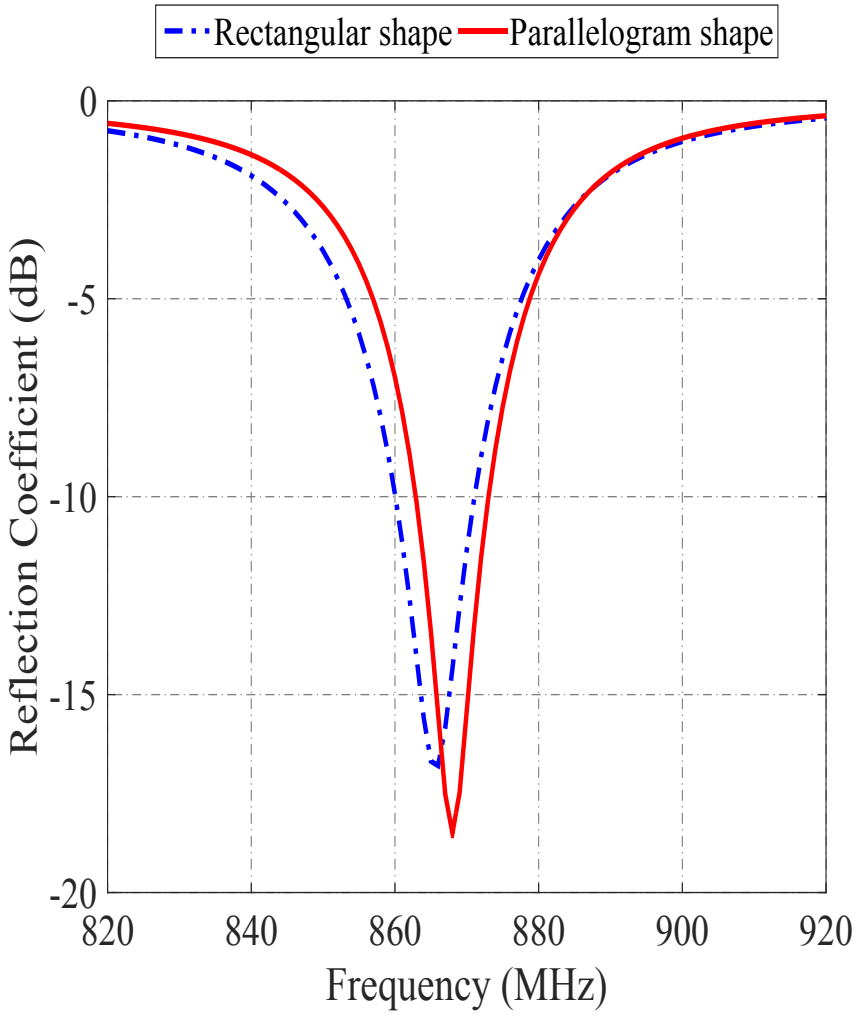

a

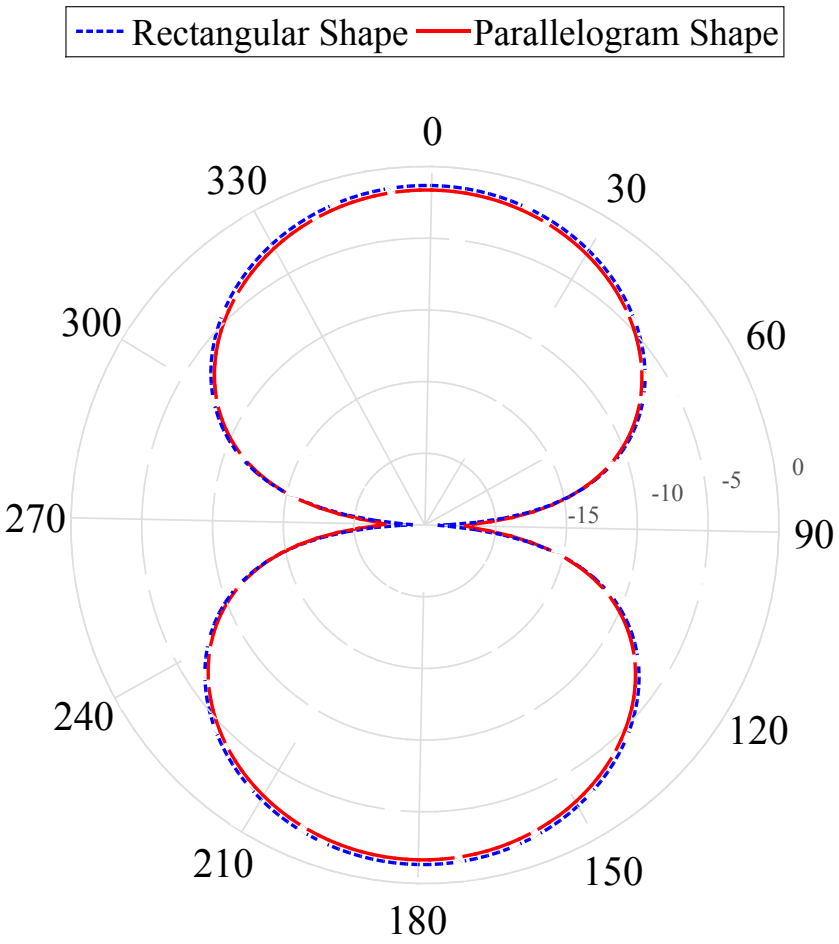

b

Fig.18. Comparison between AK tag configurations rectangular versus parallelogram a) Reflection coefficient b) Gain

A parametric study on the optimum coupling position of the AK tag has been achieved. Figure 19 shows three different positions of coupling where the optimum performance is realized when the AK Tag is centered in a way that the upper branch of the AK tag and the stubs connecting the bars are very close or overlapped (Position A).

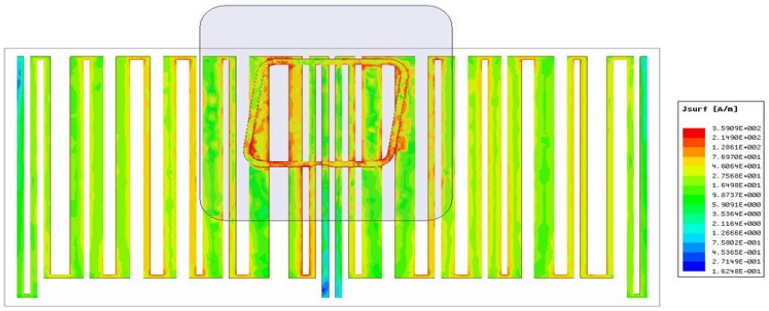

Position A

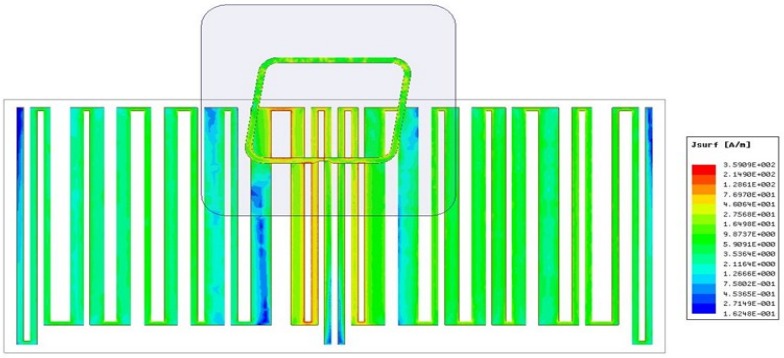

Position B

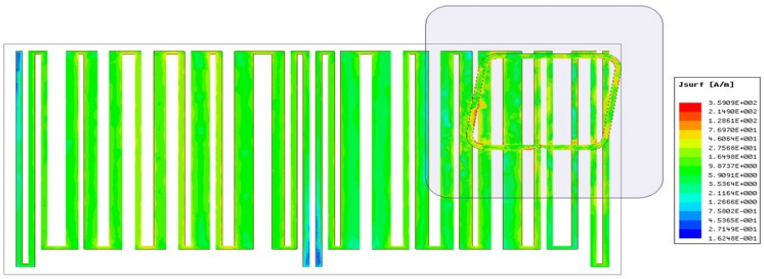

Position C

Fig.19. Parametric study on the position of the AK tag: a) optimum performance as the AK tag is centered b) weak coupling as the AK tag is shifted 5 mm away from the stubs c) lower coupling as the AK tag is placed on the edge of the structure.

This is because, in a meander line structure, the surface current responsible for radiation is the horizontal part of the meander lines as it cancels each other in the vertical direction. The directivity of the structure decreases as the AK tag is placed 5 mm away from the stubs as in position (B). The tag directivity also decreased at third position C as the AK Tag is placed on the edge of the barcode instead of the center as in position A. Figure 20 shows the read range of an AK Tag coupled to EAN barcode at the optimum position. The measured read range shows a good agreement with the simulation where the maximum read distance is around 7 meters instead of 0.5 meters for the AK tag alone without external radiator.

This configuration has a smaller read range compared to the other tags of the same size (≈ 12 cm²) because of the coupling which reduces the overall tag gain compared to direct soldering and also due to the chip (Monza 5) which has a lower sensitivity of -17.8 dBm compared to the Monza-R6 (-20 dBm) as shown in table 2.

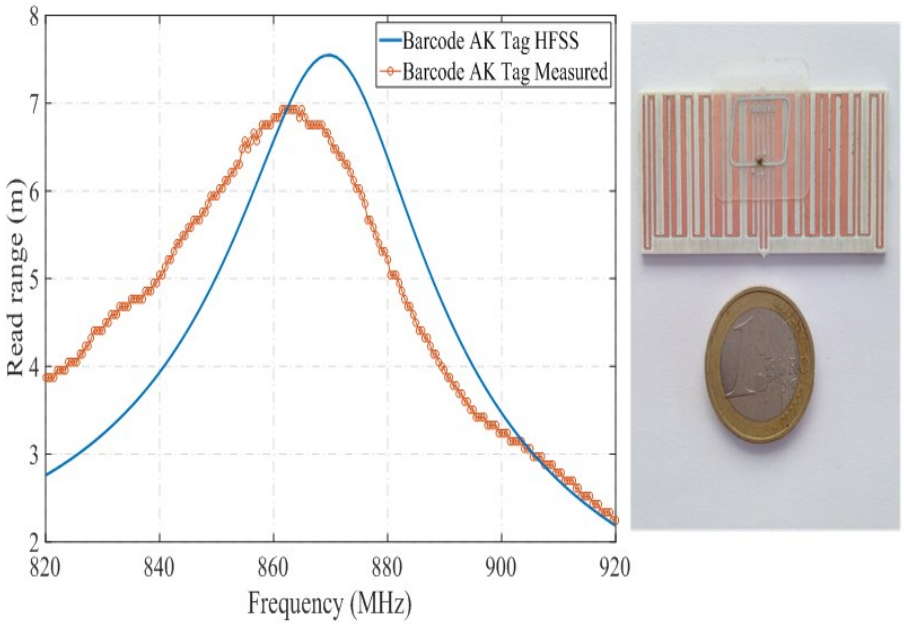

Fig. 20. Measured read range vs. HFSS simulation of an AK Tag coupled to EAN barcode at the optimum coupling position.

Table 2. Main characteristics of the realized tags at 866 MHz

Tag	Reflection coefficient Simulated (dB)	Gain HFSS (dB)	Area (cm^2)	Measured Read range (m)	Chip sensitivity (dBm)
Code128	-10	0.346	11.9	12.5	-20
EAN (Large)	-9	-0.596	9.2	11	-20
EAN (Small)	-11	-3.58	6.4	7.5	-20
EAN AKTag	-12	-1.78	12.4	7	-17.8

5. Conclusion

This chapter presented a comparison between read ranges of different tag designs in a real industrial environment using a handheld reader. Despite the multipath effect and reader output power limitation, all tag configurations were successfully detected. In order to provide a robust RFID traceability solution for food sector, we proposed a new technique based on sweeping the linear polarized signal of the transmitter antenna on the reader side, and thus makes the detection of tags independent of their orientations without reducing the system efficiency. Concept validation and measurements in practical environment were realized using a commercial UHF RFID tag in different orientations. Remarkable results are obtained with a precision of ±10 degrees due to attenuators accuracy, with the possibility of improving the system performance in future works using correlation technique and smaller attenuators steps.

Finally, we presented a proof of concept for smart labels combining the advantages of barcode and RFID technologies on the same label. Two different barcode standards were simulated and tested. The maximum read range achieved is 12.5 meters for a 12 cm^2 tag whereas the smaller configuration of 6.3 cm^2 presents a lower read range of 7.5 meters. A novel smart label configuration based on electromagnetic coupling with AK tag is presented. Parametric study on the coupling position was realized where the tag achieved a read range of 7 meters at the optimum position.

References

[1] "EUR-Lex - 32003R1830 - EN - EUR-Lex." [Online]. Available: http://eur-lex.europa.eu/legal-content/en/ALL/?uri=CELEX%3A32003R1830. [Accessed: 20-Feb-2018].

[2] *Council Regulation (EC) No 2991/94 of 5 December 1994 laying down standards for spreadable fats*, vol. 316. 1994.

[3] "Tagformance Pro," *Voyantic*. [Online]. Available: http://voyantic.com/products/tagformance-pro. [Accessed: 19-Oct-2017].

[4] "RF Attenuators - Fixed Precision Attenuators, High-Power Attenuators, Digital Step/Programmable Attenuators | Mini-Circuits." [Online]. Available: https://ww2.minicircuits.com/WebStore/Attenuators.html. [Accessed: 02-Jun-2018].

[4] Romero, Alejandro & Lefebvre, Elisabeth, Combining barcodes and RFID in a hybrid solution to improve hospital pharmacy logistics processes. International Journal of Information Technology and Management. 14. . 10.1504/IJITM.2015.068504, 2015.

[5] J. Han, G. Wang, and J. Sidén, "Fragment-type UHF RFID tag embedded in QR barcode label," Electron.Lett., vol. 51, no. 4, pp. 313–315, 2015.

[6] E. C. Jones and C. A. Chung, RFID in logistics: a practical introduction. CRC press, 2007.

[7] https://internationalbarcodes.com/ean-13-specifications/

[8] http://www.idautomation.com/barcode-faq/code-128/

[9] http://www.idautomation.com/barcode-faq/gs1-128/#Symbol_Size

[10] G. Marrocco, "The art of UHF RFID antenna design: impedance-matching and size-reduction techniques," in *IEEE Antennas and Propagation Magazine*, vol. 50, no. 1, pp. 66-79, Feb. 2008.doi: 10.1109/MAP.2008.4494504

Chapter 6

Design of RFID sensor Tag for food quality monitoring

1. Introduction

In this chapter, we will discuss the design of an RFID tag for detecting the level of cheese maturation during ripening. Several parameters are studied in order to determine the correlation between their variations and the level of cheese maturation. A significant variation of cheese permittivity and loss tangent can have an important effect on the RF matching and radiation efficiency of tag antenna. At the beginning of this work, it has been decided to track the variation of the permittivity and loss tangent as an indicator of maturation level. However, for some types of cheese, these variations can be very weak which makes it difficult to consider dielectric properties as sensing parameters for quality monitoring. Therefore, it was absolutely necessary to study other parameters.

The cheese maturation process is usually accompanied with significant amounts of gazes released during ripening and thus an important variation in the cheese wheel volume takes place. Therefore, measurements of carbon dioxide (CO_2) were achieved during ripening of Emmental cheese. Measurement results showed the possibility of using the amount of CO_2 as a sensing parameter during cheese maturation. Indeed, the increase of amount of released gazes as well as the

variation of physical parameters such as cheese volume have strong correlation with cheese ripening. Two configurations of RFID tags enhanced with different types of sensors were designed to measure the variation of amount of gazes and the increase of the cheese wheel dimensions during ripening process. Several measurements have been realized on different cheese samples in a real industrial environment and usefulresults are obtained for both configurations.

2. Permittivity as a sensing parameter

In the food sector, the variation of dielectric properties of some food products can be exploited as sensing parameter for quality monitoring. As discussed previously in chapter 3, the dielectric characterization analysis of different types of cheese products showed that the level of variation of cheese permittivity during maturation can be very different from one type to another. Therefore, the feasibility of designing an RFID sensor tag based on the variation of cheese permittivity depends on the significance of these variations during the maturation process. In this section, the effect of dielectric properties variation on the performance of UHF RFID passive tags simulated in direct contact with the cheese surface is studied. Three different scenarios are considered for the three studied cheese types: Emmental, Morbier, and Grimont. The measured dielectric properties of three types of pressed cheese presented in Table 1 are used for simulation models.

Table 1. Variation of dielectric properties of three types of cheese during ripening process

	Emmental		**Morbier**		**Grimont**	
	Start of ripening	*End of ripening*	*Start of ripening*	*End of ripening*	*Start of ripening*	*End of ripening*
ε_r	20	25,6	20,8	13,7	22	4
Tg (δ)	0,875	0,56	1	0,45	1,29	0,18

In this context, the evolution in cheese permittivity leads to the variation of the RFID tag's parameters such as gain and impedance of the antenna structure and therefore it affects the read-range of the RFID tag according to the Friis formula:

$$ReadRange = \frac{\lambda}{4\pi}\sqrt{\frac{P_{eirp}G_{tag}\ p(1-|S|^2)}{P_{th}}} \quad (6.1)$$

where λ is the wavelength of the carrier emitted by the reader, P_{eirp} is the regulated equivalent isotropic radiated power, P_{th} is the activation power of the chip, G_{tag} is the tag antenna gain, p is the polarization loss factor between reader and tag antennas. $|S|^2$ is the power reflection coefficient.

Assuming UHF RFID tags are typically designed to work properly at permittivity values corresponding to the start of ripening process. As the real part of the cheese relative permittivity ε_r increases, the impedance matching between the tag antenna and the RFID chip will decrease considerably due to antenna detuning reducing thus the tag read range performance. On the other hand, the decrease in loss tangent between start and end of ripening will mainly improve the tags radiation efficiency for the three scenarios and thus the tag read range performance will increase. In order to avoid this trade-off between the variations of dielectric constant and loss tangent, we used a design methodology that can maintain the effective bandwidth of the read-range and ensure the impedance matching between the chip and antenna for UHF RFID tags over a wide range of dielectric constant values [11]. This tag configuration is based on coupling of a near field RFID module (AK tag) to a meander antenna. The AK tag principle is inspired from the famous T-Match technique where a simple loop compensates the capacitance of the RFID chip while the two branches of the meander line increase the radiation resistance. By applying this configuration, the imaginary part of the tag's impedance will mainly depend on the loop dimensions and thus will be less dependent on the substrate's permittivity as shown in figure 1 where the complex impedance of the proposed design is simulated as function of dielectric constant.

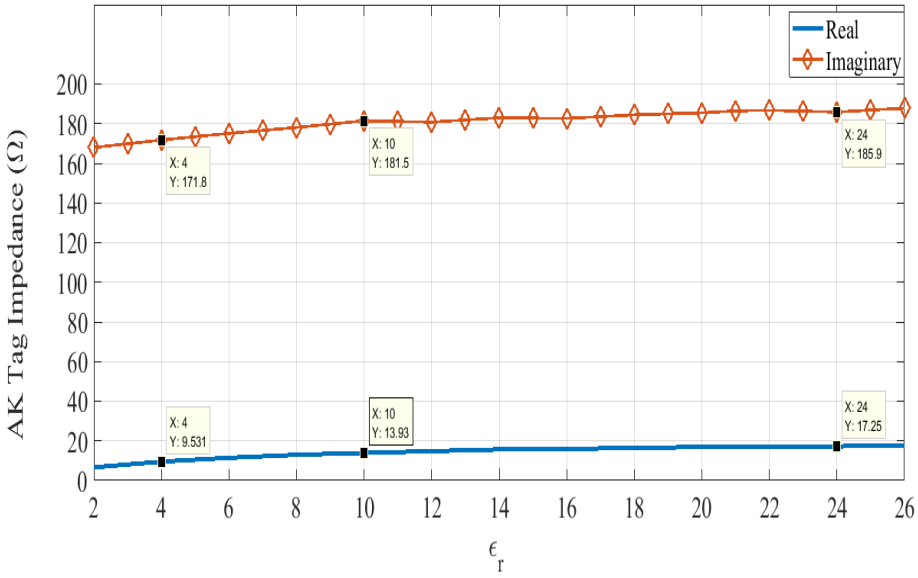

Fig. 1. AK Tag complex impedance as function of substrate permittivity ε_r

Over a range of ε_r between 4 and 24, the imaginary part of AK tag impedance varies around 15 Ω which represents less than 10% of the minimum value at ε_r = 4. However, the relative variation of the real part of the tag's impedance is more important versus the variation of ε_r (almost the double from ε_r = 4 to ε_r = 24) as it depends on the meander structure. Therefore, the variation of ε_r will not strongly affect the resonance frequency of the tag but rather it will affect the amplitude of the tag reflection coefficient. However, these variations due to ε_r are less significant compared to the variation of $\tan(\delta)$ which will be the main parameter affecting the tag performance during cheese ripening.

As the three types of cheese have quite similar values of dielectric constant at the start of their ripening, the same tag design was used for testing. The main differences in the tag performance in each case will be simply due to the radiation efficiency of the tag on different samples due to variation of their loss tangent values during ripening. The realized prototype is based on AK5 tag module which uses Monza 5 chip. This chip was modeled for simulation as a parallel RC model of 1,8 KΩ as resistance and 1,73 pF as capacitance respectively. The tag was simulated and designed on polymide substrate on casein fixture as shown in figure 2.

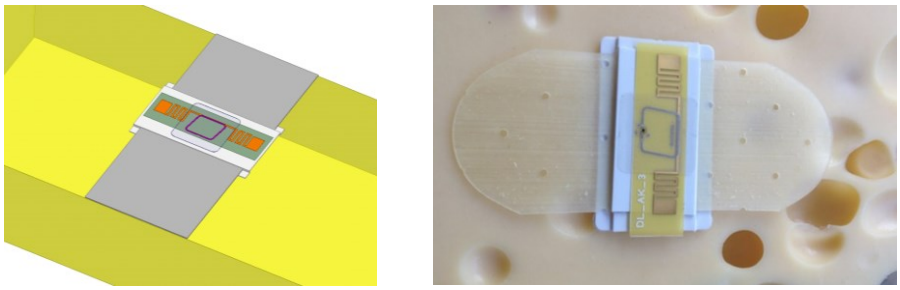

a b

Fig. 2.a) Simulation design model of Ak tag coupled to meander antenna b) Realized prototype on casein fixture

The final prototype was enhanced with reference points indicating the optimum position of coupling the AK tag module and thus guaranteeing the best performance. Measurements of the read range were realized using Voyantic Tagformance where the tag was placed beneath a sample of each type of cheese as shown in figure 3.

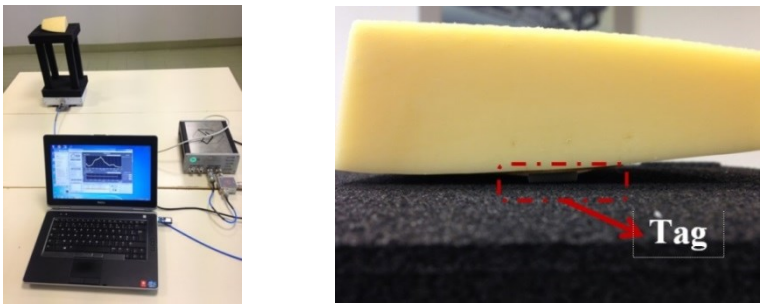

Fig. 3. Read range measurement setup using Voyantic Tagformance.

For Emmental samples, the difference in read range performance is in the range of just 10 cm maximum as shown in figure 4. This weak variation is due to quite low variation of dielectric losses of Emmental between start and end of ripening ($\tan(\delta)$ from 0.85 to 0,56) and therefore the increase in the tag performance was not very significant. More significant variations are realized in the cases of Morbier and Grimont samples as their dielectric losses decrease considerably during their maturation. This leads to significant improvement in the tag's read range performance at the end of ripening of both samples as shown in figure 4 b & c where the read range increased about 30 cm in the case of Morbier and Grimont samples as they had higher variation of $\tan(\delta)$ between start and end of ripening and thus more significant variation of read range compared to Emmental.

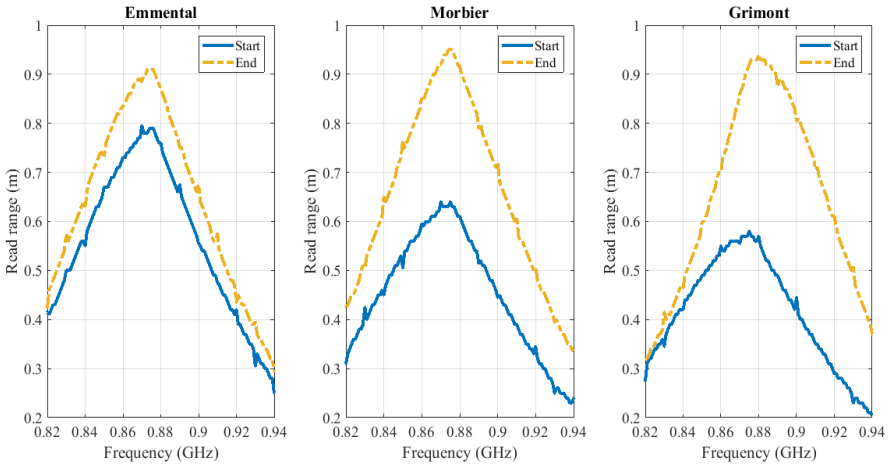

a *b* *c*

Fig. 4. AK5 tag read range comparison between start and end of ripening for three types of cheese a) Emmental b) Morbier c) Grimont

Despite the significance of dielectric properties variations of some types of cheese on the read range performance, this approach of RFID sensing tag is not very practical to be applied for cheese quality monitoring as the variation of the read range is just dozens of cm and when measured in a real environment it will be affected by multi-path which will reduce the accuracy of measurements. Moreover, the cheese permittivity will vary due to other parameters than the maturation such as humidity and temperature which makes it difficult to provide a robust sensing solution just based on variation of dielectric properties of food products.

3. Production of gas in foods

Many types of gases are produced during the fabrication process of different food products such as carbon dioxide (CO_2), hydrogen (H_2), hydrogen sulfide (H_2S) and ammonia (NH_3) [1]. Numerous metabolic pathways are responsible for the production of these gases, and they vary according to the microbial species and the substrate on which they grow. The production of gas by microorganisms may be desired in the production of fermented foods. This is the case for

Propionibacterium freudenreichii [2] responsible for the formation of characteristic eyes [3] during the ripening process of Emmental cheese.

In this section, we have studied the possibility of using commercial CO_2 sensors in order to detect the amount of CO_2 released during the ripening of Emmental cheese wheels. CO_2-source in this type of cheese is propionic acid bacteria (PAB). The ripening of these cheeses includes a step during which cheeses are stored at warm temperature (about 2-3 weeks at 20-25 ºC) for stimulating the PAB fermentation. During this step, CO_2 is intensively produced, leading to the growth of eyes [4]. Cheeses are often foil ripened and a plastic packaging is used to wrap the cheeses during the whole ripening period in order to retain moisture content and thus reduce the transformation of valuable cheese into rind [5]. Moreover, this technique helps avoiding excessive loss of gaseous compounds which give the Emmental its characteristic flavor [6].

A CO_2 sensor incorporated into food package can efficiently monitor product quality until it reaches the consumer [7]. The CO_2 sensors can be divided into two types, electrochemical and optical, based on the type of transducer. The objective is to integrate a gas sensor inside the cheese packaging during maturation and to determine the feasibility of using a commercial CO_2 sensor considering the amount of gases released, the complexity of the measurements, the power consumption of the sensor and the final cost.

3.1. Electrochemical CO_2 sensors

Electrochemical CO_2 sensors are further sub-categorized into potentiometric, amperometric, and conductometric types [8]. The main difference between these sensors is their behavior when exposed to a mixture of different gases. MQ-135 sensor [9] is sensitive to different types of gases including NH_3, benzene, alcohol and CO_2, whereas MG-811 [10] is less reactive to other gases and is mainly sensitive to CO_2 which makes it more suitable for applications where the CO_2 is the main parameter to follow as in the case of cheese ripening. Chemical Sensor MG-811 adopts solid electrolyte battery principle to detect carbon dioxide. When the sensor is exposed to an increase in the CO_2 concentration, ElectroMotive Force (EMF) is generated between the sensor sensitive electrode and reference electrode according to Nernst's equation [11] that relates the reduction potential of an

electrochemical reaction to the standard electrode potential, temperature, and concentrations of the chemical species undergoing reduction and oxidation as follows :

$$EMF = E_0 - \frac{RT}{2F} ln(Q)$$

E_0 : Standard cell potential

R : Gas Constant (8.314 J/mol.K)

T : Absolute Temperature in Kelvin

F : Faraday constant

Q : Reaction quotient which measures the relative amounts of products and reactants present during a reaction (Concentration of CO_2)

When the internal heating element is activated, this gas sensor responds to CO_2 by generating a small voltage in proportion to the amount of CO_2 present in the air exposed to the internal element. The sensor is a high impedance device and requires a buffer/amplifier to measure the output where the voltage from the sensor actually drops as CO_2 concentration increases.

In order to work properly, these sensors need fairly precise calibration and therefore they incorporate a potentiometer that can be adjusted to specific threshold to return meaningful results. The major drawback of electrochemical CO_2 sensors is that they must be allowed to 'warm up' before measurements are stable (typically a couple of hours minimum) which makes using these sensors very power consuming and difficult to use for food packaging applications.

3.2 Optical CO_2 sensors

NDIR (Non-Dispersive Infrared) sensors are simple spectroscopic devices often used for gas analysis. The key components of a NDIR sensor are an infrared source (lamp), a sample chamber or light tube, an optical wavelength filter, and an infrared detector as shown in figure 5.

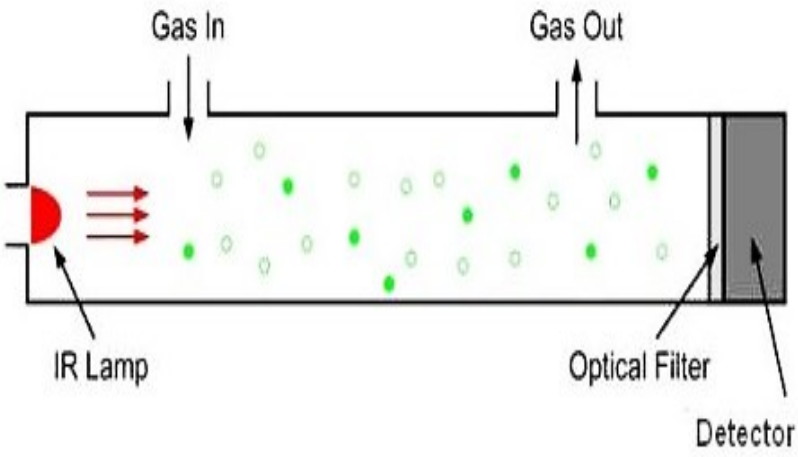

Fig. 5. Non-Dispersive Infrared (NDIR) gas measurement system [12]

The gas is pumped or diffuses into the sample chamber and gas concentration is measured electro-optically according to the absorption of a specific wavelength in the infrared (IR) spectrum. The IR light is directed through the NDIR sample chamber towards the detector. The detector has an optical filter in front of it that eliminates all light except the wavelength that the selected gas molecules can absorb. Other gas molecules do not absorb light at this wavelength, and do not affect the amount of light reaching the detector. The IR signal from the source lamp is usually chopped or modulated so that thermal background signals can be offset from the desired signal [13]. For greater optical efficiency, a reflector assembly can surround the lamp used for the NDIR sensor. The reflector is usually parabolic in shape to collimate the IR light through the sample chamber towards the detector. The use of a reflector can increase available light intensity by two to five times. The intensity of IR light that reaches the NDIR detector is inversely related to the concentration of target gas in the NDIR sample chamber. When the concentration in the chamber is zero, the detector will receive the full light intensity. As the concentration increases, the intensity of IR light striking the detector decreases. Beer's Law [14] describes the exact relationship between IR light intensity and gas concentration as follows:

$$I = I_0 e^{-kP}$$

where:

I = the intensity of light striking the NDIR detector

I_0 = the measured intensity of an empty NDIR sample chamber

k = a system dependent constant

P = the concentration of the gas to be measured

NDIR sensors can be used to measure practically all inorganic and organic gases, but they are most often used for measuring carbon dioxide because no other sensing method works as simply and reliably for this gas. Calibration gases of specific concentration are available for determining the NDIR system constant k for any particular sensor design. Compared to electrochemical gas sensors, NDIR gas sensors have better measurement accuracy and they are more suitable to be integrated in food packaging.

3.3 VOC sensors

Volatile Organic Compounds (VOC) are just one aspect of the plethora of chemicals present in foods where the total amount of VOCs found in a single food item can range from 24 to 5328 ppb [15]. VOCs include electrochemical, semiconductor with solid electrolyte and PID-type sensors (photoionization detectors) [16].

In Metal Oxide Semiconductor Sensors, particles diffuse towards the receptor surface and interact with the metal oxide (maintained at suitable temperature using heater). This interaction results in change of resistance of the receptor element which corresponds to the VOC concentration [17], [18].

On the other hand, the photoionization detector (PID) uses ultraviolet light to irradiate the VOC molecules, thus ionizing them. The analysis chamber is composed of two plates between which a difference of potential is applied as illustrated in Figure 6. Upon production of ionized molecules, a current is created and recorded where the intensity of the current is a direct measurement of the amount of ionized molecules.

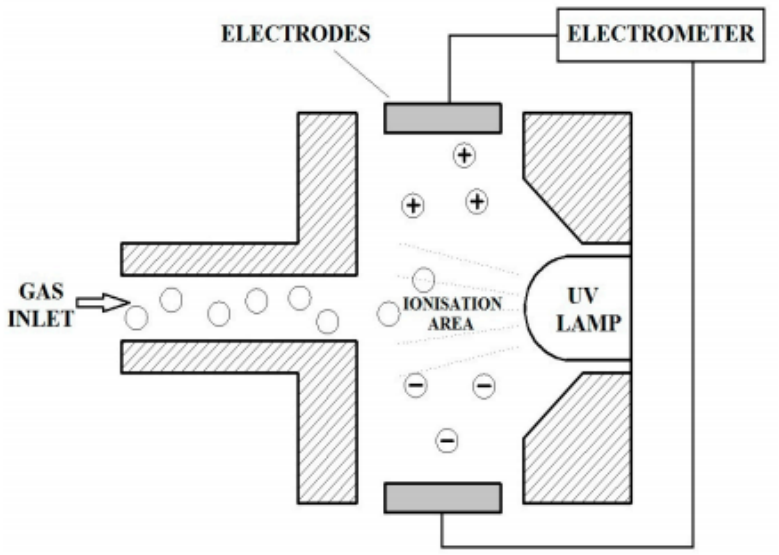

Fig. 6. Photoionization VOC sensor design [19]

During Emmental cheese ripening, several volatile compounds are produced such as propionic acid ($C_3H_6O_2$) which is an important parameter indicating the level of fermentation as well as cheese flavor [20]. However, the majority of these organic compounds are kept dissolved in the cheese texture and very little amount is released outside the cheese curd which makes it very difficult to be detected.

3.4 CO2 sensor for monitoring gas production during cheese ripening

As discussed in the previous section, the objective is to study the production of carbon dioxide which is released during the cheese ripening due to fermentation. A commercial sensor Telaire 6700 [21] is used in order to measure the amount of CO_2 inside the packaging of an Emmental cheese wheel provided for testing purpose. The sensor circuit consists of a microcontroller unit which communicates with the sensor and then the measured data is transferred to an RTC-SD module to be registered with time and date. The main challenge of this configuration is the power source to activate the circuit. As the sensor will be integrated inside the package, it was not possible to use a battery and at the same time these types of

sensors cannot be powered by means of energy harvesting as their power consumption is in the range of 750 mW (150 mA; 5 Volt). Therefore a wireless power transceiver module [22] is used as shown in figure 7. This module is based on inductive coupling between TX and RX coils and it can provide a maximum output of 5 V and 600 mA.

a *b*

Fig. 7. CO_2 sensor powered by coupling a) Rx coupling module connected to the sensor circuit b) Tx coupling module powered by a USB battery pack

3.4.1 Sensor installation

Before installation on cheese wheel, all the circuit components were protected against humidity and isolated using food safe acrylic coating [23] in order to avoid any short circuit during measurements while leaving access just to the sensor zone. Also, the cheese wheel was identified with additional labels in order to differentiate it from the other cheeses and thus avoid any error during the transportation to ripening caves. Then, some parts of the cheese curd are removed to install the sensor on the cheese wheel as illustrated in figure 8.

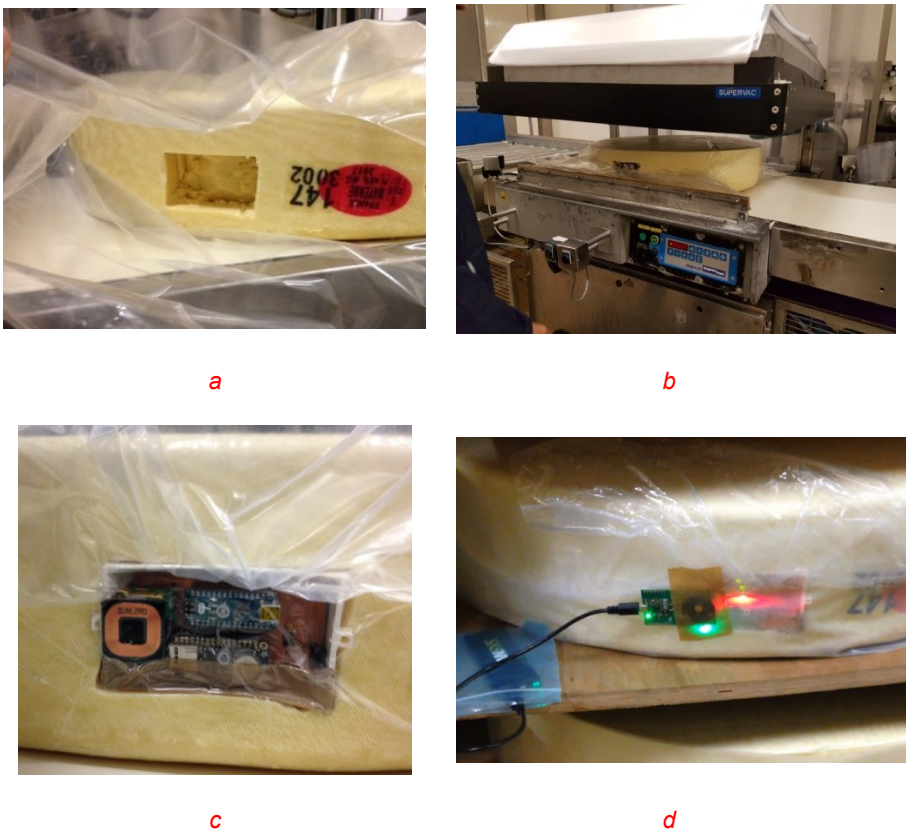

a *b*

c *d*

Fig.8. CO_2 sensor installation a) Removing parts of the curd to install the sensors b) Cheese wheel wrapping c) Sensor integrated in the cheese packaging d) Measurement setup in warm cave where the sensor is powered by inductive coupling.

A 3D printed box based on Polylactic Acid (PLA) is used as a shield for the circuit (Fig.8.c) which helps avoiding any direct contact between the components and the cheese. At the same time, this box creates a small gap between the wrapping foil and the surface of cheese near the sensor which allows better circulation of released gases leading thus to an improved sensitivity for gas detection.

The selected cheese wheel for testing was at the end of the cold ripening chamber. After sensors installation, the cheese wheel was directly transported to the warm ripening chamber where gas releases will take place. The TX wireless power module is coupled to the RX module by fixing it on the outer surface of the

plastic foil while it is connected by USB cable to a portable power pack as shown in Fig.8.d. This configuration allows powering the circuit without removing the TX module and thus provides easier and more stable measurements. Moreover, the LEDs integrated in the power modules and the sensor circuit provide visual verification of the circuit functionality and thus any error due to bad coupling can be easily detected and fixed.

3.4.2 Measurement results and discussion

According to the datasheet of the sensor, a period of around 2 to 10 minutes is required for warming up the sensor and for calibration in order to get accurate results. As the measurements are realized over discrete periods and not in continuous, we had to verify the stability of the measurements when the sensor is powered off and then activated again after some time for the next measurement. Figure 9 shows the results obtained by the CO_2 sensor when the power was turned off in the middle of measurements. The sensor was powered for around 15 minutes then it was turned off for 5 minutes (red zone) before resuming the measurements for another 15 minutes.

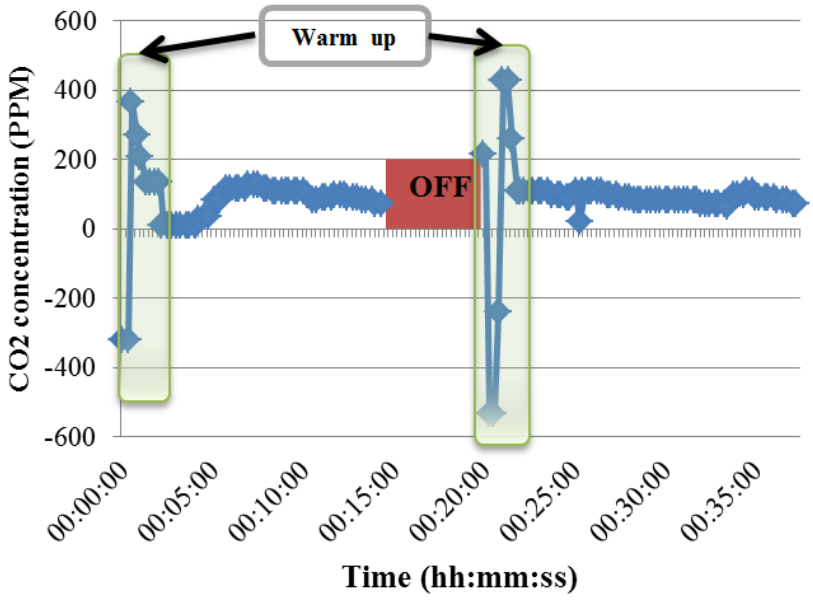

Fig. 9. Results obtained from CO_2 sensor with a turn off period between measurements

The peaks detected at the beginning and at the middle correspond to the warm up periods before the measurements stabilize. During the first measurements, the sensor value began around 0 ppm and kept increasing until it stabilized around 100 ppm. After turning off the sensor and resuming the measurements, the measured value began where the previous measurement stopped around 100 ppm which means that the turning off period did not affect the calibration of the sensor and thus the measurements were kept stable.

These measurements were realized directly after wrapping the cheese wheel. The little amount of CO_2 detected is due to the fact that the packaging was not 100% under vacuum and thus small amount of air was still inside the foil which explains the values of 100 ppm measured by the sensor. The cheese wheel was then transported to the warm ripening chamber for testing. The main advantage of ripening cheese wrapped in foil is that it requires less time for maturation which reduces the period of the ripening stage in warm chamber for just two weeks. Moreover, compared to cheese ripened in open air, the amount of CO_2 released during maturation is held inside the packaging which improves considerably the measurement sensitivity.

Unfortunately, it was not possible to realize these measurements during the entire period of ripening due to many restrictions applied in an industrial site. First, there are restrictions on mobility inside the factory, especially for visitors, which makes it difficult to access the cheese for measuring regularly. Also, it was not allowed to leave a power pack inside the ripening chamber without close surveillance in order to avoid fire risks. Therefore, we decided to realize the measurements in the second week when the cheese wheel starts swelling and considerable amounts of gases are released. Figure 10 shows the measurements realized in two days during the second week of ripening in the warm chamber. In the first day, the concentration detected by the sensor increased slowly until it reached around 400 ppm after one hour of measurements. In the next day, we decided to extend the time of measurements until the power pack is off in order to see the behavior of the sensor over a larger period. As the first day, the measurements increased slowly until reaching around 1300 ppm after 2 and half hours. The sensor stabilized around these values of 1300 ppm for the rest of measurements until the power pack was totally discharged and the measurements stopped.

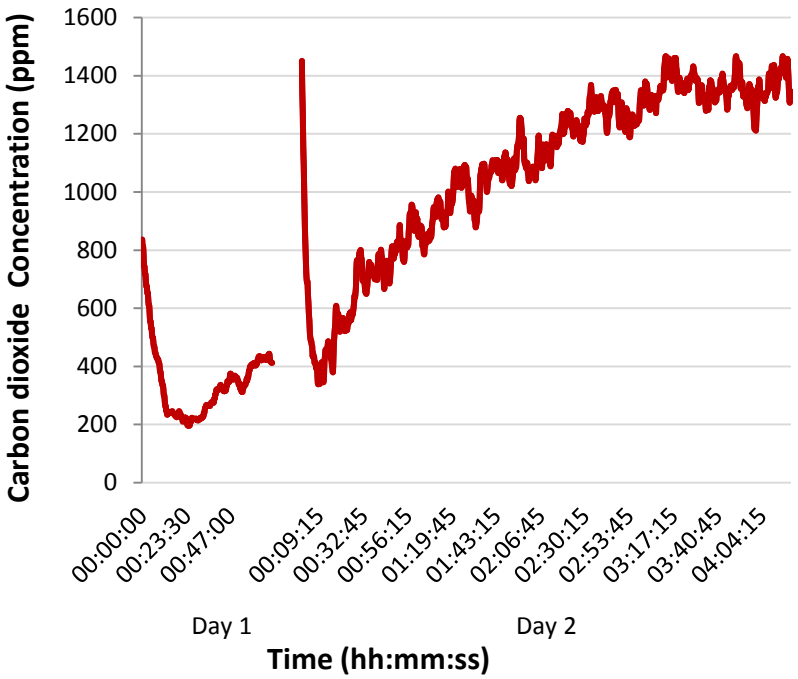

Fig. 10. Results obtained from the CO_2 sensor over two days in the warm ripening chamber.

These results showed the potential of following the carbon dioxide as a sensing parameter for the cheese ripening. A variation of 1000 ppm in the CO_2 concentration during maturation can give significant indication about fermentation activity as well as cheese flavor. Considering the complexity of measurements and the sensor cost, this solution based on available commercial sensors is still unpractical to be applied commercially. Moreover, the high power consumption of gas sensors requires using a power source or a battery inside the packaging which adds more costs and conflicts with the food norms of safety.

However, measuring other parameters highly correlated to gas production can be considered as an interesting alternative. Following other parameters directly related to carbon dioxide will provide more flexibility at the level of tag design which allows reducing the total cost as well as the power consumption.

4. Physical parameters

Some microorganisms produce gas as they grow in food, thereby causing the food itself or the packaging to swell. The gas production during cheese ripening is usually accompanied with the formation of numerous small (1±2 mm) or larger (3±6 mm) holes in the cheese mass [24]. In some cases, this can lead to noticeable physical changes especially in the case of very large cheese wheels (80 kilograms) where huge amounts of gases are released (CO_2, H_2 or both) which makes the cheese wheel swell considerably.

The objective of this section is to design a sensor based on RFID tag which is capable of following the changes occurring in physical parameters during cheese ripening. Two design configurations were considered for measuring the variation of cheese wheel size due to swelling as well as the variation of pressure inside the packaging caused by the significant amount of CO_2 released. Interesting results are obtained showing the possibility of following physical parameters using cost effective tag designs which can be considered as an alternative to gas sensors.

4.1. Stretch sensor

There are several types of stretch sensors which are mainly based on elastomers such as silicone, acrylic, and natural rubber. These materials are electrical insulators, however, by adding particles of a conductive material such as carbon black or nickel to the uncured polymer, they can be turned into a conductor [25].

The objective is to use a stretchable cord sensor which can detect the volumetric change of the cheese wheel during ripening process. A stretch sensor which modifies its internal resistance in function of cheese diameter variation was found to be suitable for this application. Moreover, it shows the advantage of being much more practical as it is installed outside the package avoiding any electrical contact with the cheese. The cord is made of carbon impregnated rubber; its section is circular with a diameter of about 2mm, and its resistivity is about 140 Ω/cm. As the sensor is stretched out, its resistance increases and can be stretched more than 50-70% longer than its resting length. Therefore, it can be easily adapted to the cheese wheel size. We realized our study on the same type of Emmental cheese wheels used for gas sensor testing. The average wheel diameter at the beginning of maturation process can vary between 79 cm to 81 cm. At the

end of ripening, the cheese wheel swells considerably due to gases released and its diameter increases around 3 to 4 cm as shown in figure 11. Assuming a tolerance of 10 Ω/cm at the level of the sensor, thus our measurements are in the range between 32 KΩ at the start of ripening and 39 KΩ at the end of maturation.

a *b*

Fig. 11. Stretch resistive sensor installed on Emmental cheese wheel a) start of ripening b) end of ripening

The cheese wheel height also varies considerably during ripening; however, the cheese wheel should be flipped many times during the maturation process in order to allow better distribution of gases inside the texture. Therefore, we chose to install the sensor around the diameter to ensure the stability of measurements.

4.2. UHF RFID tag design enhanced with stretch sensor

Besides achieving good matching between the IC and the tag antenna, the main design objective for this application is to easily realize measurements and to store the sensor values in the RFID chip user memory during the entire period of cheese ripening. Recently, there are many RFID chips enhanced with communication buses (SPI or I2C) which allow using a microcontroller unit (MCU) as an intermediate device between the sensor and the RFID chip. However, there are already commercial RFID chips enhanced with analog entries to directly measure different types of sensors. The chip SL900A provided by ams [26] was considered for this study as it is enhanced with two analog entries allowing many sensor configurations. Moreover, the chip can be configured using an easy software interface which gives more flexibility and provide easy and better control of the chip internal parameters to achieve accurate measurements.

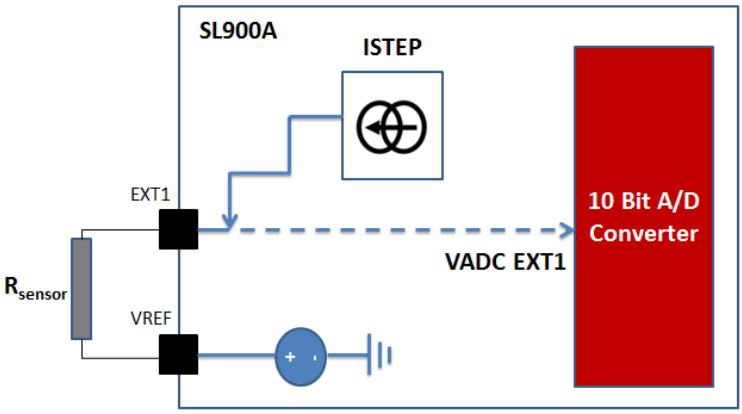

Fig.12. SL900A measurement configuration of resistive sensor

In most cases, the sensor front end (SFE) of SL900a chip can accept different types of sensors without associating additional components. This is possible by means of either the use of software reconfigurable Current source value (I_{STEP}) used with the first analog entry EXT1 or by existing software reconfigurable resistor feedback ladder (Rf) used with the second analog entry EXT2. In addition, two reconfigurable voltage references (V_{01} and V_{REF}) can be used to change the input voltage range accepted by the internal AD converter based on the resistance ranges presented by the sensor. In our design configuration we choose the first measurement approach based on I_{STEP} (figure 12) as it provides higher precision compared to the reconfigurable resistor feedback ladder configuration. The minimum and maximum resistance values that can be measured in this configuration are: $R_{Sens-min} = 6.3\ \Omega$ (maximal resolution) and $R_{Sens-max} = 2.44\ M\Omega$.

As the resistive sensor is supplied with I_{STEP}, the resistance can be calculated from:

$$R_{SENSOR} = \frac{V_{EXT1}}{I_{STEP}}$$

with

$$V_{EXT1} = AD_{code} * \frac{V_{REF} - V_{01}}{1024}$$

Thus

$$R_{SENSOR} = AD_{code} * \frac{V_{REF} - V_{01}}{I_{STEP} * 1024}$$

In this configuration, V_{REF} and V_{01} control the input range of ADC where we can select the appropriate combination through eight reference voltage levels for each. Selecting a combination where the voltage difference is high will allow covering wide range of input values; however, this will be at cost of lower resolution. On the other hand, the current I_{STEP} can be selected in a range between 0,25 µA and 7,75 µA with a step of 0,25 µA where its value mainly affects the sensitivity of the measurement. However, this value should be selected carefully along with V_{REF} and V_{01} in order not to exceed the limits of the ADC.

Figure 13 explains how to select the optimum value of I_{STEP} which corresponds to the range of ADC determined by V_{REF} & V_{01}. Considering V_{REF} = 610 mV and V_{01}= 410 mV, this configuration corresponds to the last 350 bits of the ADC (between 674 and 1024). Based on the values of R_{min} and R_{max} expected for the sensor (between 32 KΩ and 39 KΩ), the I_{STEP} should be selected in a way that the measured values do not exceed the limits of ADC and at the same time provides the highest possible sensitivity. According to this criteria, measured resistances corresponding to I_{STEP} values (4 µA, 4.25 µA,5.25 µA and 5.5 µA) fall outside the expected range of sensor over the allowed ADC bits.

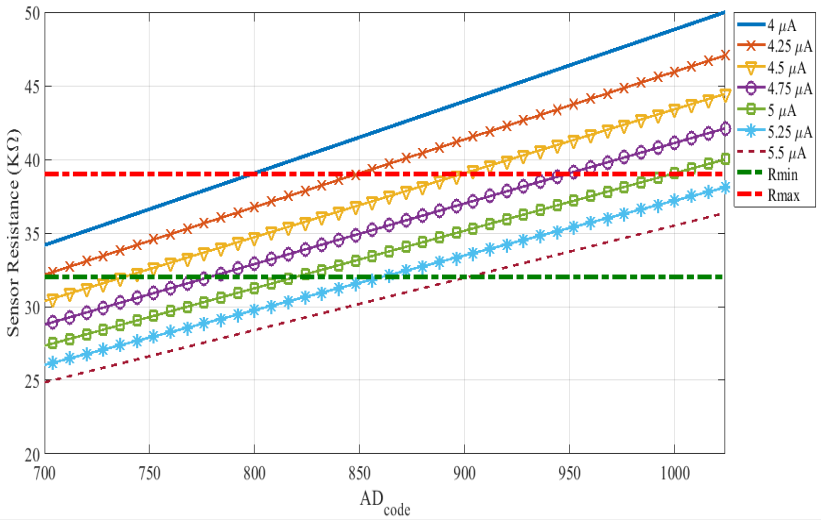

Fig. 13. Sensor resistance as function of AD_{code} for several values of I_{step}

On the other hand, I_{STEP} values (4.5 µA, 4.75 µA and 5 µA) fall in the expected range of the sensor without exceeding the ADC limits. The choice between these three values corresponds to the one which gives the best performance. As the cheese wheels can vary in terms of initial diameter and as the ADC variation is directly proportional to I_{STEP}, thus, the chip was configured with I_{STEP} = 4.5 µA in order to avoid any unexpected saturation of ADC at the end of measurements.

After configuring the chip and installing the tag on the cheese wheel, the sensor must be left for a period to settle before activating the tag and realizing the first measurement. The SL900A can be configured to work in both semi-passive and fully passive modes. As the tag is installed out of the package and there is no direct contact between the sensor and the cheese, we configured the tag to work in semi-passive mode in order to register automatically the measurements into the chip user memory and thus the measurements are recovered at the end of ripening. Two tag prototypes were installed on two different cheese wheels as shown in figure 14. The results obtained from both sensors varied between 34 and 36 KΩ which corresponds to the early estimated values. An offset of nearly 0.5 KΩ is observed between the initial values of two sensors. However, results showed quite similar behavior for both sensors where their values were almost constant during the cold chamber stage and then started to increase gradually as the cheese wheels started to swell into the warm ripening chamber where the average variation of the sensor resistance is around 1,2 KΩ.

a

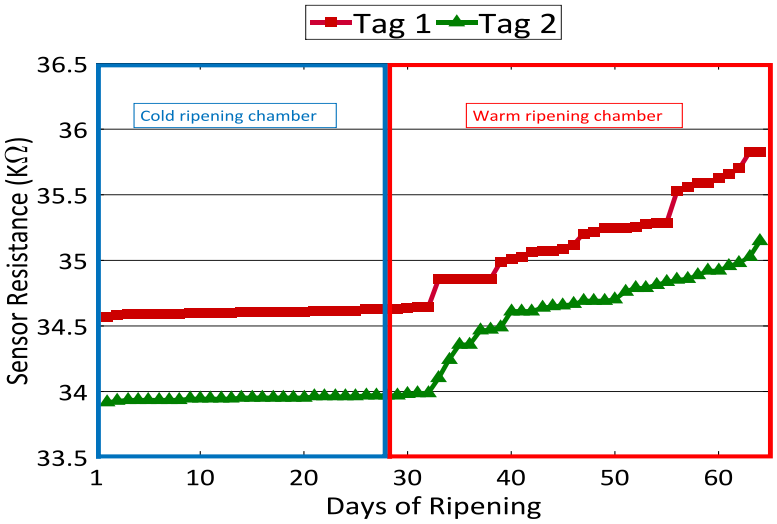

b

Fig. 14. a) Measurement setup b) Resistance variation of two stretch sensors installed on two cheese wheels during their ripening.

This sensor tag configuration showed the potential of using a simple resistive cord that can provide information about the change in the cheese size during ripening. This information is of great importance for cheese manufacturers as it allows them to quickly detect any deformation in the cheese wheel during fabrication. Moreover, these results can be correlated with other types of sensors and give indication about the amount of gas released during ripening as function of the rate of cheese swelling.

4.3. Monitoring pressure inside food packaging

Recently, food manufacturers are using smart packaging for their finished goods and products in order to monitor various aspects, such as moisture, temperature and oxygen. There are two main approaches on which intelligent packaging systems are based; the first approach is based on data systems (bars labels or RFID tags) used to store or transmit data whereas the other approach is based on indicators of incidents or biosensors in packaging that allow control of the environment and product packaging [27]. In this context, fermented food products can produce considerable amounts of gases which increase the pressure inside the packaging and cause volume expansion [28]. Therefore, a smart packaging enhanced with a pressure sensor can give an indication about the amount of gases

inside the packaging by means of correlation with pressure values. The objective of this section is to design an RFID tag for monitoring pressure variation inside the cheese wheel packaging due to fermentation and gas production. As the sensor is integrated inside the package, it is indispensable using a low power sensor which allows using a totally passive tag approach powered by energy harvesting.

There are several types of electronic pressure sensors which are based on different technologies such as piezoelectric, optical or inductive principles [29]. Micro electromechanical sensors (MEMS) based on piezoelectric or piezoresistive approaches are recently the most used for pressure monitoring. This is due to their small size, lightweight, high reliability and smart interface features which allow them to be applied easily in different applications.

Piezo-resistive based transducers rely on the piezo-resistive effect which occurs when the electrical resistance of a material changes in response to applied mechanical strain. When piezo-resistors are placed in a Wheatstone bridge configuration and attached to a pressure-sensitive diaphragm, a change in resistance is converted to a voltage output which is proportional to the applied pressure [30]. On the other hand, piezoelectric-based transducers rely on the piezoelectric effect, which occurs when a crystal reorients under stress forming an internal polarization. This polarization results in the generation of charge on the crystal face that is proportional to the applied stress [31]. Unlike strain gage sensors, piezoelectric sensors require no external excitation. However, piezoelectric sensors are effectively AC coupled devices, and thus, they are incapable of measuring a true static pressure as piezoelectric material can only sense alternating force. Therefore, piezo-resistive sensors are more suitable for our application as they offer true static pressure measurement capability without taking any special precautions.

In this work, we will use a piezo-resistive sensor module which includes a high linearity pressure sensor and an ultra-low power 24 bit ΔΣ ADC providing a resolution of 0.2 mbar [32]. The main function of the sensor is to convert the uncompensated analogue output voltage from the piezo -resistive pressure sensor to a 24-bit digital value, as well as providing a 24-bit digital value for the temperature of the sensor. The main advantages of this sensor are its very low power consumption and the possibility to be interfaced to MCU using I^2C.

4.4. UHF RFID tag design enhanced with pressure sensor

The main objective of the tag design is to provide a totally passive solution where the sensor along with the microcontroller are powered by means of energy harvesting avoiding thus the need of batteries inside the package. Therefore, RFID chip SL900A was chosen for this design as it can provide an output power based on energy recuperated from the reader interrogating signal.

The studied architecture in this work is illustrated in figure 15. It consists of a passive UHF SL900a RFID tag that can provide through its V_{Rectf} output pin a regulated voltage signal. The chip output is followed by super tantalum storage capacitor and a low forward voltage Schottky diode that prevents the discharge of the capacitor in the internal circuit of the chip. Low power consumption MCU PIC16LF1707 is used in order to perform two tasks: sampling the received sensor signals using I²C communication protocol and organizing the pressure and temperature data into the user memory of the SL900A chip using the SPI communication protocol.

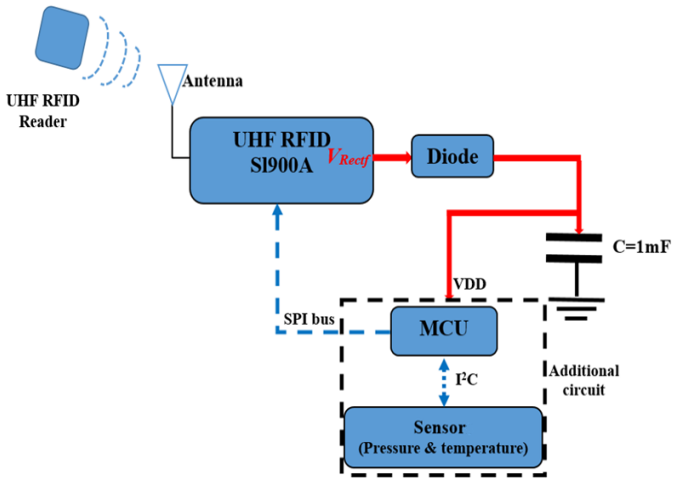

Fig. 15. The block diagram of the proposed tag architecture

Compared to previous sections, the tag is installed inside the package of smaller size cheese wheels in order to validate the concept of pressure variation for cheese wheels of different sizes. Two prototypes were realized and installed on two different wheels where the tags are placed on the upper surface of the wheel as

they are not flipped during maturation process like the big wheels. Due to high dielectric loss of the cheese ($\tan(\delta) \approx 0.8$), a compressed foam layer was inserted between the tag and the cheese surface as illustrated in figure 16 in order to reduce the amount of signal absorbed by the cheese and thus provide the best possible conditions for energy harvesting.

a

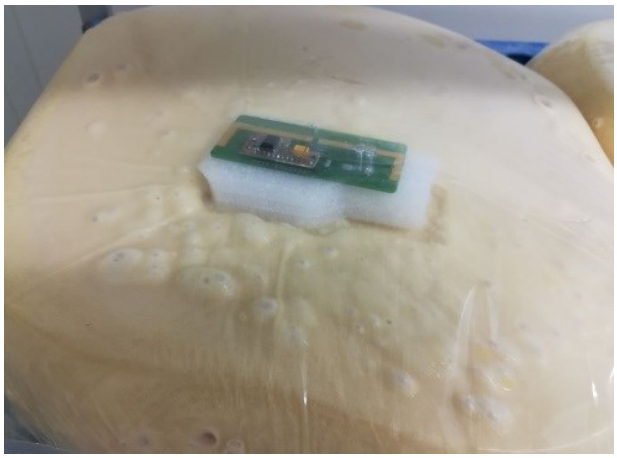

b

Fig. 16. UHF RFID tag configuration for pressure monitoring inside the cheese package a) cheese package under vacuum with tags on top b) Creation of bubbles in the cheese texture due to gas release which results into an increase of pressure

The cheese wheels were ripened in a temperature controlled ripening chamber in a period of nearly 2 months. Figure 17 shows the results obtained by the two sensors where the cheese wheels were ripened three weeks in cold chamber then in a temperature around 23°C for a period of one month.

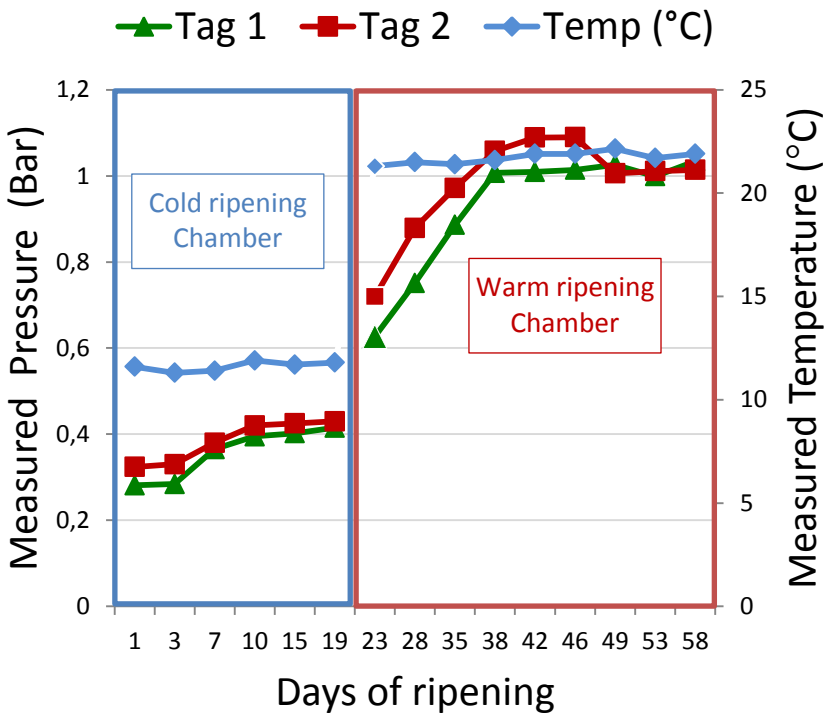

Fig. 17. Results of pressure and temperature obtained by two sensors inside the package of Emmental cheese during ripening.

The first measurements were realized after packaging where a small level of pressure is detected (250 mBar) because the cheese wheels are not enveloped under high vacuum in order not to deform their soft curd. During the first three weeks, the cold temperature decreases the fermentation activity and thus little variation of pressure (150 mBar) inside the package was detected. After increasing the chamber temperature to 23°C, the measurements were realized three days later in order to allow the temperature inside the package to stabilize. As the fermentation rate is accelerated due to temperature, the cheese wheels started to

swell gradually where the first values of pressure reached around 600 mBar. Then, the production of gases increased significantly and some bubbles started to figure on top of the cheese wheel starting from the end of the second week where the pressure inside the package reached a maximum of around 1.1 Bar.

This RFID tag showed the possibility of monitoring temperature and pressure inside a food package using a totally passive design approach. The sensor and the microcontroller were powered by an energy harvesting module where the power consumption was optimized by using a watchdog timer in the microcontroller code. An absolute pressure variation of 700 mBar inside the packaging of cheese wheels during ripening showed the potential of monitoring pressure as a sensing parameter which gives indication about the fermentation activity and gas production during ripening. Moreover, the pressure sensor can be used to monitor the package tightness of food products where any leakage due to invisible damage in the package will lead to immediate variation in the sensor value.

5. Conclusion

Sensors embedded in the food packaging enable easy tracking of the product throughout the supply chain. This enforces an efficient, controlled and well-monitored food supply chain, wherein the exact degree of damage or well-being of a food product can be monitored. Several parameters vary significantly during the maturation process of food products. In this chapter, we focused our study on observing and analyzing the main parameters which vary during the ripening period of Swiss type cheese. The main objective is to design a sensor RFID tag to detect the variation of a sensitive parameter during ripening and validate the tag feasibility when applied in real industrial conditions.

Starting by the dielectric properties of cheese, we studied the effect of permittivity and dielectric losses on the performance of the tag antenna. Measurements showed little variation on the read range of a tag installed on Emmental cheese whereas more significant variations were detected in the case of other types of cheese as their dielectric properties varied considerably compared to Emmental. However, even with significant variation in the dielectric properties, it is hard to distinguish between variations due to ripening and other variations due to environmental conditions such as humidity, temperature or other parameters

such as the texture of the material where the creation of holes can significantly affect the dielectric measurements as in the case of Emmental.

Therefore, other parameters were considered in order to monitor the quality of ripening process of cheese. One of the major parameters which characterize the quality of foods, especially the fermented ones, is the amount and type of gas released during its maturation. In the case of Emmental cheese, measurement realized using a commercial gas sensor showed an important variation at the level of CO_2 inside the cheese package. However, the complexity of measurements, high cost of sensor and the necessity of using a power source make this approach far from being applied in the industry. On the other hand, other parameters are directly related to gas production and at the same time are easier to detect using simple RFID sensor tag design.

An RFID tag was designed in order to detect the increase of the cheese wheel diameter when it starts to swell due to gas production. Two tags were enhanced with a resistive stretch sensor and installed around the rind of two cheese wheels. Results obtained from both sensors showed a significant variation of their resistances between start and end of ripening. These variations could be correlated with the amount of gas produced and thus give indirect indication about the fermentation activity and the quality of ripening.

Another RFID tag design based on low power pressure sensor was also realized and tested on two cheese wheels of smaller sizes in order to validate if the effect of gas production will be significant as in bigger cheese wheels. The tag configuration was totally passive where the sensor was powered by an energy harvesting module. After two months of ripening, results obtained by both sensors showed an important variation in the pressure inside the package between start and end of the maturation process. In addition, this sensor configuration provided an accurate temperature measurement.

A more developed configuration can be realized by combining both sensors on the same cheese wheel. This design approach will be able to provide information about three major parameters which vary during cheese maturation: pressure variation, dimensional variation, and temperature. By means of correlation between these physical parameters and other chemical parameters such as CO_2, we can have better understanding about the cheese ripening process and thus a robust sensing solution for cheese ripening.

References

[1] R. Jeantet, T. Croguennec, P. Schuck, and G. Brulé, *Handbook of Food Science and Technology 1: Food Alteration and Food Quality*. John Wiley & Sons, 2016.

[2] J. F. Kennedy and C. Bandaiphet, "Encyclopedia of Dairy Sciences (Volume 1–4): H. Roginski, J.W. Fuquay, P.F. Fox (Eds.); Academic Press, Amsterdam, 2003, ccclxvi+2799 pp., ISBN 0-12-227235-8, Price £530," *Carbohydr. Polym.*, vol. 54, no. 3, p. 394, Nov. 2003.

[3] F. G. Martley and V. L. Crow, "Open texture in cheese: the contributions of gas production by microorganisms and cheese manufacturing practices," *J. Dairy Res.*, vol. 63, no. 3, pp. 489–507, Aug. 1996.

[4] M.-T. Fröhlich-Wyder, H.-P. Bachmann, and M. Gerard Casey, "Interaction between propionibacteria and starter/non-starter lactic acid bacteria in Swiss-type cheese," *http://dx.doi.org/10.1051/lait:2001001*, vol. 82, pp. 1–15, Jan. 2002.

[5] M. V. Gurp, C. J. Hooft, J. Krijgsman, and A. A. M. Stroeks, "Process for foil ripening of cheese," US9242789B2, 26-Jan-2016.

[6] M. T. Fröhlich-Wyder and H. P. Bachmann, "Cheeses with propionic acid fermentation," in *Cheese: Chemistry, Physics and Microbiology*, vol. 2, P. F. Fox, P. L. H. McSweeney, T. M. Cogan, and T. P. Guinee, Eds. Academic Press, 2004, pp. 141–XV.

[7] C. E. Realini and B. Marcos, "Active and intelligent packaging systems for a modern society," *Meat Sci.*, vol. 98, no. 3, pp. 404–419, Nov. 2014.

[8] P. Puligundla, J. Jung, and S. Ko, "Carbon dioxide sensors for intelligent food packaging applications," *Food Control*, vol. 25, no. 1, pp. 328–333, May 2012.

[9] "MQ-135 Air Quality Sensor Hazardous Gas Detection Sensor," *SainSmart.com*. [Online]. Available: https://www.sainsmart.com/products/mq-135-air-quality-sensor-hazardous-gas-detection-sensor. [Accessed: 20-Apr-2018].

[10] "MG-811 Gas CO2 Carbon Dioxide Sensor," *SainSmart.com*. [Online]. Available: https://www.sainsmart.com/products/mg-811-gas-co2-carbon-dioxide-sensor. [Accessed: 20-Apr-2018].

[11] F. J. Vidal-Iglesias, J. Solla-Gullón, A. Rodes, E. Herrero, and A. Aldaz, "Understanding the Nernst Equation and Other Electrochemical

Concepts: An Easy Experimental Approach for Students," *J. Chem. Educ.*, vol. 89, no. 7, pp. 936–939, Jun. 2012.
[12] "How Does an NDIR CO2 Sensor Work?," *CO2 Meter*. [Online]. Available: https://www.co2meter.com/blogs/news/6010192-how-does-an-ndir-co2-sensor-work. [Accessed: 10-Apr-2018].
[13] K. Arshak, E. Moore, G. M. Lyons, J. Harris, and S. Clifford, "A review of gas sensors employed in electronic nose applications," *Sens. Rev.*, vol. 24, no. 2, pp. 181–198, Jun. 2004.
[14] L. B. Mendes, N. W. M. Ogink, N. Edouard, H. J. C. van Dooren, I. de F. F. Tinôco, and J. Mosquera, "NDIR Gas Sensor for Spatial Monitoring of Carbon Dioxide Concentrations in Naturally Ventilated Livestock Buildings," *Sensors*, vol. 15, no. 5, pp. 11239–11257, May 2015.
[15] M. E. F.-J. and and R. E. Smith*, "Volatile Organic Compounds in Foods: A Five Year Study," 02-Dec-2003. [Online]. Available: https://pubs.acs.org/doi/abs/10.1021/jf0303159. [Accessed: 09-Apr-2018].
[16] J. Gebicki and T. Dymerski, "Application of Chemical Sensors and Sensor Matrixes to Air Quality Evaluation," in *Comprehensive Analytical Chemistry*, 2016.
[17] A. Berna, "Metal Oxide Sensors for Electronic Noses and Their Application to Food Analysis," *Sensors*, vol. 10, no. 4, pp. 3882–3910, Apr. 2010.
[18] N. Yamazoe, G. Sakai, and K. Shimanoe, "Oxide Semiconductor Gas Sensors," *Catal. Surv. Asia*, vol. 7, no. 1, pp. 63–75, Apr. 2003.
[19] B. Szulczyński and J. Gębicki, "Currently Commercially Available Chemical Sensors Employed for Detection of Volatile Organic Compounds in Outdoor and Indoor Air," *Environments*, vol. 4, no. 1, p. 21, Mar. 2017.
[20] T. Langsrud and G. W. Reinbold, "Flavor development and microbiology of swiss cheese-a review," *J. Milk Food Technol.*, vol. 36, no. 12, pp. 593–609, Dec. 1973.
[21] "Telaire T6700 Series | Miniature CO2 Sensor Modules." [Online]. Available: https://amphenol-sensors.com/en/products/co2/co2-modules/3215-t6700#specifications-t6713. [Accessed: 20-Apr-2018].
[22] "WP3W-RK - Wireless Power Reference Solution for 0.5W to 3W Applications | IDT." [Online]. Available: https://www.idt.com/products/power-management/wireless-

power/wireless-power-transmitters/wp3w-rk-wireless-power-reference-solution-05w-3w-applications. [Accessed: 20-Apr-2018].
[23] "CFR - Code of Federal Regulations Title 21." [Online]. Available: https://www.accessdata.fda.gov/scripts/cdrh/cfdocs/cfCFR/CFRSearch.cfm?fr=175.300. [Accessed: 10-Apr-2018].
[24] P. L. H. McSweeney, *Cheese Problems Solved*. Elsevier, 2007.
[25] M. H. Polley and B. B. S. T. Boonstra, "Carbon Blacks for Highly Conductive Rubber," *Rubber Chem. Technol.*, vol. 30, no. 1, pp. 170–179, Mar. 1957.
[26] ams AG, "ams." [Online]. Available: http://ams.com/eng/Products/Wireless-Connectivity/Sensor-Tags-Interfaces/SL900A. [Accessed: 15-Apr-2018].
[27] K. Yam, P. Takhistov, and J. Miltz, *Intelligent Packaging: Concepts and Applications*, vol. 70. 2005.
[28] Lee Dong Sun, Kwon Ho Ryoung, and Ha Jung Uk., "Estimation of pressure and volume changes for packages of kimchi, a Korean fermented vegetable," *Packag. Technol. Sci.*, vol. 10, no. 1, pp. 15–32, Dec. 1998.
[29] W. P. Eaton and J. H. Smith, "Micromachined pressure sensors: review and recent developments," *Smart Mater. Struct.*, vol. 6, no. 5, p. 530, 1997.
[30] A. A. Barlian, W. T. Park, J. R. Mallon, A. J. Rastegar, and B. L. Pruitt, "Review: Semiconductor Piezoresistance for Microsystems," *Proc. IEEE*, vol. 97, no. 3, pp. 513–552, Mar. 2009.
[31] M. A. Cullinan, R. M. Panas, C. M. DiBiasio, and M. L. Culpepper, "Scaling electromechanical sensors down to the nanoscale," *Sens. Actuators Phys.*, vol. 187, pp. 162–173, Nov. 2012.
[32] "0-30 Bar Digital Pressure Sensor | TE Connectivity." [Online]. Available: http://www.te.com/usa-en/product-CAT-BLPS0017.html. [Accessed: 19-Apr-2018].

General conclusion

This work has addressed the design aspects for UHF RFID tags in order to develop a low-cost tag that will be used to meet the need for traceability and quality assessment for cheese production sector. This work was done in the framework of collaboration between several industrial partners and the Laboratory of Design and Integration Systems (LCIS), as well as other academic partners.

The first chapter of this thesis was dedicated to a general presentation of RFID technology and its applications in the field of food traceability and quality monitoring of different food products. The various existing RFID technologies have been introduced and the interest of the passive RFID technology has been highlighted. Compared to other food sectors, the application of RFID technology for traceability of cheese is still limited and mainly based on HF RFID. Therefore, the UHF RFID technology can be an interesting alternative which provides more reliable and flexible traceability solution for the cheese production sector.

In the second chapter, the properties of dielectric materials have been exposed along with the main parameters which affect the complex permittivity of food. The dielectric properties of several food products were stated at different frequencies, temperatures and moisture contents. Then, we presented the primary dielectric characterization methods where the choice between one method and another depends on the nature of food product and the required frequency band. Finally, a new dielectric measurement technique based on the frequency shift of a simple dipole antenna is presented. The main advantages of this method is its simplicity and being low-cost compared to other methods such as the coaxial probe. However, it is limited to the characterization of dielectric constant and future work needs to be realized in order to accurately estimate the dielectric losses.

The third chapter presented a detailed analysis on the variation of dielectric properties for three different types of cheese during ripening. Moreover, chemical analyses were realized showing the variation of different parameters such as dry matter, fats, pH, calcium, NaCl and nitrogen. The correlations between dielectric and chemical parameters showed small variations in the case of Emmental cheese whereas more significant variations were observed in the case of Grimon and Morbier respectively.

The fourth chapter discussed in detail the design steps of a passive UHF RFID tag for traceability. The first step was the dielectric characterization of different substrate materials such as casein and polypropylene which are compatible with the regulations of food labeling. Then, a comparison between different RFID chips was held and the chip Monza R6 was selected as it has the best performance in terms of sensitivity besides its unique feature of auto-tuning which allows achieving higher read range compared to other RFID chips. The chip impedance was then measured using a simple method based on a balun and the obtained values were used for antenna simulations. Different tag configurations were presented showing the possibility of achieving a read range around 1 meter for tags in direct contact with cheese. Higher read ranges were obtained for tag configurations with a ground plane where the maximum read range was around 4,5 meters.

The first section of chapter five presented the installation procedure of RFID tags on cheese in a real industrial environment and read range measurements were realized using a handheld reader. Compared to Tagformance used for the characterization of tags performance as in chapter four, the handheld reader could only send less than half of the allowed power which significantly affected the read ranges of tags. The rest of the chapter presented two solutions for improving the traceability in the cheese production sector. The first approach was based on a technique which allows the reader antenna to rotate the polarization of the transmitted signal and thus detects the randomly oriented tags without decreasing the system performance. The second approach was based on transformation barcodes into RFID tag which allows two tiered identification solution and thus combines the advantages of both technologies on the same design.

Finally, chapter six presented different design approaches of RFID sensor tag for monitoring cheese maturation. The first approach studied the effect of dielectric properties variation on a tag read range during cheese ripening. The variation of a tag read range as function of dielectric properties of three types of cheese was simulated showing very limited variations which cannot be easily detected especially in a real environment where interferences and multipath effects exist. Another sensor tag approach based on gas detection was presented. In the case of Emmental, a huge amount of Carbon dioxide is released during ripening due to the increase in fermentation activity. Measurement using a CO2 sensor based on NDIR, installed inside the package of an Emmental cheese wheel, showed a significant

variation in the level of CO2 detected during cheese maturation in the warm cave. This variation in the level of gas can be related to the level of cheese maturation; however, it is not feasible to use such kind of sensor due to its high cost and high power consumption. The rest of the chapter presented two tag configurations which allow measuring other parameters which can be related to cheese maturation. The first configuration was based on the measurement of the increase in the dimensions of cheese wheel using resistive wires, whereas the second configuration used a MEMS pressure sensor to measure the variation of pressure inside the cheese packaging due to gas release during ripening. Results obtained showed the feasibility of applying both configurations for cheese quality monitoring.

List of Publications

Journals

Accepted

[1] **A. Abdelnour**, D. Kaddour, and S. Tedjini, "Transformation of Barcode Into RFID Tag, Design, and Validation," *IEEE Microw. Wirel. Compon. Lett.*, vol. 28, no. 5, pp. 398–400, May 2018.

[2] **A. Abdelnour,** F. Buchin, D. Kaddour and S. Tedjini, "Improved Traceability Solution Based on UHF RFID for Cheese Production Sector," *in IEEE Journal of Radio Frequency Identification*, vol. 2, no. 2, pp. 68-72, June 2018.

[3] A.Rennane, **A. Abdelnour**, D. Kaddour, R.Touhami, and S. Tedjini, "Design of Passive UHF RFID sensor on Flexible Foil for Sports Balls Pressure Monitoring ," *IET Microwaves, Antennas & Propagation.2018, 12, (14), p. 2154-2160*

[4] **A. Abdelnour**, A. Lazaro, R. Villarino, D. Kaddour, S. Tedjini, and D. Girbau, "Passive Harmonic RFID System for Buried Assets Localization," Sensors, vol. 18, no. 11, p. 3635, Oct. 2018.

Conferences

[1] **A. Abdelnour**, A. Lazaro, E. Ibars, R. Villarino, D.Girbau, C. Mercier, D.Kaddour and S.Tedjini, "Design of UHF RFID tag on PLA substrate for food traceability," *2nd URSI Atlantic Radio Science Conference (URSI ATRASC 2018).*

[2] A. Rennane, N. Fonseca, **A. Abdelnour**, F. Benmahmoud, D. Kaddour, R. Touhami, S. Tedjini, "Passive UHF RFID Sensor Tag for Pressure and Temperature Conditions Monitoring," *2nd URSI Atlantic Radio Science Conference (URSI AT-RASC 2018).*

[3] S.Tedjini, H.Elmatbouly, **A.Abdelnour**, " Controlled Backscatter for Identification and Sensing" *2018 IEEE APCAP*

[4] N. Fonsêca; R. Freire; G. Fontgalland; **A. Abdelnour**; A. Rennane; S. Tedjini "A based microcontroller technique to achieve capacitive multisensing in passive RFID UHF tags," *2018 IEEE International Conference on RFID (RFID).*

[5] **A. Abdelnour**, A. Rennane, D.Kaddour and S.Tedjini, "On the transformation of symbols and figures to RFID tags," *2017 XXXIInd General Assembly and Scientific Symposium of the International Union of Radio Science (URSI GASS).*

[6] A. Rennane, **A. Abdelnour**, D.Kaddour and S.Tedjini, "Development of passive UHF RFID tag on flexible foil for sport balls pressure monitoring," *2017 XXXIInd General Assembly and Scientific Symposium of the International Union of Radio Science (URSI GASS).*

[7] **A. Abdelnour**, A. Rennane, D.Kaddour and S.Tedjini, "Non-destructive dielectric characterization method for food products," *2017 IEEE MTT-S International Microwave Symposium (IMS).*

[8] G. Andìa Vera; **A. Abdelnour**; M. Sarkis; A. Georgiadis; D. Kaddour; S. Tedjini, "Passive RFID-enabled proximity sensor," *2016 IEEE MTT-S International Microwave Symposium (IMS)*

Développement d'étiquettes RFID UHF pour la traçabilité et le contrôle de qualité des produits alimentaires,

Application: production de fromage

Résumé

Dans le secteur de l'agroalimentaire, l'utilisation de la RFID permet d'améliorer la sécurité des produits alimentaires tout en assurant une meilleure traçabilité et un meilleur suivi des produits. Le travail de cette thèse était principalement réalisé dans le cadre d'un projet en coopération avec plusieurs partenaires académiques et industriels dans le secteur fromager où l'objectif principal du projet était de maitriser l'ensemble des étapes de fabrication par un parfait suivi de la traçabilité des produits et un pilotage précis de l'affinage. Le travail réalisé dans cette thèse s'inscrit dans ce contexte et a comme objectif le développement de tags RFID UHF adaptés aux contraintes des produits alimentaires en assurant une double fonction: une fonction de traçabilité à identification unitaire, et ensuite une fonction de détection du degré de maturation de l'aliment par mesure indirecte de ses propriétés électromagnétiques et physico-chimiques.

La première étape du projet était la caractérisation des paramètres électromagnétiques des produits alimentaires durant l'affinage afin de réaliser une conception appropriée de l'antenne du tag. En radiofréquences, c'est principalement le substrat qui dicte les propriétés électromagnétiques des composants, notamment la taille des antennes et leur diagramme de rayonnement. La connaissance de ces propriétés est indispensable afin de répondre aux exigences industrielles et d'intégrer dans de bonnes conditions les systèmes dans l'environnement applicatif. En plus, une étude de corrélation est réalisée entre la variation des propriétés diélectriques et celle des propriétés chimiques durant la période d'affinage

des produits. Cette étude aide à comprendre la différence entre les différents produits et permet de déterminer les paramètres principaux à suivre durant l'affinage pour la conception du tag capteur.

La deuxième étape était la conception des tags identifiants pour la traçabilité des produits alimentaires durant la procédure de fabrication. L'objectif principal est de réaliser un tag identifiant avec une performance qui répond aux besoins des fabricants dans le secteur fromager concernant la taille, la mémoire et la distance de lecture du tag tout en respectant les normes de santé au niveau d'emballage du tag ainsi que le substrat utilisé. Plusieurs configurations de tag RFID UHF étaient réalisées et testées dans un environnement industriel où les résultats obtenus montrent l'efficacité d'utiliser un système de RFID pour automatiser la traçabilité des produits dans le secteur fromager.

La troisième étape concerne la conception des tags capteurs pour suivre le degré d'affinage des produits pendant la période de maturation. Une première solution, basée sur l'exploitation de l'effet de variation des propriétés diélectriques sur la distance de lecture de tag, montre un manque de performance due aux faibles variations ainsi qu'aux difficultés de mesure dans un environnement réel. Une deuxième solution basée sur la mesure de taux de dégagement des gaz durant l'affinage montre la possibilité d'estimer le degré d'affinage. Par contre, la puissance d'activation de capteur et le coût élevé ne permettent pas d'adopter cette solution. Finalement, deux solutions alternatives étaient réalisées pour mesurer l'augmentation du taux d'échappement des gaz d'une manière indirecte. La première configuration de tag capteur est basée sur le suivi du changement de dimensions du produit en utilisant un capteur résistif. D'autre part, la deuxième configuration de tag capteur est basée sur le suivi de changement de pression dans l'emballage du produit dû à la production de gaz. Les résultats obtenus montrent que ces deux configurations de tag RFID capteur peuvent offrir des solutions simples et efficaces pour le pilotage de l'affinage des produits alimentaires.

Communauté
UNIVERSITÉ Grenoble Alpes

Développement d'étiquettes RFID UHF pour la traçabilité et le contrôle de qualité des produits alimentaires, Application: production de fromage

Résumé

Dans le secteur de l'agroalimentaire, l'utilisation de la RFID permet d'améliorer la sécurité des produits alimentaires tout en assurant une meilleure traçabilité et un meilleur suivi des produits. Le travail de cette thèse était principalement réalisé dans le cadre d'un projet en coopération avec plusieurs partenaires académiques et industriels dans le secteur fromager où l'objectif principal du projet était de maitriser l'ensemble des étapes de fabrication par un parfait suivi de la traçabilité des produits et un pilotage précis de l'affinage. Le travail réalisé dans cette thèse s'inscrit dans ce contexte et a comme objectif le développement de tags RFID UHF adaptés aux contraintes des produits alimentaires en assurant une double fonction: une fonction de traçabilité à identification unitaire, et ensuite une fonction de détection du degré de maturation de l'aliment par mesure de ses propriétés électromagnétiques et physico-chimiques.

Development of RFID tags for traceability and sensing in the food sector, Application: Cheese production

Abstract

In the food sector, the use of RFID makes it possible to improve the safety of food while ensuring better traceability and better monitoring of products. The work of the thesis was mainly carried out within the framework of a project in cooperation with several academic and industrial partners in the cheese sector where the main objective of the project is to develop UHF RFID tags adapted to the constraints of food products by ensuring a dual function: a traceability function with unitary identification, and then a sensing function of cheese maturation by measurement of its electromagnetic and physicochemical properties.